



TECHNISCHE UNIVERSITÄT MÜNCHEN

Lehrstuhl für Biotechnologie der Nutztiere

Modelling the multi-step process of tumorigenesis in pigs

Anja B. E. Saalfrank

Vollständiger Abdruck der von der Fakultät Wissenschaftszentrum Weihenstephan für Ernährung, Landnutzung und Umwelt der Technischen Universität München zur Erlangung des akademischen Grades eines

Doktors der Naturwissenschaften

genehmigten Dissertation.

Vorsitzender: Univ.-Prof. Dr. H. Luksch

Prüfer der Dissertation:

1. Univ.-Prof. A. Schnieke, Ph.D.
2. apl. Prof. Dr. D. Saur

Die Dissertation wurde am 10.12.2014 bei der Technischen Universität München eingereicht und durch die Fakultät Wissenschaftszentrum Weihenstephan für Ernährung, Landnutzung und Umwelt am 27.04.2015 angenommen.

Für meine Mama

Abstract

The World Health Organisation has stated that the number of new cancer cases is steadily increasing. Despite tremendous knowledge about the aetiology of cancer, there has been little progress in the treatment of this deadly disease. Until now, genetically engineered mice are the most extensively used animals for biomedical cancer research. However their small size and short lifespan limit the type of preclinical studies that can be carried out. In this respect, the pig has gained much interest as an alternate animal model for human cancers. However to date, little is known about the multi-step process of tumorigenesis in pigs and how closely the fundamental mechanisms involved resemble those in humans.

This work describes the neoplastic transformation of stepwise genetically modified porcine mesenchymal stem cells (pMSCs) *in vitro* that express oncogenic $TP53^{R167H}$ (orthologous to human $TP53^{R175H}$) and $KRAS^{G12D}$ (homologous to human $KRAS^{G12D}$) from their endogenous gene loci. Conversion of pMSCs to a transformed phenotype was accompanied by p16INK4 α gene silencing. The unique *in vitro* growth characteristics of the genetically modified pMSCs suggested that they have circumvented replicative senescence. Transcriptome analysis revealed increased expression of genes associated with the “Alternative Lengthening of Telomeres” mechanism in these cells. Several *in vitro* assays were performed that confirmed the neoplastic transformation of the genetically modified pMSCs. Furthermore, the tumorigenic potential of these cells was assessed in an *in vivo* xenotransplantation model. Here, only genetically modified pMSCs with an additional deregulated cMyc expression formed palpable tumours in immune-deficient mice. In accordance with the implanted cell type, recovered tumours were classified as soft-tissue sarcomas. When implanted in an immune competent isogenic pig, the stepwise genetically modified pMSCs were rejected by the pig’s immune system, as judged by swelling and redness at the injection sites. Collectively, this work demonstrates that transformed pMSCs mimic several aspects of human mesenchymal stem cell transformation.

Zusammenfassung

Laut Weltgesundheitsorganisation steigt die Zahl der Krebserkrankungen stetig an. Trotz des enormen Forschungsfortschrittes der letzten Jahre sind die Heilungschancen dieser meist tödlich verlaufenden Krankheit gering. Bis heute gehören genetisch veränderte Mäuse zu den am häufigsten verwendeten Tiermodellen in der biomedizinischen Krebsforschung. Allerdings limitieren ihre Größe und kurze Lebenserwartung die Durchführung einiger präklinischer Studien. Das Schwein hingegen bietet sich wegen seiner anatomischen und physiologischen Ähnlichkeit zum Menschen als alternatives Modelltier für die Krebsforschung an. Bisher ist jedoch wenig über die Tumorbilogie beim Schwein bekannt und es ist ungewiss, wie sehr der Mehrstufenprozess der Tumorgenese des Schweines dem des Menschen ähnelt.

Diese Arbeit beschreibt die neoplastische Transformation schrittweise genetisch veränderter mesenchymaler Stammzellen (MSZs) des Schweines *in vitro* basierend auf der Expression von onkogenem $TP53^{R167H}$ (ortholog zu humanem $TP53^{R175H}$) und $KRAS^{G12D}$ (homolog zu humanem $KRAS^{G12D}$). Die unbegrenzte Proliferation der genetisch veränderten porzinen MSZs deutete daraufhin, dass diese replikative Seneszenz umgangen haben mussten. Molekulare Analysen zeigten, dass in diesen Zellen die Expression von p16INK4a durch Genmethylierung stillgelegt wurde, sowie die Expression von Genen erhöht war, welche in dem Prozess des „*Alternative Lengthening of Telomeres*„ involviert sind. Mehrere *in vitro* Analysen bestätigten die neoplastische Transformation der modifizierten MSZs. Bei der Implantation dieser Zellen in immundefiziente Mäuse stellte sich heraus, dass nur genetisch veränderte porzine MSZs mit einer zusätzlichen, deregulierten cMyc-Expression tastbare Tumore bildeten. Diese wurden in Übereinstimmung mit dem implantierten Zelltyp als Weichteilsarkome klassifiziert. Die Implantation der modifizierten porzinen MSZs in ein immunkompetentes, isogenes Empfängerschwein löste hingegen eine Immunreaktion aus. Zusammenfassend zeigt diese Arbeit, dass transformierte Schweine-MSZs mehrere Aspekte der neoplastischen Transformation humaner Stammzellen imitieren.

1 Introduction	1
1.1 Proto-oncogenes and tumour suppressor genes	1
1.2 Mimicking the multi-step process of tumorigenesis <i>in vitro</i>	1
1.3 Deregulated signalling pathways that contribute to cellular transformation <i>in vitro</i>	4
1.3.1 Telomere biology and human cell immortalisation	4
1.3.2 The tumour suppressor protein p53	6
1.3.3 The retinoblastoma protein pRb	8
1.3.4 The <i>CDKN2A</i> gene locus	11
1.3.5 Oncogenic Myc	13
1.3.6 The <i>RAS</i> gene family members	16
1.4 Genetically engineered mouse models in cancer research	19
1.5 Limitations of mouse cancer models	20
1.6 Genetically modified pigs in biomedical and cancer research	21
1.7 Objective	22
2 Material and Methods	23
2.1 Materials	23
2.1.1 Equipment	23
2.1.2 Consumable	24
2.1.3 Chemicals	25
2.1.4 Miscellaneous	27
2.1.5 Bacterial media	27
2.1.6 Tissue culture media, buffers and supplements	27
2.1.7 Kits	28
2.1.8 Enzymes and Buffers	29
2.1.9 Competent bacterial strains	29
2.1.10 Mammalian cell lines	29
2.1.11 Animals	30
2.1.12 Gene targeting constructs and plasmids	30
2.1.13 Oligonucleotides	30
2.1.14 Antibodies	32
2.1.15 Computer Softwares	32
2.2 Methods	33
2.2.1 Microbiological methods	33
2.2.2 Mammalian cell culture methods	35
2.2.3 Isolation of nucleic acids	39
2.2.4 Molecular biological methods	41

2.2.5 Biochemical methods	47
2.2.6 Animal experiments	51
3 Results	53
3.1 Introducing defined oncogenic mutations into porcine mesenchymal stem cells	53
3.1.1 Design of the $KRAS^{LSL-G12D}$ gene targeting vector constructs	54
3.1.2 Derivation of pMSCs carrying latent oncogenic $KRAS^{LSL-G12D}$ and $TP53^{LSL-R167H}$ alleles	54
3.2 Activation of latent oncogenic $TP53^{LSL-R167H}$ and $KRAS^{LSL-G12D}$ alleles	59
3.3 Inducing a deregulated cMyc expression in mutant $TP53^{R167H}$ and $KRAS^{G12D}$ pMSCs	65
3.4 Investigating TERT expression in stepwise genetically modified pMSCs	67
3.5 Investigating the $CDKN2A$ gene locus in stepwise genetically modified pMSCs	68
3.6 <i>In vitro</i> characterisation of genetically modified pMSCs	71
3.7 Implantation of genetically modified pMSCs into immune-deficient mice	74
3.8 <i>In vitro</i> growth characteristics and genetic signature of porcine sarcoma derived cell lines	76
3.9 Expression profile of stepwise modified pMSCs and porcine sarcoma derived cell lines	81
3.10 Implantation of genetically modified pMSCs in an immune-competent isogenic pig	84
3.11 Conclusion	85
3.12 Derivation of pigs carrying latent oncogenic $TP53^{LSL-R167H}$ and $KRAS^{LSL-G12D}$ alleles	86
3.12.1 Introducing a latent oncogenic $KRAS^{LSL-G12D}$ allele in $TP53^{LSL-R167H/+}$ gene-targeted pMSCs	86
3.12.2 Conclusion	90
4 Discussion	91
4.1 Modelling the multi-step process of porcine tumorigenesis <i>in vitro</i>	91
4.2 Generation of $TP53^{LSL-R167H}$, $KRAS^{LSL-G12D}$ double-targeted pMSC clones	91
4.2.1 Design of the $KRAS^{LSL-G12D}$ gene targeting constructs	92
4.2.2 Identification of $TP53^{LSL-R167H}$, $KRAS^{LSL-G12D}$ double-targeted pMSC clones	92
4.2.3 Efficiency of $KRAS^{LSL-G12D}$ gene targeting	92
4.3 Activation of latent oncogenic alleles by Cre protein transduction	93
4.3.1 Efficiency of Cre protein mediated cassette excision	94
4.3.2 $TP53^{LSL-R167H/LSL-R167H}$ homozygosity of the cell clone neo14	94
4.3.3 Functionality of Cre recombined $TP53^{L-R167H}$, $KRAS^{L-G12D}$ alleles	95
4.4 Transcriptional silencing of p16INK4 α	95
4.5. Deregulated cell cycle control in stepwise genetically modified pMSCs	97
4.6 Acquired immortalisation of stepwise genetically modified pMSCs	98
4.7 <i>In vitro</i> growth characteristics of stepwise genetically modified pMSCs	100
	VI

4.8. <i>In vivo</i> tumorigenicity of stepwise genetically modified pMSCs	101
4.8.1 Implantation of stepwise genetically modified pMSCs in immune-deficient mice	101
4.8.2 Isolation and culture of porcine sarcoma derived tumour cells	102
4.8.3 Amplification of oncogenic KRAS ^{G12D} in porcine sarcoma derived tumour cells	103
4.8.4 Implantation of stepwise modified pMSCs in an immune-competent isogenic pig	104
4.9 Derivation of pigs carrying latent oncogenic <i>TP53</i> ^{LSL-R167H} and <i>KRAS</i> ^{LSL-G12D} alleles	105
5 Concluding remarks and outlook	107
6 Abbreviations	108
7 List of Tables	113
8 List of Figures	114
9 Bibliography	116
10 Appendix	135
11 Acknowledgement	140
12 Curriculum Vitae	143

1 Introduction

1.1 Proto-oncogenes and tumour suppressor genes

The development of cancer arises from a stepwise accumulation of genetic and epigenetic alterations in proto-oncogenes and tumour suppressor genes that control cell cycle progression, apoptosis, genome integrity and cell differentiation. Proto-oncogenes process and transmit growth-stimulatory signals throughout the cell, thereby regulating and controlling cellular growth and proliferation after mitogenic stimulation. To date, four groups of proto-oncogenes are known: growth factors, growth factor receptors, signal transducers and transcription factors. These proto-oncogenes can be converted to oncogenes by amplifications, rearrangements, translocations or gain-of-function mutations that result in cellular growth autonomy and which consequently leads to the formation of neoplasm [reviewed in 1,2,3]. In contrast, tumour suppressors are cellular genes that receive and process growth-inhibitory signals, which lead to decreased cell proliferation. Their inactivation by point mutations or protein sequence deletions coupled with the loss of the remaining wild-type allele increases the susceptibility of tumour formation. Moreover, impairment of the functioning of tumour suppressor genes is considered to increase the rate of additional mutations and other genetic abnormalities, respectively [reviewed in 3,4]. By now, about 100 potential oncogenes, cellular and viral ones, and about 20 tumour suppressors have been described [reviewed in 5].

1.2 Mimicking the multi-step process of tumorigenesis *in vitro*

The analysis of cells obtained from cancer patients revealed that different combinations of mutant oncogenes and tumour suppressor genes could be found in the genome of distinct human cancer types. These studies allowed the identification and description of molecules and pathways important for the malignant phenotype and were thus fundamental for the current understanding of the molecular basis of cancer. However, cancer cell lines from human tumour specimens are most often established from late-stage tumours, which harbour complex karyotypes and multiple genetic mutations, making it difficult to determine, how specific mutations contribute to the initiation and progression of cancer [6-8].

An alternative approach to study and understand the multi-step process of tumorigenesis is the direct manipulation of primary cells in culture to establish experimental transformation models. These genetically engineered cell models, rodent and human ones, provided important insights into the oncogenic potential of distinct mutant genes. However soon it became obvious, that a profound difference exist in the susceptibility of rodent and human cells to transformation, as rodent cells could be converted to a transformed phenotype by very few manipulations. In particular, two laboratories showed, that primary rodent cells could

be transformed by the expression of at least two cooperating oncogenic mutations, such as Ras and Myc [9] or Ras and either the adenovirus early region 1A (E1A) protein [10] or the large T antigen of the simian virus 40 early region [11]. In contrast, the same set of oncogenes failed to transform primary human cells and instead, resulted in cells with a limited replicative capability [12]. These observations suggested that in human cells replicative senescence may function as barrier of cellular transformation and moreover that human cells require additional genetic alterations to become malignant [13].

In 1999, Hahn and colleagues reported the derivation of the first experimental human transformation model. They showed that human cells could be converted to a transformed phenotype by the ectopic expression of a combination of viral and human transgenes. In particular, the expression of large T (LT) and small T antigen (ST) of simian virus 40 early region, the catalytic subunit of the human telomerase (hTERT) and an oncogenic form of HRAS (HRAS^{G12V}) resulted in neoplastic cell transformation of normal human cells (Figure 1) [14].

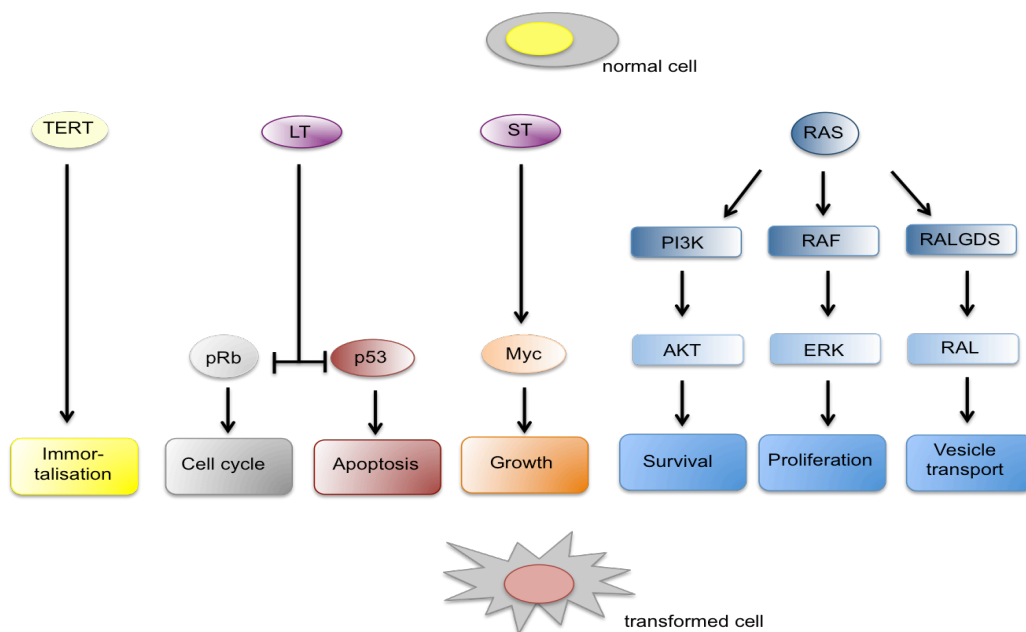


Figure 1: Cooperating pathways in human cell transformation

The disruption of several pathways results in the neoplastic transformation of human cells. Expression of the catalytic subunit of telomerase (TERT) confers telomere maintenance and thereby cellular immortalisation. The simian virus 40 early region encodes both the large T antigen (LT) and the small T antigen (ST). LT inactivates and disrupts the action of the retinoblastoma protein (pRb) as well as the p53 tumour suppressor protein. ST stabilises cMyc protein. Oncogenic Ras stimulates several signalling pathways through multiple effector pathways. Abbreviation: PI3K: phosphoinositide 3-kinase, ERK: extracellular signal-regulated kinase. (Adapted from [7])

Later, the same group proved, that the action of the LT, namely binding and sequestration of the two important tumour suppressor genes, retinoblastoma protein (pRb) and p53, could be substituted by the ectopic expression of the human papillomavirus (HPV) E6 and E7 oncoproteins [15]. Moreover, they and others uncovered that the ectopic expression of the ST leads to the stabilisation of cMyc proteins, resulting in the perturbation of the functional

Myc network [15,16]. Subsequent studies confirmed that this set of introduced modifications was also sufficient to transform a wide variety of human cell types, including glial cells, endothelial cells, airway epithelial cells and mammary epithelial cells [17-21].

Although these experimental tumour models were invaluable for our understanding of cellular transformation, one major limitation of them was, that they relied on the ectopic expression of viral proteins. Therefore further investigations were conducted to identify human genes that could substitute the action of these viral proteins in the process of malignant cell transformation *in vitro*. Hahn and colleagues (2001) showed, that an overexpression of cyclin D1 with concomitant expression of mutant CDK4 (CDK4^{R24C}) protein, which is resistant to its major inhibitor p16INK4 α [22], were sufficient to perturb the pRb signalling pathway [15]. Additionally they proved, that the expression of truncated p53 (p53^{DD}) protein, which acts as a dominant negative p53 protein [23], leads to the disruption of normal p53 signalling [15]. And a study conducted by Yeh and colleagues (2004) showed, that the expression of a stabilised version of cMyc (cMyc^{T58A}) could replace the function of the ST in the transformation process [24]. Inspired by these findings, Kendall *et al.* (2005) demonstrated that primary human cells of various cell types could be converted to neoplastic ones by using only mammalian genetic elements. In particular, the ectopic expression of hTERT, p53^{DD}, cyclin D1, CDK4^{R24C}, cMyc^{T58A} and oncogenic HRAS^{G12V} gave rise to cells, which grew in an anchorage-independent manner and which formed tumours in immuno-compromised mice [25].

Cell type	Telomere maintenance	LT or replacement	ST or replacement	Oncogene	Reference
Fibroblasts, Embryonic kidney (HEK) cells	hTERT	LT	ST	HRAS ^{G12V}	[14]
Fibroblasts, HEK cells, mammary epithelial cells (HMECs)	hTERT	HPV-E6E7	ST	HRAS ^{G12V}	[15]
Fibroblasts	hTERT	cyclinD1, CDK4 ^{R24C} , p53 ^{DD}	ST	HRAS ^{G12V}	[15]
HEK cells	hTERT	LT	cMyc ^{T58A}	HRAS ^{G12V}	[24]
HEK cells, HMECs, skeletal myoblasts	hTERT	cyclinD1, CDK4 ^{R24C} , p53 ^{DD}	cMyc ^{T58A}	HRAS ^{G12V}	[25]

Table 1: Experimental human cell transformation models

Diverse sets and combinations of viral genes, mutant oncogenes and mutant tumour suppressor genes together with the ectopic expression of the catalytic subunit of the human telomerase (hTERT) were sufficient to transform a wide variety of human cells. Abbreviations: LT: simian virus 40 early region encodes the large T antigen, ST: simian virus 40 early region encodes the small T antigen, HPV: human papillomavirus, CDK: cyclin-dependent kinase

1.3 Deregulated signalling pathways that contribute to cellular transformation *in vitro*

Taken together, these experimental cell models provide, independent of the particular viral and human transgenes used, that telomere maintenance, the perturbation of p53 and pRb signalling pathways combined with deregulated cMyc and Kras signalling pathways are sufficient to induce a tumorigenic phenotype in human cells. For that reason, these particular molecules and their signalling pathways will be described in more detail in the following sections.

1.3.1 Telomere biology and human cell immortalisation

Telomeres consist of the G-rich hexameric nucleotide sequence TTAGGG [26,27] and specialised DNA-binding proteins, which cap the termini of chromosomes. This unique telomere structure protects the chromosome ends from degradation, rearrangement and fusion with other chromosomal ends, thereby protecting chromosomal integrity [reviewed in 28]. However, due to the “end replication problem” telomeres are progressively shortened with each cell division, as DNA polymerase cannot fully replicate the ends of linear chromosomes [29,30]. To prevent the progressive shortening of telomeres, a specialised cellular ribonucleoprotein enzyme complex maintains and replicates the chromosomal ends by adding telomeric repeats onto the 3' end of the chromosomes. This ribonucleoprotein complex consists of two major components, a telomerase RNA component named TERC [31] and an enzymatic telomerase reverse transcriptase, TERT [32]. TERC acts as a template for DNA synthesis and is constitutively expressed, while the expression of TERT is restricted to pluripotent stem cells as well as to adult germ cells [33] and it is not expressed at sufficient levels in somatic cells [34]. This transcriptional repression of TERT in somatic cells entails the shortening of telomeres by 50-200 base pairs per cell division. Upon a certain threshold length, cells enter an irreversible growth arrest called replicative senescence or mortality stage 1 (M1) [35,36], which is triggered by p53- and pRb-dependent growth arrest signals [37]. Due to the limited proliferative capacity of somatic cells, telomere shortening and replicative senescence are considered as potent tumour suppressor mechanisms [38]. It is worth mentioning, that senescent cells, while not proliferating, remain in a metabolic active state for an extended period of time [reviewed in 39]. Intriguingly, some cells can escape senescence either through the up-regulation of TERT activity [40] or through the simultaneous inactivation of the potent tumour suppressors p53 and pRb [41,42]. In the latter case, cells will continue to proliferate until their telomeres reach a critical shortness, leading to a second barrier termed crisis or mortality stage 2 (M2) [43]. This crisis is characterised by a massive cell death and only 1 out of 10^7 cells will escape from crisis and becomes immortal [42]. Cells that have evaded these two barriers -senescence and

crisis- must activate an additional mechanism, which prevents the further shortening of telomeres and which finally confers cellular immortalisation. In most cases immortalisation is accomplished by up-regulating telomerase activity [44], while only a minority of immortal cell lines employ a telomerase-independent mechanism, termed Alternative Lengthening of Telomeres (ALT) to maintain stable telomere length [45,46]. Current data strongly indicate that ALT is a homologous recombination (HR)-mediated telomeric DNA replication mechanism [47]. However, the proper mechanism of telomere lengthening in ALT-positive cells remains uncertain.

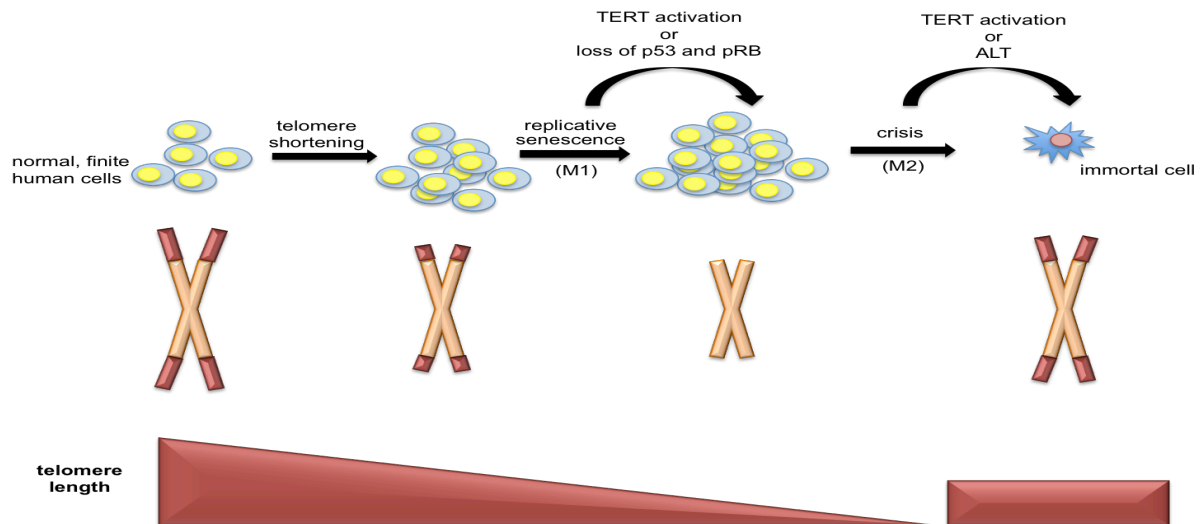


Figure 2: Barriers to immortalisation

Finite human cells have to bypass two proliferative barriers -replicative senescence and crisis- to achieve immortalisation. After a critical telomere length human cells enter an irreversible growth arrest called replicative senescence. Expression of TERT or the simultaneous inactivation of p53 and pRb allows human cells to continue proliferation with further shortening of telomeres. Such post-senescent cells continue to proliferate until they reach a second proliferative barrier called crisis. Up-regulation of TERT expression or activation of the telomerase-independent mechanism, termed Alternative Lengthening of Telomeres (ALT) allows human cells to maintain stable telomere length and immortalisation. Abbreviations: M1: mortality stage 1, M2: mortality stage 2 (Adapted from [6]).

As illustrated in Figure 2, in normal, finite cells telomeres become progressively shortened with each cell cycle that limits their replicative lifespan. This restricted lifespan is regarded to suppress neoplastic transformation [13,48]. Consistent with this idea, the majority of cancer cell lines and tumours maintain stable telomere length and show detectable telomerase activity [40,44]. Based on these observations cellular immortalisation is postulated as a hallmark of cancer [49]. In agreement with this hypothesis, the ectopic expression of hTERT was a crucial prerequisite to permit cellular transformation of a wide variety of primary human cells (see Table 1).

1.3.2 The tumour suppressor protein p53

The *TP53* gene, located on chromosome 17 in humans, on chromosome 11 in mice and on chromosome 12 in pigs encodes for the most frequently mutated tumour suppressor protein p53 [50]. In 1979, the p53 protein was first identified to be physically complexed with the SV40 LT [51]. Further analysis revealed that this protein was abundantly expressed in many human tumours, a phenomenon not observed in normal tissues. This finding led to the misinterpretation that p53 is a cellular proto-oncogene [52]. In the first decade after its discovery this assumption was furthermore reinforced by experimental model systems, which showed that p53 cooperates with oncogenic Ras in the transformation of primary cells [53-55]. In addition, overexpression of p53 in otherwise p53-null cells was reported to increase their tumorigenicity [56]. However years later, sequence analysis of the cloned p53 cDNA constructs revealed that all earlier experiments were performed with mutated p53 cDNAs derived from cancer cell lines [57,58]. These findings led to reconsider p53's role in tumour biology.

The paradigm shift that p53 is not actually a proto-oncogene but rather a tumour suppressor was first provided by work from Levine's and Oren's laboratories. They proved that the overexpression of wild-type p53 was sufficient to suppress cellular transformation [59,60]. These data and subsequent findings by Bert Vogelstein and co-workers firmly demonstrated that p53 acts as a tumour suppressor gene [61]. Now, 35 years after its discovery and intensive research, p53 is known as the "guardian of the genome" [62]. In response to cellular stress such as DNA damage, hypoxia and oncogene activation, p53 can impart cell cycle arrest, DNA repair, apoptosis, differentiation or senescence. The ability of p53 to choose between cell survival and cell death demonstrates its potent tumour-suppressive and anti-proliferative function, as it can block uncontrolled cell growth, suppress cellular transformation and thereby protect against tumour development [reviewed in 63].

1.3.2.1 Tumour suppressive function of wild-type p53

The p53 protein functions as a sequence-specific transcription factor that binds as a homotetramer to p53 response DNA-elements resulting in the transactivation of nearby genes [64]. The 53 kDa protein consists of 393 amino acids and can be divided into three functional domains. An acidic N-terminal transactivation domain, which is required for transcriptional activation, a centrally located sequence-specific DNA-binding domain and a basic C-terminal tetramerisation domain [65].

Under physiological, unstressed conditions p53 is maintained at low protein levels by its predominant negative regulator, human double minute 2 homolog (HDM2, MDM2 for its

mouse equivalent). HDM2 binds to p53 and blocks its transactivation domain [66]. Moreover, HDM2 is a E3 ubiquitin ligase that marks p53 for degradation through the ubiquitin-proteasome pathway [67]. Importantly, HDM2 is a direct transcriptional target of p53 and the p53-HDM2 complex forms a negative feedback-loop, in which the induced expression of HDM2 leads to the degradation of p53, which results in decreased p53 protein levels and low p53 activity [68].

Following cellular stress ataxia telangiectasia mutated (ATM) becomes activated and causes the phosphorylation of p53 and HDM2, blocking thereby p53-HDM2 interaction, which results in stabilisation and accumulation of p53 (Figure 3) [69,70]. Subsequent posttranslational modifications such as acetylation and phosphorylation activate p53 and cause the transcription of its downstream targets and pathways [71]. Dependent on the strength and the intensity of the stress signal p53 triggers either cell cycle arrest or apoptosis. In the case of repairable damage p53 causes cell cycle arrest by the induction of its downstream targets cyclin dependent kinase inhibitor p21, growth arrest and DNA damage-inducible protein 45 (GADD45) and cyclin G1. Overexpression of these genes results in G₁ phase arrest enabling DNA repair and survival of the cell. Whereas in cells harbouring deleterious genetic abnormalities p53 provokes an apoptotic response through transcriptional activation of pro-apoptotic genes, such as BCL2- associated X protein (BAX), p53 upregulated modulator of apoptosis (PUMA) and phorbol-12-myristate-13-acetate-induced protein 1 (NOXA) [reviewed in 72,73-75].

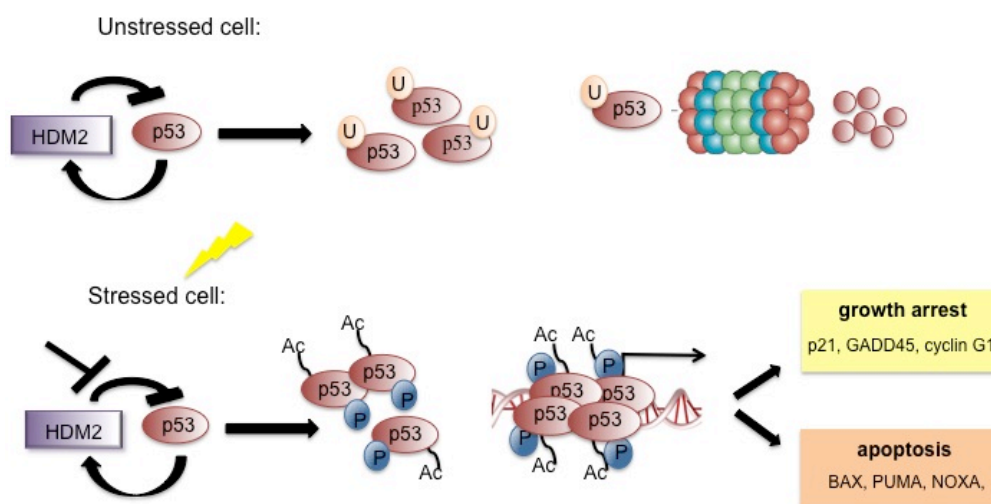


Figure 3: Regulation of p53 function

In normal, unstressed cells p53 mediates transcription of its negative regulator human double minute 2 homolog (HDM2). HDM2 marks p53 for proteasomal degradation through ubiquitylation (Ub). Cellular stress leads to interfered p53-HDM2 interaction and to the stabilisation and accumulation of phosphorylated (P) and acetylated (Ac) p53 protein. Active p53 binds as a homotetramer at its target genes and triggers their transcription. Induction of p21, GADD45 and cyclinG1 expression promote growth arrest and DNA repair. Apoptosis is induced through the transcriptional activation of BCL2-associated X protein (BAX), p53 upregulated modulator of apoptosis (PUMA) and phorbol-12-myristate-13-acetate-induced protein 1 (NOXA) (Adapted from [71]).

1.3.2.2 Loss of wild-type p53 function and tumorigenesis

On the basis of p53's multifaceted and potent tumour suppressive function, it is not surprising that somatic mutations in the *TP53* gene can be found in more than 50% of all human tumours. The majority of these cancer-associated mutations are missense mutations, which are clustered within the p53 DNA-binding domain. Data from human cancer patients revealed that most of these missense mutations are found within six "hot spot" residues (R175, G245, R248, R249, R273 and R282) that cause single amino-acid exchanges (<http://www-p53.iarc.fr/>). According to the mutated residue, the protein products can be classified as either contact (R248, R273) or structural (R175, G245, R249, R282) mutants, which can abolish the tumour suppressor function of wild-type p53 protein in a dominant negative manner [76]. In human cancers missense mutations in the *TP53* gene are frequently followed by loss of heterozygosity (LOH) of the remaining wild-type allele. This suggests that there is a selective advantage conferred by losing the remaining wild-type allele [77]. All these and additional observations have led to the "gain-of-function" hypothesis, which states that certain *TP53* gene mutations are important drivers of tumorigenesis through exerting oncogenic properties [78].

Studies conducted by Lang's and Olive's groups support this hypothesis. They have generated two mouse models of Li-Fraumeni syndrome (LFS), in which *TP53* germline mutations are the underlying cause of the early onset of tumour development. In these animal models the most two common p53 "hot spot" mutations (R172H, R270H) are expressed from their endogenous gene locus. These genetically modified mice produced tumours with a more aggressive and metastatic phenotype than heterozygous p53 knock-out animals, thereby recapitulating the disease of human LFS patients [79,80]. Taken together, these and other studies strongly demonstrate, the pro-tumorigenic potential of mutant p53 proteins.

1.3.3 The retinoblastoma protein pRb

The retinoblastoma gene (*RB1*) was the first identified tumour suppressor based on its mutational inactivation in retinoblastoma, a rare childhood tumour of the eyes. Molecular analysis of dissected tumours allowed the mapping of the locus to chromosome 13q14 [81,82]. The *RB1* gene consists of 27 exons that span 180 kb and are transcribed into a 4.7 kb long mRNA encoding 982 amino acids [83]. The 110 kDa gene product belongs together with the retinoblastoma-like proteins p107 and p130 to the family of "pocket proteins" that share sequence homology in the pocket domain [84-86]. This pocket domain mediates

interaction with members of the E2F family of transcription factors [87] and with several other proteins containing an LxCxE motif, such as D-type cyclins [88] and histone deacetylases [89]. In addition, viral oncogenes such as the adenovirus E1A, SV40 LT and the human papillomavirus E7 were also identified to bind to the LxCxE motif, causing thereby inactivation of pRb during cellular transformation [90-92]. RB family members are nuclear phosphoproteins that play a key role in cell cycle regulation and cell proliferation, since they negatively modulate G₁-to-S phase transition [83]. The G₁-to-S phase transition is a complex process, involving not only pRb and E2F but also various cyclins and cyclin-dependent kinases (CDKs). Since the progression through the cell cycle is a strictly regulated interplay of cyclin-CDK complexes, this stringently regulated network will be described in more detail.

1.3.3.1 pRb and cell cycle progression

The cell cycle can be divided into four major phases. During the presynthetic G₁ phase proliferating somatic cells harbour a diploid number of chromosomes and grow in size. In early G₁ phase hypo-phosphorylated pRb interacts with E2F transcription factors leading to their transcriptional inactivation. During the middle of G₁ phase CDK4 or CDK6, depending on the cell type, associate with D-type cyclins (cyclinsD1-D3) and phosphorylate pRb. Hyper-phosphorylation of pRb causes the release of E2F, which in turn stimulates its own transcription as well as transcription of cyclin E. In late G₁ phase cyclin E complexes with CDK2 causing further phosphorylation of pRb and complete disruption of the pRb/E2F interaction. At this point, the G₁-to-S phase transition occurs and the synthesis of cyclin A begins. Interaction of cyclin A with CDK2 triggers DNA synthesis. During S phase cyclin B is expressed and its concentration increases as cells proceed through G₂ phase. Here, cells increase their size and prepare themselves for cell division. Formation of cyclinB-CDK1 complexes induces entry into mitosis. During mitosis the cell divides into two daughter cells. At the end of mitosis cyclin B levels drop and pRb becomes stepwise dephosphorylated by protein phosphatases. Hypo-phosphorylated pRb binds to E2F and inhibits its activity during early G₁ phase of the next cell cycle. Intriguingly, post mitotic cells can exit the cell cycle in G₁ phase and enter a quiescent state, called G₀ phase, in which cells can remain for days, weeks or in some cases their whole lifetime without proliferating further (Figure 4) [reviewed in 93,94,95].

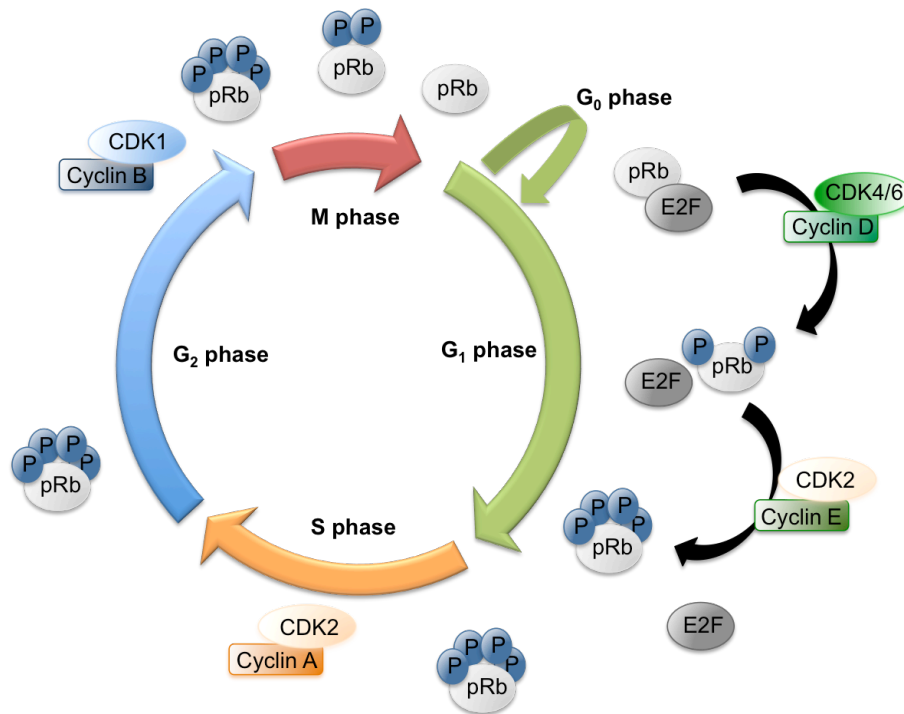


Figure 4: Regulation of cell cycle progression

Hypo-phosphorylated Retinoblastoma protein (pRb) blocks the G₁-to-S phase transition by binding E2F transcription factors. To enter S phase, pRb has to become hyper-phosphorylated through the action of several cyclins and cyclin-dependent kinases (CDKs) complexes. During G₁ phase cyclinD-CDK4/6 and cyclinE-CDK2 complexes phosphorylate (P) pRb. Hyper-phosphorylation of pRb causes fully release from E2F and cells progress through G₁ phase. Interaction of cyclin A with CDK2 causes DNA synthesis during S phase. During G₂ phase cyclin B concentrations increase. The formation of cyclinB-CDK1 complexes induces entry into mitosis (M phase), in which pRb becomes stepwise hypo-phosphorylated. After cell division, cells can enter a quiescent state called G₀ phase or enter a new cell cycle (Adapted from [93]).

Apart from its role in regulating cell cycle progression, pRb is recognised as a crucial tumour suppressor since it mediates cell cycle arrest and growth suppression through transcriptional repression of genes required for DNA replication. As mentioned before, direct interaction of pRb with E2F transcription factors represses their transcriptional activity. As a consequence the expression of genes implicated in cell proliferation and cell cycle progression are not induced [96]. Additionally, when complexed with E2F, pRb binds to E2F-regulated promoters causing thereby their transcriptional inhibition [97,98], as pRb functions as molecular adapter allowing histone deacetylases to be recruited to these promoters [99].

1.3.3.2 Disruption of the pRb network in cancer

Despite of its potent tumour suppressive function, loss or mutation of the *RB1* gene in sporadic cancers is a rare event. Instead defects in the enzymes and pathways regulating pRb phosphorylation are more frequent. Thus in most tumours pRb function is impaired by deregulated CDK activity. For example in non-small-cell lung cancers the expression of D-type cyclins is frequently increased through translocations or amplifications [100] and cyclin E was reported to be overexpressed in several cancer entities [reviewed in 101]. In addition,

overexpression of CDK4 and CDK6 has also been documented [102]. However, the most frequently mutated genetic locus that affects pRb regulation in human cancers is *CDKN2A*.

1.3.4 The *CDKN2A* gene locus

The *CDKN2A* locus is located on chromosome 9p21 in humans, on chromosome 4 in mice and on chromosome 1 in pigs, respectively. This locus is inactivated in approximately one third of all human cancers and it is recognised as the most frequently mutated gene, only secondary to p53 [103]. This observation reflects its potent tumour suppressive function. Genetic inactivation of the *CDKN2A* locus is most often a consequence of deletions, promoter methylations or point mutations [104,105].

As shown in Figure 5 this locus has a complex genomic organisation, as it encodes two physically linked but distinct tumour suppressor proteins, INK4A (also known as p16 or p16INK4 α) and ARF (also known as p14 or p14ARF in humans and pigs and 19 or p19ARF in mice, respectively). P16INK4 α and p14ARF have different and unique first exons (1 β and 1 α) but share second and third exons. Both p16INK4 α and p14ARF are transcribed from their own promoters and the proteins are encoded in alternative reading frames [106,107].

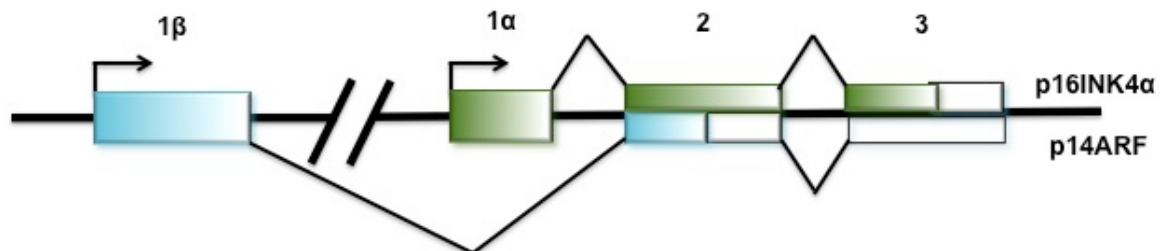


Figure 5: Genomic structure of the *CDKN2A* gene locus

The genomic locus is depicted as a bold line, with exons indicated by coloured boxes. The coding regions of p16INK4 α are shown in green, those of p14ARF in blue and untranslated regions in white (Adapted from [108]).

Both proteins show no structural homology and exhibit distinct biological functions. P16INK4 α acts as an inhibitor of cyclin- dependent kinases by binding to CDK4 and CDK6, respectively (Figure 6). This interaction induces an allosteric change of CDK4 and CDK6 conformations that abrogates the binding of these kinases to D-type cyclins. As a consequence the assembly of catalytically active cyclinD-CDK complexes is blocked [109,110]. This in turn leads to a decreased CDK4/6 kinase activity ensuring that hypophosphorylated pRb remains in complex with the transcription factor E2F, blocking thereby G₁-to-S phase transition [111]. Collectively, p16INK4 α is a potent regulator of cell cycle progression that acts in concert with CDK4/CDK6 and pRb in coordinating cellular proliferation [112].

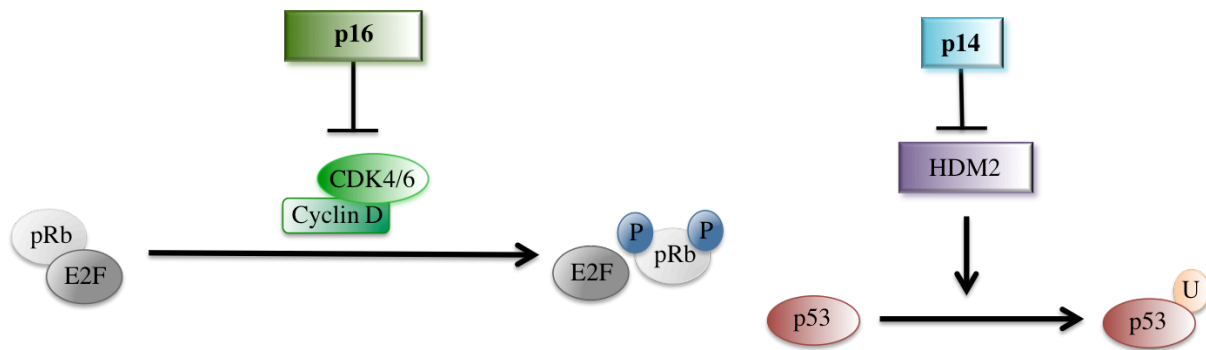


Figure 6: Regulation of the pRb and p53 pathways by p16INK4 α and p14ARF

Left: p16 (p16INK4 α) inhibits the interaction of the cyclinD-CDK4/6 complex. As a consequence pRb remains in its hypo-phosphorylated conformation bound to E2F. Complexed with E2F, pRb blocks G₁-to-S phase progression. **Right:** p14 (p14ARF) binds to human double minute 2 homolog (HDM2) and inhibits its ubiquitin ligase activity. As a consequence p53 is stabilised and activates the transcription of its target genes. Abbreviation: P: Phosphorylation, U: Ubiquitylation (Adapted from [108]).

In contrast, p14ARF binds to HDM2 and inhibits its ubiquitin ligase activity (Figure 6). This in turn leads to the stabilisation of p53 permitting p53-induced growth arrest or apoptosis [113].

1.3.4.1 The *CDKN2A* locus and its role in mediating cellular senescence

One prominent function of the *CDKN2A* locus is triggering cellular senescence, which is often elicited by oncogenic signalling. In proliferating normal cells, the expression of p16INK4 α as well as p14ARF are kept at low levels, whereas distinct cellular stresses invoke their expression leading to stable cell cycle arrest [114]. Intriguingly, the relative contribution of p16INK4 α and p14ARF to oncogene-induced senescence varies between different species and cell types [reviewed in 115]. *In vitro* data revealed that p16INK4 α plays a major role in mediating cellular senescence and tumour suppression in human cells [116], whereas p19ARF exerts a predominant role in the senescence program in mouse cells [112]. In addition, murine cells can escape from culture-induced growth arrest by shutting down the p19ARF-p53 axis [117]. Consistent with these findings, *p19Arf*-null mouse embryonic fibroblasts (MEFs) are immortal, whereas *p16Ink4 α* -null MEFs are not [118]. It is generally agreed that cellular senescence plays a pivotal role in tumour suppression by acting as a barrier to cancer [reviewed in 119]. Thus evasion from replicative senescence combined with an extended lifespan seems to be a prerequisite for malignant cell transformation, as it greatly increases the susceptibility to acquire successive mutations.

1.3.4.2 The *CDKN2A* locus and its contribution to neoplastic transformation

As the *CDKN2A* locus exerts a crucial role in mediating cellular senescence, a barrier to malignant transformation, it is not surprisingly, that this gene locus is frequently homozygously deleted in a variety of human cancers [120,121]. In agreement with these

observations, the *CDKN2A* locus is designated as the familial-melanoma locus, because inherited germline mutations are associated with a high incidence of familial melanoma [121,122]. However, the loss of *CDKN2A* gene function does not only predispose to the development of melanoma, it is also fundamental in the development of pancreatic ductal adenocarcinoma (PDAC) [123,124] and non-small-cell lung carcinoma (NSCLC) [125]. Apart from homozygous deletions of the gene locus other molecular alterations, which target the expression of either p16INK4 α or p14ARF, are also common in human cancers. In this respect, methylation of the *P16/INK4A* gene promoter is most frequently observed in primary gastric carcinoma, esophageal adenocarcinoma and hepatocellular carcinoma [126-128]. In contrast, *P14ARF* gene promoter methylation is preferentially detected in colorectal cancer [129-131].

1.3.5 Oncogenic Myc

The discovery of the Myc proto-oncogene can be traced back to studies in the early 1960s, when Ivanov and co-worker reported, that the avian myelocytomatosis retrovirus (MC29) was able to induce leukaemogenesis in chickens [132]. Molecular cloning and DNA sequence analysis revealed, that MC29 was an acute transforming, replication defective virus, in which most of the proviral sequences were replaced by the chicken-derived *myc* sequence coding for a Gag-Myc fusion protein [133]. Genomic mapping proved, that the sustained Myc expression was a consequence of retroviral promoter insertion adjacent to the chicken *cMYC* gene [134-136]. Soon after this, molecular analysis of human Burkitt's lymphoma specimen revealed, that in this human malignancy the *cMYC* gene is often placed under the control of the immunoglobulin heavy chain enhancer through chromosomal translocation [137,138]. Besides in lymphoid tumours [139], the *cMYC* gene contributes to the genesis of many human malignancies, predominantly through gene amplification [140].

The *cMYC* gene consists of three exons, an untranslated first exon and two translated ones. The translated protein product functions as a DNA-binding transcription factor that regulates cell growth and proliferation [141]. In normal cells, the expression of cMyc is under tight control and its expression levels are virtually undetectable. Several reports have shown, that the short-lived cMyc mRNA transcript is posttranscriptionally regulated by several microRNAs [142-144] and the cMyc protein is usually degraded very rapidly with a half-life in the order of 15-20 minutes [145]. However, upon mitogenic stimulation, expression levels of cMyc increase and induce the expression of target genes required for protein biosynthesis, DNA replication, cell growth and metabolism [reviewed in 146]. In contrast, cancer cells express high levels of cMyc and as a consequence cellular proliferation is no longer

dependent on growth factor stimulation [reviewed in 147]. This leads to uncontrolled cell growth and proliferation, a hallmark of cellular transformation [49].

1.3.5.1 Transcriptional functions of cMyc

Myc is a nuclear phosphoprotein that functions as a sequence-specific DNA-binding transcription factor. Genomic binding studies revealed that approximately 10-15% of all genomic loci are bound by cMyc, indicating that Myc is a global transcriptional regulator [148-151]. The cMyc oncoprotein belongs to the family of basic helix-loop-helix-leucine zippers (HLH-Zip) and contains a N-terminal transcriptional transactivation/repression domain followed by a nuclear localisation signal and a C-terminal HLH-Zip dimerisation domain [152-154]. These two regulatory regions facilitate that cMyc can both activate and repress the transcription of its target genes. By forming a heterodimer with its binding partner Max, c-Myc acts as a transcriptional activator *in vivo*. After heterodimerisation this complex locks onto 5'-CACA/GTG-3' DNA sequences termed E-boxes, which are located near core promoter elements [154]. The DNA-bound Myc-Max dimer recruits and interacts with the adapter protein transformation/transcription domain-associated protein (TRRAP), a core subunit of the histone acetyltransferase (HAT) complex [155]. The activity of recruited HATs induces the opening of chromatin and consequently transcription of Myc-bound target genes (Figure 7) [156-158].

Besides acting as a transcriptional activator, cMyc can also repress the transcription of its target genes by interacting with the Myc-interacting zinc finger protein 1 (Miz1). In the absence of Myc, Miz1 and its cofactors are attached to the transcriptional start site of several Myc repressed genes, thereby stimulating their transcription [159]. For example, when bound to the promoter of cell cycle inhibitors, such as CDKN1A (p21) and CDKN2B (p15IN4b), Miz1 drives the transcription of these negative cell cycle regulators. In contrast, binding of the Myc-Max heterodimer to Miz1 disrupts the interaction between Miz1 with its cofactors. As a consequence the transcription of these negative regulators of cell proliferation is repressed [160,161]. The interaction of Myc-Max heterodimers with Miz1 recruits histone deacetylase 3 (HDAC3) as well as DNA methyltransferase 3a (DNmt3a) that permit strict transcriptional silencing of the bound gene promoters (Figure 7) [162,163].

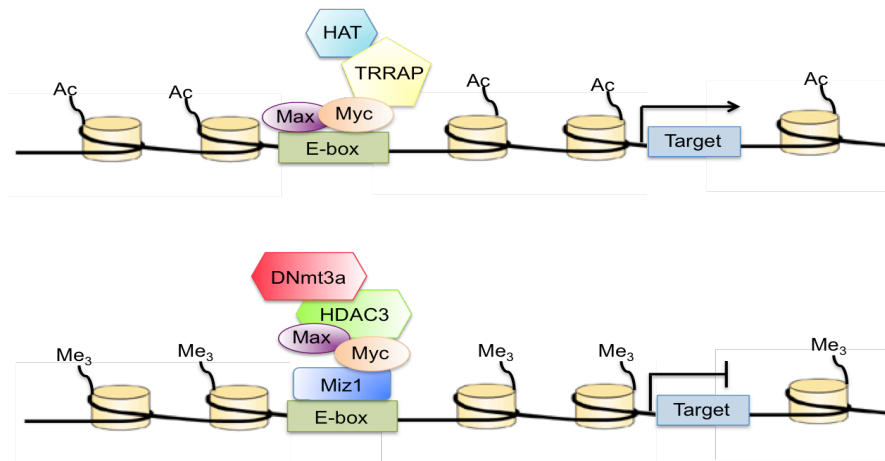


Figure 7: Transcriptional properties of Myc

Top: Transcriptional activation mediated by Myc; Myc attaches with its binding partner Max to E-box elements. Binding of transformation/transcription domain-associated protein (TRRAP) and histone acetyltransferases (HATs) to the Myc-Max heterodimer results in open chromatin and subsequently in gene transcription. **Bottom:** Transcriptional repression mediated by Myc; Myc represses Myc-interacting zinc finger protein 1 (Miz1)-dependent transcriptional activation of its target genes. Interaction of the Myc-Max heterodimere with Miz1 leads to the recruitment of histone deacetylase 3 (HDAC3) and DNA methyltransferase 3a (DNmt3a). These histone and DNA remodelling enzymes cause the transcriptional repression of bound gene promoters. Abbreviations: Ac: acetylation, Me₃: methylation (Adapted from [164,165]).

1.3.5.2 Deregulated expression of oncogenic Myc and its contribution to cellular transformation

Although chromosomal translocations of the *MYC* locus are found in almost all Burkitt's lymphoma patients [166], such rearrangements are not common in other human cancer types, where rather genomic amplifications of the *MYC* locus are prevalent [146]. Consistent with these observations, analysis of more than 3000 cancer specimens revealed that the *MYC* gene is one of the most frequently amplified oncogene among different human cancer types [140] and genetic amplification of *MYC* results in constitutive and elevated expression levels of this oncoprotein [49,147]. Due to its potent growth promoting properties, it is not surprisingly, that cMyc plays a pivotal role in tumour initiation and maintenance [164]. However, deregulated expression of Myc alone fails to transform either rodent or human cells. In fact, Myc requires the cooperation with another oncogene such as oncogenic Ras to convert primary rat cells to a neoplastic phenotype [9]. Worth mentioning, Myc transgenic mice develop tumours with relatively long latencies and most often, these established tumours harbour additional genetic alterations [167,168]. Although transgenic mice with inducible Myc expression developed tumours, these established tumours regressed after MYC withdrawal [169,170]. Overall, these findings indicate that oncogenic Myc requires additional mutagenic events to initiate tumour formation *in vivo* and moreover that established tumours are addicted to deregulated Myc expression.

1.3.6 The *RAS* gene family members

In 1983, the oncogenic potential of the three members of the *RAS* gene family (*HRAS*, *KRAS* and *NRAS*) was reported, as mutated versions of these proto-oncogenes, isolated from different human cancer specimen, caused the transformation of NIH3T3 cells in culture [171-173]. These genes were shown to be homologs of the former described Harvey and Kirsten murine sarcoma viruses [174,175]. Based on these findings the human *RAS* genes were identified as the first isolated human oncogenes. Although oncogenic *HRAS*, *KRAS* and *NRAS* mutations are found in a wide variety of human cancers, their incidence varies considerably with particular tumour types. Quantitative analysis of human tumour specimen revealed that each member of the *RAS* gene family, in its oncogenic version, preferentially contributes to the tumorigenesis of particular human tumour types. For example, activating *KRAS* mutations are frequently detected in three of the four most deadliest cancers, namely NSCLC (15-20%) [176], colon cancer (40%) [177] and pancreatic cancer (95%) [178]. Whereas *HRAS* mutations contribute to the tumorigenesis of bladder cancer [179] and *NRAS* mutations are frequently found in haematological malignancies [180]. According to the COSMIC database (www.sanger.ac.uk/genetics/CGP/cosmic/) *KRAS* is the most frequently mutated proto-oncogene in human neoplasms (25-30%) followed by *NRAS* (8%) and *HRAS*, which is the least frequently mutated *RAS* gene in human cancers (3%). The high frequency of activating *KRAS* mutations and the observation that they preferentially occur at early stages of tumour progression, points to a causative role of mutant *KRAS* as a driver in human tumorigenesis [181].

1.3.6.1 Gene structure and function of *KRAS*

The human *KRAS* gene is located on chromosome 12 and is composed of a 5' noncoding exon and four coding exons, which are translated into two highly related 21 kDa GTPase protein isoforms of 189 amino acids (*KRAS4A*) and 188 amino acids (*KRAS4B*), respectively [182]. These two isoforms, A and B, are products of the alternative splicing of exon 4 [183], whereby transcript variant 4B is more abundantly expressed than variant 4A [172,184]. The protein product encompasses of three domains. The N-terminal domain (85 amino acids) is identical among all *RAS* gene family members and the second protein domain, consisting of 80 amino acids, covers 80% of sequence homology among the three *RAS* genes. These two regions jointly form the effector domain (also known as G domain) including the GTP-binding pocket that is important for the interaction with all downstream target molecules. In contrast, the C-terminal domain (amino acids 165-188/189) comprises a hypervariable region, which shows no sequence similarity among the ras proteins, except for the conserved CAXX motif (C: cysteine, A: aliphatic amino acid, X: any amino acid) [185,186]. This C-terminal end

directs posttranslational modifications and trafficking of the protein product to subcellular membrane compartments [187]. The membrane-anchored Kras protein can cycle between an active guanosine triphosphate (GTP)-bound and an inactive guanosine diphosphate (GDP)-bound conformation [188]. The biological function of this low molecular GTPase is to transmit extracellular mitogenic stimuli from membrane-associated receptor tyrosine kinases to cytoplasmic kinases. Binding of extracellular mitogens, like the epidermal growth factor [189] or the platelet-derived growth factor [190], or the binding of cytokines such as Interleukin-2 [191] to their respective receptors activates guanine nucleotide exchange factors (GEFs). These GEFs cause the release of GDP from inactive Kras and permit the binding of GTP [192].

In its active conformation, Ras stimulates a multitude of signalling pathways and cascades, including the intracellular mitogen-activated protein kinase (MAPK) pathway, the phosphoinositide 3-kinase (PI3K) cascade and other small GTPases such as RAL that trigger proliferation, differentiation, cell survival and cytoskeletal dynamics [reviewed in 193]. The first identified interaction partner of Ras was the RAF serine/threonine kinase [194,195], a member of the MAPK cascade. RAF mediates the activation of the MAP kinase kinase (MEK) and the downstream extracellular signal-regulated kinase (ERK) [196,197], which triggers cell proliferation. In addition, GTP-bound Ras interacts with PI3K, which phosphorylates and activates the serine/threonine kinase AKT. Activation of the Ras-PI3K-AKT pathway mediates anti-apoptotic signals, conferring cell survival [198]. As a third effector of activated Ras the family of Ral proteins was identified, including the Ral guanine nucleotide dissociation stimulator (RALGDS) [199]. Activation of the Ras-RALGDS pathway is implicated in vesicle sorting, organisation of the actin cytoskeleton and the regulation of gene expression [200]. After completed signal transduction, active, GTP-bound Ras proteins become rapidly inactivated by GTPase-activating proteins (GAPs). These GAPs elicit an increase of the intrinsic GTPase activity of Ras causing thereby the recurrence to its inactive, GDP-bound conformation [201]. Figure 8 depicts the Ras signalling cascade.

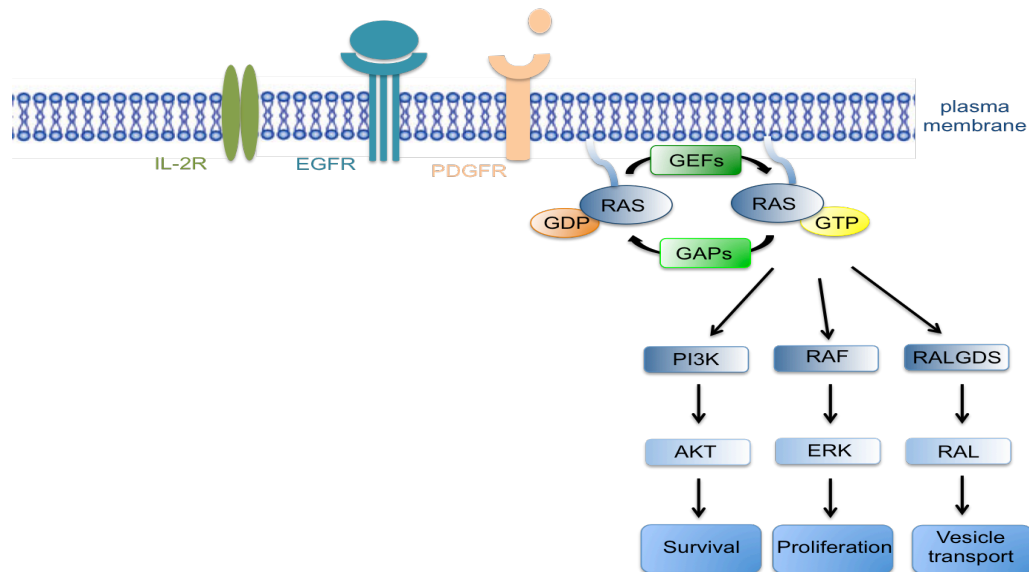


Figure 8: Ras signalling cascade

Binding of extracellular mitogens to their relative receptors activates guanine nucleotide exchange factors (GEFs). These GEFs catalyse the replacement of bound guanosine diphosphate (GDP) with guanosine triphosphate (GTP) resulting in active, GTP-bound Ras. In its active, GTP-bound state, Ras interacts and stimulates the activity of several downstream effector proteins. Activation of the Phosphoinositide 3- kinase (PI3K)-AKT pathway mediates cell survival. Activation of the RAF-ERK signalling cascade regulates cell cycle progression and stimulation of the RALGDS pathway induces vesicle transport and cytoskeleton organisation. Active, GTP-bound Ras is converted to its inactive, GDP-bound state by GTPase-activating proteins (GAPs). Abbreviation: IL-2R: Interleukin-2 receptor, EGFR: epidermal growth factor receptor, PDGFR: platelet-derived growth factor receptor, ERK: extracellular signal-regulated kinase. (Adapted from [193]).

1.3.6.2 Oncogenic *KRAS* and its contribution to tumorigenesis

Numerous publications show that oncogenic *KRAS* contributes to the initiation and progression of several human cancers including PDAC, colorectal cancer and NSCLC. The oncogenic potential of mutant Kras proteins is most often a consequence of missense mutations at one of the three hot spot codons 12, 13 or 61, which account for 97-99% of all *KRAS* mutations in human malignancies. With G12 being the most frequently mutated residue (www.sanger.ac.uk/genetics/CGP/cosmic/). This hot spot codon is located near the GTP-binding site, which leads to a 10-fold impaired, intrinsic GTPase activity of the mutant protein [202,203] and a diminished GAP-stimulated GTP hydrolysis [204]. Mutations at this codon lead to the accumulation of constitutively active, GTP-bound Kras [205]. Constitutively active Kras results in sustained proliferative signalling, independent of any growth factor signals, a hallmark of cancer [206]. Although Der *et al.* (1982) showed, that mutant Ras alone was sufficient to convert immortalised NIH3T3 cells to a tumorigenic state [207], various experimental approaches, trying to transform primary rodent cells by mutant Ras alone, failed. Instead, Land *et al.* (1983) and Ruley *et al.* (1983) evidenced, that mutant Ras requires a collaborating oncogene, like Myc, or the concomitant inactivation of a tumour

suppressor gene to impart cellular transformation of primary rodent cells [9,10]. In agreement with these *in vitro* findings, the requirement for a cooperating genetic event in the process of Ras-mediated tumorigenesis was proven in genetically engineered mouse models (GEMM) of pancreatic cancer. While the majority of transgenic mice, expressing merely mutant *Kras*^{G12D} in the pancreatic epithelium developed only premalignant pancreatic intraepithelial neoplasia (PanINs) [208], mice with the concomitant expression of mutant *Trp53*^{R172H} or the loss of either Ink4a/Arf or SMAD4, progressed to PDAC [209-211]. Consistent with these observations in animal models, the initiation of human pancreatic cancer relies on the expression of oncogenic KRAS, however additional genetic events have to occur to progress to PDAC [212]. A similar picture is seen in the development of colorectal cancer (CRC), where the expression of mutant KRAS is detected at an early stage of this disease, but progression to malignant CRC requires further genetic alterations [213]. These data indicate that oncogenic KRAS is a potent driver of various human malignancies, however additional genetic events must occur to advance to full transformation.

1.4 Genetically engineered mouse models in cancer research

Overall, the design and validation of experimental human cancer models provided considerable insights into the action and cooperation of individual oncogenes and tumour suppressor genes on the initiation and progression of cellular transformation *in vitro*. However these models completely disregard, that cancer is a complex disease with extensive cell-cell interactions between cancerous cells and the surrounding tissue. In particular, many facets of tumorigenesis, including angiogenesis, tissue invasion and metastasis cannot be assessed in these models [reviewed in 214].

For this reason a new research area emerged, dedicated to generate and use genetically engineered rodent models of human cancers. Until now, the laboratory mouse is the best-studied model system for cancer biology mainly due to its small size, short gestation and lifespan and its entirely sequenced genome [215]. In addition, the derivation of mouse pluripotent embryonic stem (ES) cells [216] and the ease with which they can be genetically modified through homologous recombination entailed the establishment of GEMMs [217]. Consequently, multiple germline mutant mice have been generated, in which the expression of mutant oncogenes and tumour suppressor genes is driven from their native promoters. This allowed studying the pathophysiological and molecular features of human hereditary cancer syndromes [reviewed in 218,219]. However, as most cancers arise by somatic mutations in proto-oncogenes and tumour suppressor genes in specific cells of a given organ, more sophisticated endogenous GEMMs had to be established, that allowed the modelling of sporadic cancers in mice. For this purpose, conditional activatable cancer-prone GEMMs have been generated, in which the expression of mutant oncogenes and tumour

suppressor genes can be controlled in a temporal- and tissue-specific manner [reviewed in 214]. In this context, the Cre-lox site-specific recombination system of the bacteriophage P1 is the most often applied site-specific recombination system in conditional GEMMs. Here, the 38 kDa site-specific Cre recombinase recognises 34 bp sites, called loxP sites, that consist of an 8 bp nonpalindromic region flanked by two 13 bp inverted repeats [220]. Cre mediated recombination between two directly repeated loxP sites catalyses the excision of the flanked, intervening DNA sequence within the two loxP sites [221]. This Cre-loxP site-specific recombination system has allowed the creation of several conditional activatable cancer-prone GEMMs, as the targeted insertion of a floxed transcriptional and translational termination (loxP-STOP-loxP, also called LSL) cassette between the promoter and the coding sequence of the oncogenic allele blocks its expression [222]. In the presence of Cre recombinase this LSL cassette is excised allowing expression of the mutant allele. To date, numerous GEMMs carrying conditional mutant oncogenes and tumour suppressor genes have been created (eg. LSL-KrasG12D, LSL-Trp53R172H, LSL-BrafV600E) [80,223,224]. In these mice the expression of the floxed mutant alleles can be activated in any given tissue by crossing them with mice, in which the expression of the Cre recombinase is under the control of a tissue-specific promoter. Overall, these spatial inducible mutant mice provided invaluable tools for recapitulating several human cancer entities [209,223,225-228].

1.5 Limitations of mouse cancer models

Although mouse models are the most extensively used animal models for biomedical cancer research and preclinical studies, their relative small size hampers their use for imaging and radiation therapy studies. In addition, the high heartbeat rate of mice with about 600 beats per minute leads to a faster clearance of most chemicals from their body compared to humans. Thus this pharmacokinetic difference makes it difficult to translate the drug dosage from mice to humans [reviewed in 229]. Moreover, discrepancies were reported between mice and humans regarding drug metabolism [230] and immunology [231,232]. Apart from these anatomical and physiological differences, there are also clear discrepancies regarding tumour biology of these two species. For example, primary mouse cells are more easily transformed than primary human cells. The perturbation of the p53 and Kras signalling pathways alone are sufficient to induce cellular transformation of murine cells *in vitro*, while human cells need the disruption of at least five pathways [233]. Although mice and humans are pretty similar at the genomic level, subtle variations have to exist with respect to physiological and biological properties, as similar germline mutations of known human cancer-associated genes yield different tumour phenotypes in these two species [reviewed in 115]. For example, humans with germline or somatic *RB1* gene loss develop retinoblastomas and sarcomas [reviewed in 234]. In contrast, engineered mice with *RB1* gene deletions fail to

develop these tumours [235]. In addition, germline mutations of the tumour suppressor gene adenomatous polyposis coli (APC) predispose patients to familial adenomatous polyposis (FAP). Human FAP is characterized by dysplasia in the colon and rectum that develop to adenomatous polyps and adenocarcinoma, whereas *Apc*-heterozygous mice develop polyposis of the small intestine [236,237]. These examples indicate, that albeit similar genetic lesions murine cancer models do not always accurately recapitulate the human cancer phenotype. However, these differences do not diminish the importance and usefulness of GEMMs as cancer models. Rather, they indicate that more reliable animal models are needed that more closely resemble humans in body size, anatomy and physiology and most importantly phenocopy human cancer pathophysiology [reviewed in 6,214].

1.6 Genetically modified pigs in biomedical and cancer research

Due to the limitations of rodent models, there is a significant need for relevant animal models that more closely resemble humans. As such, pigs are increasingly recognised as favourable animal models due to their shared anatomical and physiological characteristics with humans. Pigs have been already widely used as biomedical models for studying cardiovascular diseases, organ transplantation, developing medical devices and training surgical procedures [reviewed in 238]. Given, the similarity of several porcine cytochrome P450 isoforms with their human orthologous and their comparability in drug metabolism [239,240], minipigs are widely recognised as experimental models for toxicity testing of pharmaceuticals [241,242]. The recently published high-quality draft pig genome sequence [243] and the high sequence homology between pigs and humans [244] lending further support to the use of pigs as relevant large animal models for human diseases. In addition, the development and improvement of transgenesis techniques, such as gene targeting and synthetic endonucleases (e.g. ZFN, TALENs and CRISPR/Cas9) [245-249] allow the introduction of precise genetic modifications into the porcine genome. These techniques in combination with the ability to clone pigs through somatic cell nuclear transfer (SCNT) [250] provide the opportunity to generate tailored-made large animal models. Due to these technical achievements, genetically modified pigs were created as biomedical models for diabetes [251], cystic fibrosis [252] and muscular dystrophy [253]. Given, that these genetically modified pigs closely resemble the human disease phenotype it was just a logical consequence to derive porcine cancer models. In this regard, the first gene targeted porcine cancer model was attempted by recombinant adeno-associated virus mediated breast cancer associated gene 1 (BRCA1) knockout in Yucatan minipig fibroblasts. Unfortunately, all piglets died within 18 days after birth [254]. In 2012, our group reported the first viable gene-targeted porcine APC¹³¹¹ animal model (equivalent to human severe FAP mutation APC¹³⁰⁹). Examination of a one year old founder animal carrying the APC¹³¹¹ mutation revealed more

than 60 polyps in the colon and rectum [255]. These findings indicate that pigs predisposed to colorectal cancer reflect more closely the location and onset of human FAP than genetically engineered mice do [236]. Moreover, in the same year we have reported the generation of gene-targeted pigs carrying conditional Cre activatable oncogenic $TP53^{R167H}$ alleles (orthologous to human $TP53^{R175H}$ and mouse $Trp53^{R172H}$) [256]. Since genetic alterations in a relative small set of genes such as APC, KRAS, TP53 are implicated in a variety of human cancers [257], we also wish to derive pigs carrying latent oncogenic $KRAS^{G12D}$ alleles. Derivation of pigs carrying any combination of these aforementioned mutant alleles and the possibility to induce their expression by Cre recombinase in any chosen tissue will thus allow to replicate different cancer types.

However, to date little is known about the multi-step process of tumorigenesis in pigs and there is only one report, which shows that primary porcine cells can be converted to a fully transformed phenotype by the enforced expression of cyclin D1, CDK4^{R24C}, p53^{DD}, HRAS^{G12V}, cMyc^{T58A} and hTERT [258]. It is worth to mention that this set of genetic modifications is in full accordance with those necessary to transform human cells *in vitro* [25]. Although this experimental porcine transformation model provided useful insights into porcine tumorigenesis, it falls short as a representative cancer model, as it relies on the ectopic expression of oncogenes and dominant-negative tumour suppressors, which are driven by viral promoters. For this reason, we aimed to model the process of neoplastic porcine cell transformation by the expression of endogenous oncogenic TP53^{R167H} (orthologous to human R175H and mouse R172H) and KRAS^{G12D}, respectively.

1.7 Objective

The objective of this work was to provide *in vitro* proof that oncogenic mutant porcine $TP53^{R167H}$ (orthologous to human $TP53^{R175H}$ and mouse $Trp53^{R172H}$) and $KRAS^{G12D}$ (homologous to human $KRAS^{G12D}$ and mouse $Kras^{G12D}$) alleles are functionally equivalent to their human and murine orthologous. In addition, it should be investigated if the expression of mutant $TP53^{R167H}$ and $KRAS^{G12D}$ alleles is sufficient to convert primary porcine cells to a transformed phenotype. For this purpose, a Cre recombinase activatable mutant $KRAS^{G12D}$ allele had to be introduced by gene targeting into genetically modified pMSCs that carried already a Cre inducible mutant $TP53^{R167H}$ allele. Double gene-targeted pMSCs, expressing mutant $TP53^{R167H}$ and $KRAS^{G12D}$ from their endogenous gene loci, had to be characterised and their tumorigenic potential assessed by several *in vitro* and *in vivo* assays.

Furthermore, $TP53^{LSL-R167H}$ and $KRAS^{LSL-G12D}$ double gene-targeted porcine mesenchymal stem cells (pMSCs) had to be established that could be used as nuclear donors for SCNT.

2 Material and Methods

2.1 Materials

2.1.1 Equipment

+4°C fridge	Beko Technologies, Dresden, GER
-20°C freezer	Siemens, Munich, GER
-80°C ultra low temperature freezer	Thermo Electron GmbH, Dreieich, GER
7500 Fast Real-Time PCR System	Applied Biosystems, <i>Warrington, UK</i>
Analytic balance	Denver Instrument GmbH, Göttingen, GER
AxioCAM MRc camera	Carl Zeiss Vision GmbH, Munich, GER
Axiovert 40 CFL microscope	Carl Zeiss Vision GmbH, Munich, GER
Bio Imaging System Gene Genius	Syngene, Cambridge, UK
Biophotometer	Eppendorf, Hamburg, GER
Centrifuge 1-15	Sigma, Osterode, GER
Centrifuge 3-15	Sigma, Osterode, GER
Centrifuge 4K15C	Sigma, Osterode, GER
Centrifuge 5810	Eppendorf, Hamburg, GER
Centrifuge Minispin	Eppendorf, Hamburg, GER
Countess™ automated cell counter	Invitrogen, Karlsruhe, GER
Countess™ cell counting chamber slides	Invitrogen, Karlsruhe, GER
Digital graphic printer UP-D895MD	Syngene, Cambridge, UK
Electrophoresis horizontal gel system	PeqLab, Erlangen GER
Electrophoresis Power Supply E-105	Thermo Electron GmbH, Dreieich, GER
Electroporator Multiporator	Eppendorf, Hamburg, GER
Hybaid Shake 'n' Stack	Thermo Electron GmbH, Dreieich, GER
Ice maker	Manitowoc Company Inc., Manitowoc, USA
Ika-Combimag	IKA-Werke GmbH & Co. KG, Staufen, GER
Improved Neubauer chamber	Brand, Wertheim, GER
Incubator	Binder GmbH, Tuttlingen, GER
Laminar Flow Hood HERAsafe Type HSP	Heraeus Instrumente, München, GER
Microwave N-E202 W	Panasonic, Hamburg, GER
Mini-PROTEAN 3 Cell	BioRad, Munich, GER
Mini-PROTEAN 3 System	BioRad, Munich, GER

Mr.Frosty freezing device	Nalgene, Rochester, USA
Multiscan Spectrum	Thermo LabSystem, Dreieich, GER
Orbitakl shaker	Thermo Electron GmbH, Dreieich, GER
PCR-Cycler DYAD DNA Engine	MJ Resaerch, Watertown, USA
pH meter Cyberscan 510	Thermo Scientific, Waltham, USA
Pipette controller accu-jet® pro	Brand, Wertheim, GER
Power Supply	Amersham Bioscience, Freiburg, GER
Pure water system, micro Pure	Thermo Scientific, Waltham, USA
RAININ Pipet-Lite (2,20,200,1000µl)	Mettler Toledo GmbH, Giessen, GER
Repetitive pipette HandyStep® S	Brand, Wertheim, GER
Rocker Shaker KH500	Noctua GmbH, Mössingen, GER
Scale 440-33N	Kern & Sohn GmbH, Balingen, GER
Scale APX-1502	Denver Instrument GmbH, Göttingen, GER
Steri-Cycle CO ₂ -Incubator	Thermo Electron GmbH, Dereich, GER
Trans-Blot SD Semi-dry Transfer Cell	BioRad, Munich,GER
Tube block heater	Gefran, Seligenstadt, GER
Vortex Mixer	VELP Scientifica, Usmate, ITA
Waterbath	Thermo Electron GmbH, Dereich, GER

2.1.2 Consumable

0.5, 1.5, 2.0ml reaction tubes	Brand GmbH & Co. KG, Wertheim, GER
1.0, 2.0, 5.0 , 10.0, 25.0ml disposable serological pipettes	Corning Inc., New York, USA
14ml round-bottom tubes	BD, Baltimore, USA
15ml and 50ml conical bottom centrifugation tubes	Greiner Bio-One GmbH, Frickenhausen, GER
Disposable pipet tips	Brand GmbH & Co. KG, Wertheim, GER
Cell culture dishes (10,15 cm)	Corning Inc., New York, USA
Cell culture flasks (25,75,150 cm ²)	Corning Inc., New York, USA
Cell culture plates (6-,12-,24-,48-, 96-well)	Corning Inc., New York, USA
Cell scraper	Faust Lab Science, Klettgau, GER
Cryo Tube TM vials 1.8ml	Nunc, Wiesbaden-Biebrich, GER
Econo-Pac® disposable chromatography columns	BioRad, Munich, GER
Electroporation cuvettes (2, 4mm)	Peqlab Biotechnologie GmbH, Erlangen, GER

Glassware	Paul Mirienfeld GmbH & Co KG, Lauda Königshofen, GER
HybondN+ positively charged nylon transfer membrane	Amersham Bioscience, Freiburg, GER
MicroAmp® fast optical 96-well reaction plate with barcode, 0.1ml	Applied Biosystems, <i>Warrington, UK</i>
MicroAmp® optical adhesive film	Applied Biosystems, <i>Warrington, UK</i>
Petri dish (10cm)	Brand GmGH & Co. KG, Wertheim, GER
RAININ pipette tips (2,20,200, 1000µl) normal and filter tips	Mettler Toledo GmbH, Giessen, GER
Roti® PVDF membrane, pore size 0.45µm	Carl Roth GmbH, Karlsruhe, GER
Sterile filter 0.22µm	Sartorius AG, Göttingen, GER
Syringes	BD, Baltimore, USA

2.1.3 Chemicals

Acetic acid	Sigma-Aldrich GmbH, Steinheim, GER
Ammonium persulfate (APS)	Carl Roth GmbH, Karlsruhe, GER
Ampicillin	Sigma-Aldrich GmbH, Steinheim, GER
Bromophenol blue	Sigma-Aldrich GmbH, Steinheim, GER
Boric acid	AppliCHEM GmbH, Darmstadt, GER
Bovine Serum Albumin Fraction V	PAA, Laboratories GmbH, Pasching AUT
Crystal violet	Sigma-Aldrich GmbH, Steinheim, GER
Dithiothreitol (DTT)	Omnilab, Bremen, GER
Ethanol absolute	Riedel-de-Haen, Seelze, GER
Ethidium bromide	Sigma-Aldrich GmbH, Steinheim, GER
Ethylenediaminetetraacetic acid	AppliCHEM GmbH, Darmstadt, GER
Formaldehyde	Sigma-Aldrich GmbH, Steinheim, GER
Glucose	Sigma-Aldrich GmbH, Steinheim, GER
Glycine	Carl Roth GmbH, Karlsruhe, GER
Glycerol	AppliCHEM GmbH, Darmstadt, GER
GenAgarose L.E.	Genaxxon Bioscience GmbH, Biberach, GER
HEPES	Invitrogen, Karlsruhe, GER
Hydrochloric acid	Sigma-Aldrich GmbH, Steinheim, GER
IGEPAL-630	Sigma-Aldrich GmbH, Steinheim, GER
Imidazole	Carl Roth GmbH, Karlsruhe, GER

Isopropanol	Carl Roth GmbH, Karlsruhe, GER
Isopropyl β -D-thiogalactopyranosid	Omnilab, Bremen, GER
L-tartaric acid disodium salt	Sigma-Aldrich GmbH, Steinheim, GER
Maleic acid	Sigma-Aldrich GmbH, Steinheim, GER
Magnesium chlorid	Sigma-Aldrich GmbH, Steinheim, GER
Methanol	Carl Roth GmbH, Karlsruhe, GER
Milk powder	Carl Roth GmbH, Karlsruhe, GER
N-acetylcystein	Sigma-Aldrich GmbH, Steinheim, GER
Ni-NTA Agarose	Life Technologies GmbH, Darmstadt, GER
Nonidet P-40	Sigma-Aldrich GmbH, Steinheim, GER
Phenol	Sigma-Aldrich GmbH, Steinheim, GER
Phenol:Chloroform:Isoamylalcohol (25:24:1)	Sigma-Aldrich GmbH, Steinheim, GER
Potassium phosphate dibasic	AppliChem GmbH, Darmstadt, GER
Potassium chlorid	Sigma-Aldrich GmbH, Steinheim, GER
Potassium phosphate monobasic	AppliChem GmbH, Darmstadt, GER
Rothiphorese Gel 40	Carl Roth GmbH, Karlsruhe, GER
Sodium acetate	Carl Roth GmbH, Karlsruhe, GER
Sodium bicarbonate	Carl Roth GmbH, Karlsruhe, GER
Sodium chloride	Carl Roth GmbH, Karlsruhe, GER
Sodium citrate	Sigma-Aldrich GmbH, Steinheim, GER
Sodium dihydrogen phosphate	Merck, Darmstadt, GER
Sodium dodecyl sulfate	Omnilab, Bremen, GER
Sodium hydroxide pellets	Riedel-de Hen, Seelte, GER
Sodium phosphate	Sigma-Aldrich GmbH, Steinheim, GER
Sodium thiosulfat	Sigma-Aldrich GmbH, Steinheim, GER
Sucrose	Fluka, Seelze, GER
Tetramethylethylenediamine (TEMED)	Carl Roth GmbH, Karlsruhe, GER
Trizma Base	Sigma-Aldrich GmbH, Steinheim, GER
Trizma hydrochloride	Sigma-Aldrich GmbH, Steinheim, GER
TRizol®	Life Technologies GmbH, Darmstadt, GER
Tween 20	Sigma-Aldrich GmbH, Steinheim, GER

2.1.4 Miscellaneous

Advanced Protein Assay Reagent	Cytoskeleton Inc., Denver, USA
AGFA Cronex 5 X-Ray film	Röntgen Bender, Baden-Baden,GER
AGFA Developer G150 for X-Ray film	Röntgen Bender, Baden-Baden,GER
AGFA Fixier G 354 for X-Ray film	Röntgen Bender, Baden-Baden,GER
Anti-Digoxigenin-AP Fab fragment	Roche Diagnostic GmbH, Mannheim, GER
Blocking Reagent	Roche Diagnostic GmbH, Mannheim, GER
CDP-Star	Roche Diagnostic GmbH, Mannheim, GER
Complete mini protease inhibitor	Roche Diagnostic GmbH, Mannheim, GER
DIG Easy Hyb	Roche Diagnostic, Mannheim, GER
Digoxigenin-11-2'-deoxy-uridine-5'-triphosphate (dUTP)	Roche Diagnostic, Mannheim, GER
DNA marker (100 bp, 1kb)	New England Biolabs GmbH, Frankfurt,GER
DNA marker VII, digoxigenin-labeled	Roche Diagnostic GmbH, Mannheim, GER
dNTPs	Biomers.net GmbH, Ulm, GER
Matrigel™ Basement Membrane Matrix, high concentrated	BD, Baltimore, USA
Noble Agar	Sigma-Aldrich GmbH, Steinheim, GER
PageBlue™ protein staining solution	Fermentas GmbH, St. Leon-Rot, GER
Pierce™ ECL Western Blotting substrate	Thermo Scientific, Waltham, USA
Phosphatase inhibitor	Roche Diagnostic, Mannheim, GER
Spectra™ Broad Range Protein Ladder	Fermentas GmbH, St. Leon-Rot, GER

2.1.5 Bacterial media

Difco™ LB Agar, Miller	BD, Heidelberg, GER
Difco™ Luria Broth Base, Miller	BD, Heidelberg, GER
Tryptone	Fluka, Seelze, GER
Yeast extract	Fluka, Seelze, GER

2.1.6 Tissue culture media, buffers and supplements

Advanced Dulbecco's Modified	Gibco BRL, Paisley, UK
------------------------------	------------------------

Eagle's Medium (Advanced DMEM)	
Accutase	PAA Laboratories GmbH, Pasching, AUT
Amphotericin B solution	PAA Laboratories GmbH, Pasching, AUT
Basic fibroblast growth factor, (FGF-2)	PromoKine, Heidelberg, GER
Blasticidin S	InvivoGen, San Diego, USA
Cell culture water, EP-grade	PAA Laboratories GmbH, Pasching, AUT
DMEM powder	Gibco BRL, Paisley, UK
Dimethylsulfoxide	AppliChem GmbH, Darmstadt, GER
Dulbecco's PBS	PAA Laboratories GmbH, Pasching, AUT
Fetal Calf serum (FCS)	PAA Laboratories GmbH, Pasching, AUT
G418-Sulfate Solution	PAA Laboratories GmbH, Pasching, AUT
GlutaMAX	Gibco BRL, Paisley, UK
Hank's Balanced Salt Solution	Biochrom AG, Berlin, GER
Heparin	Sigma-Aldrich GmbH, Steinheim, GER
Hypoosmolar Buffer	Eppendorf AG, Hamburg, GER
LSM 1077 Lymphocyte Separation Medium	PAA Laboratories GmbH, Pasching, AUT
Non essential amino acids (NEAA)	PAA Laboratories GmbH, Pasching, AUT
Penicillin/Streptomycin	PAA Laboratories GmbH, Pasching, AUT
Trypan blue stain 0.4%	Invitrogen, Karlsruhe, GER

2.1.7 Kits

CloneJET PCR Cloning Kit	Fisher Scientific, Schwerte, GER
EpiTect Fast Bisulfite Conversion Kit	Qiagen, Hilden, GER
Fast SYBR® Green PCR Master Mix	Applied Biosystems, <i>Warrington, UK</i>
Plasmid DNA purification	Macherey-Nagel GmbH&Co.KG, Düren, GER
NucleoBond® Xtra	
Ras Activation Assay Kit	Merck Millipore, Darmstadt, GER
SuperScript® III First-Strand Synthesis System	Life Technologies GmbH, Darmstadt, GER
SurePrep™ RNA/DNA/Protein Purification Kit	Fisher Scientific, Schwerte, GER
TURBO DNA- <i>free</i> ™ Kit	Ambion Inc., Austin, USA
Wizard® SV Gel and PCR Clean-up	Promega, Mannheim, GER

System

2.1.8 Enzymes and Buffers

5x Green® GoTaq Reaction Buffer	Promega GmbH, Mannheim, GER
5x Phire Reaction Buffer	Fisher Scientific, Schwerte, GER
10x PCR Extender Buffer	5 PRIME GmbH, Hilden, GER
Benzonase	Novagen, Darmstadt, GER
Collagenase type I-A	Sigma-Aldrich GmbH, Steinheim, GER
Collagenase type IV	Worthington, New Jersey, USA
Exonuclease I	Fermentas GmbH, St. Leon-Rot, GER
GoTaq® Polymerase	Promega GmbH, Mannheim, GER
Lysozyme	Sigma-Aldrich GmbH, Steinheim, GER
NEBuffer 1-4 10x	New England Biolabs GmbH, Frankfurt, GER
PCR Extender Polymerase Mix	5 PRIME GmbH, Hilden, GER
Phire Hot Start II DNA polymerase	Fisher Scientific, Schwerte, GER
ProteinaseK	Sigma-Aldrich GmbH, Steinheim, GER
Purified BSA 100x	New England Biolabs GmbH, Frankfurt, GER
Restriction endonucleases	New England Biolabs GmbH, Frankfurt, GER
RNase A	Sigma-Aldrich GmbH, Steinheim, GER
Shrimp alkaline phosphatase	Fermentas GmbH, St. Leon-Rot, GER

2.1.9 Competent bacterial strains

Bacterial strain	Genotype	Supplier
<i>DH10B</i>	<i>F⁻ mcrA Δ(mrr-hsdRMS-mcrBC)</i> <i>Φ80dlacZΔM15 ΔlacX74 deoR recA1</i> <i>araD139 Δ(ara, leu)7697 galU galK rpsL</i> <i>endA1 nupG</i>	Invitrogen, Karlsruhe, GER
Tuner™(DE3) pLacI	<i>F⁻ ompT hsdS_B (r_B⁻m_B⁻) gal dcm</i> <i>lacY1(DE3) pLacI (Cam^R)</i>	Novagen, Darmstadt,GER

2.1.10 Mammalian cell lines

Bone-marrow derived porcine mesenchymal stem cells (090210)	Isolated by Marina Durkovic and Simon Leuchs, TU Munich, GER
neo14	Isolated by Simon Leuchs, TU Munich, GER

Bone-marrow derived porcine mesenchymal stem cells (080812) Isolated during this work

Adipose-tissue derived porcine mesenchymal stem cells (080812) Isolated during this work

2.1.11 Animals

Mouse strain	Genotype	Supplier
NOD <i>scid</i> gamma	NOD.Cg- <i>Prkdc</i> ^{<i>scid</i>} <i>Il2rg</i> ^{<i>tm1Wjl</i>} /SzJ	Jackson Laboratory, Bar Harbor, Maine, USA

2.1.12 Gene targeting constructs and plasmids

KRAS^{LSL-G12D} gene targeting vector constructs M.Sc. Alexander Tschukes, TU Munich, GER

pPGK-pocMyc-IRES-BS-pA M.Sc. Lena Glashauser, TU Munich, GER

pTriEX-HTNC Addgene Inc., Cambridge, USA

pJET1.2/blunt Fermentas GmbH, St. Leon Rot, GER

2.1.13 Oligonucleotides

Oligonucleotides were synthesized by Eurofins MWG GmbH, Ebersberg, Germany.

Name	Sequence (5'-3')	Anneal [C°]	Size
KRAS^{G12D} screenings			
KRAStarg_F	ACGCGGGGAATGAGGAAT	65	3.8 kb
KRAStarg_R	AGCCCTCCCACACATAACCA		
KRAStarg_F	ACGCGGGGAATGAGGAAT	58	3.4 kb
SA_R	GAAAGACCGCGAAGAGTTTG		
KRAStarg_F	ACGCGGGGAATGAGGAAT	58	3.3 kb
loxP Screen rev	TGAGGAAAAGAACAGTGCAAA		
KRAStargLA_F	CCAGCCATCTGTTGTTTGCC	64	10.8 kb
KRAStargLA_R	GAAGAAGGGACTGGGGTGTG		
Mut_F	GAGCAACGGCTACAATCA	61	2.8 kb
Mut_R	TGAAAAGGACTGCACAGGA		
KRASLoxP_F	AAAGCGGTACTTGCCTTTAAT	57	LSL: 1.5 kp loxP: 201 bp WT: 167 bp
KRASLoxP_R	TGAGGAAAAGAACAGTGCAAA		
KRASEx1_F	CATTTCCGACTGGGAGCTA	58	536 bp
bs_R	GGCAGCAATTCACGAATC		
KRASEx1_F	CATTTCCGACTGGGAGCTA	58	646 bp
neo_R	GCTCTTCGTCCAGATCATCC		
KRASEx1_F	CATTTCCGACTGGGAGCTA	58	145 bp

KRASEx2_R	TGTCAAGGCACTCTTGCCTAC		
KRASEx1_F	CATTTTCGGAAGTGGGAGCTA	65	492 bp
KRASEx4_R	TCCTGAGCCTGTTTTGTGTC		
KRASEx1_F	CATTTTCGGAAGTGGGAGCTA	65	522 bp
KRASEx5_R	GCTGATGTTTCAATAAAAGG		
bs-probe_F	ATGGCCAAGCCTTTGTCTC	58	402 bp
bs-probe_R	GATTTAGCCCTCCCACACAT		
neo probe_F	GCCACCATGATTGAACAAGA	58	784 bp
neo-probe_R	AAGGCGATAGAAGGCGATG		
TP53^{R167H} screenings			
TP53LoxP_F	TGAGGAATTTGTATGCCAAGG	57	LSL: 1.9 kb
TP53LoxP_R	TTCCACCAGTGAATCCACAA		loxP: 254 bp
			WT: 198 bp
TP53Ex1_F	GCAGGTAGCTGCTGGTCTC	58	630 bp
neo_R	GCTCTTCGTCCAGATCATCC		
TP53Ex1-F	GCAGGTAGCTGCTGGTCTC	58	1.3 kb
TP53Ex11-R	AGGGACTTCAAAGGGGATG		
RT-PCRs			
po_TERT_for	TGAACCTCCCTGTGGAGGAC	58	387 bp
po_TERT_rev	GGAGGAAAAATGAGGGGTTT		
p16_RT for	AACGCACCGAACCGTTAC	61	176 bp
p16_RT rev	AGGACCACCAAAGTGTCC		
p14_Ex1_1_forw	CGTGCTGTTGCTAGTGAGGA	61	361 bp
p16_Ex2_1 rev	GCGGGATCTTCTCCAGAGTT		
GAPDH_F	TTCCACGGCACAGTCAAGGC	57-61	576 bp
GAPDH_R	GCAGGTCAGATCCACAACC		
Quantitative real time RT-PCR			
cMyc exon2F	CCTCGGACTCTCTGCTCTCCT		369 bp
cMyc exon3R	ATTTTCGGTTGTTGCTGATCTGT		
p16_RT for	AACGCACCGAACCGTTAC		176 bp
p16_RT rev	AGGACCACCAAAGTGTCC		
p14_Ex1_1_forw	CGTGCTGTTGCTAGTGAGGA		234 bp
p16_Ex2_2_rev	AGGCGTCTCGCACGTCTA		
GAPDH_F	TTCCACGGCACAGTCAAGGC		576 bp
GAPDH_R	GCAGGTCAGATCCACAACC		
Analysis of bisulfite converted genomic DNA			
BSp16_F	GGGAGTAGTATGGAATTTT	51	266 bp
BSp16_R	CAAAAAAAAAAACTCCAACCTC		
pJet_forw	CGACTCACTATAGGGAGAGCGGC	51	387 bp
pJet_rev	AAGAACATCGATTTTCCATGGCAG		
Investigation of pPGK-pocMyc-IRES-BS-pA integration			
Kana_pUCori_for	TGCTCCTGCCGAGAAAGTAT	58	1.7 kp
Kana_pUCori_rev	CCTGACGAGCATCACAAAAA		
IRES-BS-forw	TGGCTCTCTCAAGCGTATT	58	1.6 kb
BS-SV40pro_rev	CGGGACTATGGTTGCTGACT		
Copy number alteration			
CNV_KRAS_forw	AGAGGGCTTGATAGCGTTTG	61	251 bp
CNV_KRAS_rev	GCCTGCACAAGTCAATATGC		
CNV_GAPDH_forw	TAGGTTTGGGTTGGAACAGC	58	223 bp
CNV_GAPDH_rev	AACCCAGTCTTGTCAGTGG		

2.1.14 Antibodies

Antibody	Catalogue number	Company
Primary antibodies		
DO-1 (Anti-p53)	P6874	Sigma- Aldrich
N-262 (Anti-cMyc)	sc-764	Santa Cruz Biotech
Akt (pan) (C67E7)	4691	Cell Signaling
Anti-GAPDH	G8795	Sigma- Aldrich
Clone RAS10	05-516	Merck Millipore
Erk1/2	9102	Cell Signaling
Phospho-Akt (Ser473)	4060	Cell Signaling
Phospho-Akt (Thr308)	2965	Cell Signaling
Phospho-Erk1/2	9101	Cell Signaling
Secondary antibodies		
Goat Anti-Rabbit IgG (HRP)	A9169	Sigma- Aldrich
Rabbit Anti-Mouse IgG (HRP)	ab6728	abcam

2.1.15 Computer Softwares

7500 Software v2.0.5	Applied Biosystemes, Warrington, UK
Axiovision 3.1	Zeiss AG, Oberkochen, GER
Basic local alignment serach tool (BLAST)	http://blast.ncbi.nlm.nih.gov/Blast.cgi
BiSearch	http://bisearch.enzim.hu
everyVECTOR	http://everyvector.com
GeneSnap 6.01	Syngene, Cambridge;UK
Microsoft Office: Mac 2011	Microsoft Deutschland GmbH, Unterschleißheim, GER
Primer3	http://bioinfo.ut.ee/primer3-0.4.0/
Quantification tool for Methylation analysis (QUMA)	http://quma.cdb.riken.jp nvitrogen GmbH, Darmstadt,GER
VectorNTI 10	Invitrogen GmbH, Darmstadt,GER

2.2 Methods

2.2.1 Microbiological methods

2.2.1.1 Bacterial culture

Escherichia coli (E.coli) DH10B cells and TUNERTM(DE3)pLacI cells were grown either in LB-medium in an orbital shaker at 230rpm or on agar plates in an incubator at 37°C O/N. LB-medium and agar plates were supplemented with 100µg/ml of the appropriate antibiotic. For liquid culture a single colony was picked with a sterile pipette tip, inoculated into 5 to 150ml LB-medium supplemented with the appropriate antibiotic and incubated at 37°C O/N.

2.2.1.2 Bacterial Transformation

Recombinant DNA-molecules were introduced into electrocompetent DH10B cells or TUNERTM(DE3)pLacI cells by electroporation. For this purpose, 50µl of frozen bacterial cells were thawed on ice and mixed with 2µl of recombinant DNA-molecules, transferred into a 2mm electroporation cuvette and pulsed at 2500V for 5ms in an Eppendorf Multiporator. Afterwards 500µl of prewarmed LB-medium were added to the electroporated cell suspension and incubated at 37°C for 30min in an orbital shaker. Subsequently, the bacterial suspension was plated onto agar plates containing the appropriate antibiotic and incubated at 37°C O/N.

2.2.1.3 Cryopreservation of bacterial cultures

For the long-term storage of bacteria, 500µl of an over-night culture were transferred to a 2ml cryopreservation tube containing 500µl 99% (v/v) glycerol, mixed gently by inversion and stored at -80°C.

2.2.1.4 Measurement of the optical density of bacterial suspensions

To monitor the growth of bacterial liquid cultures the optical density was determined at a wavelength of 600nm (OD600) with the Eppendorf BioPhotometer according to the manufacturer's instructions.

2.2.1.5 Expression of recombinant Cre protein

To express recombinant His-TAT-NLS-tagged Cre (HTNCre) protein, the vector pTriEx-HTNC (Addgene) was used. For the preparation of an over-night culture, LB-medium

supplemented with 100µg/ml ampicillin and 1.0% (w/v) glucose was inoculated with pTriEx-HTNC transformed TUNER™ (DE3)pLacI bacteria and incubated at 37°C O/N. The next day, a bacterial expression culture was set up. For this purpose, TB-medium (1.2% peptone, 2.4% yeast extract, 72mM K₂HPO₄, 17mM KH₂PO₄ and 0.4% (v/v) glycerol) supplemented with 0.5% (w/v) glucose was inoculated in a ratio 1:50 with the over-night culture and grown in an orbital shaker at 37°C until an OD₆₀₀ of 1.5. Subsequently, expression of recombinant HTNCre protein was induced by adding 0.5mM isopropyl β-D-thiogalactopyranosid (IPTG) and bacterial growth proceeded in an orbital shaker at 37°C for 4h. Thereafter bacterial cells were collected by centrifugation at 5000rpm and 4°C for 10min and the bacterial cell pellet was stored at -20°C O/N.

2.2.1.6 Extraction and purification of recombinant HTNCre protein from bacteria

Frozen bacterial cell pellets were resuspending in Lysis Buffer (50mM NaH₂PO₄, 5mM Trizma Base, pH 7.8 supplemented with 1x complete mini protease inhibitor) at 10ml/L expression culture and subsequently mechanically dissociated by mixing the suspension on a magnetic stirrer for 15min at RT. While mixing, 2mg/ml lysozyme was added for 15min at RT, followed by adding 25U/ml benzonase for 15min at RT. After sonification on ice for 1.5min with 0.5 pulses at 45% of power, 1ml ice-cold Tartaric Salt Buffer (TSB) (50mM NaH₂PO₄, 5mM Trizma Base, pH 7.8, 2M L-tartaric acid disodium salt, 20mM imidazole) per ml cell suspension was added and incubated while mixing for 5min at 4°C. Thereafter the suspension was centrifuged at 30000xg for 25min at 4°C. Then the supernatant, which contained the recombinant HTNCre protein was mixed with 2ml of 50% Ni-NTA slurry and incubated for 1h at 4°C under agitation.

In addition, to enhance the recovery of recombinant HTNCre protein, the cell pellet was additionally resuspended in 10ml Lysis Buffer and pressed ten times through a 18G needle. Thereafter the bacterial suspension was processed as after sonification and mixed with 2ml of 50% Ni-NTA slurry and incubated for 1h at 4°C under agitation. Prior to loading, EconoPac columns were equilibrated with 10ml Lysis Buffer equilibrated. Unbound material was removed from the columns by washing them twice with 5ml Washing Buffer (50mM NaH₂PO₄, 5mM Trizma Base, pH 7.8, 500mM NaCl, 15mM imidazole). The HTNCre protein-containing fraction was eluted with 3ml Elution Buffer (50mM NaH₂PO₄, 5mM Trizma Base, pH 7.8, 500mM NaCl, 250mM imidazole) and dialyzed against Salt Buffer (600mM NaCl, 20mM HEPES, pH 7.4). After 1h the buffer was exchanged and dialysis was performed O/N. To allow further concentrating and stable storage of recombinant HTNCre protein, the protein solution was dialyzed against Glycerol Buffer (50% (v/v) glycerol, 500mM NaCl, 20mM HEPES, pH 7.4) for 5h, then the buffer was renewed and dialysis proceeded O/N. The purified, recombinant HTNCre protein stock solution was aliquoted and stored at -20°C.

2.2.2 Mammalian cell culture methods

2.2.2.1 Mammalian cell culture

Mammalian cell culture work was carried out in a sterile class II laminar flow hood with sterile or autoclaved material and pipette filter tips. Unsterile solutions and solvents were filter sterilized through a 0.22µm filter prior to use. All media and supplements were prewarmed in 37°C water bath prior to use. Mammalian cell culture medium was changed every second to third day and at a confluence of 80–90% cells were passaged. For this purpose, old cell culture medium was aspirated, cells rinsed with PBS and detached by the use of Accutase. After incubation at 37°C and 5% CO₂ humidified atmosphere for 5min the action of Accutase was stopped by resuspending detached cells with the appropriate culture medium containing serum. Depending on the growth characteristics of the cells, cells were split in a ratio 1:2 to 1:10. All cells were cultivated at 37°C in a 5% CO₂ humidified atmosphere in a Steri-Cycle CO₂ incubator. Cell morphology and the absence of bacterial infections were regularly checked under an inverted microscope and photographs were taken with the AxioVision System.

2.2.2.2 Isolation of primary porcine mesenchymal stem cells (pMSCs)

For the isolation of primary pMSCs, pigs in the age of 6 to 7 months were slaughtered. Neck fat tissue, femur and tibia of the sacrificed pigs were sprayed with Barrycidal, placed in PBS supplemented with 100U/ml Penicillin, 100µg/ml Streptomycin and 2.5µg/ml Amphotericin B and transported to the laboratory in a thermo box at 37°C. Prior to isolation, all tissues and equipment used were cleaned thoroughly with 80% ethanol.

2.2.2.3 Isolation of bone marrow-derived mesenchymal stem cells (pBM-MSCs)

For the isolation of pBM-MSCs the epiphysis of tibia and femur were sawed off and the bone marrow was flushed out with prewarmed heparin solution (1000U heparin/ ml Hank's Salt Solution) using a 20G needle. The aspirated bone marrow was collected in a 150mm cell culture dish and in each case 20ml of the aspirated marrow were loaded onto 25ml of Lymphocyte Separation Medium and centrifuged at 1000xg for 20min with slow acceleration and deceleration. Then 7ml of the gradient interphase, containing mononuclear cells, were transferred to new 50ml falcon tube and washed with 35ml Hank's Salt Solution. After centrifugation at 600xg for 10min, the cell pellet was resuspended in pMSC culture medium (Advanced DMEM, 2mM GlutaMax, 1x NEAA, 5ng/ml FGF-2, 10% FCS) supplemented with

100U/ml Penicillin, 100µg/ml Streptomycin and 2.5µg/ml Amphotericin B, seeded onto one T150 cell culture flask per bone and cultured. The next three days, primary cells were rinsed twice with PBS and fresh culture medium was added. At the fourth day, cells were cultivated in culture medium without any antibiotics and antimycotics.

2.2.2.4 Isolation of adipose tissue-derived mesenchymal stem cells (pAD-MSCs)

Fat tissue was placed in a 10mm petri dish containing 10ml Collagenase Type I-A solution (0.01% (w/v) collagenase Type I-A in PBS) and finely minced with a scalpel. For proper tissue degradation the in Collagenase Type I-A solution minced fat tissue was transferred into a conical flask with a magnetic stir bar and incubated on a magnetic stirrer at 37°C for 20min. After enzymatic and mechanic tissue degradation, undigested tissue pieces were removed by filtering the muddy cell suspension through a 100µm cell strainer. The liquid was collected in a 50ml falcon tube, mixed with an equal volume of pMSC culture medium and centrifuged at 1000xg for 10min. The cell pellet was resuspended in pMSC culture medium supplemented with antibiotics and antimycotics and cultivated as described in 2.2.2.3.

2.2.2.5 Cryopreservation and thawing of mammalian cell lines

For the long-term storage of mammalian cells, cells were cryopreserved and stored in liquid nitrogen. For this purpose, cells were detached, resuspended in pMSC culture medium and pelleted at 340xg for 5min. Afterwards the cell pellet was resuspended in freezing medium (70% pMSC culture medium, 20% FCS, 10% DMSO), transferred to 2ml cryogenic vials, which were conveyed to a Mr. Frosty box and stored at -80 °C. Two days later, the cryogenic vials were transferred into liquid nitrogen.

To thaw porcine cells, a cryogenic vial of cryopreserved cells was prewarmed in a 37°C water bath until the cell suspension liquefied. In the meanwhile a 15ml falcon tube was prepared containing 10ml of pMSC cell culture medium. Then the liquefied cell suspension was transferred into the 15ml falcon tube using a disposable pipette. After centrifugation at 340xg for 5min, the supernatant was aspirated, the cell pellet resuspended in 8 ml culture medium, transferred to T25 cell culture flask and cultured.

2.2.2.6 Cell counting and determination of cell number

Using a Neubauer counting chamber 10µl of detached, resuspended single cell solution was transferred to a hemocytometer and four squares were counted. Cell number per ml suspension was calculated according to the following formula:

$$\text{number of cells per ml} = \frac{\text{number of cells in four squares}}{4} \times 10^4 / \text{ml}$$

2.2.2.7 Cell preparation for somatic cell nuclear transfer (SCNT)

Two days prior to SCNT, primary pMSCs were induced to cell cycle synchronisation by serum starvation. For this purpose, primary pMSCs were rinsed twice with PBS and starvation medium (Advanced DMEM, 2mM GlutaMax, 1x NEAA, 0.5% FCS) was added.

2.2.2.8 Transfection of primary pMSCs by electroporation

To introduce recombinant plasmid DNA molecules into primary pMSCs, cells were transfected by electroporation. For this purpose, 1×10^6 pMSCs were pelleted at 340xg for 5 min, the supernatant was discarded and the cell pellet was resuspended in 400 μ l prewarmed, hypoosmolar buffer. Then 10 μ g of linearized plasmid DNA was added to the cell suspension, mixed and incubated for 10min at RT. Afterwards the cell suspension was transferred into a 4mm cuvette and pulsed at 1200V for 85 μ s in an Eppendorf Multiporator. After pulsing, the cell suspension was incubated for 10min at RT and electroporated cells were seeded onto a T75 cell culture flask and cultured.

2.2.2.9 Selection of transfected pMSCs and derivation of single cell clones

48 hours after electroporation, pMSCs were split into selection medium (pMSCs culture medium supplemented with either G418 or Blastcidin S) and plated onto 150mm cell culture dishes. Culture proceeded in pMSCs selection medium until single cell colonies were visible. For picking sufficiently large single cell colonies, dishes were rinsed with PBS and small autoclaved in Accutase soaked filter papers were placed onto each colony and incubated for 3min at 37°C and 5% CO₂ in humidified atmosphere. Thereafter filter papers were transferred to 24-well plates containing selection medium. Two days after single cell clone picking filter papers were removed and culture continued.

2.2.2.10 HTNCre protein transduction into primary pMSCs

To investigate HTNCre mediated recombination, genetically modified pMSCs containing floxed transcriptional stop cassettes were transduced with purified, recombinant Cre protein. One day prior to protein transduction, 4×10^4 pMSCs were plated per well of a 12-well plate and cultured. The next day, 5.0 μ M of recombinant HTNCre protein were diluted in pMSCs starvation medium. After HTNCre containing medium was filter sterilized through a 0.22 μ m filter disk, the cells were rinsed with PBS and subsequently incubated with HTNCre

containing medium at 37°C and 5% CO₂ in humidified atmosphere for 8h. After HTNCre protein transduction, cells were rinsed twice with PBS and culture proceeded in standard pMSC culture medium.

2.2.2.11 Derivation of single cell clones by limiting dilution cloning

72 hours after HTNCre protein transduction, pMSCs were subjected to limiting dilution cloning. For this purpose, cells were detached, counted and a cell concentration of 2.5 cells/ml pMSC culture medium was adjusted by serial dilution. Subsequently, 200µl of the cell suspension were transferred per well of a 96-well plate and cultured at 37°C and 5% CO₂ in humidified atmosphere.

2.2.2.12 Assessment of cellular proliferation

For analysing the growth characteristics and population doubling time of primary and genetically modified pMSCs 1x10⁴ cells were seeded either per well of a 6-well plate or per T25 cell culture flask. Over a time period of 72h, cell numbers were determined daily in triplicates with the Countess[®] automated cell counter according to the manufacturer's instructions.

Population doubling time (PDT) was calculated according to the following formula, whereby Δt is the duration between two time points, N₁ the determined cell number at time point 1 and N₂ the determined cell number at time point 2:

$$\text{PDT} = \frac{\log 2 \times \Delta t}{\log N_2 - \log N_1}$$

In addition, the proliferation capacity of primary and genetically modified pMSCs was assessed by a colony formation assay. Therefore 1x10³ cells were seeded onto a 100mm cell culture dish and culture proceeded with regular medium change for three weeks.

For visualising formed colonies, they were stained with crystal violet. For this purpose, cells were rinsed twice with PBS and 10ml crystal violet solution (0.5% crystal violet in 20% methanol) were added to the cells and incubated for 10min at RT. Thereafter the crystal violet solution was aspirated, cells were rinsed twice with PBS and photographs were taken.

2.2.2.13 *In vitro* cell transformation assays

To determine the transformation potential of primary and genetically modified pMSCs their loss of contact inhibition and their anchorage-independent growth in soft agar were investigated.

To assess the growth characteristics of primary and genetically modified pMSCs at high cell densities, cells were detached by using Accutase, counted and 1×10^5 cells were plated per 100mm cell culture dish in triplicates. Mammalian cell culture proceeded with regular medium change for four weeks. Thereafter photographs were taken with the AxioVision System.

Since anchorage-independent growth is considered as the most stringent *in vitro* assay for proving cellular transformation, primary and genetically modified pMSCs were resuspended and cultured in soft agar. For this purpose, 0.6% (v/v) bottom agar medium was prepared by mixing 1.2% (w/v) Noble agar in a ratio 1:1 with 2x DMEM⁺⁺ medium (2x DMEM, 2x NEAA, 4mM GlutaMax, 88mM NaHCO₃, 20% FCS, 200µg/ml Penicillin/Streptomycin). Thereafter 6-well plates were coated with 0.6% (v/v) bottom agar medium and incubated at RT to allow the agar to solidify. In the meanwhile, the 0.4% (v/v) top agar was prepared by mixing 0.8% (w/v) Noble agar with 2x DMEM⁺⁺ medium. Then cells were detached, counted and 1×10^3 cells were suspended in 0.4% top agar medium and plated on top of the solidified bottom agar. Each cell clone was plated in triplicates. After solidification at RT, 6-well plates were incubated at 37°C and 5% CO₂ in humidified atmosphere. The day after plating, standard pMSC culture medium was added to the cells and culture proceeded for three weeks. Colonies greater than 50µm in diameter were considered as a colony, counted and photographs were taken with the AxioVision System.

2.2.3 Isolation of nucleic acids

2.2.3.1 Isolation of plasmid DNA from bacterial cells

2.2.3.1.1 Miniprep

To isolate plasmid DNA in a small-scale from a 5ml over-night bacterial suspension culture the alkaline lysis method was applied. Therefore 2ml of the bacterial suspension were centrifuged and the pellet was resuspended in 100µl of Alkaline Lysis Solution I (5mM sucrose, 10mM EDTA, 25mM Tris, pH 8.0) to ensure lysis of bacterial cells. Afterwards 200µl of Alkaline Lysis Solution II (0.2M NaOH, 1% (w/v) SDS) and subsequently 150µl of Alkaline Lysis Solution III (3 M sodium acetate) were added and incubated on ice for 30min to allow the precipitation of bacterial DNA and proteins. After centrifugation the supernatant was transferred to a fresh 2ml reaction tube and 1ml of 95% (v/v) EtOH was added, mixed and spun down. After removing the supernatant, the plasmid DNA pellet was washed with 80% (v/v) EtOH and again with 95% (v/v) EtOH. Finally, the air-dried pellet was dissolved in 50µl of ddH₂O supplemented with RNase.

2.2.3.1.2 Midiprep

For the extraction of greater plasmid DNA amounts, plasmid DNA from an 150ml over-night bacterial suspension culture was isolated with the NucleoBond Xtra Plasmid Purification Kit according to the manufacturer's instructions. After isolation, the air-dried pellet was dissolved in 150µl low Tris-EDTA (10mM Trizma base, 0.1mM EDTA).

2.2.3.2 Genomic DNA isolation from gene targeted cell clones using Igepal-Lysis Buffer

For the screening of positive targeting events, single cell clones grown on 24-well plates were detached with 100µl Trypsin. While half of the detached cell suspension was plated onto 12-well plates, 50µl of this cell suspension was stored at -20°C O/N. The next day, the cell suspension was spun down at 7000xg for 5min and the cell pellet was resuspended in 50µl Igepal-Lysis Buffer (50mM KCl, 1.5mM MgCl₂, 10mM TrizmaBase, pH 8.0, 0.5% (v/v) NP40, 0.5% (v/v) Tween20, pH 8.0) supplemented with 100µg/ml ProteinaseK solution. After incubation at 60°C for 1h the reaction was heat inactivated at 95°C for 15min and spun down at 14000xg for 5min. The supernatant was transferred to a fresh reaction tube and 5µl of isolated, genomic DNA was applied for PCR screenings.

2.2.3.3 Genomic DNA isolation by Phenol Chloroform Isoamyl alcohol extraction

To isolate genomic DNA from tissue samples or mammalian cells, phenol chloroform isoamylalcohol extraction was performed. The material was mixed with 1ml of Lysis Buffer (1M Tris-HCl pH 8.5, 0.5M EDTA, 20% (w/v) SDS, 5M NaCl) supplemented with 100µg/ml ProteinaseK solution and incubated on a rocking platform at 55°C O/N. The next day, 20µg of RNaseA solution was added to the samples and incubated for 5min at RT. Subsequently, the lysed sample was transferred to a fresh 2ml reaction tube and an equal volume of phenol chloroform isoamyl alcohol (25:24:1) solution was added, mixed gently and incubated for 10min at RT. To separate the aqueous phase from the organic phase, the sample was centrifuged at 14000xg for 15min. Then, the aqueous phase containing genomic DNA was transferred to a fresh 2ml reaction tube and an equal volume of chloroform was added, vortexed and centrifuged at 14000xg for 10min. In order to precipitate genomic DNA, the aqueous phase was transferred to a fresh reaction tube mixed with 0.7 volume of 100% (v/v) isopropanol and spun down at 14000xg for 15min. Subsequently, the pellet was washed with 70% (v/v) EtOH and centrifuged at 14000xg for 15min. Thereafter the pellet was air-dried and dissolved in low Tris-EDTA and stored at 4°C.

2.2.3.4 Total RNA isolation using TRIzol

For microarray analysis RNA of primary and genetically modified porcine cells was isolated using TRIzol. Therefore cells were cultured on T75 cell culture flasks and at a confluence of 80% 3ml of TRIzol were added and incubated for 5min at RT. After cell lysis, in each case 1ml of the cell suspension was transferred to a fresh 2ml reaction tube. Per 1ml of lysed cells 200µl chloroform were added, mixed for 15sec, then incubated for 3min at RT and centrifuged at 12000xg for 15min at 4°C. Afterwards the transparent aqueous phase was transferred to a fresh 1.5ml reaction tube and mixed with 500µl ice-cold isopropanol. After incubation for 10min at RT, the mix was centrifuged at 12000xg for 10min at RT. Afterwards the pellet was washed with 1ml 75% EtOH and vortexed. After centrifugation at 7500xg for 5min at 4°C and the pellet was air-dried and dissolved in 50µl ultra pure H₂O, aliquoted and stored at -80°C.

2.2.3.5 Isolation of total RNA and genomic DNA using the SurePrep* RNA/DNA/Protein Purification Kit

The application of the SurePrep* RNA/DNA/Protein Purification Kit allowed the sequential isolation and purification of total RNA and genomic DNA from a single sample. Here, total RNA and genomic DNA from cultured porcine cells were isolated according to the manufacturer's instructions.

2.2.3.6 DNase treatment of RNA preparations

To remove residual genomic DNA contaminations from isolated RNA preparations, the TURBO DNA-free™ Kit was applied according to the manufacturer's instructions.

2.2.3.7 Photometric determination of nucleic acid concentrations

Concentrations of nucleic acids were measured photometrically at a wavelength of 260nm with the Eppendorf BioPhotometer according to the manufacturer's instructions.

2.2.4 Molecular biological methods

2.2.4.1 Preparation of bisulfite converted DNA

To analyse the DNA methylation pattern of primary and genetically modified porcine cells, 500ng of genomic DNA were used for bisulfite conversion applying the EpiTect Fast Bisulfite

Conversion Kit. Thermal cycling conditions for bisulfite conversion were: Denaturation 5min, 95°C; Incubation 20min, 60°C; Denaturation 5min, 95°C; Incubation 20min, 60°C.

Converted DNA was cleaned up and processed according to the manufacturer's instructions.

2.2.4.2 Synthesis of complementary DNA (cDNA)

For expression analysis total RNA was reversed transcribed into cDNA by applying SuperScript® III Reverse Transcriptase (Invitrogen™). cDNA synthesis was performed with 700ng of total RNA and random hexamer primers according to the manufacturer's instructions.

2.2.4.3 Polymerase chain reaction (PCR)

For the amplification of specific DNA fragments from plasmid DNA, genomic DNA and cDNA polymerase chain reactions (PCRs) were carried out. Depending on the amplification purpose different DNA polymerases were applied according to the manufacturer's instructions. Phire polymerase was used to detect positive *KRAS* targeting events and the presence of the G12D mutation in exon 2 of the targeted allele. Whereas 5'PRIME DNA polymerase was employed to perform a PCR over the long arm of the *KRAS* targeting construct. For all other analytical PCRs GoTaq DNA polymerase was utilised. Table 2 summarises thermal cycling conditions for the different DNA polymerases used.

DNA polymerase	Step	Temperature	Time	Cycles
Phire	Initial denaturation	98C°	3min	1
	Denaturation	98C°	5sec	
	Annealing	61C° - 65°C	5sec	40
	Elongation	72C°	50sec - 1:45min	
	Final elongation	72C°	1min	1
	Final hold	8°C	∞	
	5'PRIME	Initial denaturation	93C°	3min
Denaturation		93C°	15sec	
Annealing		64°C	30sec	10
Elongation		68C°	10min	
Denaturation		93C°	15sec	
Annealing		64°C	30sec	
Elongation		68C°	10min with 20sec time increment for each elongation step	17
Final hold		8°C	∞	
GoTaq	Initial denaturation	95°C	5min	1
	Denaturation	95°C	30sec	
	Annealing	57°C - 61°C	30sec	30 - 40
	Elongation	72°C	1:00min - 3:30min	
	Final elongation	72°C	5min	1
	Final hold	8°C	∞	

Table 2: Polymerases used with the respective PCR programs

2.2.4.4 Subcloning of PCR products

Purified PCR products were subcloned into the pJet1.2 Blunt cloning vector of the CloneJET PCR Cloning Kit. Blunting and ligation reactions were performed according to the manufacturer's instructions, with the modification that the ligation mix was incubated at 4°C O/N.

2.2.4.5 Colony PCR

As a fast and convenient method for screening of recombinant transformants colony PCR was conducted. For colony PCR DNA was obtained directly from bacterial transformants and primers were used, which flanked the cloning site of the pJet1.2 Blunt cloning vector. After the PCR reaction was set up and aliquoted, single colonies were picked from antibiotic containing plates with a sterile pipette tip, resuspended in the PCR reaction mix and streaked onto LB agar plates supplemented with the appropriate antibiotic as a backup.

2.2.4.6 Quantitative real-time PCR (qRT-PCR)

For relative quantification of gene expression two-step qRT-PCR experiments were performed using Fast SybrGreen PCR MasterMix and the 7500 Fast Real-Time PCR System. Primer specificity, cDNA dilutions and PCR efficiencies were determined by melting curve analysis. For relative quantification of gene expression levels 1µl of 1:5 diluted cDNA, 0.4µM forward primer, 0.4µM reverse primer and 1x Fast SybrGreen PCR MasterMix were applied. The reaction was performed in a total volume of 10µl and each sample type was run in triplicates. Thermal cycling conditions were 95°C, 10 min; 40 cycles of 95°C for 15 s, 60°C for 1 min. The $\Delta\Delta C_T$ method was used to calculate the fold-differences in expression levels normalised to endogenous GAPDH expression.

2.2.4.7 Microarray analysis

In order to dissect the transcriptional changes, which arose along defined stages of malignant porcine mesenchymal stem cell transformation microarray analysis was performed. In the case of unmodified pMSC, unrecombined and recombined pMSCs total RNA from three biological replicates was isolated using TRIzol. Whereas in the case of stable selected Myc transfectants and porcine sarcoma derived tumour cells total RNA from three technical replicates was prepared. Gene expression experiments were performed by Morgane Ravon (Global NCS Molecular Pathology) at the F. Hoffmann-La Roche AG in Basel.

2.2.4.8 Assessment of copy number alterations

To detect and quantify variations in copy number alterations quantitative PCR (qPCR) was carried out using Fast SybrGreen PCR MasterMix. After optimisation of qPCR conditions, relative quantification of copy number alterations were performed in a total volume of 10µl with 10ng of genomic DNA and 0.3µM primer stocks and 1x Fast SybrGreen PCR

MasterMix. Thermal cycling conditions were 95°C, 10 min; 40 cycles of 95°C for 15 s, 60°C for 1 min. Each sample was run in triplicates and data were normalised to GAPDH as a reference gene. For the calculation of copy number alterations the $\Delta\Delta C_T$ method was applied.

2.2.4.9 Restriction endonuclease digestion

For DNA restriction enzyme digestion of plasmid DNA and genomic DNA 5 units (U) of restriction endonuclease per μg DNA were used. Whereas restriction fragment length polymorphism (RFLP) were detected by cleaving 20 μl of un-purified PCR samples with 5U of the respective restriction endonuclease. The reaction was performed according to the manufacturer's instructions and incubated for 2h at the temperature appropriate for the endonuclease.

2.2.4.10 Electrophoretic separation of DNA fragments

Agarose gel electrophoresis was carried out for separating DNA fragments according to their size. Thereby the concentration of the agarose gel was adjusted to the size of the expected DNA fragments. For this purpose, 0.7% to 2.0% (w/v) low melting agarose powder was dissolved in either TAE Buffer (40mM Trizma base, 20mM acetic acid, 1mM EDTA, pH 8.0) or TBE Buffer (90mM Trizma base, 90mM boric acid, 2mM EDTA, pH 8.0) and heated. Subsequently the cooled agarose gel was supplemented with 0.1 $\mu\text{g}/\text{ml}$ ethidium bromide and poured into a cast with a comb. Prior to electrophoretic separation, DNA samples were mixed with 5x DNA loading dye (50% (v/v) glycerol, 10mM EDTA, 0.1% (w/v) SDS and traces of bromphenol blue) and loaded onto the solidified agarose gel together with 100 bp or 1 kb DNA markers, that enabled the comparison of DNA fragment sizes. The gels were run at a voltage of 80V to 120V for 90min and electrophoretically separated DNA fragments were visualised under UV light (254 nm) using the Gene Genius Bioimaging System.

2.2.4.11 Isolation of DNA fragments from agarose gels

To isolate DNA fragments from agarose gels, the gels were put onto a UV table and the desired DNA fragments were cut out with a clean scalpel and purified using the Wizard SV Gel and PCR Clean-up system according to the manufacturer's instructions.

2.2.4.12 Sequencing of DNA fragments

DNA sequencing was performed by Eurofins Genomics GmbH (Ebersberg, GER). Prior to shipping, PCR samples were cleaned up by applying either the Wizard SV Gel and PCR Clean-up system or by shrimp alkaline phosphatase (SAP) and Exonuclease I (ExoI) treatment. In the latter case, 10µl of the PCR sample were mixed with 0.1U SAP and 6U ExoI and filled up with ddH₂O to obtain a reaction volume of 12µl. The reaction was incubated at 37°C for 30min and then heat inactivated at 80°C for 15min. Subsequently, the purified PCR samples were sent for sequencing.

2.2.4.13 Plasmid DNA precipitation

For transfection experiments of mammalian cells sterile plasmid DNA was needed. For this purpose, linearized plasmid DNA was mixed with 0.1 volumes of 3M NaCl and 2 volumes of ice-cold 100% EtOH, vortexed and stored at -20°C O/N. The next day, the solution was centrifuged at 14000xg for 10min and all subsequent steps were performed under sterile conditions. Firstly, the supernatant was discarded, the pellet washed with 70% EtOH and centrifuged at 14000xg for 20min. Thereafter the DNA pellet was air-dried and dissolved in 50µl low Tris-EDTA and stored at 4°C.

2.2.4.14 Southern Blot analysis

Southern blot hybridisation was carried out to confirm the integration of the *KRAS* targeting construct at the endogenous *KRAS* gene locus in porcine cells. This analysis allowed discriminating targeted cell clones from randomly integrated ones.

2.2.4.14.1 Preparation of DIG-labelled probe

Digoxigenin-11-2'-deoxy-uridine-5'-triphosphate (DIG) labelled probes were used to detect single copy DNA sequences on a blot. Two internal DIG-labelled probes, a BS-probe and a NEO-probe, were prepared by PCR labelling using GoTaq Polymerase and 10ng of the relative targeting construct as DNA template according to the manufacturer's instructions. To evaluate the efficiency of DIG labelling, a PCR reaction without labelled-UTPs was set up to compare the shift in molecular weight of labelled and unlabelled probe by gel electrophoresis.

2.2.4.14.2 Southern blot

Per sample 12.5µg of genomic DNA was cleaved with *ScaI-HF* for 5h and loaded onto a 1% TAE gel without ethidium bromide. For size control 4µl of DIG-labelled molecular weight marker were used. The gel was run at 40V for 16h. To enhance transfer of genomic DNA fragments larger than 5kb, the gel was submerged in Depurination Solution (250mM HCl) for 10min. Then, the gel was incubated twice with Denaturation Solution (0.5M NaOH, 1.5M NaCl) for 15min and subsequently twice in Neutralisation Solution (0.5M Tris-HCl, pH 7.5, 1.5M NaCl) for 15min. Prior to blot transfer, the gel was equilibrated in 20x SSC Buffer (3M NaCl, 300mM sodium citrate, pH 7.0) for 10min. Thereafter the capillary blot transfer device was assembled and transfer proceeded O/N. After rinsing the membrane in 2xSSC Buffer (0.3M NaCl, 30mM sodium citrate, pH 7.0) the membrane was baked at 120°C for 30min, which allowed the fixation of the transferred genomic DNA to the membrane. Thereafter the membrane was put in a roller bottle and incubated with 10ml of prewarmed Prehybridisation Buffer (DIG Easy Hyb) at the appropriate temperature of the relative probe used (BS-probe: 45°C; NEO-probe: 47.5°C) for 3h with gentle rotation. After the prehybridisation step, the Hybridisation Solution (3µl of denatured DIG-labelled probe per ml DIG Easy Hyb) was prepared and added to the membrane. Probe hybridisation was carried out at the appropriate temperature of the relative probe used O/N with gentle rotation. After the hybridisation procedure, the membrane was washed twice in Low Stringency Buffer (2x SSC containing 0.1% (w/v) SDS) for 15min, then twice in 68°C preheated High Stringency Buffer (0.5x SSC containing 0.1% (w/v) SDS) for 15min and finally in Washing Buffer (0.1M Maleic acid, 0.15M NaCl, pH 7.5, 0.3% (v/v) Tween20) for 2min. All washing steps were performed on a rocking platform with gentle agitation at RT. Then blocking was carried with 1x Blocking Solution (Roche) for 1h at RT. For visualising probe-target hybrids the membrane was incubated with an Anti-Digoxigenin-AP Fab fragment (diluted 1:10000 in 1x Blocking Solution) for 30min at RT. Thereafter the membrane was rinsed twice in Washing Buffer for 15min and finally in Detection Buffer (0.1M Tris-HCl, 0.1M NaCl, pH 9.5) for 3 min. After adding the chemiluminescent substrate (CDP-Star diluted 1:100 in Detection Buffer) the membrane was sealed in a plastic wrap and exposed to a X-ray film for 45min at 37°C.

2.2.5 Biochemical methods

2.2.5.1 Protein extraction from mammalian cells

For the isolation of proteins for conventional Western blotting procedures cells grown on 100mm cell culture dishes were rinsed twice with ice-cold PBS and dissociated mechanically

with 250µl ice-cold Lysis Buffer (50mM HEPES, 150mM NaCl, 1mM EDTA, 0.5% IGEPAL-630, 10% (v/v) glycerol, pH 7.9 supplemented with 1x phosphatase inhibitor and 1x complete mini protease inhibitor) using a cell scraper. After mechanic dissociation the cell suspension was stored at -80°C for 30min to enhance cell lysis. Thereafter the cell suspension was spun down at 16000xg for 30min at 4°C. The cleared lysate was aliquoted and stored at -80°C. To prepare protein lysates for the Raf-GST Pull-Down Assay adherent cells grown on 150mm cell culture dishes were rinsed twice with ice-cold PBS and dissociated mechanically with 1ml ice-cold 1x MLB Buffer (25mM HEPES, pH7.5, 150mM NaCl, 1% Igepal-CA630, 10mM MgCl₂, 1mM EDTA, 10% (v/v) glycerol supplemented with 1x phosphatase inhibitor and 1x complete mini protease inhibitor) using a cell scraper. After centrifugation at 14000xg for 5min at 4°C the cleared lysate was snap frozen in liquid nitrogen and extracts were stored at -80°C.

2.2.5.2 Determination of protein concentrations

The concentration of protein lysates was measured by using the Advanced Protein Assay Reagent. Samples were set up according to the manufacturer's instructions and transferred to a 96-well plate. Subsequently the absorbance at 590nm was measured with a Multiscan Ex device and protein concentrations were calculated according to the following formula:

$$1.0 \text{ OD}_{590\text{nm}} = 37.5\mu\text{g protein per ml reagent per } 0.8\text{cm}$$

2.2.5.3 Sodiumdodecylsulfate Polyacrylamide Gelelectrophoresis (SDS-PAGE)

Denaturing SDS-PAGE was applied to separate proteins according to their molecular mass. Therefore 12% to 15% resolving gels and 5% stacking gels were prepared according to Table 3.

Reagent	12% resolving gel	15% resolving gel	5% stacking gel
Polyacrylamide (40%)	900µl	1125µl	125µl
1M Tris (pH 8.8)	1125µl	1125µl	
0.5M Tris (pH 6.8)			250µl
10% SDS	30µl	30µl	10µl
10% APS	30µl	30µl	10µl
TEMED	1.2µl	1.2µl	1µl
ddH ₂ O	913.8µl	688.8µl	604µl

Table 3: Formulation of 12% and 15% resolving gels and 5% stacking gel for SDS-PAGE

Between 20µg to 40µg of total protein lysates were mixed with 4x Lämmli Buffer (250mM Trizma-HCl, pH 6.8, 1% (w/v) SDS, 1M sucrose, 24mM dithiothreitol (DTT) and a trace of bromphenol blue), heated at 95°C for 5min and spun down. In the meanwhile, the Mini-PROTEAN 3 Cell was assembled according to the manufacturer's instructions and filled with

1x Running Buffer (25mM Trizma base, 200mM glycine, 0.1% (w/v) SDS). After boiling, pre-stained protein marker and samples were loaded onto the gel. For electrophoretic separation, an electric field of 100V and 400mA was applied for 20min, followed by 200V and 400mA for at least 40min.

2.2.5.4 PageBlue staining of separated proteins after SDS-PAGE

For fast and sensitive staining of separated proteins after SDS-PAGE the gel was incubated in PageBlue™ protein staining solution according to the manufacturer's instructions.

2.2.5.5 Western blot analysis

Separated proteins were transferred from the polyacrylamide gel to a PVDF membrane (Immobilon-P) by semidry blotting. For this purpose, filter papers, fibre pads and the polyacrylamide gel were equilibrated in Semidry Blotting Buffer (25mM Trizma base, 192mM glycine, 20% (v/v) methanol) for 5min under agitation. In the meanwhile the PVDF membrane was activated in 100% methanol for 1min and subsequently soaked in Semidry Blotting Buffer. The Trans-Blot SD Semi-dry Electrophoretic Transfer Cell was assembled according to the manufacturer's instructions and electro-blotting was performed at 10V and 400mA for 30min. After blotting, the PVDF membrane was incubated in Blocking Buffer (20mM Trizma base, 140mM NaCl, 0.1% (v/v) Tween20 and 5% (w/v) BSA (TBST-BSA)) on an orbital shaker for 90min at RT. After blocking, the membrane was washed three times with Washing Buffer (20mM Trizma base, 140mM NaCl, 0.1% (v/v) Tween20) on an orbital shaker for 15min. Then the membrane was incubated with the primary antibody diluted in Blocking Buffer on an orbital shaker at 4°C O/N (antibodies with the appropriate dilutions are listed in Table 4). The day after, the membrane was again washed three times in Washing Buffer for 15min and subsequently incubated with an appropriate peroxidase-labelled secondary antibody diluted in Blocking Buffer on an orbital shaker for 1h at RT (antibodies with the appropriate dilutions are listed in Table 4) After three additional washing steps the membrane was placed in a plastic wrap and chemiluminescence detection was performed using the Pierce ECL Western Blotting substrate according to the manufacturer's instructions. The sealed membrane was exposed to X-ray films for 5 to 20min.

2.2.5.6 Ras Activation Assay

To investigate the abundance of GTP-bound Ras proteins, 1mg of protein extract was mixed with 10µg of the Ras Assay Reagent (a GST fusion protein, corresponding to the Ras binding domain of Raf-1, bound to glutathione agarose beads) and incubated for 3 hours at

4°C with gentle agitation. Thereafter the agarose beads were pelleted at 14000xg for 50sec at 4°C and washed for three times with 500µl of 1x MLB Buffer. After the last washing step, the pellet was resuspended in 40µl of 4x Lämmli Buffer and 2µl of 1M DTT were added, which should improve the release of GTP-bound Ras proteins from agarose beads. Prior to SDS-PAGE, samples were boiled for 5min at 95°C and spun down. 20µl of processed samples were loaded per lane. And as a loading control 20µg of unprocessed total protein extracts were loaded per lane. SDS-PAGE and blotting were conducted as described in 2.2.5.5.

After SDS-PAGE, the membrane was rinsed twice with ddH₂O and incubated in Blocking Solution (PBS containing 0.05% Tween-20 and 3% (w/v) dry milk powder (PBST-MLK)) for 2h at RT on an orbital shaker. Thereafter the primary anti-Ras antibody, clone RAS10, diluted 1:2000 in PBST-MLK was added and the membrane was incubated at 4°C O/N on a rocking platform. The next day, the membrane was washed twice with PBST for 10min with constant agitation. Subsequently the secondary antibody diluted 1:6000 in PBST-MLK was added to the membrane and incubated for 60min at RT with gentle agitation. Finally the membrane was washed three times with PBST for 10min before chemiluminescent detection was performed as described above.

Antibody	Antigene	Source	Dilution	Blocking Buffer
DO-1	p53	Mouse	1:5000	TBST-BSA
N-262	c-Myc	Rabbit	1:250	TBST-BSA
Anti-GAPDH	Glyceraldehyde-3-phosphate dehydrognease	Mouse	1:5000	TBST-BSA
Akt (pan)	Akt	Rabbit	1:1000	TBST-BSA
Phospho-Akt (Ser473)	Phospho-Akt (Ser473)	Rabbit	1:1000	TBST-BSA
Phospho-Akt (Thr308)	Phospho-Akt (Thr4308)	Rabbit	1:1000	TBST-BSA
Erk1/2	p44/42 MAPK	Rabbit	1:1000	TBST-BSA
Phospho-Erk1/2	Phospho-p44/42 MAPK	Mouse	1:1000	TBST-MLK
Clone RAS10	Ras	Mouse	1:2000	PBST-MLK
HRP-conjugated anti rabbit IgG		Goat	1:20000	TBST-BSA
HRP-conjugated anti mouse IgG		Horse	1:6000	TBST-BSA PBST-MLK

Table 4: Antibodies used with the respective dilutions

2.2.6 Animal experiments

To assess the tumorigenicity of genetically modified pMSCs, these cells were injected subcutaneously into immunological nonresponsive as well as in immunological responsive animals and their capability to give rise to tumours was monitored.

2.2.6.1 Assessing the tumorigenicity of genetically modified pMSCs in immune-deficient mice

2.2.6.1.1 Xenotransplantation

To examine the tumorigenicity of genetically modified pMSCs in immune-deficient mice, 1×10^7 porcine cells were pelleted and suspended in chilled advanced DMEM medium without any additives. Subsequently the cell suspension was mixed 1:1 (v/v) with high concentrated Matrigel™ Basement Membrane Matrix (BD Biosystems) and kept on ice until cells were injected subcutaneously into the back of NOD *scid* gamma mice. Implantations of porcine cells into NOD *scid* gamma mice were performed by Stefan Eser (Department of Medicine II) at the Klinikum rechts der Isar.

2.2.6.1.2 Isolation of primary porcine tumour cells

In the case, that injected genetically modified pMSCs formed a tactile tumour in NOD *scid* gamma mice a porcine tumour cell line was isolated by Stefan Eser (Department of Medicine II) at the Klinikum rechts der Isar. For this purpose, the animal was sacrificed, the skin opened and a piece of tumour was resected and placed into DMEM medium supplemented with 100µg/ml Penicillin/Streptomycin. The tumour tissue was finely minced with a scalpel and digested with 200U/ml Collagenase Type IV (Worthington, USA) in DMEM medium supplemented with 100µg/ml Penicillin/Streptomycin at 37°C O/N. The next day digested tissue was centrifuged at 100rpm for 5min. The cell pellet was resuspended in normal pMSC medium supplemented with 100U/ml Penicillin/Streptomycin and cells were cultivated at 37°C in a 5% CO₂ humidified atmosphere.

2.2.6.1.3 Histological examination of resected tumours

Paraffin embedding and sectioning of porcine tumour samples were carried out by Vanessa Klein (Department of Medicine II) at the Klinikum rechts der Isar. For histological examination, the H&E stained tumour sections were analysed by Prof. Dr. Esposito (Institute of Pathology) at the Klinikum rechts der Isar.

2.2.6.2 Assessing the tumorigenicity of genetically modified pMSCs in an isogenic immune-competent pig

To assess the capability of genetically modified pMSCs to give rise to tumours in immunological responsive large animals, the parental unmodified pMSCs were used to clone isogenic host animals. For syngeneic cell transplantation 1×10^8 porcine cells were pelleted and resuspended in chilled PBS and kept on ice until cell transplantation. In two experiments cells were resuspended in chilled advanced DMEM medium without any additives and mixed 1:1 (v/v) with high concentrated Matrigel™ Basement Membrane Matrix (BD Biosystems) and kept on ice. Dr. Barbara Kessler (Molecular Animal Breeding and Biotechnology, LMU) preformed all subcutaneous injections behind the ears of a syngeneic immune-competent pig.

3 Results

3.1 Introducing defined oncogenic mutations into porcine mesenchymal stem cells

Most of the established tumour progression models are based either on the expression of viral oncogenes or on the ectopic expression of oncogenes and dominant-negative tumour suppressors that are under the control of constitutively active promoters. Although these experimental cancer models provided considerable insights into the action and cooperation of individual oncogenes and tumour suppressor genes in the multi-step process of cellular transformation *in vitro*, they fall short, as they rely on the ectopic overexpression of introduced transgenes. In this regard, these experimental transformation models do not accurately recapitulate the situation *in vivo*, where oncogenes and mutant tumour suppressor genes are expressed at physiological expression levels, as they are transcribed from their endogenous gene promoters. To mimic the multi-step process of porcine neoplastic cell transformation we aimed in introducing latent oncogenic $TP53^{R167H}$ (orthologous to human $TP53^{R175H}$ and mouse $Trp53^{R172H}$) and $KRAS^{G12D}$ (homologous to human $KRAS^{G12D}$ and mouse $Kras^{G12D}$) alleles into the endogenous gene loci by homologous recombination. These two potent drivers of cellular transformation were chosen, as they are sufficient to induce full transformation of primary mouse cells *in vitro* [233] and cooperate in the multi-step process of tumorigenesis *in vivo* [209,259,260]. To test if this is also the case for porcine mesenchymal stem cells (pMSCs) a Cre recombinase inducible latent mutant $TP53^{LSL-R167H}$ allele had been introduced into the endogenous $TP53$ gene locus in pMSCs (Figure 9) [256].

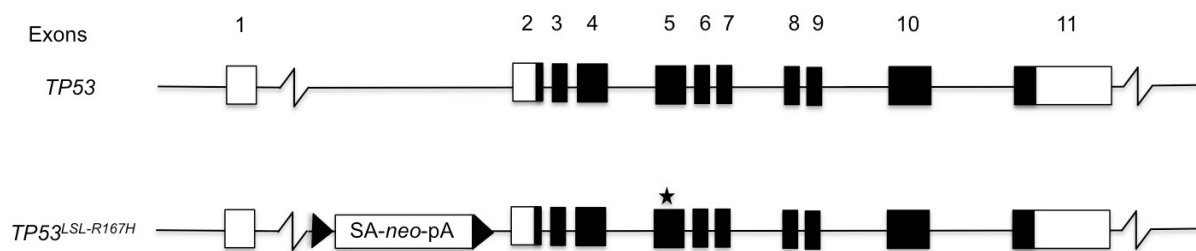


Figure 9: Schematic overview of the porcine wild-type and modified $TP53$ gene locus

Top: Porcine $TP53$ gene locus. Exon numbers are indicated, coding and non-coding regions are marked as black and open boxes. **Below:** Porcine $TP53^{LSL-R167H}$ gene locus. Black triangles mark loxP sites that flox a transcriptional termination cassette in intron 1, an asterisk indicates the G to A substitution in exon 5. Abbreviations: SA: splicing acceptor, *neo*: neomycin resistance gene, pA: poly adenylation signal. (Adapted from [256])

PCR analysis and sequencing of the mutation site in exon 5 conducted by Simon Leuchs, indicated the loss of the wild-type $TP53$ allele in one of the cell clones. This cell clone was designated as neo14. However, at the beginning of my work it was uncertain if the loss of the wild-type $TP53$ allele had been due to $TP53^{LSL-R167H}$ homo- or hemizygosity. Therefore, the

genotype of clone neo14 was designated as $TP53^{LSL-R167H/?}$. This cell clone was subjected to a second round of gene targeting to introduce a latent oncogenic $KRAS^{LSL-G12D}$ allele.

3.1.1 Design of the $KRAS^{LSL-G12D}$ gene targeting vector constructs

The $KRAS$ promoter trap gene vector comprised a 3.090 kb 5' short arm of homology corresponding to a region of $KRAS$ intron 1. 996 bp 5' of exon 2 a 1.3 kb floxed transcriptional termination cassette (LSL) was inserted. This contained either a blasticidin resistance gene (*bsr*) or a neomycin resistance gene (*neo*) as described previously [256]. The LSL cassette was followed by a 9.194 kb long arm of homology that also includes an engineered G to A point mutation within exon 2 that results in an amino acid substitution from glycine to aspartic acid at codon 12 (G12D) (Figure 10). The $KRAS-BS$ and $KRAS-NEO$ gene targeting vectors were constructed by Alexander Tschukes at our lab.

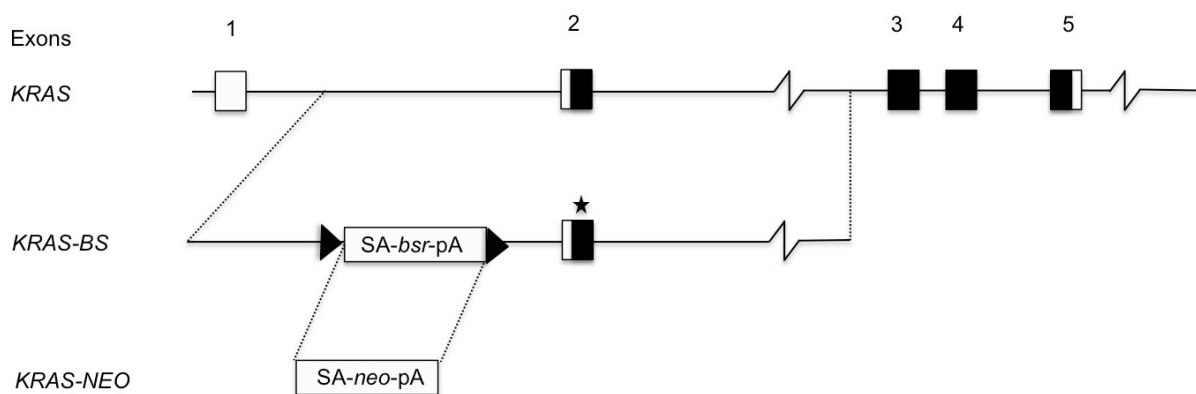


Figure 10: Schematic overview of the porcine $KRAS$ gene locus and design of the porcine $KRAS^{LSL-G12D}$ gene targeting vectors

Top: Porcine $KRAS$ gene locus. Exons are numbered, coding and non-coding exons are marked in black and open boxes. **Below:** $KRAS-BS$ and $KRAS-NEO$ gene targeting vectors, respectively. Vectors present the regions of homology, black triangles indicate loxP sites that flox the transcriptional termination cassette in intron 1, the A to G point mutation in exon 2 is indicated by an asterisk. Abbreviations: SA: splicing acceptor, *bsr*: blasticidin resistance gene, *neo*: neomycin resistance gene, pA: poly adenylation signal. (Adapted from [261])

3.1.2 Derivation of pMSCs carrying latent oncogenic $KRAS^{LSL-G12D}$ and $TP53^{LSL-R167H}$ alleles

To introduce a Cre recombinase activatable oncogenic $KRAS^{LSL-G12D}$ allele into the pMSC derived cell clone neo14, 1×10^6 cells at passage seven were electroporated with $10 \mu\text{g}$ of linearised $KRAS-BS$ gene targeting vector. Figure 11 shows the schematic overview of the $KRAS^{LSL-G12D}$ gene locus.

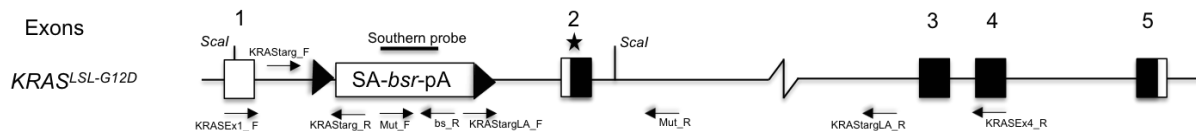


Figure 11: Schematic overview of the modified *KRAS*^{LSL-G12D} gene locus

Exons are numbered, coding and non-coding exons are marked in black and open boxes. Black triangles indicate loxP sites that flox the transcriptional termination cassette in intron 1, the A to G point mutation in exon 2 is indicated by an asterisk. PCR and RT-PCR primers that were used to identify targeted cells clones are indicated. *ScaI* restriction sites and the hybridisation probe used for Southern analysis are also shown. Abbreviations: SA: splicing acceptor, *bsr*: blasticidin resistance gene, pA: polyadenylation signal

BS-resistant single cell clones were screened for a *KRAS* targeting event by PCR using primers designed to amplify a 3.8 kb DNA fragment across the 5' junction of the short arm (*KRAS*starg_F) to the *bsr* gene (*KRAS*starg_R). In total, 65 single cell clones (designated as neo14/K- subclones) out of 119 were positive for the diagnostic 3.8 kb DNA fragment. This corresponds to a relative *KRAS*^{LSL-G12D} targeting efficiency of 54.6%. A representative screening result is depicted in Figure 12.

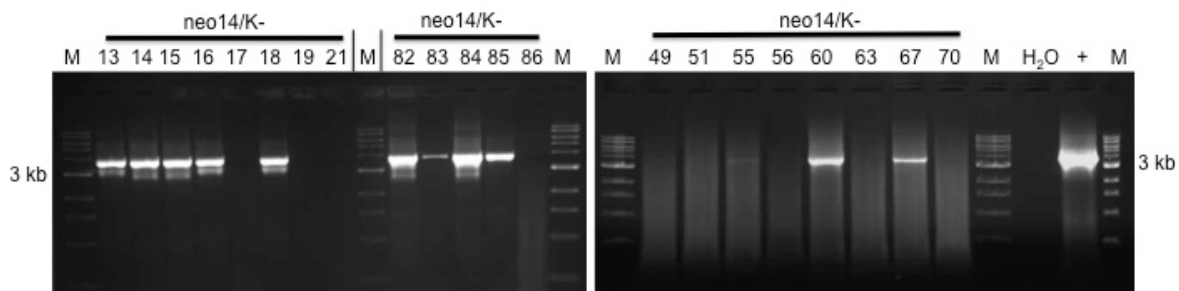


Figure 12: 5' targeting PCR of BS-resistant neo14/K- subclones

M: 1 kb DNA ladder; neo14/K- subclones 13, 14, 15, 16, 17, 18, 19, 21, 82, 83, 84, 85, 86, 49, 51, 55, 56, 60, 63, 67, 70, H₂O: water control, +: positive control, *KRAS*^{G12D} targeted cell clone
Eleven clones amplified the diagnostic 3.8 kb DNA fragment.

Figure 12 illustrates the *KRAS* targeting PCR over the short arm of 21 BS-resistant neo14/K- subclones. Twelve subclones show the expected 3.8 kb PCR product. Subclones neo14/K39 (not shown in Figure 12), neo14/K67, neo14/K82, neo14/K83 and neo14/K84 were characterised in more detail.

Next, a long range PCR was performed to confirm the integrity of the 3' end of the targeted *KRAS* gene locus. Primers were designed to amplify a 10.8 kb DNA fragment across the LSL cassette (*KRAS*stargLA_F) to the 3' junction of the targeting site (*KRAS*stargLA_R) spanning the long arm of the *KRAS*-BS gene targeting vector (Figure 13).

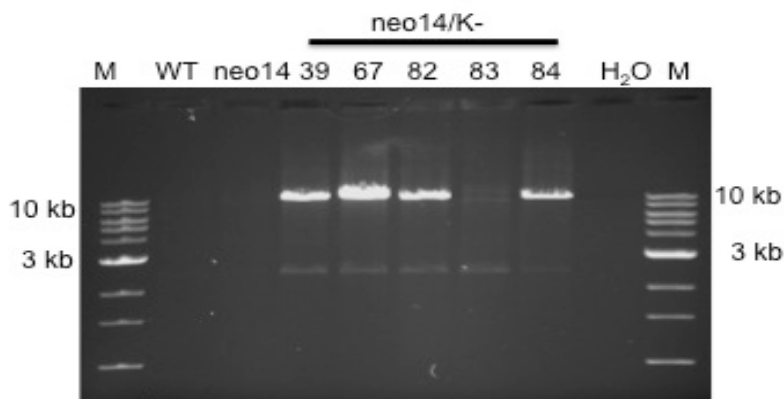


Figure 13: 3' targeting PCR of BS-resistant neo14/K- subclones

M: 1 kb DNA ladder; WT: wild-type pMSCs; neo14: parental cell clone neo14; neo14/K subclones: 39, 67, 82, 83 and 84, H₂O: water control. BS-resistant subclones neo14/K39, neo14/K67, neo14/K82 and neo14/K84 amplified the diagnostic 10.8 kb DNA fragment.

PCR screening over the long arm of the *KRAS-BS* gene targeting vector revealed the integrity of the 3' end of the targeted site in the subclones neo14/K39, neo14/K67, neo14/K82 and neo14/K84.

Next, these four cell clones were analysed for the presence of the *KRAS*^{G12D} mutation in exon 2. Since the G to A substitution in codon 12 results in gain of a *BclI* restriction enzyme recognition site, restriction fragment length polymorphism (RFLP) test was used to detect the presence of the G12D mutation. PCR was performed with oligonucleotides binding in the *bsr* gene (Mut_F) and 649 bp 3' of the second exon (Mut_R). The 2.8 kb amplified DNA fragment was subjected to *BclI* digest. The Table in Figure 14A shows sizes of expected DNA fragments after *BclI* restriction enzyme digest for wild-type *KRAS* (*KRAS*^{WT}) and mutant *KRAS* (*KRAS*^{G12D}) targeted alleles, respectively.

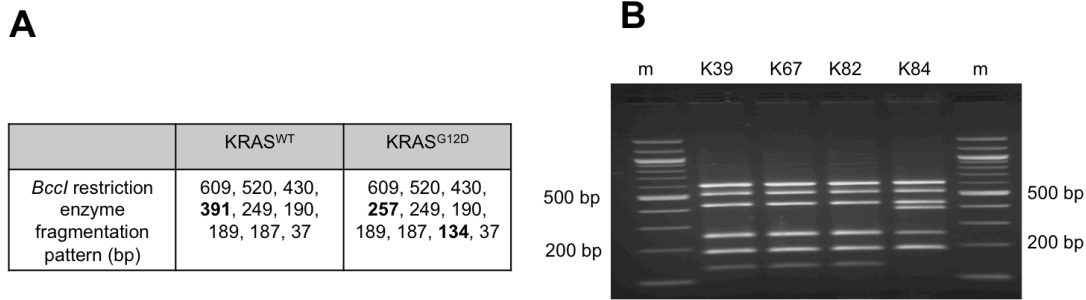


Figure 14: *BccI* RFLP test of BS-resistant neo14/K- subclones

A: *BccI* restriction enzyme fragmentation pattern of wild-type *KRAS*^{WT} and mutant *KRAS*^{G12D} targeted alleles. *BccI* digest of the 2.8 kb *KRAS*^{WT} DNA fragment results in a diagnostic 391 bp DNA fragment containing codon 12. The presence of the G to A mutation in exon 2 leads to an additional *BccI* restriction enzyme recognition site, whereby the 391 bp DNA fragment is cleaved into 257 bp and 134 bp DNA fragments. **B:** *BccI* digest of the 2.8 kb amplified DNA fragment of BS-resistant neo14/K- subclones. m: 100 bp DNA ladder; neo14/K- subclones 39, 67, 82, 84; Subclones neo14/K39, neo14/K67 and neo14/K82 showed the diagnostic *KRAS*^{G12D} restriction fragmentation pattern, while subclone neo14/K84 harbours the *KRAS*^{WT} sequence.

Figure 14B illustrates the results of the RFLP test of cell clones neo14/K39, neo14/K67, neo14/K82 and neo14/K84. Clones neo14/K39, neo14/K67 and neo14/K82 were verified for the presence of the *G12D* mutation in exon 2, while clone neo14/K84 possess the wild-type sequence at the targeted *KRAS* allele.

As PCR analysis and RFLP test evidenced positive *KRAS*^{LSL-G12D} targeting events for the clones neo14/K39, neo14/K67 and neo14/K82, these clones were subjected to Southern blot analysis to investigate the lack of any additional random integrations of the *KRAS-BS* targeting construct in these cell clones. The used BS probe hybridizes to the *bsr* gene and detects a 6.5 kb *ScaI* fragment indicative for the integration of the LSL-BS cassette at the endogenous *KRAS* gene locus. As negative controls wild-type pMSCs and the non-targeted subclone neo14/K83 were included. As shown in Figure 15, the 6.5 kb DNA fragment, indicative for a targeted *KRAS*^{LSL-G12D} allele, was present in the subclones neo14/K39, neo14/K67 and neo14/K82 and absent in wild-type pMSCs and subclone neo14/K83. Moreover, no additional random integration of the *KRAS-BS* targeting construct was observed.

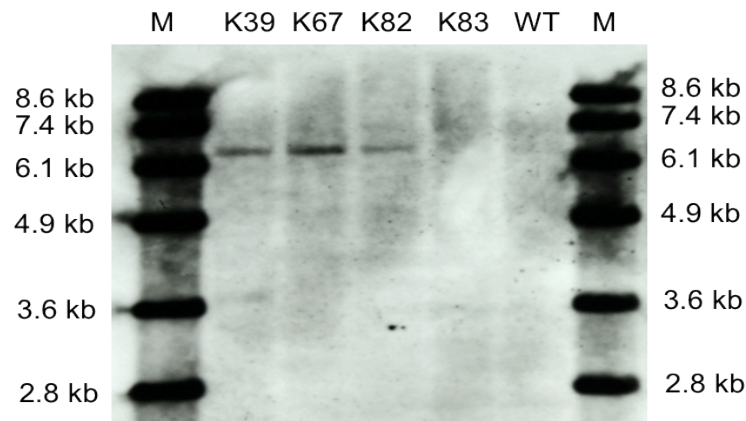


Figure 15: Southern blot analysis of BS-resistant neo14/K- subclones

M: Dig-UTP labelled marker; neo14/K- subclones 39, 67, 82, 83; WT: wild-type pMSCs. The applied DIG-UTP labelled probe hybridizes to the *bsr* gene in the LSL-BS cassette. The diagnostic 6.5 kb *ScaI* fragment is indicative for the integration of the LSL-BS cassette at the endogenous *KRAS* gene locus. The $KRAS^{LSL-G12D}$ targeted subclones neo14/K39, neo14/K67 and neo14/K82 show the expected 6.5 kb *ScaI* fragment, while it is absent in wild-type pMSCs and the subclone neo14/K83.

Next, RT-PCR analyses were carried out to assess the expression of wild-type *KRAS* mRNA and truncated *KRAS*-BS mRNA transcripts. Therefore, primers designed to amplify a 492 bp DNA fragment from exon 1 (*KRASEx1_F*) to exon 4 (*KRASEx4_R*) were used to detect expression of wild-type *KRAS* mRNA. Whereas the expression of truncated *KRAS*-BS mRNA was verified by the amplification of a 536 bp DNA fragment from exon 1 to the *bsr* selectable marker gene (*bs_R*). As illustrated in Figure 16, wild-type pMSCs and the parental cell clone neo14 expressed only wild-type *KRAS* mRNA, while $KRAS^{LSL-G12D}$ targeted cell clones additionally expressed the truncated *KRAS*-BS mRNA species.

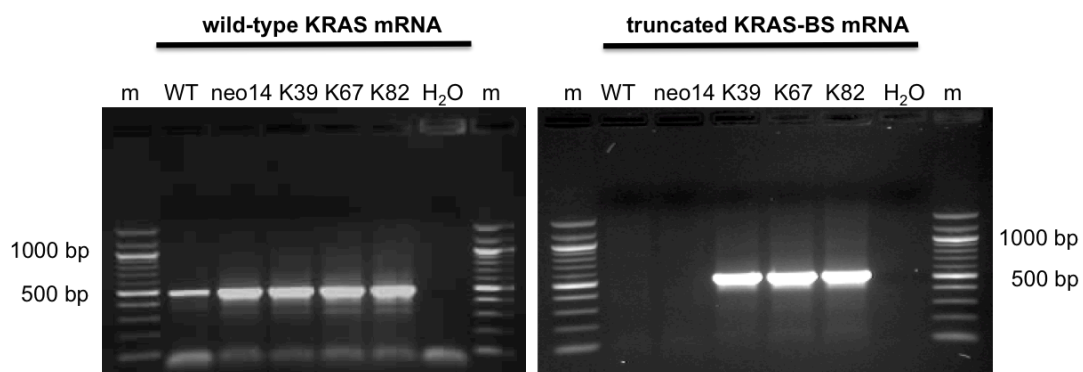


Figure 16: RT-PCR analysis of BS-resistant neo14/K- subclones

m: 100 bp DNA ladder; WT: wild-type cpMSCs; neo14: parental cell clone neo14; neo14/K- subclones: 39, 67, 82, H₂O: water control; All assessed cell samples expressed the wild-type *KRAS* mRNA transcript (492 bp). The expression of the truncated *KRAS*-BS mRNA transcript (536 bp) was detected only in the $KRAS^{LSL-G12D}$ targeted cell clones neo14/K39, neo14/K67 and neo14/K82.

In summary, PCR and RT-PCR analyses proved the integrity and the functionality of the targeted $KRAS^{LSL-G12D}$ allele in the subclones neo14/K39, neo14/K67 and neo14/K82. For that reason, the genotypes of them are designated as $TP53^{LSL-R167H/?}$, $KRAS^{LSL-G12D/+}$. The

next step was to show that the latent oncogenic $TP53^{LSL-R167H}$ and $KRAS^{LSL-G12D}$ alleles can be activated by Cre recombinase mediated cassette excision.

3.2 Activation of latent oncogenic $TP53^{LSL-R167H}$ and $KRAS^{LSL-G12D}$ alleles

To induce the expression of the porcine $TP53^{R167H}$ and $KRAS^{G12D}$ mutations in genetically modified pMSCs, the cell clone neo14/K67 ($TP53^{LSL-R167H/+}$; $KRAS^{LSL-G12D/+}$) was subjected to Cre recombinase mediated cassette excision and single cell clones were obtained by limiting dilution of cells into 96-well dishes. Cre mediated recombination should lead to the excision of the floxed transcriptional stop cassettes and the relative selectable marker genes at the distinct targeted gene loci (Figure 17).

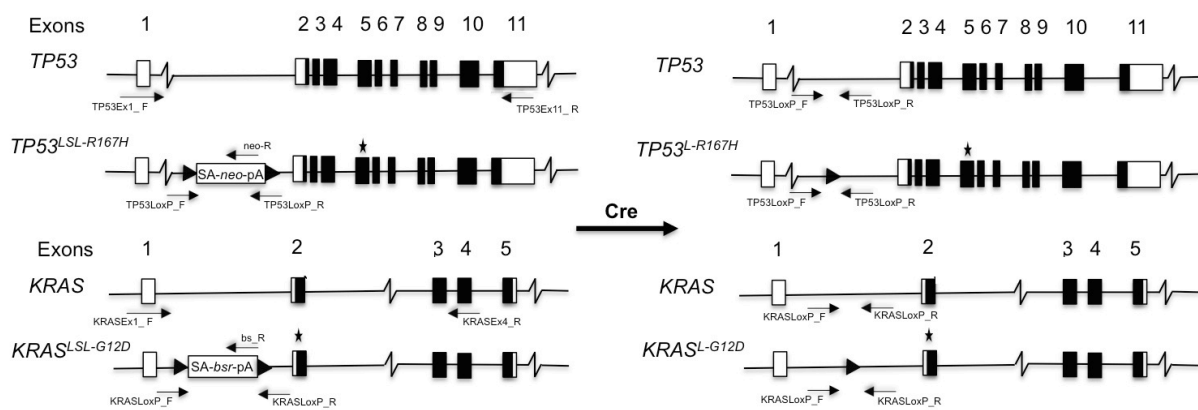


Figure 17: Schematic overview of the wild-type and gene targeted $TP53$ and $KRAS$ gene loci before and after Cre recombinase mediated cassette excision

Left: Porcine wild-type and gene targeted $TP53$ and $KRAS$ gene loci before Cre recombinase mediated cassette excision. **Right:** Porcine wild-type and gene targeted $TP53$ and $KRAS$ gene loci after Cre recombinase mediated cassette excision. Exons are numbered, coding and non-coding exons are marked in black and open boxes. Black triangles indicate loxP sites that flox the transcriptional termination cassettes in intron 1, introduced point mutations in exons are indicated by an asterisk. PCR and RT-PCR primers that were used to identify the excision of the relative floxed transcriptional termination cassettes are also shown. Abbreviations: SA: splicing acceptor, *bsr*: blasticidin resistance gene, *neo*: neomycin resistance gene pA: poly adenylation signal.

To get a rough idea of the efficiency of Cre mediated cassette excision a functional screen for loss of the respective floxed selection cassettes was conducted. In this regard, 22 single cell clones were split into culture medium supplemented with either 8 $\mu\text{g/ml}$ BS or 600 $\mu\text{g/ml}$ G418, while the rest of the cells was expanded in medium without any selection additives. As illustrated in Figure 18 the floxed LSL-BS cassette at the endogenous mutant $KRAS^{LSL-G12D}$ gene locus was excised in all analysed single cell clones (Blasticidin S selection). While six out of the 22 single cell clones still harboured the floxed transcriptional stop cassette at the endogenous mutant $TP53^{LSL-R167H}$ gene locus (G418 selection). Collectively, these data indicate that Cre mediated cassette excision was very efficient at the targeted $KRAS$ gene locus and less so at the targeted $TP53$ gene locus.

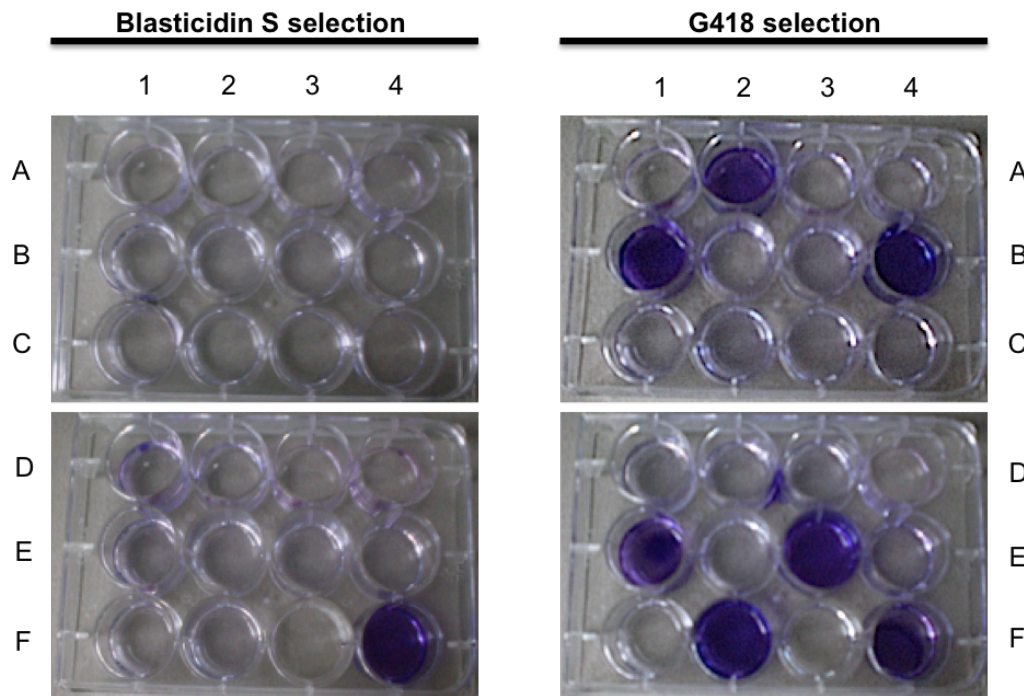


Figure 18: Functional screen for loss of floxed selection cassettes

A1-A4: cell clones neo14/K67/1.1-1.4; B1-B4: cell clones neo14/K67/1.5-1.8; C1-C4: cell clones neo14/K67/1.9-1.12; D1-D4: cell clones neo14/K67/1.13-1.16; E1-E4: cell clones neo14/K67/1.17-1.20; F1-F2: cell clones neo14/K67/1.21-1.22; F3: no cells; F4: un-induced cell clone neo14/K67. None of the single cell clones (A1-F2) survived Blasticidin S selection, indicating the successful excision of the floxed LSL-BS cassette at the targeted $KRAS^{LSL-G12D}$ allele. As a control the parental, un-induced cell clone neo14/K67 (F4) was cultured in parallel. This cell clone survived Blasticidin S selection due to the non-excised floxed LSL-BS cassette. Like the parental clone neo14/K67, the subclones neo14/K67/1.2 (A2), neo14/K67/1.5 (B1), neo14/K67/1.8 (B4), neo14/K67/1.17 (E1), neo14/K67/1.19 (E3) and neo14/K67/1.21 (F2) survived G418 selection, indicating the presence of the LSL-neo cassette at the targeted $TP53^{LSL-R167H}$ allele.

After this functional screen, genomic DNA of the fully recombined cell clones neo14/K67/1.1, neo14/K67/1.3, neo14/K67/1.4 and the partially recombined cell clone neo14/K67/1.8 was isolated and PCR was performed to confirm the successful recombination of the floxed stop cassettes. Excision of the LSL-BS cassette leaves a single 34 bp loxP site in the first intron of the recombined $KRAS^{L-G12D}$ allele. Excision of LSL-NEO cassette leaves a 34 bp loxP site plus a 22 bp vector remnant in the first intron of the recombined $TP53^{L-R167H}$ allele. Using primer pairs spanning the respective LSL integration sites allowed the discrimination of wild-type, unrecombined and recombined mutant alleles. The KRAS PCR screen was designed to amplify a diagnostic 167 bp fragment from the wild-type $KRAS$ allele (KRAS-WT), a 1.486 kb fragment from the unrecombined targeted $KRAS^{LSL-G12D}$ allele (KRAS-LSL), and a 201 bp fragment from the recombined mutant $KRAS^{L-G12D}$ allele (KRAS-loxP), respectively. The TP53 PCR screen was designed in a similar manner to amplify a diagnostic 198 bp fragment from the wild-type $TP53$ allele (TP53-WT), a 1.929 kb fragment from the unrecombined $TP53^{LSL-R167H}$ allele (TP53-LSL), and a 254 bp fragment from the recombined $TP53^{L-R167H}$ allele (TP53-loxP), respectively.

As shown in Figure 19, in wild-type pMSCs only the 167 bp KRAS-WT fragment and the 198 bp TP53-WT fragment were detected. In the un-induced cell clone neo14/K67 (genotype: $TP53^{LSL-R167H/?}$, $KRAS^{LSL-G12D/+}$) the 167 bp KRAS-WT as well as the 1.486 kb unrecombined KRAS-LSL fragments and the 1.929 kb non-excised TP53-LSL fragment were amplified. Demonstrating the lack of a functional wild-type $TP53$ allele in this cell clone. In Cre protein transduced cell clones neo14/K67/1.1, neo14/K67/1.3, and neo14/K67/1.4 (genotype: $TP53^{L-R167H/?}$, $KRAS^{L-G12D/+}$) the 167 bp KRAS-WT as well as the 201 bp KRAS-loxP remnant fragments and the 254 bp TP53-loxP remnant fragment were detected. In contrast, in clone neo14/K67/1.8, which survived G148 selection, additionally to the 254 bp TP53-loxP remnant fragment the 1.929 kb unrecombined TP53-LSL fragment was amplified. This indicates that cell clone neo14/K67/1.8 harbours an unrecombined $TP53^{LSL-R167H}$ allele and a recombined $TP53^{L-R167H}$ allele, explaining the results of the functional selection screen. Furthermore, these findings evidence that both $TP53$ alleles were targeted. In this regard, the partially recombined cell clone neo14/K67/1.8 can be designated as $TP53^{L-R167H/LSL-R167H}$, $KRAS^{L-G12D/+}$. In addition, based on these results it can be concluded, that the parental cell clone neo14 was rather homozygous than hemizygous for a $TP53^{LSL-R167H}$ gene targeting and is therefore designated as $TP53^{LSL-R167H/LSL-R167H}$.

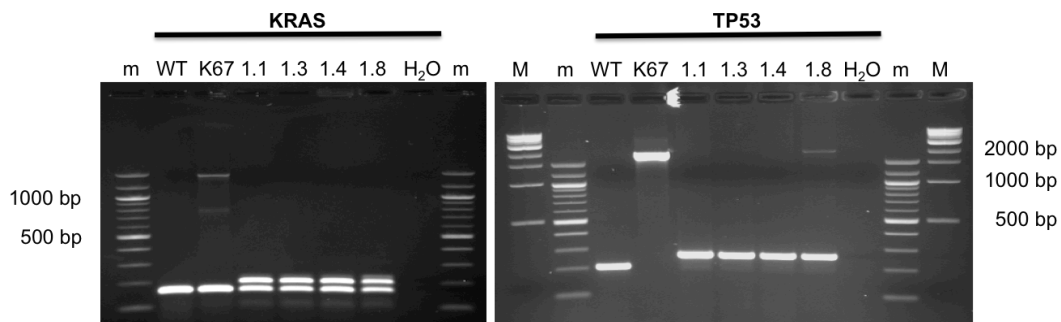


Figure 19: PCRs across the LSL integration sites before and after Cre protein transduction

m: 100 bp DNA ladder; WT: wild-type pMSCs; K67: un-induced cell clone neo14/K67; 1.1: Cre recombined cell clone neo14/K67/1.1; 1.3: Cre recombined cell clone neo14/K67/1.3; 1.4: Cre recombined cell clone neo14/K67/1.4; 1.8: partially recombined cell clone neo14/K67/1.8; H₂O: water control; **KRAS**: Wild-type pMSCs amplified only the 167 bp KRAS-WT fragment. Clone neo14/K67 amplified the 167 bp KRAS-WT fragment as well as the 1.486 kb unrecombined KRAS-LSL fragment. Cre recombined clones neo14/K67/1.1, neo14/K67/1.3, neo14/K67/1.4 and neo14/K67/1.8 amplified besides the 167 bp KRAS-WT fragment the 201 bp recombined KRAS-loxP fragment. **TP53**: In wild-type control cells only the 198 bp TP53-WT fragment was detected. The un-induced cell clone neo14/K67 amplified only the 1.929 kb unrecombined TP53-LSL fragment. In contrast, Cre recombinase transduced cell clones neo14/K67/1.1, neo14/K67/1.3 and neo14/K67/1.4 amplified only the 254 bp TP53-loxP fragment. The cell clone neo14/K67/1.8, which survived G148 selection, showed the amplification of the 1.929 kb unrecombined TP53-LSL fragment as well as the 254 bp recombined TP53-loxP fragment.

Next, RT-PCRs were performed to confirm on the one hand the lack of truncated KRAS-BS and TP53-NEO mRNA transcripts after Cre recombinase cassette exchange, and on the other hand the release of the expression of mutant KRAS-G12D and TP53-R167H mRNA species. As seen in Figure 20 un-induced neo14/K67 cells ($TP53^{LSL-R167H/LSL-R167H}$, $KRAS^{LSL-$

$G^{12D/+}$) expressed both the 492 bp truncated KRAS-BS mRNA (left) and the 630 bp truncated TP53-NEO mRNA species (right). Cre transduced cell clones neo14/K67/1.1, neo14/K67/1.3 and neo14/K67/1.4 ($TP53^{L-R167H/L-R167H}$, $KRAS^{L-G12D/+}$) lacked the expression of these truncated mRNA transcripts. And as expected, the partially recombined cell clone neo14/K67/1.8 ($TP53^{LSL-R167H/L-R167H}$, $KRAS^{L-G12D/+}$) still expressed the 630 bp truncated TP53-NEO mRNA transcript.

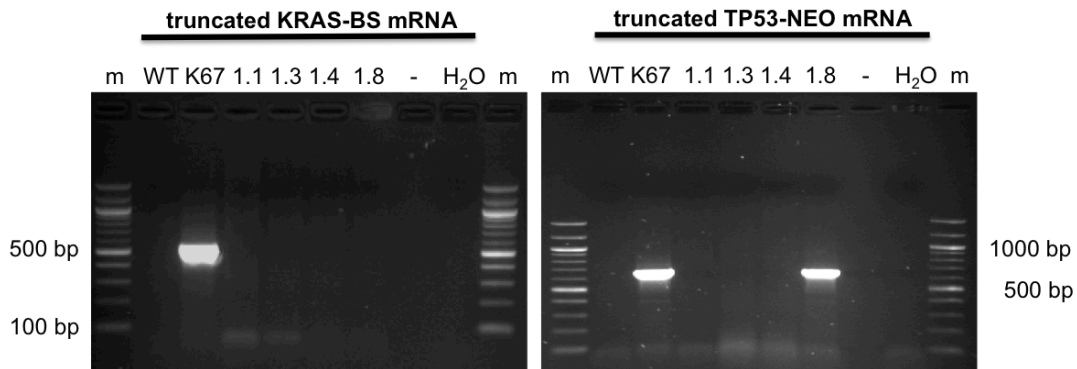


Figure 20: RT-PCR of truncated KRAS-BS and TP53-NEO mRNA transcripts before and after Cre protein transduction

m: 100 bp DNA ladder; WT: wild-type pMSCs; K67: un-induced cell clone neo14/K67; 1.1: fully recombined cell clone neo14/K67/1.1; 1.3: fully recombined cell clone neo14/K67/1.3; 1.4: fully recombined cell clone neo14/K67/1.4; 1.8: partially recombined cell clone neo14/K67/1.8; H₂O: water control; Only the un-induced cell clone neo14/K67 expressed both the 492 bp truncated KRAS-BS and the 630 bp TP53-NEO mRNA species. The lack of these transcript variants was detected in the Cre protein transduced cell clones neo14/K67/1.1, neo14/K67/1.3 and neo14/K67/1.4. In contrast, the partially recombined cell clone neo14/K67/1.8 still expressed the truncated TP53-NEO mRNA transcript.

As the excision of the floxed transcriptional stop signals should lead to the expression of mutant KRAS-G12D mRNA and mutant TP53-R167H mRNA transcripts, RT-PCR amplification followed by RFLP analysis were carried out to verify the expression of the distinct mutant mRNA species. To confirm the expression of mutant KRAS-G12D mRNA the 492 bp RT-PCR product from exon 1 to exon 4 was digested with *BccI* restriction enzyme that allowed the discrimination of wild-type KRAS from mutant KRAS-G12D transcripts. In the case of wild-type KRAS expression the 492 bp fragment is cleaved into 261 bp and 231 bp, whereas the appearance of 261 bp, 126 bp and 105 bp *BccI* fragments are consistent with the expression of mutant KRAS-G12D mRNA species. Figure 21 depicts the restriction fragmentation pattern of the 492 bp RT-PCR product after *BccI* RFLP test. Wild-type pMSCs and the un-induced cell clone neo14/K67 transcribed only the wild-type *KRAS* alleles, as indicated by the 261 bp and 231 bp DNA fragments after *BccI* digest. The presence of 261 bp, 126 bp and 105 bp was only detected for the recombined cell clones neo14/K67/1.1, -1.3, -1.4 and -1.8. These results prove that these clones expressed the mutant KRAS-G12D mRNA transcript.

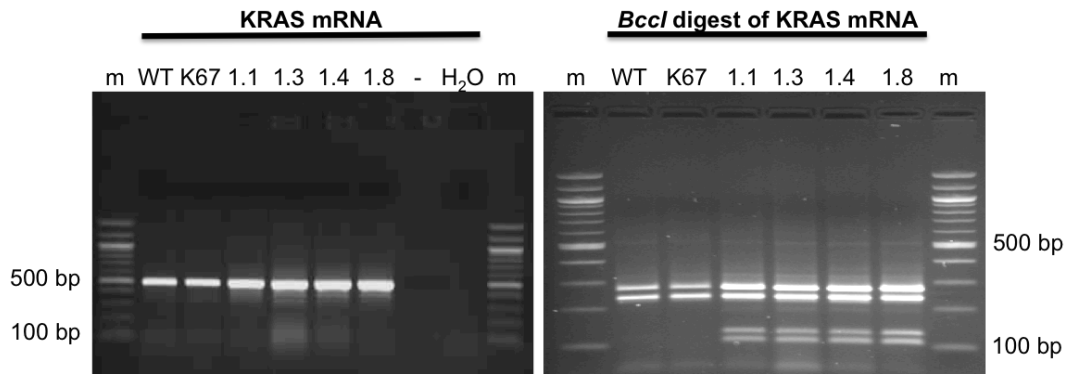


Figure 21: *BclI* RFLP test of KRAS mRNA species before and after Cre protein transduction

m: 100 bp DNA ladder; WT: wild-type pMSCs; K67: un-induced clone neo14/K67; 1.1: fully recombined cell clone neo14/K67/1.1; 1.3: fully recombined cell clone neo14/K67/1.3; 1.4: fully recombined cell clone neo14/K67/1.4; 1.8: partially recombined cell clone neo14/K67/1.8; -: free lane; H₂O: water control; **KRAS mRNA**: Expression of a 492 bp RT-PCR product from exon 1 to exon 4 in all analysed cell clones. ***BclI* digest of KRAS mRNA**: Wild-type control cells and the un-induced cell clone neo14/K67 expressed only wild-type KRAS mRNA transcripts as indicated by the restriction fragmentation pattern of 261 bp and 231 bp. In contrast, Cre recombined cell clones neo14/K67/1.1, neo14/K67/1.3, neo14/K67/1.4 and neo14/K67/1.8 expressed both wild-type (261 bp, 231 bp) and mutant KRAS-G12D (261bp, 126 bp and 105 bp) mRNA species.

The expression of mutant TP53-R167H mRNA species was detected in a similar manner. Here, the 1.313 kb RT-PCR product from exon 1 to exon 11 was subjected to *HaeIII* digest. The G to A substitution mutation in codon 167 results in loss of a restriction recognition site for *HaeIII* allowing to distinguish wild-type from mutant TP53-R167H mRNA. *HaeIII* digest of wild-type TP53 mRNA species generates DNA fragments with a size of 698 bp, 310 bp, 287 bp and 18 bp. Mutant TP53-R167H mRNA species is cleaved into 985 bp, 310 bp and 18 bp. As illustrated in Figure 22, wild-type pMSCs transcribed only the wild-type *TP53* alleles (698 bp, 310 bp and 287 bp), whereas no p53 expression was detected in the unrecombined cell clone neo14/K67, consistent with a homozygous *TP53*^{LSL-R167H} targeting event. In contrast, after Cre protein transduction all recombined cell clones expressed the mutant TP53-R167H mRNA transcript (985 bp and 310 bp).

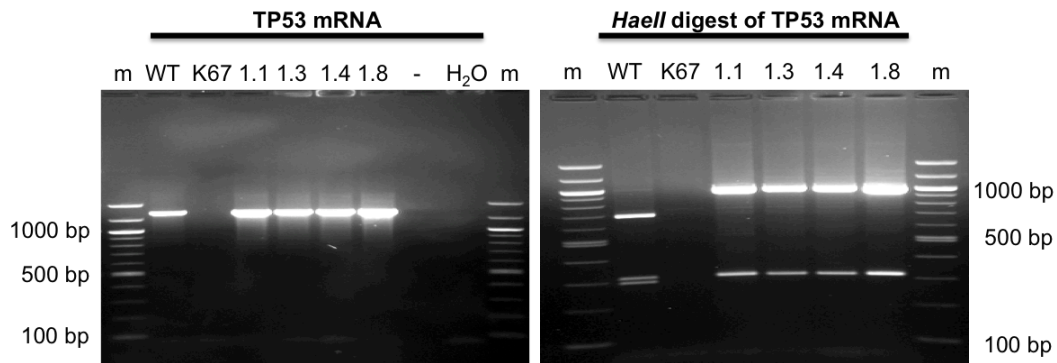


Figure 22: *Haell* RFLP test of TP53 mRNA species before and after Cre protein transduction

m: 100 bp DNA ladder; WT: wild-type pMSCs; K67: un-induced cell clone neo14/K67; 1.1: fully recombined cell clone neo14/K67/1.1; 1.3: fully recombined cell clone neo14/K67/1.3; 1.4: fully recombined cell clone neo14/K67/1.4; 1.8: partially recombined cell clone neo14/K67/1.8; -: free lane; H₂O: water control; **TP53 mRNA**: Expression of the 1.313 kb RT-PCR product from exon 1 to exon 11 was detected in all analysed cell clones, except for the un-induced cell clone neo14/K67. ***Haell* digest of TP53 mRNA**: Wild-type pMSCs expressed only wild-type TP53 mRNA transcripts, as indicated by the restriction fragmentation pattern of 698 bp, 310 bp, 287 bp and 18 bp (the smallest fragment of 18 bp was not detectable). In the case of the un-induced cell clone neo14/K67 no p53 expression was detected. After the excision of the LSL-NEO cassette, the expression of mutant TP53-R167H mRNA species was induced in all analysed cell clones. In this case, *Haell* cleaves the 1.313 kb RT-PCR product into 985 bp and 310 bp DNA fragments (again, the smallest fragment with 18 bp was not detectable).

To summarise, all analysis performed on RNA level have proven that the excision of the relative transcriptional stop cassettes leads to the expression of both mutant KRAS-G12D and mutant TP53-R167H mRNA species in the Cre recombined cell clones. As predicted for the un-induced cell clone neo14/K67, the expression of mutant mRNA transcripts is blocked by the presence of the relative LSL cassettes.

Next, we were interested in investigating if the activated mutant *KRAS*^{L-G12D} allele and *TP53*^{L-R167H/L-R167H} alleles have similar biochemical functions and effects as their human and murine orthologous. In humans, the missense R175H mutation in the *TP53* gene leads to the expression of stabilised p53 protein that has a prolonged half life compared to wild-type p53 protein [76]. The G12D mutation in the *KRAS* gene was shown to result in a permanently GTP-bound Kras protein (Ras-GTP) that causes constitutive downstream signalling [262]. To evaluate the expression and abundance of wild-type and mutant p53 proteins, Western blot analysis was performed with wild-type pMSCs, the un-induced cell clone neo14/K67 and the fully Cre recombined cell clone neo14/K67/1.1. In addition, the expression of constitutive active GTP-bound Ras protein was assessed by a Ras Activation Assay (see Figure 23).

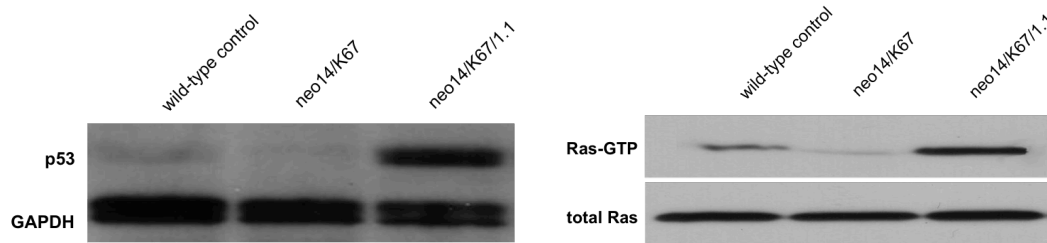


Figure 23: p53 Western blot and Ras Activation Assay

Left: For p53 Western blot analysis wild-type pMSCs, neo14/K67 and neo14/K67/1.1 samples were loaded. Recombined neo14/K67/1.1 cells show abundant p53 protein (46 kDa) levels compared to wild-type control cells and un-induced neo14/K67 cells. As expected for un-induced neo14/K67 cells, no p53 protein was detected. As loading control the expression of GAPDH (36 kDa) was investigated. **Right:** Ras Activation Assay was performed with wild-type pMSCs, neo14/K67 and neo14/K67/1.1 samples. Expression of the $KRAS^{L-G12D}$ allele in fully recombined neo14/K67/1.1 cells cause an increase in Ras-GTP (21 kDa) levels compared to wild-type pMSCs and un-induced neo14/K67 cells. As loading control total Ras protein (21 kDa) levels were assessed.

As depicted in Figure 23, expression of mutant $TP53^{L-R167H/L-R167H}$ alleles in porcine mesenchymal stem cells leads to the accumulation of stabilised p53-R167H protein. This result is in full agreement with data gained from expression analysis of oncogenic human p53-R175H and murine p53-R172H proteins, respectively. Moreover, the expression of the mutant $KRAS^{L-G12D}$ allele causes elevated GTP-bound Ras levels in porcine cells, indicating that the porcine $KRAS^{G12D}$ mutation has similar effects as their human and murine orthologous [226,263].

Collectively, all these data demonstrate that we were successful in deriving porcine mesenchymal stem cells that express mutant TP53-R167H mRNA and oncogenic KRAS-G12D mRNA transcripts from their endogenous gene loci. However, the most important finding is, that both mutant p53-R167H and oncogenic Kras-G12D proteins show similar effects as their human and murine counterparts.

3.3 Inducing a deregulated cMyc expression in mutant $TP53^{R167H}$ and $KRAS^{G12D}$ pMSCs

It is well documented that expression of oncogenic *RAS* and dominant-negative *TP53* genes alone are sufficient to convert mouse cells, but not human cells, to a fully transformed phenotype [233]. Since the *MYC* gene is the most frequently amplified oncogene in human cancers [140] and plays a pivotal role in the transformation process of primary human cells [25,264,265] we wanted to evaluate its contribution to porcine tumorigenesis.

To mimic amplification of the porcine *cMYC* gene *in vitro* 1.327 kb of porcine *cMYC* cDNA (GenBank:NM_001005154.1) flanked by 158 bp and 41 bp fragments of 5' and 3' untranslated regions (UTRs), respectively, were expressed from a vector containing the mouse phosphoglycerate kinase (PGK) promoter. As a selectable marker the bsr coding sequence linked by an internal ribosome entry site (IRES) sequence was placed behind the *cMYC* coding sequence. For cloning the *cMyc* expression vector, designated as pPGK-

pocMyc-IRES-BS-pA, the mammalian expression vector pcDNA3 was used. Figure 24 illustrates the structure of the expression vector.



Figure 24: Schematic design of the pPGK-pocMyc-IRES-BS-pA expression vector

PGK: phosphoglycerate kinase promoter; cMyc: coding sequence of porcine cMYC; IRES: internal ribosome entry site; *bsr*: blasticidin resistance gene, pA: poly adenylation signal; SV40: Simian virus 40 promoter; *Kana/neo*: neomycin resistance gene

The vector pPGK-pocMyc-IRES-BS-pA was used to induce a deregulated cMyc expression in Cre recombined neo14/K67/1.1 cells. Before adding the vector to the cells, the plasmid-DNA was subjected to *FspI* digest generating a linearised plasmid at the *neomycin* resistance gene. Transfected cells were split into Blasticidin S selection medium and RNA was isolated from pooled stable selected transfectants designated as neo14/K67/1.1+cMyc (genotype: $TP53^{L-R167H/L-R167H}$, $KRAS^{L-G12D/+}$, *cMyc*). Quantitative real-time PCR revealed that transfected neo14/K67/1.1+cMyc cells showed an averaged 1.7 fold increase in cMyc mRNA expression compared to the parental, untransfected cell clone neo14/K67/1.1 (Figure 25A). Furthermore, these results were also confirmed on protein level by Western blot analysis (Figure 25B).

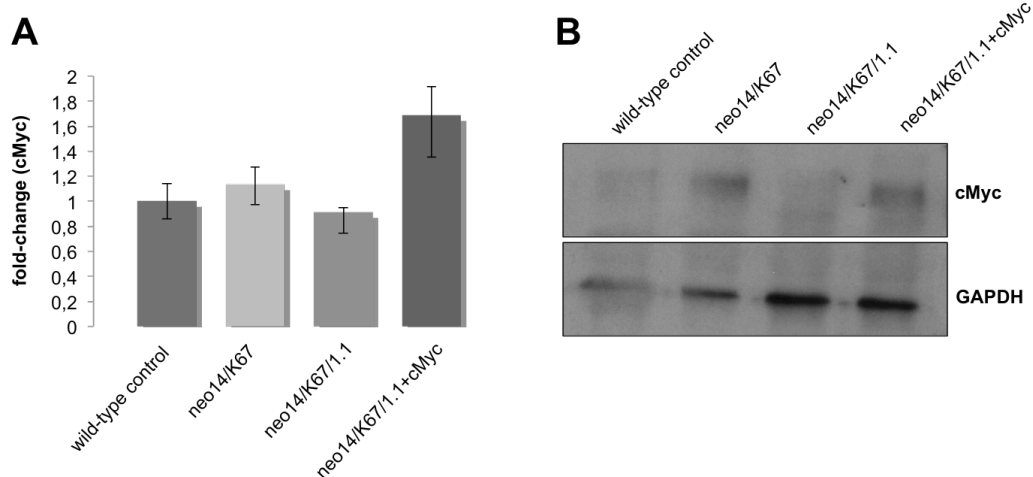


Figure 25: Investigating cMyc expression levels

A: Relative cMyc expression levels in the stepwise modified porcine cells compared to the distinct parental cell clone. Depicted are fold-change values of the cell clones, normalised to GAPDH mRNA expression. Transfected neo14/K67/1.1+cMyc cells show an averaged 1.7 fold increase in cMyc mRNA expression compared to the parental, untransfected neo14/K67/1.1 cells. **B:** cMyc Western blot analysis. Transfected neo14/K67/1.1+cMyc cells showed increased cMyc protein levels (50kDa) compared to untransfected neo14/K67/1.1 cells. As loading control the expression of GAPDH (36 kDa) was investigated.

The results in Figure 25 demonstrate that stable selected cMyc transfectants show increased cMyc mRNA and protein levels compared to parental, untransfected neo13/K67/1.1 cells. These data indicate the functionality of the pPGK-pocMyc-IRES-BS-pA vector construct.

3.4 Investigating TERT expression in stepwise genetically modified pMSCs

Typically, primary porcine cells become rapidly senescent after gene targeting and single cell cloning [266]. However, this was not the case with the cell clone neo14, which lacks p53 expression. Moreover, these cells showed considerably extended lifespan in culture [256] that enabled a second round of gene targeting and repeated isolation of single cell clones (neo14/K- and neo14/K67/- subclones). These unique growth characteristics led to the assumption that neo14 cells and all subclones had bypassed replicative senescence and have been immortalised. As mentioned before, unlimited replicative lifespan is an essential prerequisite for neoplastic cell transformation [267]. In the majority of human cancers telomere lengths are maintained by the reactivated expression of the telomerase reverse transcriptase (TERT) [40]. To test if this was also the case for the stepwise genetically modified pMSCs, RT-PCR was conducted to figure out if the expression of TERT was reactivated in these cells (Figure 26).

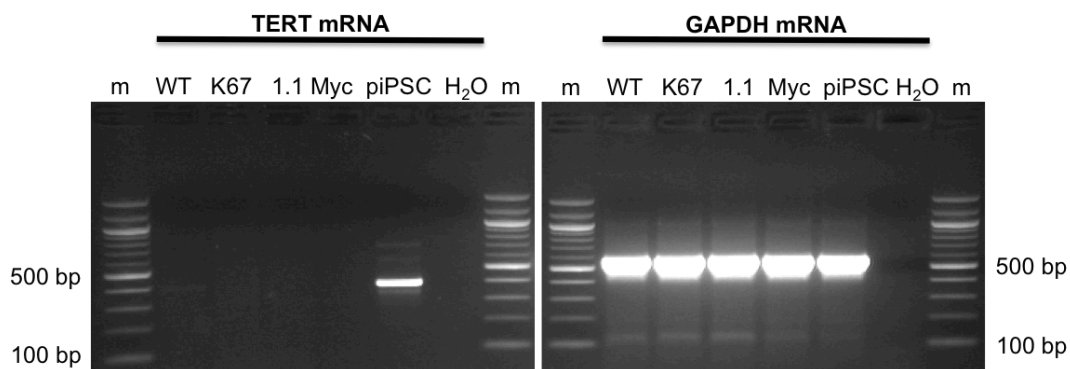


Figure 26: RT-PCR to detect TERT reactivation

m: 100 bp DNA ladder; WT: wild-type pMSCs; K67: un-induced cell clone neo14/K67, 1.1: Cre recombined cell clone neo14/K67/1.1; Myc: cell pool neo14/K67/1.1+cMyc; piPSC: putative porcine induced pluripotent stem cells, H₂O: water control; The expression of TERT was detected only in piPSC by a diagnostic 387 bp DNA fragment. GAPDH (567 bp) was run as loading control.

As shown in Figure 26 only putative porcine iPS cells, which were established by Xinxin Cui in our lab, express TERT at detectable levels. These results demonstrate that the extended lifespan of the genetically modified pMSCs was not a result of reactivated TERT expression. Thus the observed unrestricted replicative capacity of the modified pMSCs must be a consequence of a telomerase-independent mechanism. Consistent with this idea, several studies have shown, that some cells can escape cellular senescence and extend their replicative lifespan by the simultaneous inactivation of the potent tumour suppressors p53 and pRb [41,42]. Recent findings revealed that the *CDKN2A* locus and its gene products,

which are pivotal regulators of the p53 and pRb pathways, mediate culture- and oncogene-induced senescence [116,268,269]. In this regard, the concomitant inactivation of normal p53 and p16INK4 α -Rb signalling cascade was shown to allow primary human cells to escape replicative senescence [37,270,271]. For that reason the expression of the CDKN2A's gene products was investigated in more detail.

3.5 Investigating the *CDKN2A* gene locus in stepwise genetically modified pMSCs

The *CDKN2A* gene locus encodes two important tumour suppressors, p16INK4 α and p14ARF in overlapping but distinct reading frames. Both gene products play a potent role in regulating either the p53 or the pRb pathway. While p14ARF is a critical component of the p53 pathway by stabilising p53, p16INK4 α is a crucial element of the pRb pathway by regulating posttranslational modifications of pRb. Compelling evidences stated, that p14ARF exerts a predominant role in coordinating senescence in murine cells, while the opposite is seen for p16INK4 α , which is the main senescence mediator in human cells. In accordance with these findings, it was noted, that the loss of normal ARF function in murine embryonic fibroblasts elicits immortalisation, whereas the loss of INK4 α is required to immortalise primary human cells [118,272]. Based on these findings RT-PCRs were conducted to analyse the expression of the tumour suppressors p16Ink4 α and p14ARF in the genetically modified pMSCs (Figure 27).

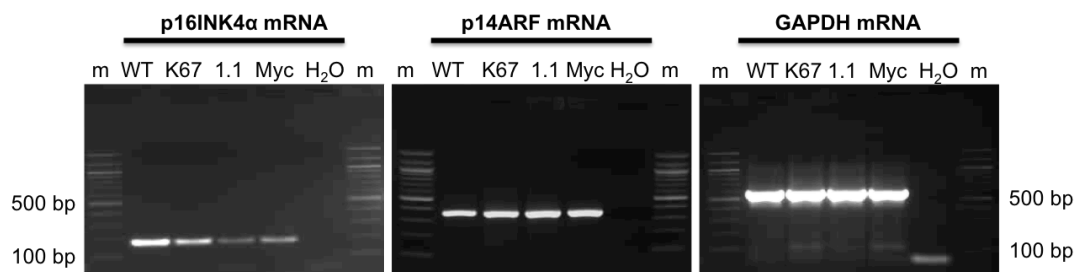


Figure 27: RT-PCR analysis of p16INK4 α and p14ARF expression levels

m: 100 bp DNA ladder; WT: wild-type pMSCs; K67: un-induced cell clone neo14/K67; 1.1: Cre recombined cell clone neo14/K67/1.1; Myc: cell pool neo14/K67/1.1+cMyc; H₂O: water control; **p16INK4 α mRNA:** The expression of p16INK4 α mRNA was detected by a diagnostic 176 bp fragment. While the expression of p16INK4 α is abundantly in wild-type pMSCs, it gradually decreases in the stepwise modified pMSCs. **p14ARF mRNA:** The expression of p14ARF was detected in all analysed cell isolates by a diagnostic 361 bp fragment. As a loading control the expression of GAPDH (567 bp) was investigated.

As shown in Figure 27, un-induced neo14/K67 cells express less p16Ink4 α than wild-type control cells. Neo14/K67/1.1 cells and neo14/K67/1.1+cMyc expressing mutant *TP53*^{R167H} and *KRAS*^{G12D} showed a further reduction in p16INK4 α expression. In contrast, the expression of p14ARF remains very similar in all analysed samples. Next, the relative gene expression levels of p16INK4 α and p14ARF were analysed by quantitative real-time RT-PCR

As depicted in Figure 28A the expression of p16INK4 α was greatly diminished in neo14/K67 cells lacking p53 (eleven fold down-regulation) and almost absent in neo14/K67/1.1 cells. The same was seen in cells with a deregulated cMyc expression. Importantly, while mRNA expression levels of p16INK4 α decreased in the genetically modified pMSCs, p14ARF mRNA expression increased (Figure 28B).

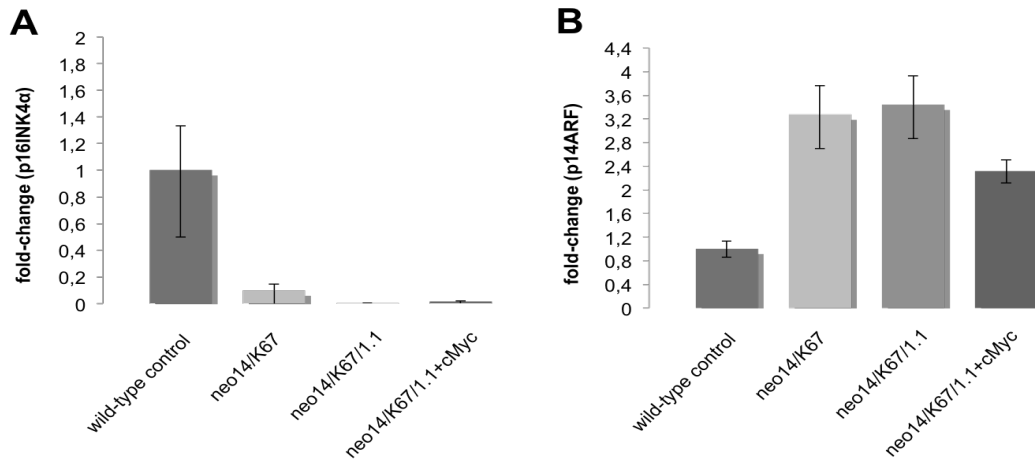


Figure 28: Quantification of p16INK4 α and p14ARF expression levels

Depicted are fold-change values of the distinct cell clones relative to wild-type pMSCs. Values were normalised to GAPDH mRNA expression. **A:** Relative expression levels of porcine p16INK4 α . Gradual down-regulation of p16INK4 α mRNA expression in stepwise genetically modified pMSCs compared to wild-type pMSCs. **B:** Relative expression levels of porcine p14ARF. Increased p14ARF mRNA expression in the stepwise genetically modified pMSCs compared to wild-type pMSCs.

To investigate if the expression of p16INK4 α was already downregulated in the parental cell clone neo14 quantitative real-time RT-PCR was conducted. Surprisingly, the data revealed that the expression of p16INK4 α remained pretty similar in the parental cell clone neo14 compared to wild-type pMSCs (one fold down-regulation).

To summarize, genetically modified pMSCs (neo14/K67, neo14K67/1.1 and neo14K67/1.1+cMyc) have downregulated the expression of p16INK4 α , while the expression of p14ARF increased. These expression data may indicate, that the downregulated expression of p16INK4 α in combination with loss of wild-type p53 function facilitated the unrestricted proliferative capacity of the modified pMSCs.

Since the expression analyses demonstrated the repression of p16INK4 α mRNA expression in the stepwise modified pMSCs, we were interested in uncovering the underlying mechanism. According to the results in Figure 28 it can be concluded that the impaired p16INK4 α expression is neither a consequence of homozygous deletion of the gene locus nor of point mutations or small deletions of the second and third exons, as p16INK4 α and p14ARF are encoded in overlapping but distinct reading frames [273]. As p16INK4 α and p14ARF are transcribed from distinct independent promoters [107] it was more likely that the underlying mechanism of p16INK4 α mRNA silencing was a consequence of epigenetic

modifications, such as gene methylation. Therefore, the methylation status of a 5' region of porcine *P16INK4A* comprising part of the first exon and first intron was investigated. Primers used covered the ATG start codon and 131 bp 3' of exon 1. PCR amplification of bisulfite-converted gDNA resulted in a 266 bp fragment encompassing 21 CpGs. As depicted in Figures 29A and 29B all 21 CpGs were non-methylated in wild-type pMSCs, while in neo14/K67 cells 71.4% of all analysed CpGs were methylated. For neo/K67/1.1 cells, expressing mutant p53-R167H and Kras-G12D proteins, 81.0% of CpGs showed a methylation signature and in stable selected cMyc transfectants 90.5% of CpGs were methylated.

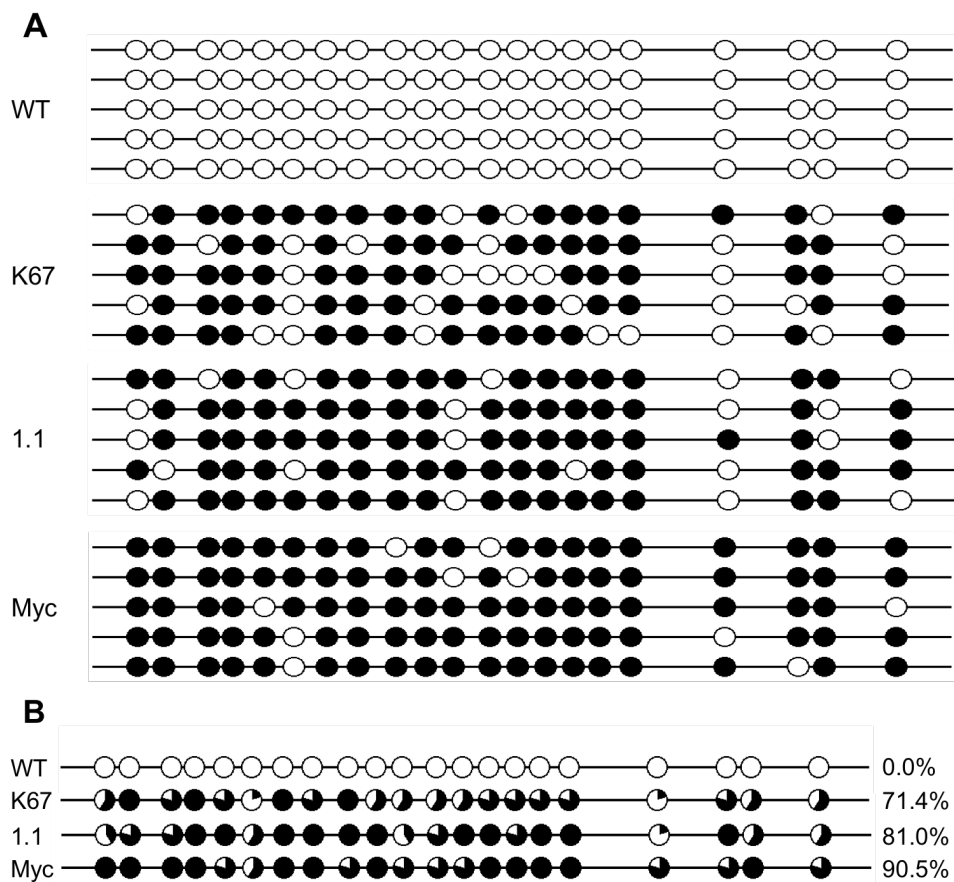


Figure 29: Methylation analysis of porcine *P16INK4A* gene region (-10 to +256)

Circles indicate CpG methylation sites; black circles represent methylated and open circles non-methylated sites. **A:** CpG methylation sites and their methylation pattern in wild-type pMSCs (WT), un-induced neo14/K67 cells (K67), Cre recombined neo14/K67/1.1 (1.1) cells, and cells with an overexpression of cMyc, neo14/K67/1.1+cMyc (Myc). **B:** Quantitative comprehension of methylation pattern sites in the distinct cells.

The results of the methylation analysis prove that the impaired p16INK4 α expression in the stepwise modified pMSCs is a consequence of gradual *P16INK4A* hyper-methylation.

Summing up, we have generated pMSCs (neo14/K67/1.1) expressing mutant *TP53*^{R167H} and mutant *KRAS*^{G12D} from their endogenous gene loci. These cells show features of unlimited replicative capacity and lack detectable p16INK4a expression levels. Moreover, cells with

similar characteristics were established with an additional deregulated cMyc expression (neo14/K67/1.1+cMyc).

3.6 *In vitro* characterisation of genetically modified pMSCs

Next, we were interested in analysing the *in vitro* growth characteristics of wild-type pMSCs and stepwise modified pMSCs. Neoplastic cells can be distinguished from their normal counterparts by their unique cellular growth characteristics, for example, unlimited replicative capacity, loss of density-dependent growth inhibition and the ability to proliferate in semisolid medium [274].

Since disruption of the p53 and pRb pathways results in diminished G₁-to-S phase checkpoint control, that causes increased cell proliferation, DNA synthesis and cell growth [reviewed in 275], we determined the population doubling time for all cell isolates. Figure 30A illustrates the growth curve of wild-type pMSCs and genetically modified pMSCs. Wild-type pMSCs have an estimated population doubling time of 25.7h (+/- 2.6h), the un-induced neo14/K67 cell clone is similar at 23.6h (+/- 0.4h). Expression of mutant *TP53*^{R167H} and *KRAS*^{G12D} markedly reduced population doubling time (15.4h +/- 1.7h) and deregulated cMyc expression resulted in a slight further reduction 14.7h (+/- 0.8h). Colony formation assay demonstrated that both neo14/67/1.1 cells and neo14/67/1.1+cMyc cells were able to form large colonies when seeded at low cell densities (Figure 30B). This indicates that these cells exhibit high plating efficiencies.

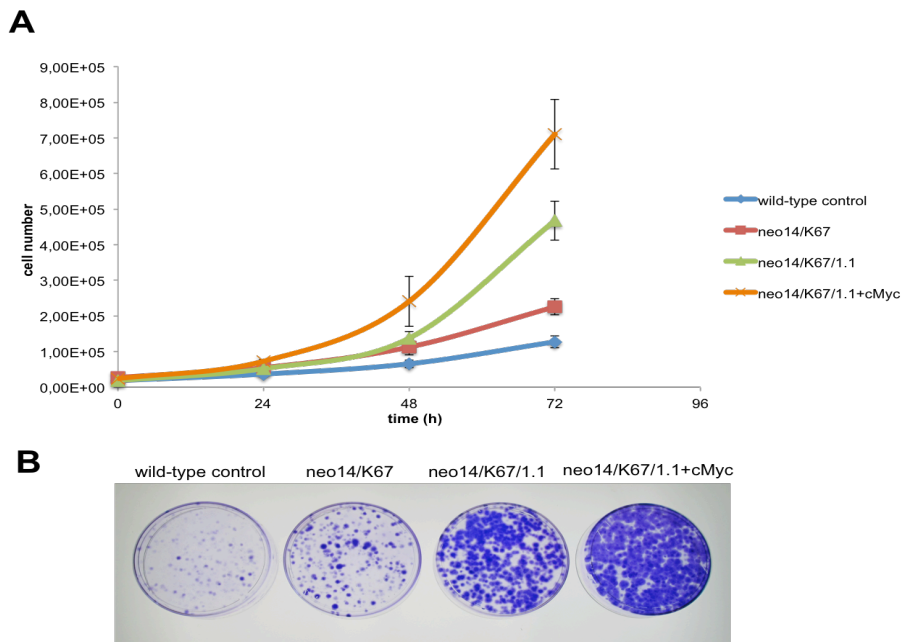


Figure 30: Determining the population doubling time of genetically modified pMSCs

A: Growth curve of wild-type pMSCs, un-induced neo14/K67 cells, Cre recombined neo14/67/1.1 cells and neo14/67/1.1+cMyc cells. Genetically modified porcine cells expressing mutant p53-R167H and oncogenic Kras-G12D show increased cell proliferation compared to wild-type control cells. **B:** Colony formation assay mirrors the increased plating efficiency of genetically modified pMSCs compared to their wild-type counterparts.

Overall, these investigations show that cells expressing mutant $TP53^{R167H}$ and $KRAS^{G12D}$ proliferate almost twice as fast as wild-type control cells and un-induced neo14/K67 cells. Moreover, these results prove that the perturbation of p53 and pRb pathways in combination with expression of oncogenic $KRAS^{G12D}$ exert a considerable impact on the growth characteristics of genetically modified pMSCs.

Another feature of transformed cells is that they do not respond to contact inhibition. Contact inhibition is a process that results in arrested cell growth when cells reach confluence. As a consequence, normal cells stop proliferation when grown to confluence, while cancer cells continue to proliferate, piling up on top of each other and form multi-layered foci [276,277]. In this regard, the morphological and phenotypic changes of the distinct cell clones were assessed by the ability to form multi-layered foci when reaching confluence (Figure 31).

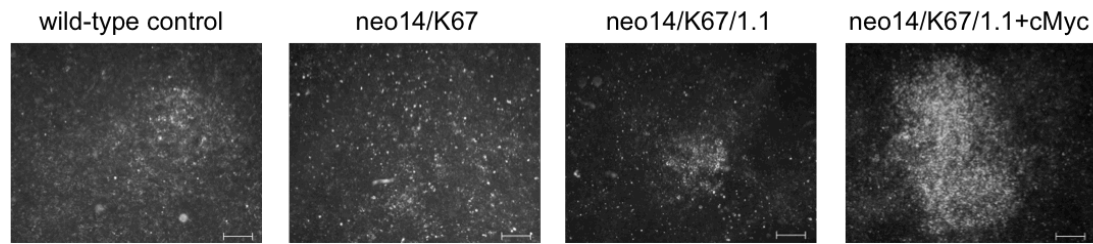


Figure 31: Validating density-dependent growth inhibition

Only neo14/K67/1.1+cMyc cells expressing mutant $TP53^{R167H}$ and $KRAS^{G12D}$ and deregulated cMyc levels form obvious multi-layered foci when grown to higher densities. Bars indicate 400 μm .

Figure 31 highlights the distinct growth characteristics of wild-type pMSCs and genetically modified pMSCs when grown to confluence. Wild-type pMSCs and neo14/K67 cells grow as dense monolayers, but arrest their growth when reaching confluence. In contrast, cells expressing mutant $TP53^{R167H}$ and $KRAS^{G12D}$ grow to higher cell density, indicating their decreased density-dependent inhibition of growth. However, only neo14/K67/1.1+cMyc cells form multi-layered foci, illustrating that these cells have lost contact inhibition.

Next, pMSCs were assessed for their anchorage-independent growth in soft agar. This assay is considered as the most stringent *in vitro* test for evaluating cellular transformation. As seen in Figure 32A, wild-type control pMSCs did not form colonies in soft agar, while cells lacking p53 (neo14/K67) gave rise to 5 colonies. In contrast, cells expressing mutant p53-R167H and Kras-G12D formed 54 colonies and the cMyc transfected cell pool neo14/K67/1.1+cMyc 24 colonies. Although stable selected cMyc transfectants formed fewer colonies in soft agar than its parental cell clone neo14/K67/1.1, these colonies were much larger (Figure 32B).

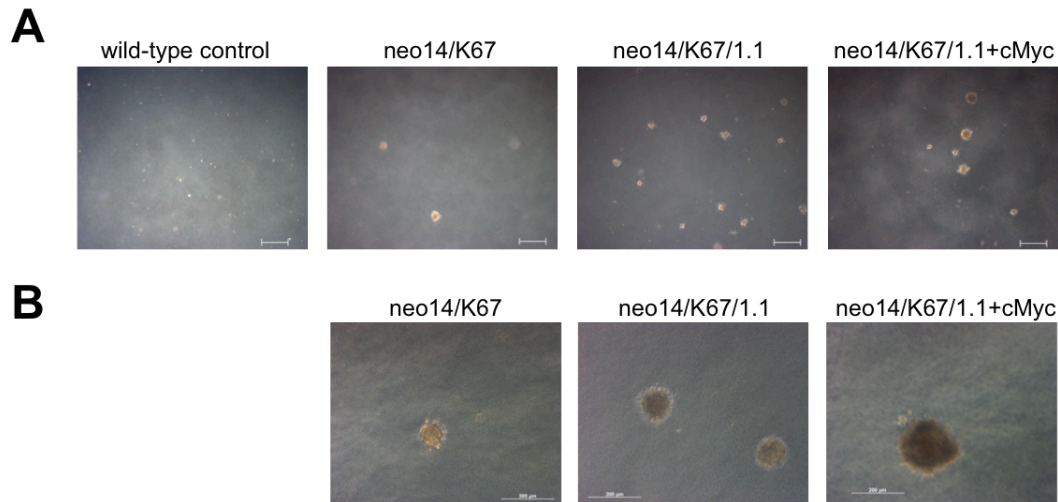


Figure 32: Anchorage-independent growth in soft agar

A: Colonies formed in semisolid medium, bars indicate 400 μm **B:** Colonies formed in semisolid medium, bars indicate 200 μm . Wild-type pMSCs grow as single cells in semisolid medium, while cells lacking p53 form three-dimensional colonies. This effect was even more pronounced in Cre recombined cells (neo14/K67/1.1) expressing mutant $TP53^{R167H}$ and $KRAS^{G12D}$ as well as in cells with a deregulated cMyc expression (neo14/K67/1.1+cMyc).

Collectively, these findings indicate that neo14/K67/1.1 cells as well as neo14/K67/1.1+cMyc cells have acquired a transformed phenotype, as these cells proliferate in semisolid medium. However, only stable selected cMyc transfectants formed multi-layered foci when grown to higher cell density, indicating that these cells have additionally lost contact inhibition. Since there is a considerable correlation between the *in vitro* anchorage-independent growth in soft agar and *in vivo* tumorigenicity [278], the tumorigenic potential of transformed pMSCs was assessed in an *in vivo* xenotransplantation experiment.

3.7 Implantation of genetically modified pMSCs into immune-deficient mice

The most rigorous test for assessing tumorigenicity of neoplastic cells is their ability to form tumours when injected into immune-deficient animals. To analyse the *in vivo* tumorigenic potential of neo14/K67/1.1 cells and the cMyc transfected cell pool (neo14/K67/1.1+cMyc), 1×10^7 cells were mixed 1:1 (v/v) with Matrigel™ Basement Membrane Matrix and injected subcutaneously into four sites at the back of an immune-deficient mouse. The tumour engraftment was monitored over a time period of 45 days.

Neo14/K67/1.1 cells formed one small tumour nodule, as seen in Figure 33. Histological examination however revealed, that this tumour was composed mainly of the coinjected Matrigel™ Basement Membrane Matrix and only of few atypical cells, which produced their own matrix (black arrows).

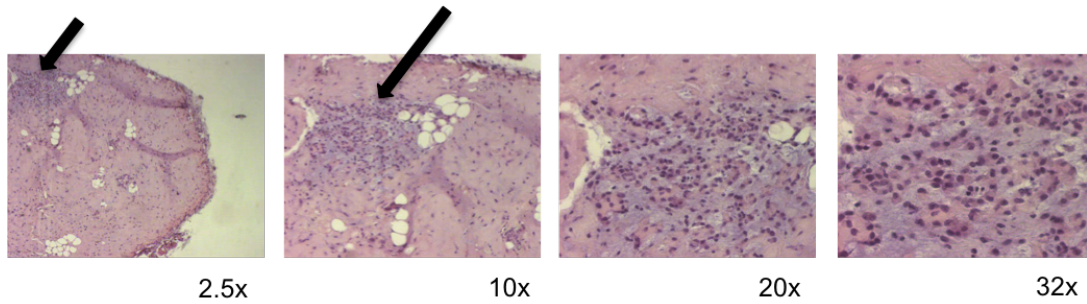


Figure 33: Histology of the neo14/K67/1.1 cells derived tumour

Depicted are HE stained sections of the tumour, which originates from neo14/K67/1.1 cells. Given are different magnifications (5x, 10x, 20x, 32x). Black arrows indicate atypical, transformed porcine cells that produced their surrounding matrix.

In contrast, cells with a deregulated cMyc expression (neo14/K67/1.1+cMyc) gave rise to three tumours within 45 days. Tumours were examined and classified as low-grade myxoinflammatory fibroblastic sarcoma (MIFS) (Figure 34).

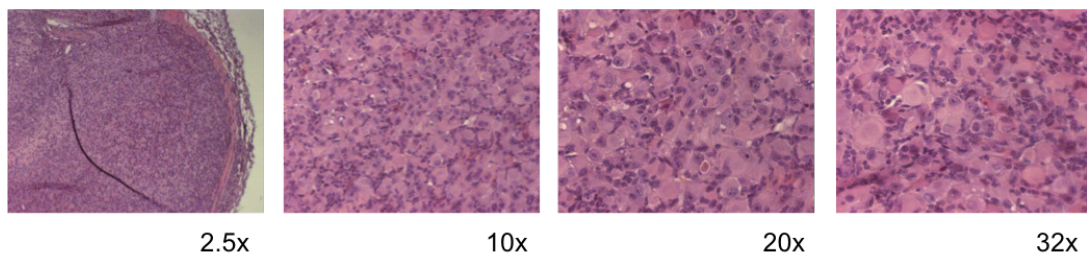


Figure 34: Histology of the neo14/K67/1.1+cMyc cells derived tumour

Depicted are HE stained sections of the low-grade myxoinflammatory fibroblastic sarcoma (MIFS) at different magnifications (5x, 10x, 20x, 32x).

Since neo14/K67/1.1+cMyc cells gave rise to three tumours, two tumours were used to derive a primary porcine tumour cell line (pPTC) and the third tumour was directly re-implanted under the peritoneum of another immune-deficient mouse. After 38 days the tumour was recovered, examined and classified as a pleomorphic-undifferentiated sarcoma (PUS) (Figure 35A). Interestingly, histological examination revealed that re-implanted porcine tumour cells migrated to and invaded the murine pancreas (Figure 35B). Again, a porcine sarcoma derived tumour cell line was established from the recovered, re-implanted tumour. This cell line is designated as re-implanted porcine tumour cell line (rePTC).

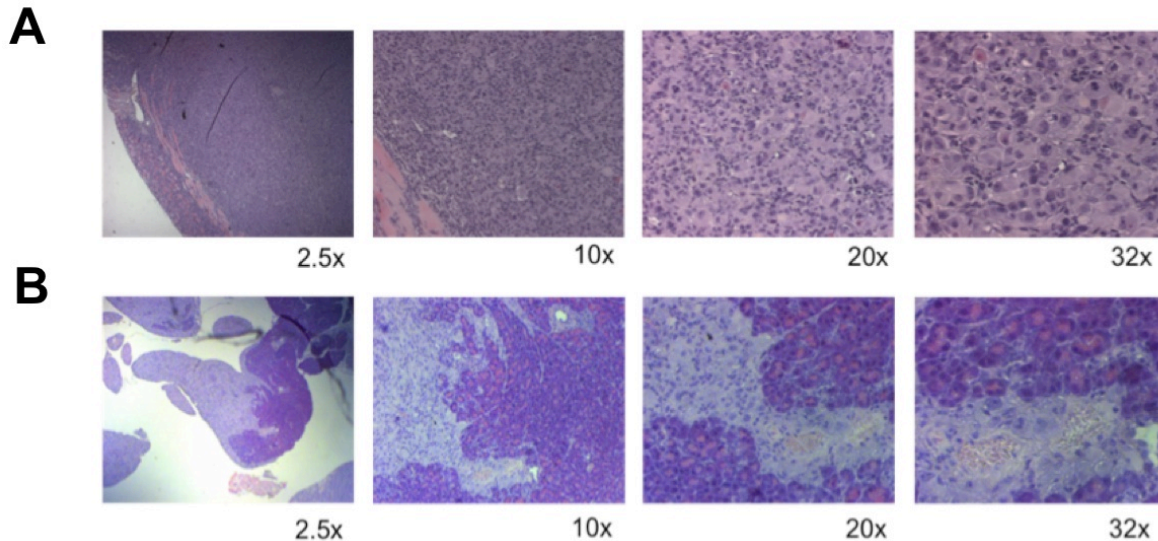


Figure 35: Histology of the re-implanted tumour

Depicted are HE stained sections at different magnifications (2.5x, 10x, 20x, 32x). **A:** HE stained sections of the pleomorphic-undifferentiated sarcoma (PUS) **B:** Invasive re-implanted tumour cells migrated to the murine pancreas

These findings show that genetic alterations in the *TP53*, *KRAS* and *INK4A* gene locus combined with cellular immortalisation are sufficient to convert normal pMSCs to a transformed phenotype *in vitro*. And an additional deregulated expression of cMyc prompted *in vivo* tumorigenicity. Moreover, these results show that tumorigenic porcine mesenchymal stem cells give rise to sarcomas in an immune-deficient host. The short time course of the xenotransplantation experiment does however leave open the possibility of long latency tumorigenesis from neo14/K67/1.1 cells.

3.8 *In vitro* growth characteristics and genetic signature of porcine sarcoma derived cell lines

Next, neo14/K67/1.1+cMyc derived tumour cell lines, pPTC and rePTC, were analysed in more detail. At first the morphological and growth characteristics of these tumour cells were investigated compared to those of the parental cell pool neo14/K67/1.1+Myc. As depicted in Figure 36A the cell pool neo14/K67/1.1+cMyc exhibit a polygonal morphology with a stellate-like shape. Cells of the pPTC line show similar morphological features. In contrast, re-implanted tumour cells exhibit elongated and spindle-shape morphology and tend to grow on top of each other. Another feature of these cells is that they attached just poorly to the culture vessel surface and therefore most of the cells were floating in the media. The colony formation assay confirms the poor adherence of the rePTC to plastic culture dishes (Figure 36B).

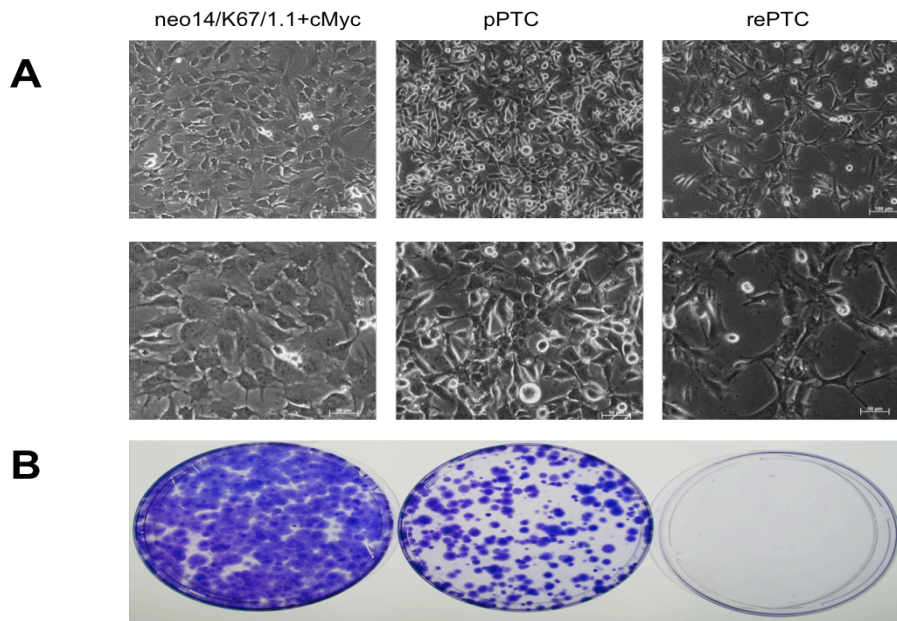


Figure 36: Morphology and growth characteristics of porcine sarcoma derived cell lines

neo14/K67/1.1+Myc: stable selected cMyc transfectants, pPTC: primary porcine tumour cell line, rePTC: re-implanted porcine tumour cell line. **A:** Phase contrast images of the distinct porcine cells, bars indicate 100 μ m (top) and 50 μ m (below). **B:** Colony formation assay of neo14/K67/1.1+cMyc cells, pPTCs and rePTCs. rePTCs formed no visible colonies when plated at low densities onto plastic culture dishes.

All these results indicate, that rePTCs exhibit markedly changed morphological and proliferative characteristics compared to the cell pool neo14/K67/1.1+cMyc and pPTCs.

To assure that the sarcoma derived cell lines originated from the cMyc transfected cell pool, two PCR reactions were conducted to detect the presence of the pPGK-pocMyc-IRES-BS-pA expression vector in these cell lines. One primer pair was designed to amplify a 1628 bp fragment from the IRES sequence to the SV40 promoter, while the other primer pair amplified a 1652 bp fragment from the *Kana/Neo* resistance gene to the pUC ori sequence (Figure 37A). Figure 37B shows that both tumours arose from neo14/K67/1.1+cMyc cells, as both amplified the diagnostic DNA fragments.

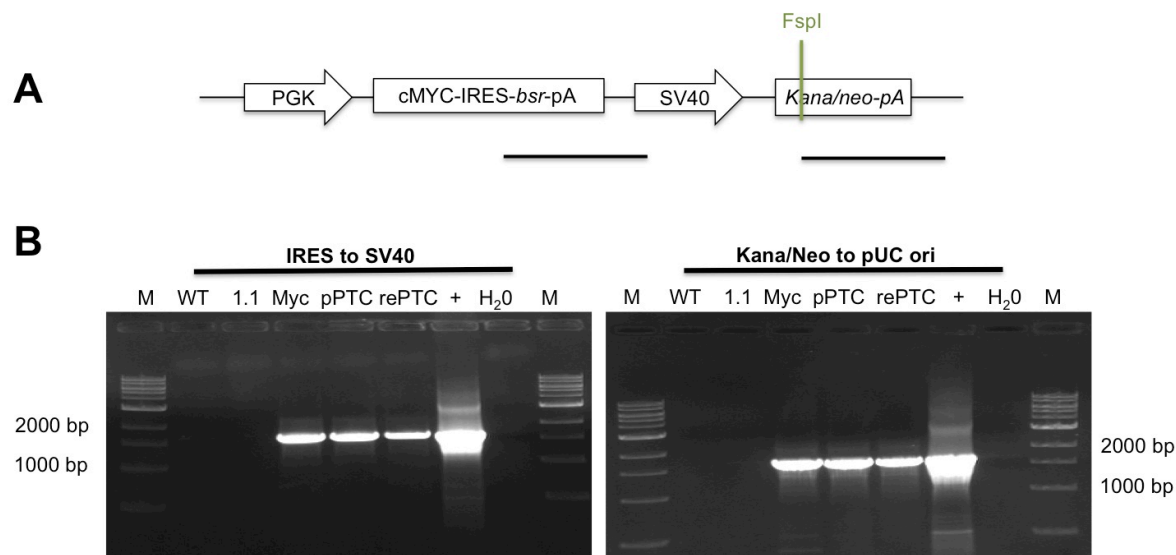


Figure 37: Verifying the cellular origin of porcine sarcoma derived cell lines

A: Design of the expression vector pPGK-pocMyc-IRES-BS-pA, *FspI* indicates the recognition site for the restriction enzyme *FspI*, which was used to linearise the vector before transfection; black bars indicate the relative amplified PCR products. **B:** PCR screenings to detect the presence of the pPGK-pocMyc-IRES-BS-pA expression vector in the distinct cells. M: 1 kb DNA ladder; WT: wild-type pMSCs; 1.1: Cre recombined cell clone neo14/K67/1.1; Myc: stable selected cMyc transfectants neo14/K67/1.1+cMyc; pPTC: primary porcine tumour cells; rePTC: re-implanted porcine tumour cells; +: plasmid-DNA pPGK-pocMyc-IRES-BS-pA; H₂O: water control; **IRES to SV40:** In stable selected cMyc transfectants (Myc) and the two porcine sarcoma derived tumour cell lines (pPTC and rePTC) the diagnostic 1628 bp fragment was detected. No PCR product was detected in wild-type pMSCs and the untransfected neo14/K67/1.1 cells. **Kana/Neo to pUC ori:** Like the expression vector, cMyc transfectants and the two porcine tumour cell lines (pPTC and rePTC) amplified the diagnostic 1652 bp fragment.

Next, PCRs across the LSL integration sites were performed with all established cell lines (see Figure 38). As expected, in porcine sarcoma derived tumour cells the diagnostic recombined TP53-loxP fragment and the 167 bp KRAS-WT fragment as well as the diagnostic 201 bp KRAS-loxP fragment were detected.

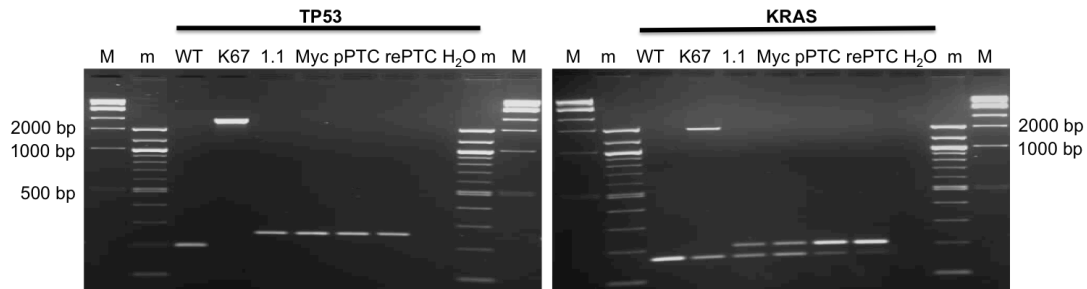


Figure 38: PCRs across the LSL integration sites before and after *in vivo* xenotransplantation

M: 1 kb DNA ladder; m: 100 bp DNA ladder; WT: wild-type pMSCs; K67: un-induced cell clone neo14/K67; 1.1: Cre recombined cell clone neo14/K67/1.1; Myc: stable selected cMyc cell pool neo14/K67/1.1+cMyc; pPTC: primary porcine tumour cells; rePTC: re-implanted porcine tumour cells; H₂O: water control; **TP53**: In wild-type pMSCs only the 198 bp fragment from the wild-type allele was detected. For the un-induced cell clone neo14/K67 only the 1.929 kb TP53-LSL fragment was detected. Cre recombined neo14/K67/1.1, neo14/K67/1.1+cMyc, primary porcine tumour and re-implanted porcine tumour cells amplified only the recombined 254 bp TP53-loxP fragment. **KRAS**: Wild-type pMSCs amplified only the 167 bp fragment from wild-type alleles, the clone neo14/K67 amplified the 167 bp fragment from the wild-type allele as well as the 1.486 kb KRAS-LSL fragment. In Cre recombined neo14/K67/1.1 cells, neo14/K67/1.1+cMyc cells, primary porcine tumour and re-implanted porcine tumour cells besides the 167 bp fragment from the wild-type allele the 201 bp KRAS-loxP fragment were detected.

The intensities of the recombined KRAS-loxP fragment compared to the KRAS-WT fragment in the porcine sarcoma derived cell lines (pPTC and rePTC) led to the assumption that the recombined *KRAS*^{L-G12D} allele has been amplified in these cells. To test if this was the case, quantitative PCR was carried out. For assessing *KRAS* copy number alterations a 251 bp PCR product was amplified, covering the second exon of the *KRAS* gene. As an unrelated reference sequence GAPDH was selected and a 233 bp genomic DNA PCR product was amplified spanning exon 4. Quantitative PCR revealed the amplification of the *KRAS* gene in the two porcine sarcoma derived tumour cell lines. Six copies of the second exon of the *KRAS* gene were detected in the cell line pPTC and 9 copies in the re-implanted porcine tumour cells, respectively. Sequence analysis of *KRAS* mRNA species comprising exon 1 to exon 4, revealed higher expression of mutant *KRAS*-G12D mRNA (GAT) than wild-type *KRAS* mRNA (GGT) (Figure 39). Collectively, these findings show that the increase in *KRAS* copy numbers in the porcine sarcoma derived tumour cells was due to the amplification of the recombined *KRAS*^{L-G12D} allele.

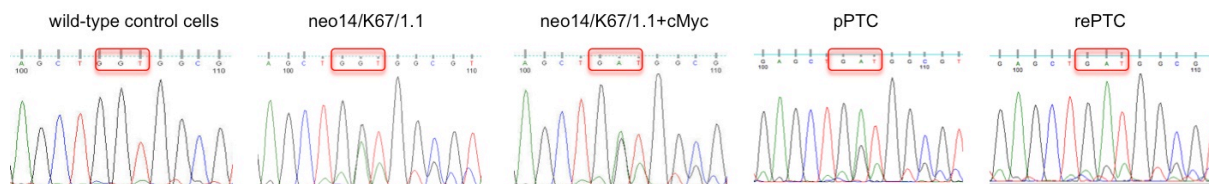


Figure 39: Chromatograms of KRAS mRNA transcripts

Red framings highlight the G12D mutation, which is the predominant species in primary porcine tumour cells (pPTC) and re-implanted porcine tumour cells (rePTC).

All these findings indicate that the mutant $KRAS^{L-G12D}$ locus has been amplified in the neo14/K67/1.1+cMyc derived tumours. As seen in Figure 40 these results were also affirmed on protein level.

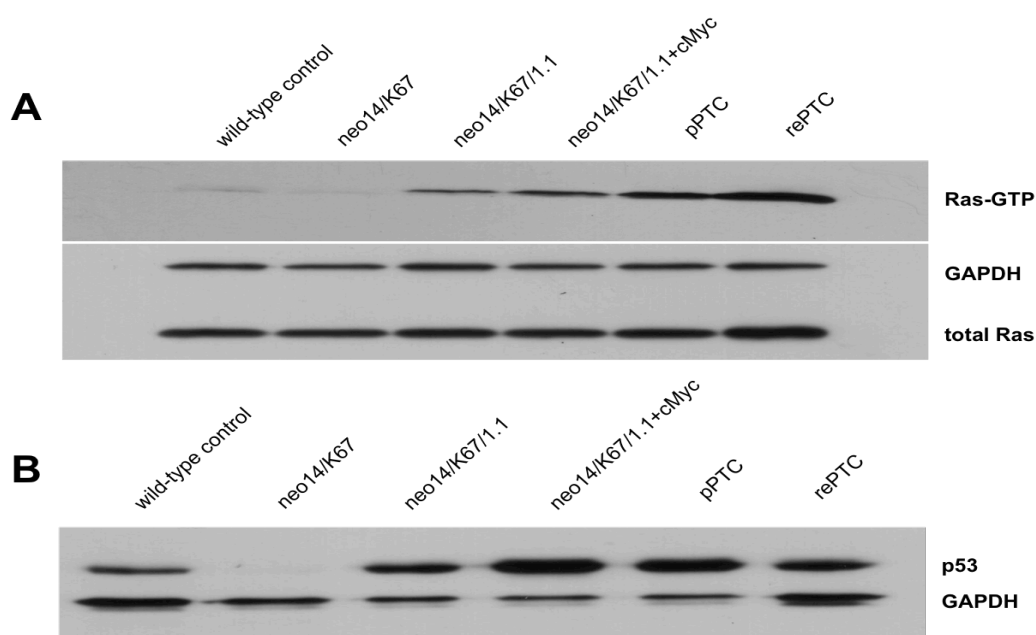


Figure 40: Ras Activation Assay and p53 Western blot analysis with lysates of cells before and after *in vivo* xenotransplantation

A: Sarcoma derived tumour cell lines express higher levels of constitutive active GTP-bound Ras proteins than the parental neo14/K67/1.1+cMyc cells. Total Ras (21 kDa) and GAPDH (36 kDa) protein levels were investigated as loading controls. **B:** Before *in vivo* xenotransplantation neo14/K67/1.1+cMyc cells express abundant levels of mutant p53-R167H (46 kDa), which is diminished in the rePTCs. As loading control the expression of GAPDH (36 kDa) was assessed.

As displayed in Figure 40A pPTCs and rePTCs express high amounts of constitutive active GTP-bound Ras proteins, whereas the expression of mutant p53-R167H proteins decreased in the rePTCs compared to the parental neo14/K67/1.1+cMyc cells (Figure 40B).

Since the oncoprotein Kras-G12D controls multiple downstream signalling pathways such as Raf, PI3-Kinase and the Ral guanine nucleotide exchange factors (Ral-GEFs) that are crucial for cellular transformation [279] we investigated the activation of phosphorylated Akt and ERK1/2. Figure 41 depicts the Western blot analysis.

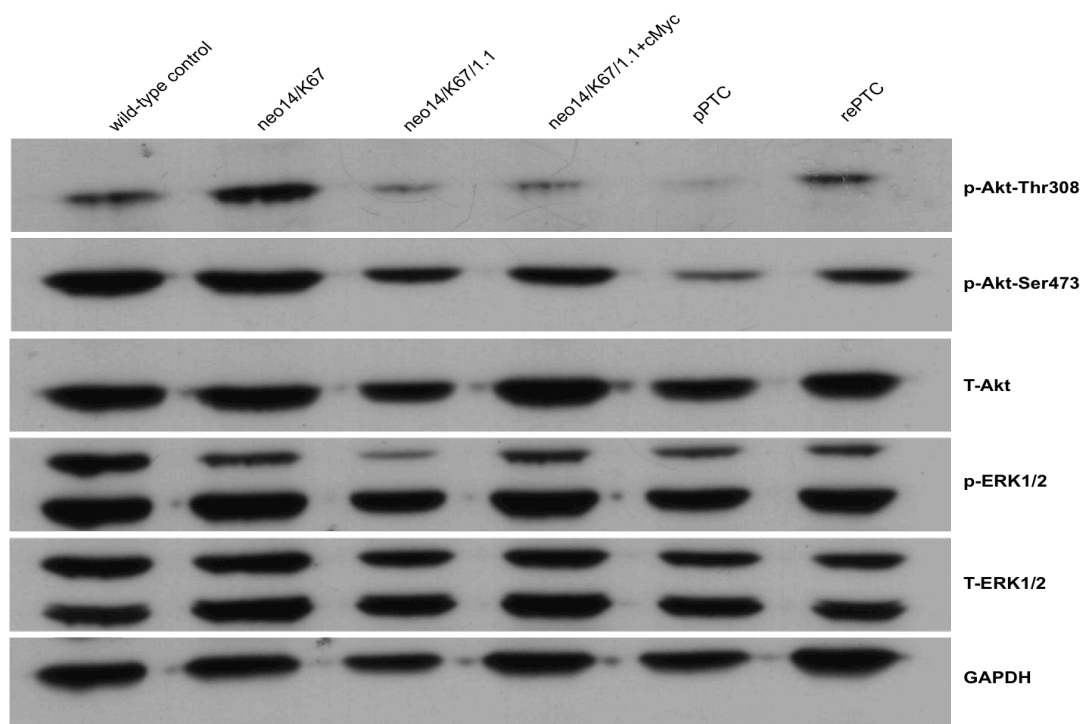


Figure 41: Western blot analysis of phosphorylated Akt and ERK1/2 proteins in pMSCs before and after xenotransplantation

No increase of phosphorylated Akt and ERK1/2 protein levels were detected in Cre recombinated porcine cells as well as in the porcine sarcoma derived cell lines.

Unexpectedly, cells after Cre recombinase treatment as well as the porcine sarcoma derived tumour cells showed similar or even decreased levels of phosphorylated Akt and phosphorylated ERK1/2, compared to wild-type pMSCs and un-induced neo14/K67 cells.

3.9 Expression profile of stepwise modified pMSCs and porcine sarcoma derived cell lines

The above-described findings show that genetic alterations of signalling molecules (KRAS), core cell cycle regulators (p16INK4 α) and transcription factors (p53 and cMyc) cause neoplastic transformation of primary porcine cells. All the introduced genetic alterations drive aberrant signal transduction pathways. In order to dissect the transcriptional changes that occurred along defined stages of malignant porcine mesenchymal stem cell transformation, microarray analyses were carried out. In the case of parental wild-type pMSCs, un-induced pMSCs (neo14/K- subclones) and Cre recombinated pMSCs (neo14/K67/- subclones) three biological replicates were analysed. Whereas in the case of the cMyc transfected cell pool and the porcine sarcoma derived cell lines three technical replicates were used.

Figure 42 illustrates the heatmaps with fold-changes in gene expression of the stepwise genetically modified pMSCs compared to wild-type pMSCs. Heatmaps are grouped as five categories: key genes of cellular transformation, ALT-associated genes, cell cycle regulatory genes, p53 target genes and tissue invasion and metastatic marker genes.

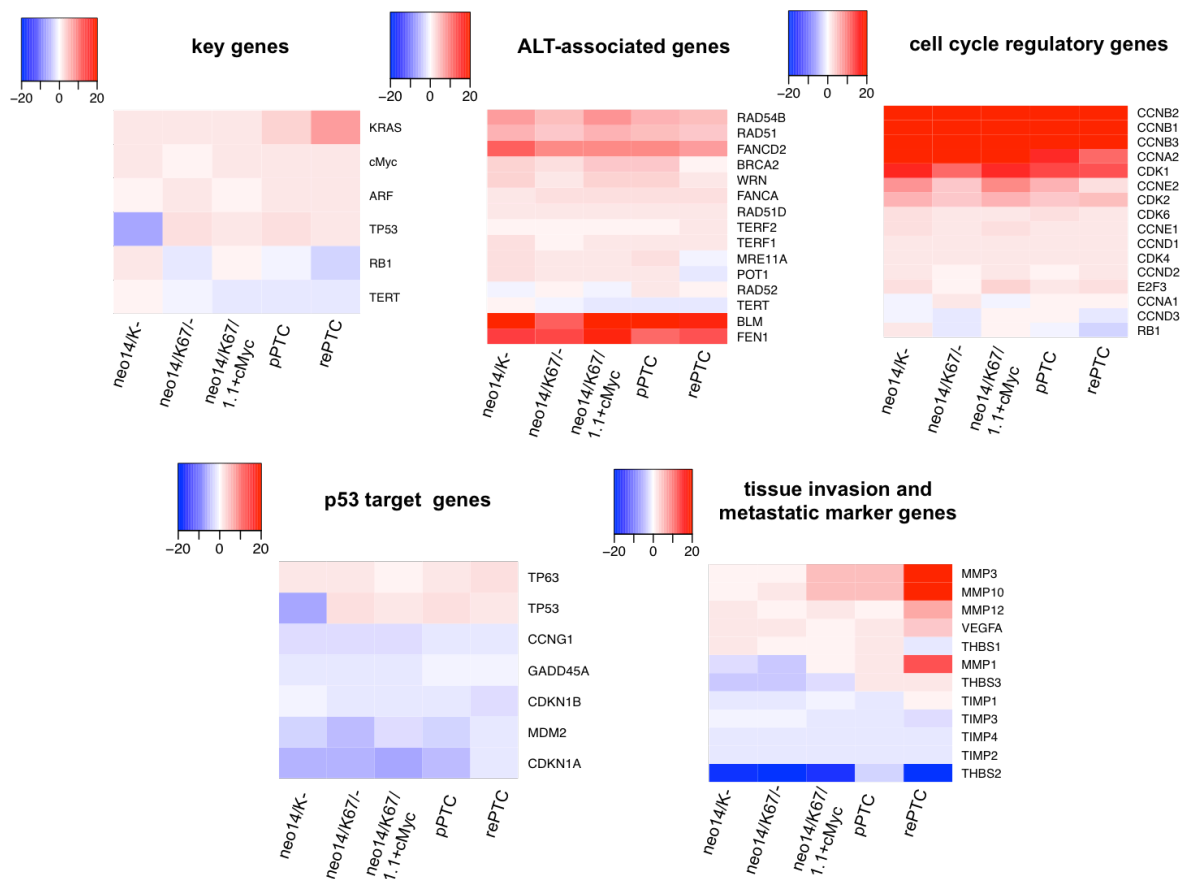


Figure 42: Expression profile of stepwise modified pMSCs and porcine sarcoma derived cell lines

neo14/K⁻: un-induced cell clones, neo14/K67/⁻: Cre recombined cell clones; neo14/K67/1.1+cMyc: stable selected Myc transfectants; pPTC: primary porcine tumour cells; rePTC: re-implanted porcine tumour cells. Heatmaps depict the fold-changes in gene expression levels of the distinct cell lines relative to wild-type pMSCs. Fold-change values are represented as a gradient colour from blue (down-regulation) to red (up-regulation). Abbreviations: CDK: cyclin-dependent kinases, CCN: cyclin

The heatmap “key genes” represents the expression levels of key genes that are known to play a pivotal role in cellular transformation (Figure 42, top left). For KRAS, a gradual up-regulation of its expression is detected along the stages of cellular transformation. In particular, an up to 7-fold increase in expression is observed in the re-implanted porcine tumour cells (rePTC). These results are in line with the finding, that porcine sarcoma derived tumour cells have amplified the KRAS^{L-G12D} allele. Fold-changes in cMyc expression levels are consistent with the data gained from quantitative real-time PCR analysis (for comparison see Figure 25). Transfection of the pPGK-pocMyc-IRES-BS-pA expression vector induced a marginal increase of cMyc expression in neo14/K67/1.1+cMyc cells compared to the untransfected parental neo14/K67/⁻ cell clones. No further increase of cMyc expression was detected in the neo14/K67/1.1+cMyc derived tumour cell lines pPTC and rePTC. The expression levels of ARF (p14ARF) vary along the defined stages of cellular transformation. Again, these data are concordant with those of the quantitative real-time PCR analysis

(Figure 28B). The same is seen for RB1 (pRb). The expression profile of TP53 reveals a significant down-regulation of TP53 expression in the un-induced neo14/K- cell clones, which is line with the blocked expression of the *TP53*^{LSL-R167H/LSL-R167H} alleles in these cells. In agreement to the results of the p53 western blot in Figure 40B, the transcription of TP53 is downregulated in rePTCs. As depicted in the heatmap, genetically modified pMSCs as well as porcine sarcoma derived tumour cells show no reactivated TERT expression. Again, these findings indicate that the transformed pMSCs must have been immortalised by a telomerase-independent mechanism.

As seen in the heatmap “ALT-associated genes” some of these genes were differentially expressed in the stepwise modified pMSCs compared to wild-type pMSCs (Figure 42, top middle). In particular, genes essential for the recombinational repair of broken replication forks, such as FEN1 and FANCD2 were upregulated in the stepwise modified porcine cells. Moreover, genes involved in the elongation and capping of telomeres, such as RAD51, RAD54B and BRCA2 are also upregulated. The same is seen for the Bloom syndrome helicase. This RecQ helicase is considered to play an important role in the ALT mechanism, as its overexpression results in increased telomeric DNA synthesis [280]. Collectively, these data indicate that the genetically modified pMSCs have activated the Alternative Lengthening of Telomeres mechanism to prevent telomere attrition

The heatmap “cell cycle regulatory genes” shows the fold-changes in expression levels of genes involved in the control of cell cycle progression (Figure 42, top right). The expression of most of these cell cycle regulatory genes are upregulated in the in the MSC derivatives, although RB1 expression remained at low baseline levels. Genes regulating the G₁-to-S phase progression, like Cyclin E and CDK2 were upregulated. The same is seen for B-type cyclins and CDK1, which control the progression from G₂- into M-phase. Also the expression of Cyclin A that is involved in the G₁-to-S and G₂-to-M transitions was markedly increased. These data indicate deregulated cell cycle control in the pMSC derivatives.

TP53 is known to exert its tumour suppressive function by acting as a sequence-specific transcription factor [64]. The heatmap “p53 target genes” (Figure 42, bottom left) illustrates that the expression of p53's direct transcriptional target and negative regulator MDM2 is downregulated in all analysed cell lines. Moreover, the expression of genes involved in mediating p53-triggered cell cycle arrest, such as CDKN1A (also known as p21), CDKN1B (also known as p27) and GADD45 is also reduced in the pMSC derivatives. Collectively, these data show that the expression of direct transcriptional targets of p53 is downregulated in p53 deficient pMSCs (neo14/K-) as well as in pMSCs expressing mutant p53-R167H (neo14/K67/-, neo14/K67/1.1+Myc, pPTC and rePTC). These results indicate that mutant p53-R167H is defective in activating the transcription of its predominant negative regulator MDM2 as well as in mediating cell cycle arrest.

The heatmap “tissue invasion and metastatic marker genes” shows that the expression of matrix-degrading extracellular proteases and protease inhibitors is markedly increased in the invasive rePTCs. In particular, high expression of matrix metalloproteinases-3 and -10 (MMP-3 and MMP10) and the vascular endothelial growth factor α (VEGF α) are detected. Moreover, the expression of thrombospondin 2 (THBS2), a potent inhibitor of tumour growth and angiogenesis is notably downregulated in rePTCs. Collectively, these data affirm the invasive and metastatic phenotype of the rePTCs, which was observed in the xenotransplantation experiment.

3.10 Implantation of genetically modified pMSCs in an immune-competent isogenic pig

As the results from the murine xenotransplantation experiment showed that transformed pMSCs can give rise to tumours in immune-deficient animals we were interested in, if these cells could also form tumours in immune-competent isogenic pigs. Therefore the parental, unmodified wild-type pMSCs were used to clone isogenic host animals by nuclear transfer. Two piglets were born, of which only one survived. This animal was used as an immune-competent isogenic host to assess the tumour growth of Cre recombined neo14/K67/1.1 cells, the Myc transfected cell pool (neo14/K67/1.1+cMyc) and the primary porcine tumour cells. As a negative control unmodified wild-type pMSCs were implanted. In each case 1×10^8 cells were implanted subcutaneously into the tissue of both ears. In addition 1×10^8 cells of the clone neo14/K67/1.1 and the cell pool neo14/K67/1.1+cMyc were mixed 1:1 (v/v) with Matrigel™ Basement Membrane Matrix and implanted into the subcutaneous tissue of each ear. The tumour growth was monitored daily and at day 8 marked swellings appeared at all injections sites, where cells were coinjected with Matrigel™ Basement Membrane Matrix. A small bulge was visible at the injection site of the neo14/K67/1.1+cMyc cells. However, all of them regressed at day 15 indicating that the swellings were most likely a consequence of an immune response against either the coinjected Matrigel™ Basement Membrane Matrix or the selectable marker genes, which are encoded by the pPGK-pocMyc-IRES-BS-pA expression vector. Furthermore, at day 15 a bulge was palpable at the injection site, where the pPTCs were implanted, which also regressed few days later. Up to now, tumour growth monitoring is ongoing.

3.11 Conclusion

The expression of oncogenic $TP53^{R167H}$ and $KRAS^{G12D}$ in combination with p16INK4a gene silencing and deregulated cMyc expression resulted in immortalised, neoplastic porcine MSCs. Implantation of these cells in immune-deficient mice resulted in tumour growth within 45 days. Isolation and propagation of porcine sarcoma derived cell lines enabled us to analyse them in more detail (Figure 43). When implanted in an immune-competent isogenic pig, transformed pMSCs failed to form tumours in this host. This was most likely due to an immune response against the coinjected Matrigel™ Basement Membrane Matrix and/or the selectable marker gene products, which are encoded by the cMyc expression vector.

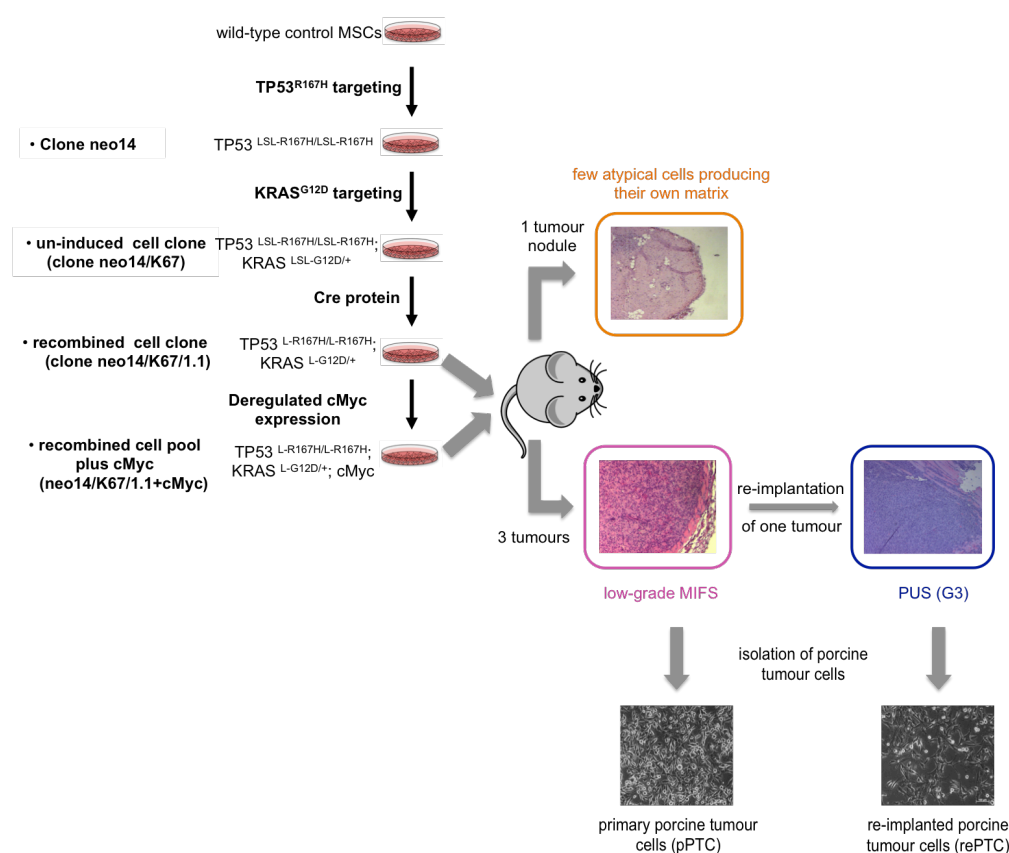


Figure 43: Work flow for the generation of transformed pMSCs *in vitro*

Wild-type pMSCs were used to introduce a latent oncogenic $TP53^{L-SL-R167H}$ allele by gene targeting. One cell clone was established that was homozygous for the $TP53^{R167H}$ mutation (clone neo14) [256]. This cell clone neo14 was subjected to a second round of gene targeting to introduce a latent oncogenic $KRAS^{L-SL-G12D}$ allele. Cre protein transduction mediated the excision of the floxed transcriptional stop cassettes and the expression of mutant p53-R167H and Kras-G12D proteins. Moreover, Cre recombined cells were transfected with a cMyc encoding expression vector that resulted in a deregulated cMyc expression. Stable selected cMyc transfectants and untransfected neo14/K67/1.1 cells were injected subcutaneously in immune-deficient mice. Only stable selected cMyc transfectants formed tumours in an immune-deficient host. Re-implantation of one of these tumours in another immune-deficient mouse resulted in invasive tumour growth in this host. Primary tumours and the re-implanted tumour were used to isolate and propagate porcine tumour cells. Abbreviation: MIFS: myxoinflammatory fibroblastic sarcoma, PUS: pleomorphic-undifferentiated sarcoma, G3: grading, pPTC: primary porcine tumour cells, rePTC: re-implanted porcine tumour cells.

To sum up, we were successful in demonstrating that the perturbation of RAS, TP53 and the pRb signalling pathways in combination with an immortalisation step and deregulation of cMyc expression are sufficient to convert pMSCs to a fully transformed phenotype. This set of genetic modifications is consistent with the set of genetic alterations that induce tumorigenicity in primary human cells.

3.12 Derivation of pigs carrying latent oncogenic $TP53^{LSL-R167H}$ and $KRAS^{LSL-G12D}$ alleles

Since cancer is a leading cause of human death and morbidity worldwide, one of our research interests is to provide a series of genetically defined pigs that model serious and common human cancers. As shown in the section before, oncogenic mutations in porcine $KRAS$ and $TP53$ alleles exert similar functions and pathological effects as their human and murine counterparts. As both oncogenic $KRAS$ and $TP53$ contribute to the pathogenesis of lung and pancreatic cancer [209,281], we decided to generate double gene-targeted pigs carrying mutations in both $KRAS$ ($KRAS^{LSL-G12D}$) and $TP53$ ($TP53^{LSL-R167H}$) genes that can be activated by the action of Cre recombinase in a tissue-specific manner.

3.12.1 Introducing a latent oncogenic $KRAS^{LSL-G12D}$ allele in $TP53^{LSL-R167H/+}$ gene-targeted pMSCs

Although successful $KRAS^{LSL-G12D}$ gene targeting had been carried out in neo14 cells ($TP53^{LSL-R167H/LSL-R167H}$) these cells were not deemed to be suited for somatic cell nuclear transfer (SCNT), since neo14 cells did not give rise to healthy piglets after SCNT as reported by Leuchs *et al.* [256]. Therefore, to derive double gene-targeted pigs carrying latent oncogenic $KRAS^{LSL-G12D}$ and $TP53^{LSL-R167H}$ alleles bone marrow (BM-pMSCs) and adipose tissue (AD-MSCs) derived mesenchymal stem cells were isolated from a male heterozygous $TP53^{LSL-R167H}$ targeted piglet (genotype: $TP53^{LSL-R167H/+}$). Gene targeting experiments were performed using the KRAS-NEO vector (see Figure 10), as isolated $TP53^{LSL-R167H/+}$ targeted pMSCs contained already a *bsr* selectable marker gene. In each case 10 µg of the KRAS-NEO vector was electroporated into 1×10^6 porcine MSCs. In the case of transfected BM-MSCs 65 NEO-resistant single cell clones and 154 NEO-resistant AD-MSC colonies were isolated and expanded for further analysis. Since most of the cell clones ceased proliferation, only 32 adipose tissue derived and 17 bone marrow derived single cell clones could have been analysed. Due to troubles with the screening PCR on genomic DNA level, NEO-resistant clones had to be analysed on RNA level. To detect correct $KRAS$ targeting events RT-PCR was conducted using primers that amplified the 646 bp truncated KRAS-NEO mRNA transcript from exon 1 (KRASEX1_1) to the *neo* selectable marker (*neo_R*). As a control the wild-type $KRAS$ mRNA was amplified using primers that

bind in exon 1 (KRASEx1_F) and exon 4 (KRASEx4_R). Figure 44 illustrates a representative screening result.

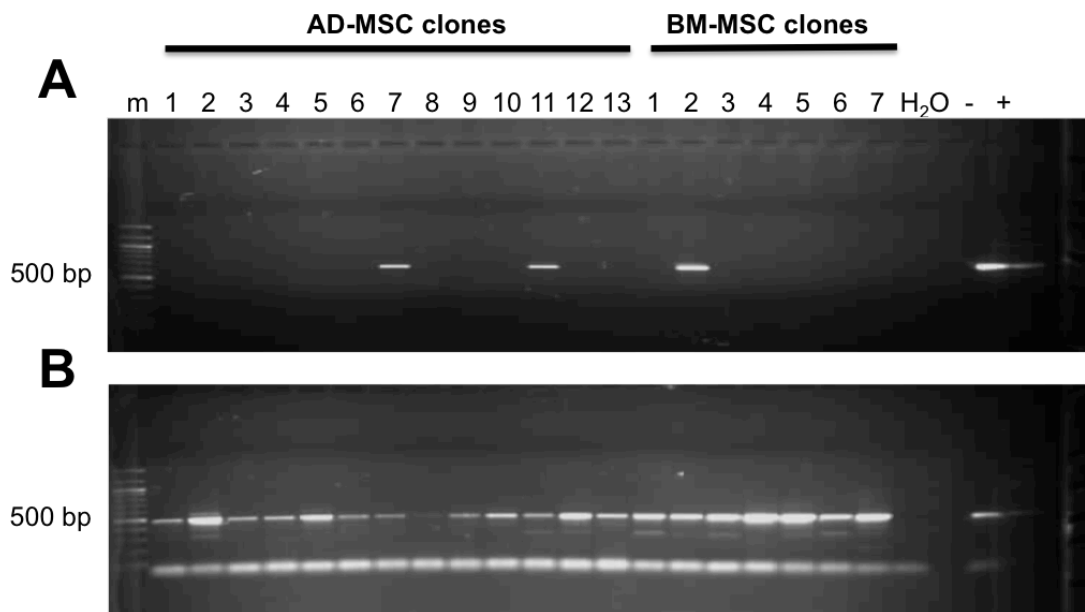


Figure 44: RT-PCR screenings of G418-resistant cell clones

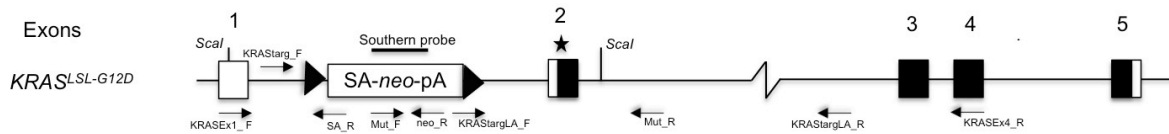
m: 100 bp DNA ladder; AD-MSC 1: clone 9; AD-MSC 2: clone 11; AD-MSC 3: clone 17; AD-MSC 4-10: clones 36-42; AD-MSC 11: clone 44; AD-MSC 12-13: clones 46-47; BM-MSC 1: clone 6; BM-MSC 2-5: clones 8-11; BM-MSC 6-7: clones 14-15; H₂O: water control, +: positive control; previously *KRAS-NEO* targeted cell clone. **A:** RT-PCR of the truncated *KRAS-NEO* mRNA transcript. The AD-MSC derived cell clones 7 and 11 (corresponding to clone AD-39 and AD-44) as well as the BM-MSC derived cell clone 2 (corresponding to clone BM-8) express the 646 bp truncated *KRAS-NEO* mRNA transcript. **B:** RT-PCR of the wild-type *KRAS* mRNA transcript. As a loading control RT-PCR was performed with primers that amplified the wild-type *KRAS* transcript from exon 1 to exon 4. All investigated cell clones amplified the 492 bp wild-type *KRAS* mRNA species.

Correct gene targeting was found for eight clones as judged by the amplification of the 646 bp *KRAS-NEO* mRNA transcript. This corresponds to a relative targeting efficiency of 12.5% in the case of analysed AD-MSC cell clones (4 out of 32) and of 23.5% in the case of investigated BM-MSC cell clones (4 out of 17). Unfortunately, three of the four retargeted AD-MSC cell clones ceased proliferation, precluding further analysis of them. The remaining five clones were used to isolate genomic DNA of better quality. That allowed us to characterise them in more detail. Next, RFLP test was carried out to assess the presence of the G12D mutation in the second exon of the targeted *KRAS*^{LSL-G12D} allele. Unfortunately, only the cell clones AD-3 and BM-19 showed the expected restriction fragmentation pattern specific for the mutant *KRAS*^{LSL-G12D} targeted allele.

Next, these two cell clones, AD-3 and BM-19, were subjected to further PCR screenings to confirm the integrity of the 5' end as well as the 3' end of the targeted *KRAS*^{LSL-G12D} gene locus (Figure 45A). To check the integrity of the 5' end a PCR was performed using primers designed to amplify a 3.4 kb DNA fragment across the 5' junction of the short arm (KRAS_{targ_F}) to the splicing acceptor (SA_R). In addition, an endogenous control PCR was

conducted that amplified a 3.3 kb DNA fragment from the wild-type *KRAS* allele (Figure 45B, left panel). The correctness of the 3' end of the targeted *KRAS*^{LSL-G12D} gene locus was examined using primers designed to amplify a 10.8 kb DNA fragment spanning the long arm of the *KRAS-NEO* targeting vector (Figure 49B, right panel).

A



B

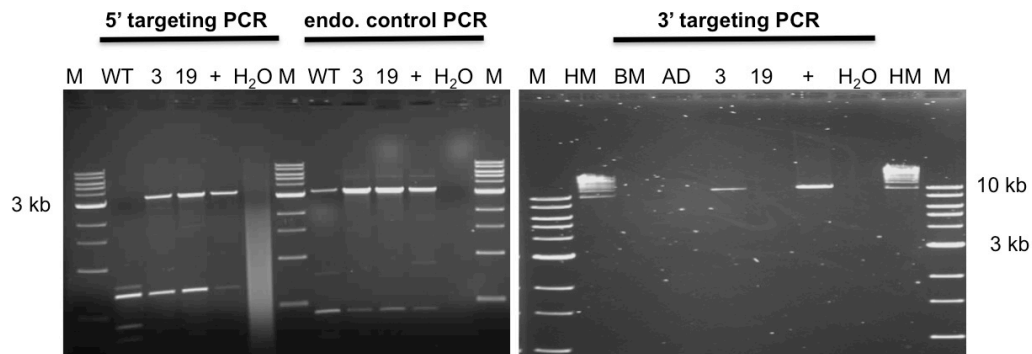


Figure 45: 5' and 3' targeting PCRs of G418-resistant cell clones

M: 1 kb DNA ladder; HM: high range DNA ladder; WT: wild-type pMSCs; BM: bone marrow derived wild-type pMSCs containing a *TP53*^{LSL-R167H} allele; AD: adipose tissue derived wild-type control cells containing a *TP53*^{LSL-R167H} allele; 3: cell clone AD-3, 19: cell clone BM-19, +: positive control, previously *KRAS-NEO* targeted cell clone, H₂O: water control. **A**: Schematic overview of the *KRAS*^{LSL-G12D} gene locus. Exons are numbered, coding and non-coding exons are marked in black and open boxes. Black triangles indicate loxP sites that flox the transcriptional termination cassette in intron 1, the A to G point mutation in exon 2 is indicated by an asterisk. PCR and RT-PCR primers that were used to identify targeted cells clones are indicated. *Scal* restriction sites and the hybridisation probe used for Southern analysis are also shown. SA: splicing acceptor, neo: neomycin resistance gene, pA: poly adenylation signal. (Adapted from 261) **B**: PCR screenings of *KRAS-NEO* retargeted porcine *TP53*^{LSL-R167H/±} MSCs. **5' targeting PCR and endogenous control PCR**: both cell clones (AD-3 and BM-19) amplified the diagnostic 3.4 kb DNA fragment indicating the correctness of the 5' end of the targeted site. **3' targeting PCR**: Only the cell clone AD-3 amplified the diagnostic 10.8 kb DNA fragment.

The results of the PCR screenings in Figure 45B confirm a correct targeting event for the adipose tissue derived cell clone, AD-3, since all performed PCRs led to the amplification of the expected DNA fragments. However, in the case of the bone marrow derived cell clone, BM-19, only the PCR across the short arm amplified the expected DNA fragment. These findings indicated the correctness of the 5' end of the targeted *KRAS*^{LSL-G12D} gene locus but not of the 3' end. Southern blot analysis revealed the integration of the LSL-NEO cassette at the endogenous *KRAS* gene locus in both cell clones and no additional random integration was observed. Figure 46 shows the Southern blot analysis.

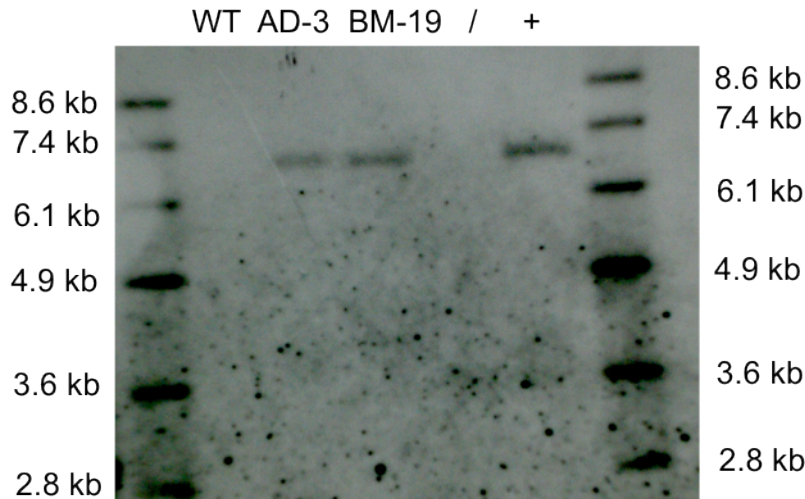


Figure 46: Southern blot analysis of putative $KRAS^{LSL-G12D}$ retargeted $TP53^{LSL-R167H/+}$ pMSCs

M: Dig-UTP labelled marker; WT: wild-type pMSCs, AD-3; BM-19; /: free lane; +: positive control, previously $KRAS-NEO$ targeted cell clone. The applied DIG-UTP labelled probe hybridizes to the *neo* gene of the LSL-NEO cassette. The diagnostic 6.9 kb *ScaI* fragment is indicative for the integration of the LSL-NEO cassette at the endogenous *KRAS* gene locus. Like the positive control, both cell clones, AD-3 and BM-19, show the expected 6.9 kb *ScaI* fragment.

As shown by Southern blot analysis the 6.9 kb DNA fragment indicative for a targeted $KRAS^{LSL-G12D}$ allele was detected in both cell clones, AD-3 and BM-19. No additional DNA fragment indicative for a random integration of the $KRAS-NEO$ targeting construct was detected. Thus, both cell clones and another $KRAS^{LSL-G12D/+}$ targeted cell clone that was established in a previous experiment were subjected to Cre recombinase mediated cassette excision to verify the expression of mutant *KRAS-G12D* mRNA transcripts. RT-PCRs were carried out to amplify the respective *KRAS* mRNA transcripts spanning exon 1 to exon 2, exon 1 to exon 3 and exon 1 to exon 4, respectively. Subsequently, PCR products were sent for sequencing. Figure 48 depicts the chromatograms of the particular cDNA fragments. The sequencing results in Figure 48 uncovered that only the positive control expresses the full-length mutant *KRAS-G12D* mRNA transcript. Whereas in the retargeted cell clones AD-3 and BM-19 the G to A substitution in codon 12 was only present in the mRNA transcript from exon 1 to exon 2 and was absent in the longer mRNA species.

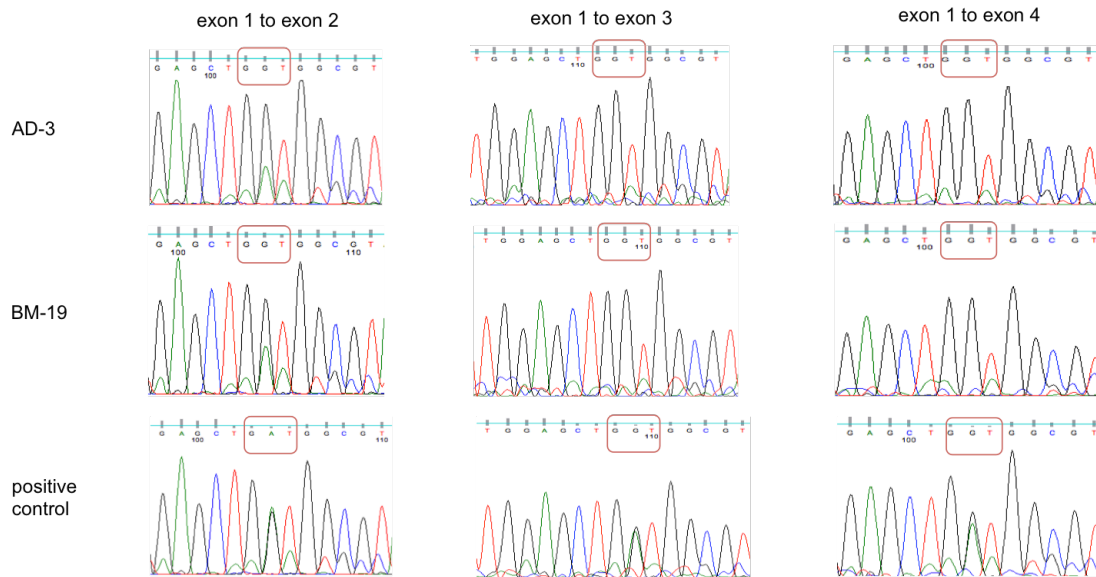


Figure 47: Chromatograms of RT-PCR products covering codon 12 of the relative *KRAS* mRNA species

exon 1 to exon 2: mRNA species comprising exon 1 to exon 2; exon 1 to exon 3: mRNA species comprising exon 1 to exon 3; exon 1 to exon 4: mRNA species comprising exon 1 to exon 4, red framing indicate the sequence of codon 12. Sequence analysis of cell clones AD-3 and BM-19 revealed the presence of the G12D mutation in the mRNA transcript spanning exon 1 to exon 2 (GAT) and lacked in the longer transcripts from exon 1 to exon 3 and exon 4 (GGT), respectively. Only the positive control expressed the full-length mutant *KRAS*-G12D mRNA species.

These results demonstrate, that none of the established cell clones harbours a correct *KRAS*^{LSL-G12D} gene targeting event.

3.12.2 Conclusion

We were unable to derive cell clones carrying both latent oncogenic *KRAS*^{LSL-G12D} and *TP53*^{LSL-R167H} targeted alleles, which could have been used for SCNT. The most surprising finding is, that although all primary screenings on genomic DNA and RNA level indicated a correct targeting event for the cell clone AD-3, Cre mediated cassette excision proved the opposite. One possible explanation of these findings could be, that the *KRAS-NEO* targeting vector might have acquired sequences of the 5' end from the genomic *KRAS* locus and might have integrated somewhere else in the genome. This phenomenon is also known as ectopic gene targeting [282]. These findings advise caution regarding the screening of putative *KRAS*^{LSL-G12D} targeted cell clones in the future. Moreover, these results demonstrate that all cell clones have to be verified for a correct *KRAS*^{LSL-G12D} gene targeting event by the activation of the latent oncogenic *KRAS*^{LSL-G12D} allele *in vitro*, before cells will be used for SCNT.

4 Discussion

4.1 Modelling the multi-step process of porcine tumorigenesis *in vitro*

Despite advanced insights into the molecular circuitry that underlies the initiation and progression of human cancers, the diagnosis and treatment for this disease remain inadequate. To this end, animal models represent important tools for the design and evaluation of novel diagnostic and therapeutic anticancer drugs. In this respect, genetically defined mice are currently the most commonly used animal model for biomedical cancer research and preclinical studies [reviewed in 283]. However, mice differ clearly from humans in terms of cancer biology, as murine cells are more easily transformed *in vitro* than human cells. In particular, the perturbation of the p53 and Kras signalling pathways alone was shown to be sufficient to induce a transformed phenotype in murine cells *in vitro*, while human cells needed the disruption of the p53, Kras, pRb and Myc signalling pathways in combination with an immortalisation step [233]. This indicates that profound differences exist in the process of cellular transformation between mice and humans. Thus, there is a considerable need for relevant animal models, in which the process of tumorigenesis is analogous to humans. To date there has been only one report, which demonstrated the derivation of fully transformed primary porcine cells *in vitro* through the enforced expression of cyclin D1, CDK4^{R24C}, p53^{DD}, HRAS^{G12V}, cMyc^{T58A} and hTERT [258]. Worth mentioning, this set of genetic alterations is in full agreement with those necessary to transform human cells *in vitro* [25]. However, this experimental porcine tumour model falls short as a representative cancer model, as it relies on the ectopic expression of oncogenes and dominant-negative tumour suppressors, which are driven by viral promoters. In this regard, the expression of introduced transgenes is driven in a non-physiological manner resembling rather gene amplifications of oncogenes and mutant tumour suppressors than the occurrence of natural mutations found in human cancers. Due to the limitations of this experimental porcine tumour model, the objective of this study was to derive an experimental porcine mesenchymal stem cell (pMSC) transformation model that recapitulates the situation *in vivo* more closely. Therefore, the expression of oncogenic *TP53*^{R167H} (orthologous to human *TP53*^{R175H} and mouse *Trp53*^{R172H}) and *KRAS*^{G12D} (homologous to human *KRAS*^{G12D} and mouse *Kras*^{G12D}) should be driven from their endogenous gene promoters and their contribution to porcine tumorigenesis should be investigated.

4.2 Generation of *TP53*^{LSL-R167H}, *KRAS*^{LSL-G12D} double-targeted pMSC clones

To mimic the multi-step process of porcine tumorigenesis *in vitro* latent oncogenic *TP53*^{LSL-R167H} and *KRAS*^{LSL-G12D} alleles should be introduced into the endogenous gene loci by

homologous recombination. As target cells, the previously $TP53^{LSL-R167H}$ targeted cell clone neo14, which lacked any detectable p53 expression [256], was subjected to a second round of gene targeting to introduce a Cre activatable mutant $KRAS^{LSL-G12D}$ allele.

4.2.1 Design of the $KRAS^{LSL-G12D}$ gene targeting constructs

Due to the commonly observed low frequency of targeted homologous recombination (HR) in somatic cells, several experiments were designed by various laboratories, which aimed at increasing the rate of targeted recombinants in somatic cells. These included positive-negative selection, promoter and polyadenylation trap strategies, extension of the homologous sequence arms of the targeting vector and introduction of double-strand breaks at the targeted locus by rare-cutting endonucleases or chimeric nucleases, respectively [284-290]. Some of these strategies were taken into account for the design of the $KRAS^{LSL-G12D}$ targeting vectors. To enrich correctly targeted $KRAS^{G12D}$ cell clones the promoter trap gene vectors comprise a 3.1kb 5' short arm of homology, followed by a floxed transcriptional stop cassette containing either a blasticidin resistance gene (*bsr*) ($KRAS-BS$) or a neomycin resistance gene (*neo*) ($KRAS-NEO$) and a 9.1kb 3' long arm of homology.

4.2.2 Identification of $TP53^{LSL-R167H}$, $KRAS^{LSL-G12D}$ double-targeted pMSC clones

Neo14 cells were electroporated with the $KRAS-BS$ promoter trap gene vector to introduce a latent oncogenic $KRAS^{G12D}$ allele in these cells. Subsequent PCR-screenings of BS-resistant single cell clones (designated as neo14/K- subclones) revealed that 54.6% of all analysed subclones amplified the expected DNA fragment across the 5' junction of the short arm to the *bsr* gene. Next, the integrity of the 3' end of the targeted $KRAS$ gene locus was investigated for five subclones (neo14/K39, neo14/K67, neo14/K82, neo14/K83 and neo14/K84). Long range PCR across the LSL cassette to the 3' junction of the long arm showed that four out of the five analysed subclones amplified the expected DNA fragment. To detect the presence of the G to A substitution in codon 12 (G12D), these four subclones (neo14/K39, neo14/K67, neo14/K82 and neo14/K84) were subjected to restriction fragment length polymorphism (RFLP) test, as the G12D mutation results in gain of a *BccI* restriction enzyme recognition site. RFLP test evidenced that three out of the four investigated subclones possess the G12D mutation in exon 2.

4.2.3 Efficiency of $KRAS^{LSL-G12D}$ gene targeting

The in this project achieved high targeting efficiency of 54.6% was quiet astounding, since targeted HR in somatic porcine cells is usually relatively inefficient with reported targeting efficiencies ranging from 2.1-9% [248,253,256,266]. With the exception of one report that

showed that gene targeting into the permissive porcine *ROSA26* gene locus resulted in targeting efficiencies of 28%-48% [291]. However our obtained high targeting efficiency of 54.68% can neither be reasoned by the design of the targeting construct nor by the gene locus or by the selection strategy applied. Thus it is more likely, that the high KRAS-BS targeting efficiency was rather a consequence of p53 deficiency in the clone neo14. Beside p53's function in mediating cell cycle arrest and/or apoptosis in response to DNA damage, p53 plays an essential role in maintaining genomic stability. In this respect, HR provides the only pathway for accurate repairing of double-strand breaks [292] and several studies have shown that p53 is directly involved in repressing the frequency of HR [293-296]. These initial findings were in accordance with the observation of the unusual cytoplasmic localisation of p53 in ES cells [297-300] reasoning their relatively high frequency of HR [301]. Although these findings pointed to a direct role of p53 in HR, several other studies were not able to show any effect of p53 on HR [302-304]. Because of these given discrepancies in the literature, a more detailed *in vitro* study was conducted to figure out the role of p53 in regulating HR. By applying different HR assays Yun *et al.* (2004) evidenced, that the frequency of gene targeting was unaffected by p53 depletion, while in the same somatic cells, the rate of intra- and extrachromosomal HR was elevated [305]. Based on their findings, the group concluded that p53 can discriminate between genome-stabilising and genome-destabilising HR [305].

In addition to p53, the RAD52 epistasis group comprises several genes (e.g. Rad51, Rad52 and Rad54), which are involved in the cell's intrinsic recombination machinery and are therefore crucial for double-strand break repair by HR [306]. Consistent with their role in HR, these genes were shown to directly influence the efficacy of gene targeting, as their depletion resulted in severely impaired targeting efficiencies [307-311]. For that reason, the transient overexpression of these genes is considered as a valuable tool for improving gene targeting efficiencies [312]. As experimentally demonstrated by microarray analysis BS-resistant neo14/K- subclones showed an increased expression of Rad51 and Rad54B -a Rad54 paralog- [313,314]. Based on these findings it can be presumed that their expression was already elevated in the parental cell clone neo14. Therefore, the lack of p53 expression and the presumable elevated expression of Rad51 and Rad54B in the parental cell clone neo14 provide a good explanation for the relative high KRAS-BS targeting efficiency achieved.

4.3 Activation of latent oncogenic alleles by Cre protein transduction

To activate the introduced latent *KRAS*^{LSL-G12D} and *TP53*^{LSL-R167H} mutant alleles in the subclone neo14/K67, cells were subjected to Cre recombinase mediated cassette excision. Cre protein transduction was applied, as Peitz *et al.* (2002) showed that cell permeable,

recombinant Cre protein is a very effective and safe tool for inducing recombination of lox-modified alleles in primary cells [315].

4.3.1 Efficiency of Cre protein mediated cassette excision

$TP53^{LSL-R167H}$, $KRAS^{LSL-G12D}$ double-targeted porcine cells were transduced with recombinant Cre protein. Excision of the floxed transcriptional stop cassettes should accomplish expression of mutant mRNA species and restoration of G418 and Blasticidin S sensitivity in fully recombined cell clones, respectively. As a functional screen 22 Cre protein transduced single cell clones (referred to as neo14/K67/- subclones) were split into culture medium supplemented with either G418 or Blasticidin S and culture proceeded. While 6 out of 22 neo14/K67 subclones survived G418 selection, none of the neo14/K67/- subclones survived Blasticidin S selection. These initial observations indicated, that the floxed transcriptional stop (LSL) cassette at the targeted mutant $TP53^{LSL-R167H}$ gene locus was recombined in 72.7% (6/22) of all analysed neo14/K67/- subclones, while the LSL cassette at the targeted mutant $KRAS^{LSL-G12D}$ gene locus was excised in all analysed neo14/K67/- subclones (22/22). This highly efficient Cre protein mediated recombination of latent oncogenic porcine alleles is in accordance with data from Peitz and colleagues (2007), who reported a virtually 100% efficiency of recombination in both primary mouse and ES cells [316].

4.3.2 $TP53^{LSL-R167H/LSL-R167H}$ homozygosity of the cell clone neo14

PCR screenings of the fully recombined subclones neo14/K67/1.1, neo14/K67/1.3, neo14/K67/1.4 and the partially recombined subclone neo14/K67/1.8, which survived G418 selection, were carried out to prove the excision of the relative LSL cassettes on genomic DNA level. To this end, PCRs across the LSL integration sites at the relative targeted gene loci were performed. Consistent with the results obtained from the Blasticidin S selection test, all subclones derived after Cre protein transduction, lacked the transcriptional stop cassette at the targeted $KRAS^{G12D}$ gene locus. PCR across the LSL integration site at the targeted $TP53^{R167H}$ gene locus revealed that the transduced subclones neo14/K67/1.1, neo14/K67/1.3 and neo14/K67/1.4 possess only the recombined $TP53^{L-R167H}$ allele, while the partially recombined subclone neo14/K67/1.8 has both a non-excised $TP53^{LSL-R167H}$ allele and a recombined $TP53^{L-R167H}$ allele. These findings showed that the parental cell clone neo14 harbours two gene-targeted $TP53^{LSL-R167H}$ alleles. However, these findings were astonishing, since Simon Leuchs was able to amplify the wild-type $TP53$ allele in early-passage neo14 cells. In addition, he recognised that the clone neo14 ceased proliferation for a short period of time after which fast growing cells arose, which had lost the wild-type $TP53$ allele (personal communication). Overall, his observations pointed to a loss of heterozygosity (LOH). Cre protein mediated recombination of lox-modified alleles revealed that the parental

cell clone neo14 was homozygous than hemizygous for a $TP53^{LSL-R167H}$ gene targeting event. One explanation for these findings can be provided by the observations that heterozygously targeted mammalian cells can become homozygous either after culture in high concentrations of G418 or spontaneously through mitotic recombination [317-319]. For that reason, it is likely that the homozygosity of clone neo14 is a consequence of a HR-dependent double-strand break repair mechanism. This assumption is strengthened by the noticed elevated HR frequency of clone neo14 (as discussed before). In addition, it is most likely that the homozygosity facilitated the clone neo14 to bypass growth arrest. This assumption is consistent with the observation that loss of wild-type p53 function enables cells to extend their replicative lifespan [320-322].

4.3.3 Functionality of Cre recombined $TP53^{L-R167H}$, $KRAS^{L-G12D}$ alleles

Besides the finding that the parental cell clone neo14 was homozygous for a latent $TP53^{R167H}$ mutant allele, Cre protein transduction evidenced the functionality of the activated oncogenic $KRAS^{L-G12D}$ and $TP53^{L-R167H}$ alleles, as Cre transduced neo14/K67/- subclones expressed both mutant KRAS-G12D and mutant TP53-R167H mRNA transcripts. Moreover, Western blot and Ras Activation Assay proved that the porcine oncogenic $KRAS^{L-G12D}$ and $TP53^{L-R167H}$ alleles have similar biochemical properties as their human and murine orthologous, namely expression of constitutively GTP-bound Kras proteins and stabilised p53 proteins, respectively [79,80,188,205,226,262,263,323].

4.4 Transcriptional silencing of p16INK4 α

Although it was shown that the perturbation of p53 and Ras signalling pathways was sufficient to convert murine cells to a transformed phenotype, human and porcine cells required additional hits for neoplastic transformation. In particular, the abrogation of five pathways -including pRb, p53, Ras, cMyc and hTERT- was necessary for full tumorigenic transformation *in vitro* [233,258]. The perturbation of normal p53 and pRb function is considered as an essential prerequisite for cellular transformation, as it leads to deregulated cell cycle progression and to an extended lifespan of human cells *in vitro* [reviewed in 275]. Based on these findings and the observation that all established cell clones (neo14, neo14/K- subclones and neo14/K67/- subclones) showed no signs of replicative senescence and instead exhibited an accelerated growth pointed to the idea that stepwise modified pMSCs had lost normal pRb function. Inhibition of normal pRb function leads to loss of G₁-to-S phase checkpoint control, which in turn accomplishes uncontrolled cell cycle progression. In this regard, the retinoblastoma protein is regarded as an important tumour suppressor gene, because it acts as a transcriptional negative regulator of G₁ phase progression. In its hypo-phosphorylated active conformation, pRb blocks G₁ phase progression resulting in cell

cycle arrest and subsequent growth suppression. Upon hyper-phosphorylation by active cyclin D1/CDK4 complexes pRb becomes inactive and G₁-to-S phase transition proceeds [reviewed in 83,324,325]. Due to its potent role in limiting uncontrolled cell growth the abrogation of the p16INK4 α /cyclinD1-CDK4/pRb signalling pathway was a basic prerequisite for the tumorigenic conversion of primary human and porcine cells *in vitro* [25,233,258,326]. This pathway can be altered either through the inactivation of the two negative regulators of cell proliferation, p16INK4 α and pRb, or through the overexpression of the two inducers of proliferation, cyclin D1 and CDK4 [327]. Consistent with these observations, several experimental human cell transformation models have shown that an overexpression of cyclin D1 and CDK4 or its mutant resistant to p16INK4 α inhibition (CDK4^{R24C}) are sufficient to inactivate the pRb pathway [15,25,265,328]. These genetic modifications cause hyper-phosphorylation and inactivation of pRb [329-331]. The same effect was observed in cells lacking expression of the cell cycle inhibitor and modulator of senescence p16INK4 α [332,333]. A growing body of evidence indicates that the *CDKN2A* gene locus and its gene products, p16INK4 α and p14ARF, take a centre stage not only in controlling cell cycle progression but also in replicative senescence. While p16INK4 α plays a central role in senescence and tumour suppression in human cells, p14ARF does so in murine cells by inducing p53-dependent cell cycle arrest [reviewed in 108]. As both are considered as potent mediators of cellular senescence, but in a species-specific manner and little is known about the circumstances regarding the porcine senescence program, their expression levels were investigated in more detail. As evidenced by RT-PCR and quantitative real-time RT-PCR, the expression of p16INK4 α was almost absent in the stepwise-modified pMSCs compared to wild-type pMSCs, whereas the expression of p14ARF increased. These results suggest that p16INK4 α is the key governor of the senescence program in porcine cells, similar to its function in mediating cellular senescence in human cells [116,271,272].

Based on the results of the expression analysis and the fact that p16INK4 α and p14ARF are encoded from the same gene locus but transcribed from distinct independent promoters [107], it was assumed that the impaired p16INK4 α expression had to be rather a consequence of epigenetic modifications of the *P16INK4A* gene region than gene deletions. Consistent with this idea aberrant DNA hyper-methylation is a common mean by which tumour suppressor genes are inactivated during carcinogenesis [103,334]. Given that the porcine *P16INK4A* promoter sequence is not fully annotated yet, the methylation signature of 5' region of the *P16INK4A* gene locus covering most of the first exon (-10 to +256) was investigated, as Brenet and colleagues showed, that DNA methylation surrounding the transcriptional start site is tightly linked to transcriptional silencing [335]. Methylation analysis revealed that this region is hyper-methylated in the genetically modified pMSCs. These findings indicate that the transcriptional repression of the *P16INK4A* gene locus might be a

consequence of gene methylation. These findings are in full agreement to those from Tsutsui *et al.* (2002), who showed that spontaneously immortalised human cells lose p16INK4 α expression mainly due to gene methylation, which in turn causes hyper-phosphorylation and inactivation of pRb [333]. Considering that neither the expression of cyclin D1 nor CDK4 was highly upregulated in the genetically modified pMSCs compared to wild-type pMSCs as evidenced by microarray analysis, it can be concluded that the transcriptional repression of p16INK4 α has to be the cause of the physiological inactivation of the pRb pathway. Consistent with this idea, an altered expression of one component of the p16INK4 α /cyclinD-CDK4/pRb pathway was reported to be sufficient to trigger G₁-to-S-phase transition and thereby cell cycle progression [275,327].

4.5. Deregulated cell cycle control in stepwise genetically modified pMSCs

Microarray analysis showed an aberrant expression of other cyclin/CDK complexes involved in cell cycle regulation. In particular, the expression of cyclin E and its interaction partner CDK2 was significantly upregulated in the stepwise modified pMSCs compared to wild-type pMSCs. In normal cells cyclin E and CDK2 accumulate near the G₁-to-S phase transition, where they control the entry into and progression through S phase [reviewed in 336]. An aberrant expression of cyclin E throughout the cell cycle has been reported in a variety of human cancers, suggesting a link between deregulated cyclin E expression and tumorigenesis [337-339]. Moreover, early *in vitro* studies showed that an ectopic expression of cyclin E accelerates entry into S phase [329,340] and cyclin E overexpression is also associated with mitotic delay and genomic instability [341,342]. In addition, an aberrant expression of cyclin A2 and its interacting cyclin dependent kinases CDK2 and CDK1 was detected in the stepwise modified pMSCs. While cyclin A2 binds to and activates CDK2 in S phase, it associates with either CDK1 or CDK2 at the G₂-to-M phase transition [343,344]. Cyclin A/CDK2 complexes control S phase progression, where they are implicated in DNA replication [345]. In agreement to these findings, an ectopic overexpression of cyclin A2 was shown to induce premature entry of G₁ cells into S phase [346,347]. In late G₂ phase cyclin A/CDK2 complexes localise to the centrosomes and coordinate the timing of entry into mitosis [348]. Given that cyclin A2 is rapidly degraded during mitosis, usually before the onset of anaphase, increased levels of cyclin A in mammalian cells delay chromosome alignment and anaphase onset [349,350]. In line with these findings, aberrant expression of cyclin A2 has been found in a variety of human cancers and deregulated cyclin A2 expression appears to be closely related to tumour cell proliferation [reviewed in 351].

Moreover, stepwise modified pMSCs showed elevated levels of B-type cyclins (B1, B2 and B3) and CDK1, which regulate the progression from G₂ into M phase. In normal cells the levels of cyclin B mRNA increase during G₂ phase and peak at the G₂-to-M transition [352-

354]. Transcription of CDK1 is initiated during G₁-to-S-phase transition and peaks at early mitosis [355]. As a consequence, inappropriate expression of Cyclin B1 and CDK1 cause premature entry into mitosis and uncontrolled cell proliferation [356,357]. Consistent with these observations, an accelerated expression of cyclin B1 and CDK1 was reported in a broad spectrum of human malignancies [358-363], indicating their pivotal role in deregulating cell cycle progression and promoting malignant transformation.

Since cell cycle progression is not only controlled by a diverse set of cyclin/CDK complexes but also by p53, the expression levels of some p53 target genes were investigated. Transcriptome analysis revealed that the expression of p53 and its two stress-induced targeted genes, p21 and GADD45, is diminished in p53-deficient neo14/K-subclones as well as in cells expressing mutant p53-R167H protein (neo14/K67/1.1+cMyc). After DNA-damage p53 inhibits G₁-to-S transition by causing the accumulation of p21 [364,365]. P21 is the key regulator of G₁ arrest, as it blocks the kinase activity of cyclin-complexed CDK2, which in turn leads to hypo-phosphorylated pRb [366]. Besides its pivotal role in mediating G₁ arrest, p21 can also trigger G₂ phase arrest by effectively inhibiting the kinase activity of CDK1 [367,368]. GADD45 binds also to CDK1 and disrupts its ability to complex with cyclin B, which is essential to enter mitosis [369,370]. These data imply, that loss of normal p53 function entails impaired DNA damage checkpoint control in porcine cells, as seen in murine and human cells [371,372].

Collectively these data indicate, that the stepwise genetically modified pMSCs have lost normal cell cycle control, mainly through the perturbation of both the pRb and p53 signal transduction pathways. Moreover, based on the aberrant expression of genes involved in sensing and repairing DNA damage or assuring correct chromosomal segregation during mitosis it can be assumed that the genetically modified pMSCs possess a high degree of genetic instability [49].

4.6 Acquired immortalisation of stepwise genetically modified pMSCs

Due to the “end replication problem” telomeres are progressively shortened with each cell division [29,30] and upon a certain threshold length, cells enter an irreversible growth arrest called replicative senescence [35,36]. For that reason, the restricted replicative lifespan of somatic cells is regarded as a potent barrier of malignant cell transformation limiting the growth potential of precancerous cells [38]. In contrast, unlimited replicative capability is a hallmark of cancer [49]. In virtually all human tumours (90%) the telomeres are maintained by an upregulated expression of telomerase, while the minority employs a telomerase-independent mechanism, termed Alternative Lengthening of Telomeres (ALT) [40,44,46]. These observations indicate that telomere maintenance and the concomitant cellular immortalisation are essential events in the multi-step process of malignant human cell

transformation. Consistent with these observations, the ectopic expression of TERT was an essential prerequisite for human cell transformation [25,233,264,326,373]. In contrast, ectopic expression of TERT was dispensable to drive murine cells to a transformed phenotype, as they readily undergo spontaneous immortalisation *in vitro* [233]. This phenomenon may be due to the relatively long telomeres (250 kb) observed in laboratory mice and their persistent expression of telomerase in somatic tissue [374-376]. Although telomere biology in humans and pigs seems to be similar, as porcine telomeres (16-18 kb) have a similar length as human ones [377,378] and several somatic porcine tissues lack detectable telomerase expression [379,380], the cell pool neo14/K67/1.1+cMyc was converted to a fully transformed phenotype without the ectopic expression of TERT. RT-PCR and microarray analysis evidenced that neither wild-type pMSCs nor stepwise modified pMSCs expressed detectable levels of this reverse transcriptase. These findings pointed to the idea that the genetically modified pMSCs must have acquired a telomerase-independent mechanism to become immortalised. As mentioned above the parental cell clone neo14 entered a growth-arrested state, after which fast growing, homozygously targeted TP53^{R167H} cells emerged. Based on these observations it is quite likely that loss of wild-type p53 function facilitated the clone neo14 to extend its proliferative lifespan. In addition, the finding that the KRAS-BS retargeted subclone neo14/K67 showed a markedly diminished p16INK4 α expression, which was almost absent in all subsequent subclones (neo14/K67/1.1 and neo14/K67/1.1+cMyc), presumes that the abrogation of both pathways are essential for porcine cells to escape replicative senescence. Consistent with these findings, several reports have shown that in human cells replicative senescence is triggered by the p53 and p16INK4 α -pRb signalling cascade [116,268,381] and their combined inactivation entails human cells to escape replicative senescence [37,270,271]. This is opposed to the relative ease with which mouse cells become immortalised and to their senescence program. In particular, in response to culture- or oncogene-induced senescence, wild-type MEFs express increased levels of p53 and ARF, whereas human cells show elevated levels of p16 and pRb [116,118,269,382]. Consistent with this, ARF- or p53-deficient murine cells escape oncogene-induced senescence [118,383,384], while human cells have to abolish normal p53 and pRb function [270,385]. The fact that p53- and p16INK4 α -deficient porcine cells showed no signs of replicative senescence suggests that both signalling pathways are involved in the porcine senescence program, consistent with that of human cells.

Although disruption of normal p53 and pRb function leads to an extended lifespan of human cells, telomeres are still progressively shortened and upon a critical shortness cells enter a second growth-arrest, called crisis [reviewed in 43]. To evade this second barrier to immortalisation human cells have either to upregulate telomerase activity or ALT, which prevents further telomere shortening [386]. In ALT-positive (ALT⁺) cells the telomeres are

maintained by a recombination-mediated DNA replication step, in which telomeric DNA from an adjacent chromosomal telomere is synthesised and copied to another telomere [47]. As the unlimited replicative capability of stepwise modified pMSCs was not a consequence of upregulated TERT expression, we investigated the expression of some ALT-associated genes. Transcriptome analysis of stepwise genetically modified pMSCs and the porcine sarcoma derived cell lines revealed that a number of genes that are crucial for telomere maintenance in ALT⁺ cells were upregulated. Among them were genes required for telomere elongation and capping, such as RAD51 and BRCA2 [387]. In addition, flap endonuclease 1 (FEN1), Fanconia anaemia group D2 (FANCD2) and Fanconi anaemia group A (FANCA) were also upregulated. These proteins are essential for the recombinational repair of broken replication forks in normal cells [388-390] and thus it is supposed, that these proteins are required for telomere maintenance in ALT⁺ cells [reviewed in 391]. Furthermore, transcriptome analysis revealed that the expression of the Bloom syndrome helicase (BLM), a RecQ helicase [392], was significantly upregulated. Studies conducted by Stavropoulos *et al.* (2002) demonstrated, that the overexpression of BLM caused a rapid increase in telomeric DNA synthesis in telomerase-deficient human cells, reasoning that BLM plays an important role in the human ALT pathway [280]. In contrast, the expression of shelterin proteins TERF2 and protection of telomeres 1 (POT1) that are implicated in the repression of ALT were kept at low levels. Shelterin proteins bind to telomeric DNA and exert anti-recombination properties, whereas reduced shelterin protein saturations at telomeres are considered as the cause of ALT [reviewed in 391].

Summing up, data from the transcriptome analysis show that pMSCs, which were converted to a transformed phenotype *in vitro* had upregulated the expression of genes that are implicated in the Alternative Lengthening of Telomeres mechanism. These results are in high accordance with human MSCs, which have a particular tendency to activate ALT [393]. It should be noticed, that the overall prevalence of ALT in tumours is relatively low, but it is observed more frequently in mesenchymal malignancies. In particular, 77% of pleomorphic-undifferentiated sarcomas (PUS) are ALT positive [394]. Again, our results are in full agreement with these data, as transformed pMSCs gave rise to sarcomas, which in humans prevent telomere attrition by the ALT mechanism.

4.7 *In vitro* growth characteristics of stepwise genetically modified pMSCs

Since unlimited replicative capacity, loss of density-dependent growth inhibition and the ability to proliferate in semi-solid medium are characteristics of neoplastic cells, several *in vitro* assays were performed to analyse the transformation-related phenotypes of the stepwise genetically modified pMSCs. Un-induced neo14/K67 cells did not proliferate considerably faster than wild-type pMSCs (population doubling time (PDT) of 23.6 +/-0.4h vs.

25.7h +/-2.6h), although an increased expression of several cyclin/CDK complexes and the perturbation of the pRb pathway were detected in un-induced neo14/K67 cells. However, these results are consistent to those from Resnitzky *et al.* (1994). The group reported that an ectopic overexpression of cyclin B1, E and D1 does not change the mean cell cycle length of rat fibroblasts relative to their non-induced counterparts. These findings were reasoned by the observation, that the constitutive ectopic expression of these cyclins did not only accelerate G₁-to-S transition but also increase the length of S and G₂ phase [329]. As opposed to this, cells expressing mutant *TP53*^{R167H} and *KRAS*^{G12D} (neo14/K67/1.1 and neo14/K67/1.1+cMyc) showed an accelerated growth with a PDT of 15.4h +/- 1.7h and 14.7h +/-0.8h, respectively. These results are in line to those from Lang *et al.* (2004). They showed that MEFs homozygous for the *Trp53*^{R172H} mutation grew faster than p53^{-/-} MEFs, supporting the idea of a gain of function of mutant p53 [79]. In addition, Tuveson *et al.* (2004) reported that the expression of endogenous mutant *Kras*^{G12D} stimulates proliferation in MEFs [226]. Surprisingly, stable selected cMyc transfectants did not proliferate considerably faster than the parental cell clone neo14/K67/1.1. However, deregulated expression of cMyc enabled neo14/K67/1.1+cMyc cells to form multi-layered foci when reaching confluence. These observations indicated that neo14/K67/1.1+cMyc cells had lost contact inhibition. Moreover, when grown in soft agar, cells expressing mutant *TP53*^{R167H} and *KRAS*^{G12D} gave rise to 54 colonies and the cMyc transfected cell pool to 24 colonies. Although the neo14/K67/1.1+cMyc cell pool formed fewer colonies in semisolid medium than the parental cell clone neo14/K67/1.1, these colonies were much larger. Collectively, the soft agar assay evidenced that both cell populations had acquired *in vitro* growth properties associated with neoplastic cell transformation [reviewed in 395].

4.8. *In vivo* tumorigenicity of stepwise genetically modified pMSCs

Since all *in vitro* assays indicated that the genetically modified pMSCs were converted to transformed phenotype, these cells were implanted into immune-deficient mice, because the most rigorous test for assessing tumorigenicity of transformed cells is their capability to form tumours when injected immune-comprised animals.

4.8.1 Implantation of stepwise genetically modified pMSCs in immune-deficient mice

To test the tumorigenic potential of stepwise modified pMSCs *in vivo*, cells were mixed 1:1 (v/v) with Matrigel™ Basement Membrane Matrix and injected subcutaneously in immune-deficient mice. However, only stable selected cMyc transfectants gave rise to rapidly growing tumours in the immune-deficient host (3/4), while the parental cell clone neo14/K67/1.1 formed only one small tumour nodule. These data show that although ALT-immortalised,

p16INK4 α -deficient pMSCs expressing endogenous mutant *TP53*^{R167H} and *KRAS*^{G12D} mimicked almost all features of neoplastic cell transformation *in vitro*, they failed to form rapidly growing tumours in the short time course of the xenotransplantation experiment. These observations indicate, that additional genetic alterations are indispensable to confer complete transformation of pMSCs. In agreement with this idea, the additional deregulated expression of cMyc promoted the *in vivo* tumorigenicity of genetically modified pMSCs in our study. One explanation for Myc's crucial role in the process of neoplastic porcine cell transformation can be provided by the observations of Lin *et al.* (2012) and Nie *et al.* (2012). They reported that elevated cMyc levels cause the transcriptional amplification of the existing gene expression program by binding to actively transcribed gene promoters [396,397]. Moreover, our results are in high agreement with those from Funes *et al.* (2007). They reported that the concomitant expression of hTERT, E6 and E7 oncoproteins of the human papillomavirus and HRAS^{V12} resulted in tumour growth in 2/10 injection sites with a latency of 69 days. In contrast, mice inoculated with telomerase-immortalised human MSCs transduced with E6 and E7, SV40 ST and HRAS^{V12}, which resulted in the perturbation of the p53, pRb, Myc and Kras signalling pathways, developed tumours with a significantly shorter latency of between 20-27 days [326]. These observations are in high accordance to an earlier study conducted by Rangarajan *et al.* (2004). The group demonstrated that the perturbation of the same signalling pathways is required for *in vivo* tumorigenicity of differentiated human cells derived from various tissue compartments (foreskin fibroblasts, embryonic kidney fibroblasts and mammary epithelial cells) [233]. And in 2007 Adam *et al.* showed that the perturbation of the identical pathways is sufficient to confer neoplastic transformation of porcine dermal fibroblasts, embryonic kidney fibroblasts, kidney epithelial cells and testis cells [258]. Collectively, our data and the previously reported one by Adam *et al.* (2007) show, that multipotent and differentiated porcine cells require the same genetic alterations as their human counterparts to be converted to a fully transformed phenotype. This conflicts with the ease how murine MSCs and differentiated cells became tumorigenic [233,398,399].

4.8.2 Isolation and culture of porcine sarcoma derived tumour cells

One of the neo14/K67/1.1+cMyc derived tumours was histological examined and classified as a low-grade myxoinflammatory fibroblastic sarcoma (MIFS). Re-implantation of one neo14/K67/1.1+cMyc derived tumour into another immune-deficient mouse resulted in the formation of a pleomorphic-undifferentiated sarcoma (PUS). These results are in line with the role of experimentally transformed murine and human MSCs in sarcomagenesis [reviewed in 400]. In addition the neo14/K67/1.1+cMyc derived MIFS and PUS were used to derive a porcine primary tumour cell line (pPTC) and a re-implanted porcine tumour cell line (rePTC), respectively. Unfortunately, rePTC adhered very poorly to plastic culture dishes and

frequently detached during standard tissue culture procedure. This feature contrasts to the tight plastic adherence of genetically modified pMSCs and pPTC. These observations assumed that the re-implanted porcine tumour cells might express another set of genes involved in adhesion and extracellular matrix pathways compared to the genetically modified pMSCs and the primary porcine tumour cells. This assumption was moreover underpinned by the finding that tumour cells of the re-implanted tumour invaded the pancreas of the immune-deficient mouse. In addition, transcriptome analysis showed that the malignant rePTCs express elevated levels of extracellular matrix (ECM) degrading and remodelling proteases, such as MMP-1, MMP-3, MMP-10 and MMP-11 and vascular endothelial growth factor α , an inducer of the “angiogenic switch” [49]. These findings confirm the invasive and migratory properties of these re-implanted porcine sarcoma derived cells. In this regard, our results are consistent to numerous studies that reported that cellular migration and invasion are governed by an altered expression of integrins and secreted proteases [reviewed in 401,402]. Collectively, these findings suggest that the modified affinity for basement membrane substrates observed in the malignant rePTCs might be most likely due to a different expression and distribution of integrins.

4.8.3 Amplification of oncogenic *KRAS*^{G12D} in porcine sarcoma derived tumour cells

Microarray analysis uncovered that both porcine sarcoma derived cell lines expressed elevated levels of *KRAS* mRNA. Molecular investigations brought to light that the elevated *KRAS* mRNA levels in both cell lines correlated with increased *KRAS* copy numbers. Six copies of the second exon of the *KRAS* gene were identified in the primary PTC line and nine copies in the re-implanted PTC line. Sequencing of *KRAS* mRNA transcripts revealed that the mutant *KRAS*-G12D mRNA species is the predominant one in the two porcine sarcoma derived tumour cell lines. In agreement with these findings, pPTC and rePTC expressed elevated levels of constitutively active GTP-bound Ras proteins compared to the genetically modified pMSCs. Taken together, these results indicate that the increased expression of active Ras-GTP in the porcine sarcoma derived cell lines is primarily due to genomic amplification of the mutant *KRAS*^{L-G12D} allele, a phenomenon that has been observed in some human tumour entities [403-405].

Since all investigations showed that the transcription of mutant *Kras*-G12D mRNA results in an increased expression of oncogenic *Kras*^{G12D} protein we assessed the levels of phosphorylated ERK1/2 and Akt. These are two well-defined indicators of the activation of the Raf/MEK/ERK and the PI3K/Akt pathway, respectively [reviewed in 406]. Unexpectedly, wild-type control pMSCs and un-induced neo14/K67 cells displayed elevated basal levels of both, pERK1/2 and pAkt, but no further increase was detected in Cre recombined pMSCs before (neo14/K67/1.1 and neo14/K67/1.1+cMyc) as well as after xenotransplantation (pPTC

and rePTC). These results were very wondrous, since these two pathways are supposed to become activated by constitutively GTP-bound Kras [reviewed in 279]. One possible explanation for this finding can be provided by study designed by Tuveson *et al.* (2004). The group reported that Kras^{L-G12D} MEFs had equal or even decreased levels of pERK and pAkt compared to wild-type MEFs and unrecombined Kras^{LSL-G12D} MEFs, while MEFs ectopically expressing super-physiological levels of oncogenic HRAS^{G12V} contained elevated levels of pERK and pAkt. In their study the underlying mechanism of Ras effector pathway attenuation in primary cells expressing endogenous oncogenic Kras^{G12D} remained also elusive [226]. Braun *et al.* (2004) reported similar results. They established an IFN-inducible genetically engineered mouse model (Mx1-Cre; Kras^{LSL-G12D}) in which recombination of the LSL cassette was directed to the bone marrow. Although Ras-GTP levels were elevated in isolated bone marrow cells of mutant Kras^{L-G12D} mice, the group did not detect elevated levels of pMEK and pAkt [407]. Based on their and our findings it can be presumed that primary cells of mesenchymal origin may require the activation of the Ral-GEFs or other downstream signalling pathways, which were not investigated in our study. Collectively, our results are in agreement with the findings of these two experimental studies, in which the expression of endogenous oncogenic Kras^{G12D} does not entail an activation of either ERK or Akt in primary cells *in vitro*.

4.8.4 Implantation of stepwise modified pMSCs in an immune-competent isogenic pig

In a final attempt, we wanted to evaluate the tumorigenic potential of genetically modified porcine cells in an immune-competent large animal. The parental, unmodified wild-type pMSCs were used to clone a syngeneic recipient animal. Subcutaneous implantation of transformed pMSCs into the cloned, syngeneic pig should not result in an immune response and cell rejection. Since the xenotransplantation experiment showed, that transformed pMSCs co-injected with MatrigelTM Basement Membrane Matrix can give rise to tumours in immune-deficient mice, it was decided to co-inject two cell preparations with MatrigelTM Basement Membrane Matrix. Few days after implantation a swelling and redness at the injections sites, where cells had been co-injected with MatrigelTM, were visible. However, these regressed again, indicating that the pig has evoked a potent immune response against the xenoantigenes presented by the MatrigelTM Basement Membrane Matrix, as this basement membrane had been extracted from an Engelbreth-Holm-Swarm mouse sarcoma [408,409]. The same phenomenon was observed at the injection sites, where stable selected cMyc transfectants (neo14/K67/1.1+cMyc) and primary porcine tumour cells (pPTCs) had been injected. In contrast, no obvious immune response was detected at the injections sites of wild-type and Cre recombined pMSCs (neo14/K67/1.1), respectively. These findings suggest that the syngeneic pig developed an immune response against the products of the

selectable marker genes *bsr* and *neoR*, which are encoded by the cMyc expression vector. Consistent with this idea, several studies have reported that the infusion of cells expressing xenogeneic reporter or selectable marker genes, such as the enhanced green fluorescent protein and the hygromycin phosphotransferase and herpes simplex thymidine kinase fusion protein induced a potent immune response in human and animal recipients even after nonmyeloablative conditioning regime [410-413]. Collectively, these data indicate that a preceding immune suppression of the syngeneic recipient would be an essential prerequisite to allow the tumour growth of implanted genetically modified porcine cells. A similar experiment was performed by Adam *et al.* (2007). Here, they had to apply an immune suppressive regime to the isogenic pig prior to cell implantation to allow tumour growth, as they used a combination of human and murine transgenes to convert porcine cells to a tumorigenic state [258].

4.9 Derivation of pigs carrying latent oncogenic $TP53^{LSL-R167H}$ and $KRAS^{LSL-G12D}$ alleles

One of our research interests is to model serious and common human cancers in genetically defined pigs. Inspired by the fact, that concomitant oncogenic mutations of *KRAS* and *TP53* are frequently found in the most deadliest human cancer types [414-416], we aim in deriving genetically modified pMSCs that carry both latent oncogenic $TP53^{LSL-R167H}$ and $KRAS^{LSL-G12D}$ alleles. Correctly double-targeted cell clones should then be used as nuclear donors for somatic cell nuclear transfer. Bone-marrow (BM) and adipose-tissue (AD) derived MSCs were isolated from a transgenic $TP53^{LSL-R167H}$ piglet. Both cell preparations were transfected with the *KRAS-NEO* gene targeting vector construct. Primary targeting screenings revealed a relative targeting efficiency of 12.5% (4 out of 32) in the case of analysed AD-MSC cell clones and of 23.5% (4 out of 17) in the case of investigated BM-MSC cell clones, respectively. However, further molecular analysis showed that only two clones (BM-19 and AD-3) were correctly targeted. These results are consistent with the overall extremely low efficiency of targeted integrations compared to the relatively high frequency of random, non-homologous integrations observed after gene targeting in mammalian cells [reviewed in 312]. Although all investigations pointed to a correct $KRAS^{LSL-G12D}$ gene targeting event in the cell clones BM-19 and AD-3, Cre recombinase cassette excision proved the opposite. While the G12D mutation in exon 2 was present in the RT-PCR product covering exon1 to exon 2, it was not detectable when amplifying exon1 to exon 3 or exon 1 to exon 4. These results were surprising, as no such problem occurred when targeting *KRAS* in the clone neo14. Having a closer look at the literature the term “ectopic gene targeting” attracted my attention. Ectopic gene targeting is described as a phenomenon, in which a transfected targeting construct can elongate its homology arms by acquiring DNA sequences from the genomic target locus and subsequently this elongated targeting construct integrates somewhere else in the genome

[282,417]. In this regard, ectopic gene targeting provides a good explanation for my results, because all performed experiments point to the assumption that the *KRAS-NEO* gene targeting construct has extended its 5' end with genomic sequences comprising the first exon of the *KRAS* gene locus. Otherwise there is no logical explanation, why the established cell clones express a "short" mutant KRAS-G12D transcript (exon 1 to exon 2), but not the longer ones (exon 1 to exon 3 and exon 1 to exon 4).

Summing up, in the course of this project no *TP53*^{LSL-R167H} and *KRAS*^{LSL-G12D} double-targeted cell clones could be derived that could have been used for somatic cell nuclear transfer.

5 Concluding remarks and outlook

In this project, the neoplastic transformation of stepwise genetically modified porcine mesenchymal stem cells (pMSCs) has been achieved. *In vitro* assays and an *in vivo* xenotransplantation experiment proved that the perturbation of normal p53, Kras, pRb and cMyc signalling in combination with an immortalisation step entails the neoplastic transformation of pMSCs. This set of genetic alterations accords with those necessary to convert human MSCs to a transformed phenotype.

This study provides the first porcine experimental cell transformation model that is mainly driven by endogenous genetic alterations (expression of endogenous mutant $TP53^{R167H}$ and $KRAS^{G12D}$, $P16INK4\alpha$ gene methylation and activation of the Alternative Lengthening of Telomeres). However, implantation of genetically modified pMSCs into immune-deficient mice revealed that a deregulated cMyc expression is an essential prerequisite to prompt the *in vivo* tumorigenicity of pMSC. Thus to provide a more elegant porcine experimental mesenchymal stem cell transformation model a conditional cMyc^{T58A} knock-in gene targeting vector should be constructed and used for gene targeting, as mutant cMyc^{T58A} has been reported to exert an enhanced transforming activity [24]. After Cre recombination this approach will allow the derivation of a porcine experimental mesenchymal stem cell transformation model that is driven only by the expression of endogenous mutant oncogenes and tumour suppressor genes. Ideally, these genetically modified pMSCs should not evoke an immune response when implanted in an immune-competent isogenic pig. If these cells will form tumours in syngeneic pigs they can be grown to very large size allowing the testing and validation of hyperthermia and radiation therapy.

Motivated by the findings of the experimental porcine transformation model, we aim in generating double-targeted pigs carrying both Cre activatable oncogenic $TP53^{LSL-R167H}$ and $KRAS^{LSL-G12D}$ alleles. Crossing these pigs with transgenic pigs expressing Cre recombinase in different tissues will allow replicating various human cancer types. Unfortunately, in the course of this project we were unable to generate correctly double gene-targeted pMSCs that could have been used for somatic cell nuclear transfer. This has to be repeated. An alternative approach would be to generate only $KRAS^{LSL-G12D}$ gene targeted pMSCs. Correctly targeted and SCNT-derived founder animals can then be crossed with our $TP53^{LSL-R167H}$ gene targeted pigs and subsequently with transgenic pigs expressing Cre recombinase in a tissue-specific manner. We are confident that these multi-transgenic oncopigs will provide powerful insights into the initiation, progression and pathogenesis of several human cancer types.

6 Abbreviations

%:	Percent
°C:	Degree celsius
µg:	Microgram
µl:	Microliter
µM:	Micromolar
µm:	Micrometer
Ac:	Acetylation
AD:	Adipose tissue
ALT:	Alternative Lengthening of Telomeres
AKT:	Protein kinase B
APC:	Adenomatous polyposis coli
ARF:	Alternative reading frame
ATM:	Ataxia telangiectasia mutated
BAX:	BCL2- associated X protein
BLM:	Bloom syndrome helicase
BM:	Bone marrow
bp:	Basepair
BRCA1:	Breast cancer 1, early onset
bsr:	Blasticidin resistance
cDNA:	Complementary deoxyribonucleic acid
CDK:	Cyclin-dependent kinase
CDKN1A:	Cyclin-dependent kinase inhibitor 1A
CDKN2A:	Cyclin-dependent kinase inhibitor 2A
CO ₂ :	Carbon dioxide
CRC:	Colorectal cancer
CRISPR:	Clustered regulatory interspaced short palindromic repeats
DIG:	Digoxigenin-11-2'-deoxy-uridine-5'-triphosphate
DMEM:	Dulbecco's Modified Eagle's Medium
DMSO:	Dimethylsulfoxide
DNA:	Deoxyribonucleic acid
DNmt3a:	DNA methyltransferase 3a
dNTP:	Deoxyribonucleotide triphosphate
DTT:	Dithiothreitol
dUTP:	Digoxigenin-11-2'-deoxy-uridine-5'-triphosphate
E1A:	Adenovirus early region 1A

ECM:	Extracellular Matrix
EDTA:	Ethylenediaminetetraacetic acid
EGFR:	Epidermal growth factor receptor
ERK:	Extracellular signal-regulated kinase
ES cell:	Embryonic stem cells
<i>et al.:</i>	<i>et alii</i>
FANCA:	Fanconi anemia group A
FANCD2:	Fanconi anemia group D2
FAP:	Familial adenomatous polyposis
FCS:	Fetal calf serum
FEN1:	Flap endonuclease 1
FGF:	Fibroblast growth factor
LFS:	Li-Fraumeni syndrome
LOH:	Loss of heterozygosity
LSL:	Transcriptional termination
LT:	Large T antigen of the simian virus 40 early region
g:	gram
g:	Gravitational acceleration
gDNA:	genomic deoxyribonucleic acid
GADD45:	Growth arrest and DNA damage-inducible protein 45
GAP:	GTPase-activating protein
GAPDH:	Glyceraldehyde-3-phosphate dehydrogenase
GDP:	Guanosine diphosphat
GEF:	Guanine nucleotide exchange factor
GEMM:	Genetically engineered mouse models
GTP:	Guanosine triphosphate
h:	hour
H ₂ O:	Water
HAT:	Histone acetyltransferase
HDAC:	Histone deacetylase
HDM2:	Human double minute 2 homolog
HEK:	Human embryonic kidney
HMEC:	Human mammary epithelial cells
HR:	Homologous recombination
HRP:	Horseradish peroxidase
HLH-Zip:	Helix-loop-helix-leucine zippers
HRAS:	Harvey rat sarcoma viral oncogene homolog

HPV:	Human papillomavirus
HTNC:	His Tag-TAT-NLS-Cre, recombinant Cre recombinase
IL-2R:	Interleukin 2 receptor
IPTG:	isopropyl β -D-thiogalactopyranosid
IRES:	Internal ribosomal entry site
kb:	Kilo basepair
kDa:	Kilo Dalton
KRAS:	Kirsten rat sarcoma viral oncogene homolog
loxP:	Locus of crossing over, bacteriophage P1
m:	Marker
M1:	Mortality stage 1
M2:	Mortality stage 2
mA:	Milliampere
Me ₃ :	Methylation
MAPK:	Mitogen-activated protein kinase
MDM2:	Mouse double minute 2 homolog
MEF:	Mouse embryonic fibroblast
MEK:	MAP kinase kinase
MIFS:	Myxoinflammatory fibroblastic sarcoma
min:	Minute
Miz1:	Myc-interacting zinc finger protein 1
ml:	Milliliter
mM:	Millimolar
MMP:	Matrix Metalloproteinase
mRNA:	Messenger ribonucleic acid
ms:	Milliseconds
MSC:	Mesenchymal stem cell
MSZ:	Mesenchymale Stammzelle
MYC:	v-myc avian myelocytomatosis viral oncogene homolog
NEAA:	Non essential amino acids
neoR:	Neomycin resistance
nm:	Nanometer
NOXA:	Phorbol-12-myristate-13-acetate-induced protein 1
NRAS:	Neuroblastoma RAS viral oncogene homolog
NSCLC:	Non-small-cell lung carcinoma
OD:	Optical density
O/N:	Over night

P:	Phosphorylation
p21:	Cyclin-dependent kinase inhibitor 1A
pA:	Poly adenylation signal
PanIN:	Pancreatic intraepithelial neoplasia
PBS:	Phosphate buffered saline
PCR:	Polymerase chain reaction
PDAC:	Pancreatic ductal adenocarcinoma
PDT:	Population doubling time
PDGFR:	Platelet-derived growth factor receptor
PGK:	Phosphoglycerat kinase
pH:	<i>potential hydrogenii</i>
PI3K:	Phosphoinositide 3- kinase
pIPSC:	Putative porcine induced pluripotent stem cell
pMSC:	Porcine mesenchymal stem cell
POT1:	Protection of telomeres 1
pPTC:	Primary porcine tumour cells
PUS:	Pleomorphic-undifferentiated sarcoma
pRb:	Retinoblastoma protein
PUMA:	p53 upregulated modulator of apoptosis
qPCR:	Quantitative polymerase chain reaction
qRT-PCR:	Quantitative real-time polymerase chain reaction
RAF:	Raf kinase
RALGDS:	Ral guanine nucleotide dissociation stimulator
rePTC:	Re-implanted porcine tumour cells
RFLP:	Restriction fragment length polymorphism
RNA:	Ribonucleic acid
rpm:	Revolutions per minute
RT:	Room temperature
RT-PCR:	Reverse transcriptase polymerase chain reaction
SA:	Splicing acceptor
SCNT:	Somatic cell nuclear transfer
SDS:	Sodium dodecyl sulfate
SDS-PAGE:	Sodium dodecyl sulfate polyacrylamide gel electrophoresis
sec:	Seconds
ST:	Small T antigen of the simian virus 40 early region
SV40:	Simian virus 40
TALEN:	Transcription activator-like effector nuclease

TEMED:	Tetramethylethylenediamine
TERC:	Telomerase RNA component
TERF2:	Telomeric repeat binding factor 1
TERT:	Telomerase reverse transcriptase
THBS2:	Thrombospondin 2
TP53:	Tumour protein p53
TRRAP:	Transformation/transcription domain-associated protein
Ub:	Ubiquitylation
UV:	Ultraviolet
V:	Volt
VEGF α :	Vascular endothelial growth factor α
WT:	wild-type
ZFN:	Zinc finger nuclease

7 List of Tables

Table 1: Experimental human cell transformation models	3
Table 2: Polymerases used with the respective PCR programs	43
Table 3: Formulation of 12% and 15% resolving gels and 5% stacking gel for SDS-PAGE	48
Table 4: Antibodies used with the respective dilutions	51
Table 5: Fold-change values and associated p-values for a series of key genes of cellular transformation	135
Table 6: Fold-change values and associated p-values of ALT-associated genes	136
Table 7: Fold-change values and associated p-values of cell cycle regulatory genes	137
Table 8: Fold-change values and associated p-values of some p53 target genes	137
Table 9: Fold-change values and associated p-values of some tissue invasion and metastatic marker genes	138

8 List of Figures

Figure 1: Cooperating pathways in human cell transformation	2
Figure 2: Barriers to immortalisation	5
Figure 3: Regulation of p53 function	7
Figure 4: Regulation of cell cycle progression	10
Figure 5: Genomic structure of the <i>CDKN2A</i> gene locus	11
Figure 6: Regulation of the pRb and p53 pathways by p16INK4 α and p14ARF	12
Figure 7: Transcriptional properties of Myc	15
Figure 8: Ras signalling cascade	18
Figure 9: Schematic overview of the porcine wild-type and modified <i>TP53</i> gene locus	53
Figure 10: Schematic overview of the porcine <i>KRAS</i> gene locus and design of the porcine <i>KRAS</i> ^{LSL-G12D} gene targeting vectors	54
Figure 11: Schematic overview of the modified <i>KRAS</i> ^{LSL-G12D} gene locus	55
Figure 12: 5' targeting PCR of BS-resistant neo14/K- subclones	55
Figure 13: 3' targeting PCR of BS-resistant neo14/K- subclones	56
Figure 14: <i>BccI</i> RFLP test of BS-resistant neo14/K- subclones	57
Figure 15: Southern blot analysis of BS-resistant neo14/K- subclones	58
Figure 16: RT-PCR analysis of BS-resistant neo14/K- subclones	58
Figure 17: Schematic overview of the wild-type and gene targeted <i>TP53</i> and <i>KRAS</i> gene loci before and after Cre recombinase mediated cassette excision	59
Figure 18: Functional screen for loss of floxed selection cassettes	60
Figure 19: PCRs across the LSL integration sites before and after Cre protein transduction	61
Figure 20: RT-PCR of truncated <i>KRAS</i> -BS and <i>TP53</i> -NEO mRNA transcripts before and after Cre protein transduction	62
Figure 21: <i>BccI</i> RFLP test of <i>KRAS</i> mRNA species before and after Cre protein transduction	63
Figure 22: <i>HaeIII</i> RFLP test of <i>TP53</i> mRNA species before and after Cre protein transduction	64
Figure 23: p53 Western blot and Ras Activation Assay	65
Figure 24: Schematic design of the pPGK-pocMyc-IRES-BS-pA expression vector	66
Figure 25: Investigating cMyc expression levels	66
Figure 26: RT-PCR to detect TERT reactivation	67
Figure 27: RT-PCR analysis of p16INK4 α and p14ARF expression levels	68
Figure 28: Quantification of p16INK4 α and p14ARF expression levels	69
Figure 29: Methylation analysis of porcine <i>P16INK4A</i> gene region (-10 to +256)	70

List of Figures

Figure 30: Determining the population doubling time of genetically modified pMSCs	72
Figure 31: Validating density-dependent growth inhibition	73
Figure 32: Anchorage-independent growth in soft agar	74
Figure 33: Histology of the neo14/K67/1.1 cells derived tumour	75
Figure 34: Histology of the neo14/K67/1.1+cMyc cells derived tumour	75
Figure 35: Histology of the re-implanted tumour	76
Figure 36: Morphology and growth characteristics of porcine sarcoma derived cell lines	77
Figure 37: Verifying the cellular origin of porcine sarcoma derived cell lines	78
Figure 38: PCRs across the LSL integration sites before and after <i>in vivo</i> xenotransplantation	79
Figure 39: Chromatograms of KRAS mRNA transcripts	80
Figure 40: Ras Activation Assay and p53 Western blot analysis with lysates of cells before and after <i>in vivo</i> xenotransplantation	80
Figure 41: Western blot analysis of phosphorylated Akt and ERK1/2 proteins in pMSCs before and after xenotransplantation	81
Figure 42: Expression profile of stepwise modified pMSCs and porcine sarcoma derived cell lines	82
Figure 43: Work flow for the generation of transformed pMSCs <i>in vitro</i>	85
Figure 44: RT-PCR screenings of G418-resistant cell clones	87
Figure 45: 5' and 3' targeting PCRs of G418-resistant cell clones	88
Figure 46: Southern blot analysis of putative $KRAS^{LSL-G12D}$ retargeted $TP53^{LSL-R167H/+}$ pMSCs	89
Figure 47: Chromatograms of RT-PCR products covering codon 12 of the relative KRAS mRNA species	90

9 Bibliography

1. Cline MJ (1987) The role of proto-oncogenes in human cancer: implications for diagnosis and treatment. *Int J Radiat Oncol Biol Phys* 13: 1297-1301.
2. Klein G (1988) Oncogenes and tumor suppressor genes. *Acta Oncol* 27: 427-437.
3. Weinberg RA (1994) Oncogenes and tumor suppressor genes. *CA Cancer J Clin* 44: 160-170.
4. Weinberg RA (1991) Tumor suppressor genes. *Science* 254: 1138-1146.
5. Kopnin BP (2000) Targets of oncogenes and tumor suppressors: key for understanding basic mechanisms of carcinogenesis. *Biochemistry (Mosc)* 65: 2-27.
6. Hahn WC, Weinberg RA (2002) Modelling the molecular circuitry of cancer. *Nat Rev Cancer* 2: 331-341.
7. Zhao JJ, Roberts TM, Hahn WC (2004) Functional genetics and experimental models of human cancer. *Trends Mol Med* 10: 344-350.
8. Boehm JS, Hahn WC (2005) Understanding transformation: progress and gaps. *Curr Opin Genet Dev* 15: 13-17.
9. Land H, Parada LF, Weinberg RA (1983) Tumorigenic conversion of primary embryo fibroblasts requires at least two cooperating oncogenes. *Nature* 304: 596-602.
10. Ruley HE (1983) Adenovirus early region 1A enables viral and cellular transforming genes to transform primary cells in culture. *Nature* 304: 602-606.
11. Michalovitz D, Fischer-Fantuzzi L, Vesco C, Pipas JM, Oren M (1987) Activated Ha-ras can cooperate with defective simian virus 40 in the transformation of nonestablished rat embryo fibroblasts. *J Virol* 61: 2648-2654.
12. Stevenson M, Volsky DJ (1986) Activated v-myc and v-ras oncogenes do not transform normal human lymphocytes. *Mol Cell Biol* 6: 3410-3417.
13. Sager R (1991) Senescence as a mode of tumor suppression. *Environ Health Perspect* 93: 59-62.
14. Hahn WC, Counter CM, Lundberg AS, Beijersbergen RL, Brooks MW, et al. (1999) Creation of human tumour cells with defined genetic elements. *Nature* 400: 464-468.
15. Hahn WC, Dessain SK, Brooks MW, King JE, Elenbaas B, et al. (2002) Enumeration of the simian virus 40 early region elements necessary for human cell transformation. *Mol Cell Biol* 22: 2111-2123.
16. Yu J, Boyapati A, Rundell K (2001) Critical role for SV40 small-t antigen in human cell transformation. *Virology* 290: 192-198.
17. Rich JN, Guo C, McLendon RE, Bigner DD, Wang XF, et al. (2001) A genetically tractable model of human glioma formation. *Cancer Res* 61: 3556-3560.
18. MacKenzie KL, Franco S, Naiyer AJ, May C, Sadelain M, et al. (2002) Multiple stages of malignant transformation of human endothelial cells modelled by co-expression of telomerase reverse transcriptase, SV40 T antigen and oncogenic N-ras. *Oncogene* 21: 4200-4211.
19. Lundberg AS, Randell SH, Stewart SA, Elenbaas B, Hartwell KA, et al. (2002) immortalization and transformation of primary human airway epithelial cells by gene transfer. *Oncogene* 21: 4577-4586.
20. Elenbaas B, Spirio L, Koerner F, Fleming MD, Zimonjic DB, et al. (2001) Human breast cancer cells generated by oncogenic transformation of primary mammary epithelial cells. *Genes Dev* 15: 50-65.
21. Liu J, Yang G, Thompson-Lanza JA, Glassman A, Hayes K, et al. (2004) A genetically defined model for human ovarian cancer. *Cancer Res* 64: 1655-1663.
22. Wolfel T, Hauer M, Schneider J, Serrano M, Wolfel C, et al. (1995) A p16INK4a-insensitive CDK4 mutant targeted by cytolytic T lymphocytes in a human melanoma. *Science* 269: 1281-1284.
23. Shaulian E, Zauberman A, Ginsberg D, Oren M (1992) Identification of a minimal transforming domain of p53: negative dominance through abrogation of sequence-specific DNA binding. *Mol Cell Biol* 12: 5581-5592.

24. Yeh E, Cunningham M, Arnold H, Chasse D, Monteith T, et al. (2004) A signalling pathway controlling c-Myc degradation that impacts oncogenic transformation of human cells. *Nat Cell Biol* 6: 308-318.
25. Kendall SD, Linardic CM, Adam SJ, Counter CM (2005) A network of genetic events sufficient to convert normal human cells to a tumorigenic state. *Cancer Res* 65: 9824-9828.
26. Meyne J, Moyzis RK (1989) Human chromosome-specific repetitive DNA probes: targeting in situ hybridization to chromosome 17 with a 42-base-pair alphoid DNA oligomer. *Genomics* 4: 472-478.
27. Moyzis RK, Buckingham JM, Cram LS, Dani M, Deaven LL, et al. (1988) A highly conserved repetitive DNA sequence, (TTAGGG)_n, present at the telomeres of human chromosomes. *Proc Natl Acad Sci U S A* 85: 6622-6626.
28. Hahn WC (2003) Role of telomeres and telomerase in the pathogenesis of human cancer. *J Clin Oncol* 21: 2034-2043.
29. Olovnikov AM (1973) A theory of marginotomy. The incomplete copying of template margin in enzymic synthesis of polynucleotides and biological significance of the phenomenon. *J Theor Biol* 41: 181-190.
30. Watson JD (1972) Origin of concatemeric T7 DNA. *Nat New Biol* 239: 197-201.
31. Feng J, Funk WD, Wang SS, Weinrich SL, Avilion AA, et al. (1995) The RNA component of human telomerase. *Science* 269: 1236-1241.
32. Bryan TM, Cech TR (1999) Telomerase and the maintenance of chromosome ends. *Curr Opin Cell Biol* 11: 318-324.
33. Wright WE, Piatyszek MA, Rainey WE, Byrd W, Shay JW (1996) Telomerase activity in human germline and embryonic tissues and cells. *Dev Genet* 18: 173-179.
34. Avilion AA, Piatyszek MA, Gupta J, Shay JW, Bacchetti S, et al. (1996) Human telomerase RNA and telomerase activity in immortal cell lines and tumor tissues. *Cancer Res* 56: 645-650.
35. Shay JW, Wright WE (2005) Senescence and immortalization: role of telomeres and telomerase. *Carcinogenesis* 26: 867-874.
36. Harley CB, Futcher AB, Greider CW (1990) Telomeres shorten during ageing of human fibroblasts. *Nature* 345: 458-460.
37. Smogorzewska A, de Lange T (2002) Different telomere damage signaling pathways in human and mouse cells. *EMBO J* 21: 4338-4348.
38. Degerman S, Siwicki JK, Osterman P, Lafferty-Whyte K, Keith WN, et al. (2010) Telomerase upregulation is a postcrisis event during senescence bypass and immortalization of two Nijmegen breakage syndrome T cell cultures. *Aging Cell* 9: 220-235.
39. Goldstein S (1990) Replicative senescence: the human fibroblast comes of age. *Science* 249: 1129-1133.
40. Kim NW, Piatyszek MA, Prowse KR, Harley CB, West MD, et al. (1994) Specific association of human telomerase activity with immortal cells and cancer. *Science* 266: 2011-2015.
41. Counter CM, Avilion AA, LeFeuvre CE, Stewart NG, Greider CW, et al. (1992) Telomere shortening associated with chromosome instability is arrested in immortal cells which express telomerase activity. *EMBO J* 11: 1921-1929.
42. Shay JW, Wright WE (1989) Quantitation of the frequency of immortalization of normal human diploid fibroblasts by SV40 large T-antigen. *Exp Cell Res* 184: 109-118.
43. Shay JW, Wright WE, Werbin H (1991) Defining the molecular mechanisms of human cell immortalization. *Biochim Biophys Acta* 1072: 1-7.
44. Shay JW, Bacchetti S (1997) A survey of telomerase activity in human cancer. *Eur J Cancer* 33: 787-791.
45. Bryan TM, Englezou A, Gupta J, Bacchetti S, Reddel RR (1995) Telomere elongation in immortal human cells without detectable telomerase activity. *EMBO J* 14: 4240-4248.
46. Bryan TM, Englezou A, Dalla-Pozza L, Dunham MA, Reddel RR (1997) Evidence for an alternative mechanism for maintaining telomere length in human tumors and tumor-derived cell lines. *Nat Med* 3: 1271-1274.

47. Dunham MA, Neumann AA, Fasching CL, Reddel RR (2000) Telomere maintenance by recombination in human cells. *Nat Genet* 26: 447-450.
48. Blackburn EH (2000) Telomere states and cell fates. *Nature* 408: 53-56.
49. Hanahan D, Weinberg RA (2000) The hallmarks of cancer. *Cell* 100: 57-70.
50. Vogelstein B, Lane D, Levine AJ (2000) Surfing the p53 network. *Nature* 408: 307-310.
51. Lane DP, Crawford LV (1979) T antigen is bound to a host protein in SV40-transformed cells. *Nature* 278: 261-263.
52. DeLeo AB, Jay G, Appella E, Dubois GC, Law LW, et al. (1979) Detection of a transformation-related antigen in chemically induced sarcomas and other transformed cells of the mouse. *Proc Natl Acad Sci U S A* 76: 2420-2424.
53. Eliyahu D, Raz A, Gruss P, Givol D, Oren M (1984) Participation of p53 cellular tumour antigen in transformation of normal embryonic cells. *Nature* 312: 646-649.
54. Parada LF, Land H, Weinberg RA, Wolf D, Rotter V (1984) Cooperation between gene encoding p53 tumour antigen and ras in cellular transformation. *Nature* 312: 649-651.
55. Jenkins JR, Rudge K, Currie GA (1984) Cellular immortalization by a cDNA clone encoding the transformation-associated phosphoprotein p53. *Nature* 312: 651-654.
56. Wolf D, Harris N, Rotter V (1984) Reconstitution of p53 expression in a nonproducer Ab-MuLV-transformed cell line by transfection of a functional p53 gene. *Cell* 38: 119-126.
57. Hinds P, Finlay C, Levine AJ (1989) Mutation is required to activate the p53 gene for cooperation with the ras oncogene and transformation. *J Virol* 63: 739-746.
58. Levine AJ, Oren M (2009) The first 30 years of p53: growing ever more complex. *Nat Rev Cancer* 9: 749-758.
59. Eliyahu D, Michalovitz D, Eliyahu S, Pinhasi-Kimhi O, Oren M (1989) Wild-type p53 can inhibit oncogene-mediated focus formation. *Proc Natl Acad Sci U S A* 86: 8763-8767.
60. Finlay CA, Hinds PW, Levine AJ (1989) The p53 proto-oncogene can act as a suppressor of transformation. *Cell* 57: 1083-1093.
61. Baker SJ, Fearon ER, Nigro JM, Hamilton SR, Preisinger AC, et al. (1989) Chromosome 17 deletions and p53 gene mutations in colorectal carcinomas. *Science* 244: 217-221.
62. Lane DP (1992) Cancer. p53, guardian of the genome. *Nature* 358: 15-16.
63. Vousden KH, Lu X (2002) Live or let die: the cell's response to p53. *Nat Rev Cancer* 2: 594-604.
64. el-Deiry WS, Kern SE, Pietenpol JA, Kinzler KW, Vogelstein B (1992) Definition of a consensus binding site for p53. *Nat Genet* 1: 45-49.
65. Laptenko O, Prives C (2006) Transcriptional regulation by p53: one protein, many possibilities. *Cell Death Differ* 13: 951-961.
66. Oliner JD, Pietenpol JA, Thiagalingam S, Gyuris J, Kinzler KW, et al. (1993) Oncoprotein MDM2 conceals the activation domain of tumour suppressor p53. *Nature* 362: 857-860.
67. Haupt Y, Maya R, Kazaz A, Oren M (1997) Mdm2 promotes the rapid degradation of p53. *Nature* 387: 296-299.
68. Wu X, Bayle JH, Olson D, Levine AJ (1993) The p53-mdm-2 autoregulatory feedback loop. *Genes Dev* 7: 1126-1132.
69. Mayo LD, Donner DB (2002) The PTEN, Mdm2, p53 tumor suppressor-oncoprotein network. *Trends Biochem Sci* 27: 462-467.
70. Khosravi R, Maya R, Gottlieb T, Oren M, Shiloh Y, et al. (1999) Rapid ATM-dependent phosphorylation of MDM2 precedes p53 accumulation in response to DNA damage. *Proc Natl Acad Sci U S A* 96: 14973-14977.
71. Brooks CL, Gu W (2010) New insights into p53 activation. *Cell Res* 20: 614-621.
72. Murray-Zmijewski F, Slee EA, Lu X (2008) A complex barcode underlies the heterogeneous response of p53 to stress. *Nat Rev Mol Cell Biol* 9: 702-712.
73. Pietenpol JA, Stewart ZA (2002) Cell cycle checkpoint signaling: cell cycle arrest versus apoptosis. *Toxicology* 181-182: 475-481.
74. Green DR, Kroemer G (2009) Cytoplasmic functions of the tumour suppressor p53. *Nature* 458: 1127-1130.

75. Roos WP, Kaina B (2006) DNA damage-induced cell death by apoptosis. *Trends Mol Med* 12: 440-450.
76. Strano S, Dell'Orso S, Di Agostino S, Fontemaggi G, Sacchi A, et al. (2007) Mutant p53: an oncogenic transcription factor. *Oncogene* 26: 2212-2219.
77. Varley JM, Thorncroft M, McGown G, Appleby J, Kelsey AM, et al. (1997) A detailed study of loss of heterozygosity on chromosome 17 in tumours from Li-Fraumeni patients carrying a mutation to the TP53 gene. *Oncogene* 14: 865-871.
78. Freed-Pastor WA, Prives C (2012) Mutant p53: one name, many proteins. *Genes Dev* 26: 1268-1286.
79. Lang GA, Iwakuma T, Suh YA, Liu G, Rao VA, et al. (2004) Gain of function of a p53 hot spot mutation in a mouse model of Li-Fraumeni syndrome. *Cell* 119: 861-872.
80. Olive KP, Tuveson DA, Ruhe ZC, Yin B, Willis NA, et al. (2004) Mutant p53 gain of function in two mouse models of Li-Fraumeni syndrome. *Cell* 119: 847-860.
81. Dryja TP, Friend S, Weinberg RA (1986) Genetic sequences that predispose to retinoblastoma and osteosarcoma. *Symp Fundam Cancer Res* 39: 115-119.
82. Friend SH, Bernards R, Rogelj S, Weinberg RA, Rapaport JM, et al. (1986) A human DNA segment with properties of the gene that predisposes to retinoblastoma and osteosarcoma. *Nature* 323: 643-646.
83. Weinberg RA (1995) The retinoblastoma protein and cell cycle control. *Cell* 81: 323-330.
84. Cobrinik D, Whyte P, Peeper DS, Jacks T, Weinberg RA (1993) Cell cycle-specific association of E2F with the p130 E1A-binding protein. *Genes Dev* 7: 2392-2404.
85. Li Y, Graham C, Lacy S, Duncan AM, Whyte P (1993) The adenovirus E1A-associated 130-kD protein is encoded by a member of the retinoblastoma gene family and physically interacts with cyclins A and E. *Genes Dev* 7: 2366-2377.
86. Mayol X, Grana X, Baldi A, Sang N, Hu Q, et al. (1993) Cloning of a new member of the retinoblastoma gene family (pRb2) which binds to the E1A transforming domain. *Oncogene* 8: 2561-2566.
87. Hiebert SW, Chellappan SP, Horowitz JM, Nevins JR (1992) The interaction of RB with E2F coincides with an inhibition of the transcriptional activity of E2F. *Genes Dev* 6: 177-185.
88. Landis MW, Brown NE, Baker GL, Shifrin A, Das M, et al. (2007) The LxCxE pRb interaction domain of cyclin D1 is dispensable for murine development. *Cancer Res* 67: 7613-7620.
89. Brehm A, Miska EA, McCance DJ, Reid JL, Bannister AJ, et al. (1998) Retinoblastoma protein recruits histone deacetylase to repress transcription. *Nature* 391: 597-601.
90. Whyte P, Buchkovich KJ, Horowitz JM, Friend SH, Raybuck M, et al. (1988) Association between an oncogene and an anti-oncogene: the adenovirus E1A proteins bind to the retinoblastoma gene product. *Nature* 334: 124-129.
91. DeCaprio JA, Ludlow JW, Figge J, Shew JY, Huang CM, et al. (1988) SV40 large tumor antigen forms a specific complex with the product of the retinoblastoma susceptibility gene. *Cell* 54: 275-283.
92. Dyson N, Howley PM, Munger K, Harlow E (1989) The human papilloma virus-16 E7 oncoprotein is able to bind to the retinoblastoma gene product. *Science* 243: 934-937.
93. Giacinti C, Giordano A (2006) RB and cell cycle progression. *Oncogene* 25: 5220-5227.
94. Hamel PA, Gallie BL, Phillips RA (1992) The retinoblastoma protein and cell cycle regulation. *Trends Genet* 8: 180-185.
95. Mittnacht S (1998) Control of pRB phosphorylation. *Curr Opin Genet Dev* 8: 21-27.
96. Helin K, Harlow E, Fattaey A (1993) Inhibition of E2F-1 transactivation by direct binding of the retinoblastoma protein. *Mol Cell Biol* 13: 6501-6508.
97. Adnane J, Shao Z, Robbins PD (1995) The retinoblastoma susceptibility gene product represses transcription when directly bound to the promoter. *J Biol Chem* 270: 8837-8843.
98. Weintraub SJ, Chow KN, Luo RX, Zhang SH, He S, et al. (1995) Mechanism of active transcriptional repression by the retinoblastoma protein. *Nature* 375: 812-815.

99. Takahashi Y, Rayman JB, Dynlacht BD (2000) Analysis of promoter binding by the E2F and pRB families in vivo: distinct E2F proteins mediate activation and repression. *Genes Dev* 14: 804-816.
100. Reissmann PT, Koga H, Figlin RA, Holmes EC, Slamon DJ (1999) Amplification and overexpression of the cyclin D1 and epidermal growth factor receptor genes in non-small-cell lung cancer. Lung Cancer Study Group. *J Cancer Res Clin Oncol* 125: 61-70.
101. Moroy T, Geisen C (2004) Cyclin E. *Int J Biochem Cell Biol* 36: 1424-1439.
102. Khatib ZA, Matsushime H, Valentine M, Shapiro DN, Sherr CJ, et al. (1993) Coamplification of the CDK4 gene with MDM2 and GLI in human sarcomas. *Cancer Res* 53: 5535-5541.
103. Baylin SB, Herman JG, Graff JR, Vertino PM, Issa JP (1998) Alterations in DNA methylation: a fundamental aspect of neoplasia. *Adv Cancer Res* 72: 141-196.
104. Ortega S, Malumbres M, Barbacid M (2002) Cyclin D-dependent kinases, INK4 inhibitors and cancer. *Biochim Biophys Acta* 1602: 73-87.
105. Poi MJ, Yen T, Li J, Song H, Lang JC, et al. (2001) Somatic INK4a-ARF locus mutations: a significant mechanism of gene inactivation in squamous cell carcinomas of the head and neck. *Mol Carcinog* 30: 26-36.
106. Zhang Y, Xiong Y, Yarbrough WG (1998) ARF promotes MDM2 degradation and stabilizes p53: ARF-INK4a locus deletion impairs both the Rb and p53 tumor suppression pathways. *Cell* 92: 725-734.
107. Quelle DE, Zindy F, Ashmun RA, Sherr CJ (1995) Alternative reading frames of the INK4a tumor suppressor gene encode two unrelated proteins capable of inducing cell cycle arrest. *Cell* 83: 993-1000.
108. Gil J, Peters G (2006) Regulation of the INK4b-ARF-INK4a tumour suppressor locus: all for one or one for all. *Nat Rev Mol Cell Biol* 7: 667-677.
109. Serrano M, Hannon GJ, Beach D (1993) A new regulatory motif in cell-cycle control causing specific inhibition of cyclin D/CDK4. *Nature* 366: 704-707.
110. Russo AA, Tong L, Lee JO, Jeffrey PD, Pavletich NP (1998) Structural basis for inhibition of the cyclin-dependent kinase Cdk6 by the tumour suppressor p16INK4a. *Nature* 395: 237-243.
111. Pavletich NP (1999) Mechanisms of cyclin-dependent kinase regulation: structures of Cdks, their cyclin activators, and Cip and INK4 inhibitors. *J Mol Biol* 287: 821-828.
112. Groth A, Weber JD, Willumsen BM, Sherr CJ, Roussel MF (2000) Oncogenic Ras induces p19ARF and growth arrest in mouse embryo fibroblasts lacking p21Cip1 and p27Kip1 without activating cyclin D-dependent kinases. *J Biol Chem* 275: 27473-27480.
113. Sherr CJ (2000) The Pezcoller lecture: cancer cell cycles revisited. *Cancer Res* 60: 3689-3695.
114. Bartkova J, Rezaei N, Liontos M, Karakaidos P, Kletsas D, et al. (2006) Oncogene-induced senescence is part of the tumorigenesis barrier imposed by DNA damage checkpoints. *Nature* 444: 633-637.
115. Rangarajan A, Weinberg RA (2003) Opinion: Comparative biology of mouse versus human cells: modelling human cancer in mice. *Nat Rev Cancer* 3: 952-959.
116. Serrano M, Lin AW, McCurrach ME, Beach D, Lowe SW (1997) Oncogenic ras provokes premature cell senescence associated with accumulation of p53 and p16INK4a. *Cell* 88: 593-602.
117. Sharpless NE, Ramsey MR, Balasubramanian P, Castrillon DH, DePinho RA (2004) The differential impact of p16(INK4a) or p19(ARF) deficiency on cell growth and tumorigenesis. *Oncogene* 23: 379-385.
118. Kamijo T, Zindy F, Roussel MF, Quelle DE, Downing JR, et al. (1997) Tumor suppression at the mouse INK4a locus mediated by the alternative reading frame product p19ARF. *Cell* 91: 649-659.
119. Campisi J (2001) Cellular senescence as a tumor-suppressor mechanism. *Trends Cell Biol* 11: S27-31.

120. Nobori T, Miura K, Wu DJ, Lois A, Takabayashi K, et al. (1994) Deletions of the cyclin-dependent kinase-4 inhibitor gene in multiple human cancers. *Nature* 368: 753-756.
121. Kamb A, Shattuck-Eidens D, Eeles R, Liu Q, Gruis NA, et al. (1994) Analysis of the p16 gene (CDKN2) as a candidate for the chromosome 9p melanoma susceptibility locus. *Nat Genet* 8: 23-26.
122. Hussussian CJ, Struewing JP, Goldstein AM, Higgins PA, Ally DS, et al. (1994) Germline p16 mutations in familial melanoma. *Nat Genet* 8: 15-21.
123. Wilentz RE, Geradts J, Maynard R, Offerhaus GJ, Kang M, et al. (1998) Inactivation of the p16 (INK4A) tumor-suppressor gene in pancreatic duct lesions: loss of intranuclear expression. *Cancer Res* 58: 4740-4744.
124. Schutte M, Hruban RH, Geradts J, Maynard R, Hilgers W, et al. (1997) Abrogation of the Rb/p16 tumor-suppressive pathway in virtually all pancreatic carcinomas. *Cancer Res* 57: 3126-3130.
125. Andujar P, Wang J, Descatha A, Galateau-Salle F, Abd-Alsamad I, et al. (2010) p16INK4A inactivation mechanisms in non-small-cell lung cancer patients occupationally exposed to asbestos. *Lung Cancer* 67: 23-30.
126. Bian YS, Osterheld MC, Fontollet C, Bosman FT, Benhattar J (2002) p16 inactivation by methylation of the CDKN2A promoter occurs early during neoplastic progression in Barrett's esophagus. *Gastroenterology* 122: 1113-1121.
127. Maeta Y, Shiota G, Okano J, Murawaki Y (2005) Effect of promoter methylation of the p16 gene on phosphorylation of retinoblastoma gene product and growth of hepatocellular carcinoma cells. *Tumour Biol* 26: 300-305.
128. Takaoka AS, Kakiuchi H, Itoh F, Hinoda Y, Kusano M, et al. (1997) Infrequent alterations of the p16 (MTS-1) gene in human gastric cancer. *Tumour Biol* 18: 95-103.
129. Esteller M, Tortola S, Toyota M, Capella G, Peinado MA, et al. (2000) Hypermethylation-associated inactivation of p14(ARF) is independent of p16(INK4a) methylation and p53 mutational status. *Cancer Res* 60: 129-133.
130. Burri N, Shaw P, Bouzourene H, Sordat I, Sordat B, et al. (2001) Methylation silencing and mutations of the p14ARF and p16INK4a genes in colon cancer. *Lab Invest* 81: 217-229.
131. Nyiraneza C, Sempoux C, Detry R, Kartheuser A, Dahan K (2012) Hypermethylation of the 5' CpG island of the p14ARF flanking exon 1beta in human colorectal cancer displaying a restricted pattern of p53 overexpression concomitant with increased MDM2 expression. *Clin Epigenetics* 4: 9.
132. Ivanov X., Mladenov Z., Nedyalkov S., Todorov T.G., Yakimov M. Experimental investigations into avian leucoses. V. Transmission, haematology and morphology of avian myelocytomatosis. *Bull. Inst. Pathol. Comp. Anim. Acad. Bulg. Sci.* 1964;10:5-38.
133. Reddy EP, Reynolds RK, Watson DK, Schultz RA, Lautenberger J, et al. (1983) Nucleotide sequence analysis of the proviral genome of avian myelocytomatosis virus (MC29). *Proc Natl Acad Sci U S A* 80: 2500-2504.
134. Neel BG, Gasic GP, Rogler CE, Skalka AM, Ju G, et al. (1982) Molecular analysis of the c-myc locus in normal tissue and in avian leukosis virus-induced lymphomas. *J Virol* 44: 158-166.
135. Watson DK, Reddy EP, Duesberg PH, Papas TS (1983) Nucleotide sequence analysis of the chicken c-myc gene reveals homologous and unique coding regions by comparison with the transforming gene of avian myelocytomatosis virus MC29, delta gag-myc. *Proc Natl Acad Sci U S A* 80: 2146-2150.
136. Westaway D, Payne G, Varmus HE (1984) Proviral deletions and oncogene base-substitutions in insertionally mutagenized c-myc alleles may contribute to the progression of avian bursal tumors. *Proc Natl Acad Sci U S A* 81: 843-847.
137. Dalla-Favera R, Bregni M, Erikson J, Patterson D, Gallo RC, et al. (1982) Human c-myc onc gene is located on the region of chromosome 8 that is translocated in Burkitt lymphoma cells. *Proc Natl Acad Sci U S A* 79: 7824-7827.

138. Taub R, Kirsch I, Morton C, Lenoir G, Swan D, et al. (1982) Translocation of the c-myc gene into the immunoglobulin heavy chain locus in human Burkitt lymphoma and murine plasmacytoma cells. *Proc Natl Acad Sci U S A* 79: 7837-7841.
139. Shou Y, Martelli ML, Gabrea A, Qi Y, Brents LA, et al. (2000) Diverse karyotypic abnormalities of the c-myc locus associated with c-myc dysregulation and tumor progression in multiple myeloma. *Proc Natl Acad Sci U S A* 97: 228-233.
140. Beroukhim R, Mermel CH, Porter D, Wei G, Raychaudhuri S, et al. (2010) The landscape of somatic copy-number alteration across human cancers. *Nature* 463: 899-905.
141. Facchini LM, Penn LZ (1998) The molecular role of Myc in growth and transformation: recent discoveries lead to new insights. *FASEB J* 12: 633-651.
142. Kim HH, Kuwano Y, Srikantan S, Lee EK, Martindale JL, et al. (2009) HuR recruits let-7/RISC to repress c-Myc expression. *Genes Dev* 23: 1743-1748.
143. Cannell IG, Kong YW, Johnston SJ, Chen ML, Collins HM, et al. (2010) p38 MAPK/MK2-mediated induction of miR-34c following DNA damage prevents Myc-dependent DNA replication. *Proc Natl Acad Sci U S A* 107: 5375-5380.
144. Sachdeva M, Zhu S, Wu F, Wu H, Walia V, et al. (2009) p53 represses c-Myc through induction of the tumor suppressor miR-145. *Proc Natl Acad Sci U S A* 106: 3207-3212.
145. Luscher B, Eisenman RN (1988) c-myc and c-myb protein degradation: effect of metabolic inhibitors and heat shock. *Mol Cell Biol* 8: 2504-2512.
146. Eilers M, Eisenman RN (2008) Myc's broad reach. *Genes Dev* 22: 2755-2766.
147. Oster SK, Ho CS, Soucie EL, Penn LZ (2002) The myc oncogene: MarvelouslyY Complex. *Adv Cancer Res* 84: 81-154.
148. Fernandez PC, Frank SR, Wang L, Schroeder M, Liu S, et al. (2003) Genomic targets of the human c-Myc protein. *Genes Dev* 17: 1115-1129.
149. Li Z, Van Calcar S, Qu C, Cavenee WK, Zhang MQ, et al. (2003) A global transcriptional regulatory role for c-Myc in Burkitt's lymphoma cells. *Proc Natl Acad Sci U S A* 100: 8164-8169.
150. Patel JH, Loboda AP, Showe MK, Showe LC, McMahon SB (2004) Analysis of genomic targets reveals complex functions of MYC. *Nat Rev Cancer* 4: 562-568.
151. Dang CV, O'Donnell KA, Zeller KI, Nguyen T, Osthus RC, et al. (2006) The c-Myc target gene network. *Semin Cancer Biol* 16: 253-264.
152. Amati B, Dalton S, Brooks MW, Littlewood TD, Evan GI, et al. (1992) Transcriptional activation by the human c-Myc oncoprotein in yeast requires interaction with Max. *Nature* 359: 423-426.
153. Amati B, Brooks MW, Levy N, Littlewood TD, Evan GI, et al. (1993) Oncogenic activity of the c-Myc protein requires dimerization with Max. *Cell* 72: 233-245.
154. Blackwood EM, Eisenman RN (1991) Max: a helix-loop-helix zipper protein that forms a sequence-specific DNA-binding complex with Myc. *Science* 251: 1211-1217.
155. McMahon SB, Van Buskirk HA, Dugan KA, Copeland TD, Cole MD (1998) The novel ATM-related protein TRRAP is an essential cofactor for the c-Myc and E2F oncoproteins. *Cell* 94: 363-374.
156. Frank SR, Schroeder M, Fernandez P, Taubert S, Amati B (2001) Binding of c-Myc to chromatin mediates mitogen-induced acetylation of histone H4 and gene activation. *Genes Dev* 15: 2069-2082.
157. McMahon SB, Wood MA, Cole MD (2000) The essential cofactor TRRAP recruits the histone acetyltransferase hGCN5 to c-Myc. *Mol Cell Biol* 20: 556-562.
158. Frank SR, Parisi T, Taubert S, Fernandez P, Fuchs M, et al. (2003) MYC recruits the TIP60 histone acetyltransferase complex to chromatin. *EMBO Rep* 4: 575-580.
159. Peukert K, Staller P, Schneider A, Carmichael G, Hanel F, et al. (1997) An alternative pathway for gene regulation by Myc. *EMBO J* 16: 5672-5686.
160. Seoane J, Le HV, Massague J (2002) Myc suppression of the p21(Cip1) Cdk inhibitor influences the outcome of the p53 response to DNA damage. *Nature* 419: 729-734.

161. Staller P, Peukert K, Kiermaier A, Seoane J, Lukas J, et al. (2001) Repression of p15INK4b expression by Myc through association with Miz-1. *Nat Cell Biol* 3: 392-399.
162. Kurland JF, Tansey WP (2008) Myc-mediated transcriptional repression by recruitment of histone deacetylase. *Cancer Res* 68: 3624-3629.
163. Brenner C, Deplus R, Didelot C, Lorient A, Vire E, et al. (2005) Myc represses transcription through recruitment of DNA methyltransferase corepressor. *EMBO J* 24: 336-346.
164. Adhikary S, Eilers M (2005) Transcriptional regulation and transformation by Myc proteins. *Nat Rev Mol Cell Biol* 6: 635-645.
165. Pelengaris S, Khan M, Evan G (2002) c-MYC: more than just a matter of life and death. *Nat Rev Cancer* 2: 764-776.
166. Dave SS, Fu K, Wright GW, Lam LT, Kluin P, et al. (2006) Molecular diagnosis of Burkitt's lymphoma. *N Engl J Med* 354: 2431-2442.
167. Elson A, Deng C, Campos-Torres J, Donehower LA, Leder P (1995) The MMTV/c-myc transgene and p53 null alleles collaborate to induce T-cell lymphomas, but not mammary carcinomas in transgenic mice. *Oncogene* 11: 181-190.
168. Eischen CM, Weber JD, Roussel MF, Sherr CJ, Cleveland JL (1999) Disruption of the ARF-Mdm2-p53 tumor suppressor pathway in Myc-induced lymphomagenesis. *Genes Dev* 13: 2658-2669.
169. Felsher DW, Bishop JM (1999) Reversible tumorigenesis by MYC in hematopoietic lineages. *Mol Cell* 4: 199-207.
170. Pelengaris S, Littlewood T, Khan M, Elia G, Evan G (1999) Reversible activation of c-Myc in skin: induction of a complex neoplastic phenotype by a single oncogenic lesion. *Mol Cell* 3: 565-577.
171. O'Toole CM, Povey S, Hepburn P, Franks LM (1983) Identity of some human bladder cancer cell lines. *Nature* 301: 429-430.
172. Capon DJ, Seeburg PH, McGrath JP, Hayflick JS, Edman U, et al. (1983) Activation of Ki-ras2 gene in human colon and lung carcinomas by two different point mutations. *Nature* 304: 507-513.
173. Hall A, Marshall CJ, Spurr NK, Weiss RA (1983) Identification of transforming gene in two human sarcoma cell lines as a new member of the ras gene family located on chromosome 1. *Nature* 303: 396-400.
174. Harvey JJ (1964) An Unidentified Virus Which Causes the Rapid Production of Tumours in Mice. *Nature* 204: 1104-1105.
175. Kirsten WH, Mayer LA (1967) Morphologic responses to a murine erythroblastosis virus. *J Natl Cancer Inst* 39: 311-335.
176. Mitsuuchi Y, Testa JR (2002) Cytogenetics and molecular genetics of lung cancer. *Am J Med Genet* 115: 183-188.
177. Grady WM, Markowitz SD (2002) Genetic and epigenetic alterations in colon cancer. *Annu Rev Genomics Hum Genet* 3: 101-128.
178. Jaffee EM, Hruban RH, Canto M, Kern SE (2002) Focus on pancreas cancer. *Cancer Cell* 2: 25-28.
179. Burchill SA, Neal DE, Lunec J (1994) Frequency of H-ras mutations in human bladder cancer detected by direct sequencing. *Br J Urol* 73: 516-521.
180. Rodenhuis S, Slebos RJ (1992) Clinical significance of ras oncogene activation in human lung cancer. *Cancer Res* 52: 2665s-2669s.
181. Jones S, Zhang X, Parsons DW, Lin JC, Leary RJ, et al. (2008) Core signaling pathways in human pancreatic cancers revealed by global genomic analyses. *Science* 321: 1801-1806.
182. O'Connell P, Lathrop GM, Law M, Leppert M, Nakamura Y, et al. (1987) A primary genetic linkage map for human chromosome 12. *Genomics* 1: 93-102.
183. McGrath JP, Capon DJ, Smith DH, Chen EY, Seeburg PH, et al. (1983) Structure and organization of the human Ki-ras proto-oncogene and a related processed pseudogene. *Nature* 304: 501-506.

184. George DL, Scott AF, Trusko S, Glick B, Ford E, et al. (1985) Structure and expression of amplified cKi-ras gene sequences in Y1 mouse adrenal tumor cells. *EMBO J* 4: 1199-1203.
185. Lowy DR, Willumsen BM (1993) Function and regulation of ras. *Annu Rev Biochem* 62: 851-891.
186. Bar-Sagi D (2001) A Ras by any other name. *Mol Cell Biol* 21: 1441-1443.
187. Clarke S (1992) Protein isoprenylation and methylation at carboxyl-terminal cysteine residues. *Annu Rev Biochem* 61: 355-386.
188. Barbacid M (1987) ras genes. *Annu Rev Biochem* 56: 779-827.
189. Rozakis-Adcock M, Fernley R, Wade J, Pawson T, Bowtell D (1993) The SH2 and SH3 domains of mammalian Grb2 couple the EGF receptor to the Ras activator mSos1. *Nature* 363: 83-85.
190. Satoh T, Fantl WJ, Escobedo JA, Williams LT, Kaziro Y (1993) Platelet-derived growth factor receptor mediates activation of ras through different signaling pathways in different cell types. *Mol Cell Biol* 13: 3706-3713.
191. Ravichandran KS, Burakoff SJ (1994) The adapter protein Shc interacts with the interleukin-2 (IL-2) receptor upon IL-2 stimulation. *J Biol Chem* 269: 1599-1602.
192. Quilliam LA, Khosravi-Far R, Huff SY, Der CJ (1995) Guanine nucleotide exchange factors: activators of the Ras superfamily of proteins. *Bioessays* 17: 395-404.
193. Downward J (2003) Targeting RAS signalling pathways in cancer therapy. *Nat Rev Cancer* 3: 11-22.
194. Warne PH, Viciano PR, Downward J (1993) Direct interaction of Ras and the amino-terminal region of Raf-1 in vitro. *Nature* 364: 352-355.
195. Dickson B, Sprenger F, Morrison D, Hafen E (1992) Raf functions downstream of Ras1 in the Sevenless signal transduction pathway. *Nature* 360: 600-603.
196. Kyriakis JM, App H, Zhang XF, Banerjee P, Brautigan DL, et al. (1992) Raf-1 activates MAP kinase-kinase. *Nature* 358: 417-421.
197. Howe LR, Leever SJ, Gomez N, Nakielny S, Cohen P, et al. (1992) Activation of the MAP kinase pathway by the protein kinase raf. *Cell* 71: 335-342.
198. Marte BM, Downward J (1997) PKB/Akt: connecting phosphoinositide 3-kinase to cell survival and beyond. *Trends Biochem Sci* 22: 355-358.
199. Hofer F, Fields S, Schneider C, Martin GS (1994) Activated Ras interacts with the Ral guanine nucleotide dissociation stimulator. *Proc Natl Acad Sci U S A* 91: 11089-11093.
200. Feig LA (2003) Ral-GTPases: approaching their 15 minutes of fame. *Trends Cell Biol* 13: 419-425.
201. Bollag G, McCormick F (1992) GTPase activating proteins. *Semin Cancer Biol* 3: 199-208.
202. McGrath JP, Capon DJ, Goeddel DV, Levinson AD (1984) Comparative biochemical properties of normal and activated human ras p21 protein. *Nature* 310: 644-649.
203. Manne V, Bekesi E, Kung HF (1985) Ha-ras proteins exhibit GTPase activity: point mutations that activate Ha-ras gene products result in decreased GTPase activity. *Proc Natl Acad Sci U S A* 82: 376-380.
204. Trahey M, McCormick F (1987) A cytoplasmic protein stimulates normal N-ras p21 GTPase, but does not affect oncogenic mutants. *Science* 238: 542-545.
205. Malumbres M, Barbacid M (2003) RAS oncogenes: the first 30 years. *Nat Rev Cancer* 3: 459-465.
206. Hanahan D, Weinberg RA (2011) Hallmarks of cancer: the next generation. *Cell* 144: 646-674.
207. Der CJ, Krontiris TG, Cooper GM (1982) Transforming genes of human bladder and lung carcinoma cell lines are homologous to the ras genes of Harvey and Kirsten sarcoma viruses. *Proc Natl Acad Sci U S A* 79: 3637-3640.
208. Hingorani SR, Petricoin EF, Maitra A, Rajapakse V, King C, et al. (2003) Preinvasive and invasive ductal pancreatic cancer and its early detection in the mouse. *Cancer Cell* 4: 437-450.

209. Hingorani SR, Wang L, Multani AS, Combs C, Deramandt TB, et al. (2005) Trp53R172H and KrasG12D cooperate to promote chromosomal instability and widely metastatic pancreatic ductal adenocarcinoma in mice. *Cancer Cell* 7: 469-483.
210. Bardeesy N, Aguirre AJ, Chu GC, Cheng KH, Lopez LV, et al. (2006) Both p16(Ink4a) and the p19(Arf)-p53 pathway constrain progression of pancreatic adenocarcinoma in the mouse. *Proc Natl Acad Sci U S A* 103: 5947-5952.
211. Bardeesy N, Cheng KH, Berger JH, Chu GC, Pahler J, et al. (2006) Smad4 is dispensable for normal pancreas development yet critical in progression and tumor biology of pancreas cancer. *Genes Dev* 20: 3130-3146.
212. Hruban RH, Goggins M, Parsons J, Kern SE (2000) Progression model for pancreatic cancer. *Clin Cancer Res* 6: 2969-2972.
213. Kinzler KW, Vogelstein B (1996) Lessons from hereditary colorectal cancer. *Cell* 87: 159-170.
214. Frese KK, Tuveson DA (2007) Maximizing mouse cancer models. *Nat Rev Cancer* 7: 645-658.
215. Johnson Mary, *Laboratory Mice and Rats* MATER METHODS 2012;2:113
216. Evans MJ, Kaufman MH (1981) Establishment in culture of pluripotential cells from mouse embryos. *Nature* 292: 154-156.
217. Thomas KR, Capecchi MR (1987) Site-directed mutagenesis by gene targeting in mouse embryo-derived stem cells. *Cell* 51: 503-512.
218. Macleod KF, Jacks T (1999) Insights into cancer from transgenic mouse models. *J Pathol* 187: 43-60.
219. Tuveson DA, Jacks T (2002) Technologically advanced cancer modeling in mice. *Curr Opin Genet Dev* 12: 105-110.
220. Hamilton DL, Abremski K (1984) Site-specific recombination by the bacteriophage P1 lox-Cre system. Cre-mediated synapsis of two lox sites. *J Mol Biol* 178: 481-486.
221. Sauer B, Henderson N (1988) Site-specific DNA recombination in mammalian cells by the Cre recombinase of bacteriophage P1. *Proc Natl Acad Sci U S A* 85: 5166-5170.
222. Lakso M, Sauer B, Mosinger B, Jr., Lee EJ, Manning RW, et al. (1992) Targeted oncogene activation by site-specific recombination in transgenic mice. *Proc Natl Acad Sci U S A* 89: 6232-6236.
223. Jackson EL, Willis N, Mercer K, Bronson RT, Crowley D, et al. (2001) Analysis of lung tumor initiation and progression using conditional expression of oncogenic K-ras. *Genes Dev* 15: 3243-3248.
224. Mercer K, Giblett S, Green S, Lloyd D, DaRocha Dias S, et al. (2005) Expression of endogenous oncogenic V600E-Braf induces proliferation and developmental defects in mice and transformation of primary fibroblasts. *Cancer Res* 65: 11493-11500.
225. Johnson L, Mercer K, Greenbaum D, Bronson RT, Crowley D, et al. (2001) Somatic activation of the K-ras oncogene causes early onset lung cancer in mice. *Nature* 410: 1111-1116.
226. Tuveson DA, Shaw AT, Willis NA, Silver DP, Jackson EL, et al. (2004) Endogenous oncogenic K-ras(G12D) stimulates proliferation and widespread neoplastic and developmental defects. *Cancer Cell* 5: 375-387.
227. Dhomen N, Reis-Filho JS, da Rocha Dias S, Hayward R, Savage K, et al. (2009) Oncogenic Braf induces melanocyte senescence and melanoma in mice. *Cancer Cell* 15: 294-303.
228. Calcagno SR, Li S, Colon M, Kreinest PA, Thompson EA, et al. (2008) Oncogenic K-ras promotes early carcinogenesis in the mouse proximal colon. *Int J Cancer* 122: 2462-2470.
229. de Jong M, Maina T (2010) Of mice and humans: are they the same?--Implications in cancer translational research. *J Nucl Med* 51: 501-504.
230. Martignoni M, Groothuis GM, de Kanter R (2006) Species differences between mouse, rat, dog, monkey and human CYP-mediated drug metabolism, inhibition and induction. *Expert Opin Drug Metab Toxicol* 2: 875-894.
231. Shay T, Kang J (2013) Immunological Genome Project and systems immunology. *Trends Immunol* 34: 602-609.

232. Seok J, Warren HS, Cuenca AG, Mindrinos MN, Baker HV, et al. (2013) Genomic responses in mouse models poorly mimic human inflammatory diseases. *Proc Natl Acad Sci U S A* 110: 3507-3512.
233. Rangarajan A, Hong SJ, Gifford A, Weinberg RA (2004) Species- and cell type-specific requirements for cellular transformation. *Cancer Cell* 6: 171-183.
234. Kleinerman RA, Schonfeld SJ, Tucker MA (2012) Sarcomas in hereditary retinoblastoma. *Clin Sarcoma Res* 2: 15.
235. Jacks T, Fazeli A, Schmitt EM, Bronson RT, Goodell MA, et al. (1992) Effects of an Rb mutation in the mouse. *Nature* 359: 295-300.
236. Boivin GP, Washington K, Yang K, Ward JM, Pretlow TP, et al. (2003) Pathology of mouse models of intestinal cancer: consensus report and recommendations. *Gastroenterology* 124: 762-777.
237. Heyer J, Yang K, Lipkin M, Edelmann W, Kucherlapati R (1999) Mouse models for colorectal cancer. *Oncogene* 18: 5325-5333.
238. Swindle MM, Makin A, Herron AJ, Clubb FJ, Jr., Frazier KS (2012) Swine as models in biomedical research and toxicology testing. *Vet Pathol* 49: 344-356.
239. Anzenbacher P, Soucek P, Anzenbacherova E, Gut I, Hruby K, et al. (1998) Presence and activity of cytochrome P450 isoforms in minipig liver microsomes. Comparison with human liver samples. *Drug Metab Dispos* 26: 56-59.
240. Soucek P, Zuber R, Anzenbacherova E, Anzenbacher P, Guengerich FP (2001) Minipig cytochrome P450 3A, 2A and 2C enzymes have similar properties to human analogs. *BMC Pharmacol* 1: 11.
241. van der Laan JW, Brightwell J, McAnulty P, Ratky J, Stark C, et al. (2010) Regulatory acceptability of the minipig in the development of pharmaceuticals, chemicals and other products. *J Pharmacol Toxicol Methods* 62: 184-195.
242. Forster R, Bode G, Ellegaard L, van der Laan JW (2010) The RETHINK project on minipigs in the toxicity testing of new medicines and chemicals: conclusions and recommendations. *J Pharmacol Toxicol Methods* 62: 236-242.
243. Groenen MA, Archibald AL, Uenishi H, Tuggle CK, Takeuchi Y, et al. (2012) Analyses of pig genomes provide insight into porcine demography and evolution. *Nature* 491: 393-398.
244. Humphray SJ, Scott CE, Clark R, Marron B, Bender C, et al. (2007) A high utility integrated map of the pig genome. *Genome Biol* 8: R139.
245. Watanabe M, Nakano K, Matsunari H, Matsuda T, Maehara M, et al. (2013) Generation of interleukin-2 receptor gamma gene knockout pigs from somatic cells genetically modified by zinc finger nuclease-encoding mRNA. *PLoS One* 8: e76478.
246. Xin J, Yang H, Fan N, Zhao B, Ouyang Z, et al. (2013) Highly efficient generation of GGTA1 biallelic knockout inbred mini-pigs with TALENs. *PLoS One* 8: e84250.
247. Carlson DF, Tan W, Lillico SG, Stverakova D, Proudfoot C, et al. (2012) Efficient TALEN-mediated gene knockout in livestock. *Proc Natl Acad Sci U S A* 109: 17382-17387.
248. Dai Y, Vaught TD, Boone J, Chen SH, Phelps CJ, et al. (2002) Targeted disruption of the alpha1,3-galactosyltransferase gene in cloned pigs. *Nat Biotechnol* 20: 251-255.
249. Whitworth KM, Lee K, Benne JA, Beaton BP, Spate LD, et al. (2014) Use of the CRISPR/Cas9 System to Produce Genetically Engineered Pigs from In Vitro-Derived Oocytes and Embryos. *Biol Reprod*.
250. Lai L, Kolber-Simonds D, Park KW, Cheong HT, Greenstein JL, et al. (2002) Production of alpha-1,3-galactosyltransferase knockout pigs by nuclear transfer cloning. *Science* 295: 1089-1092.
251. Renner S, Fehlings C, Herbach N, Hofmann A, von Waldthausen DC, et al. (2010) Glucose intolerance and reduced proliferation of pancreatic beta-cells in transgenic pigs with impaired glucose-dependent insulinotropic polypeptide function. *Diabetes* 59: 1228-1238.
252. Rogers CS, Stoltz DA, Meyerholz DK, Ostedgaard LS, Rokhlina T, et al. (2008) Disruption of the CFTR gene produces a model of cystic fibrosis in newborn pigs. *Science* 321: 1837-1841.

253. Klymiuk N, Blutke A, Graf A, Krause S, Burkhardt K, et al. (2013) Dystrophin-deficient pigs provide new insights into the hierarchy of physiological derangements of dystrophic muscle. *Hum Mol Genet* 22: 4368-4382.
254. Luo Y, Li J, Liu Y, Lin L, Du Y, et al. (2011) High efficiency of BRCA1 knockout using rAAV-mediated gene targeting: developing a pig model for breast cancer. *Transgenic Res* 20: 975-988.
255. Flisikowska T, Merkl C, Landmann M, Eser S, Rezaei N, et al. (2012) A porcine model of familial adenomatous polyposis. *Gastroenterology* 143: 1173-1175 e1171-1177.
256. Leuchs S, Saalfrank A, Merkl C, Flisikowska T, Edlinger M, et al. (2012) Inactivation and inducible oncogenic mutation of p53 in gene targeted pigs. *PLoS One* 7: e43323.
257. Futreal PA, Coin L, Marshall M, Down T, Hubbard T, et al. (2004) A census of human cancer genes. *Nat Rev Cancer* 4: 177-183.
258. Adam SJ, Rund LA, Kuzmuk KN, Zachary JF, Schook LB, et al. (2007) Genetic induction of tumorigenesis in swine. *Oncogene* 26: 1038-1045.
259. Zheng S, El-Naggar AK, Kim ES, Kurie JM, Lozano G (2007) A genetic mouse model for metastatic lung cancer with gender differences in survival. *Oncogene* 26: 6896-6904.
260. Tsumura H, Yoshida T, Saito H, Imanaka-Yoshida K, Suzuki N (2006) Cooperation of oncogenic K-ras and p53 deficiency in pleomorphic rhabdomyosarcoma development in adult mice. *Oncogene* 25: 7673-7679.
261. submitted *Transgenic Research*: Li S, Edlinger M, Saalfrank A, Flisikowski K, Tschukes A, Kurome M, Zakhartchenko V, Kessler B, Saur D, Kind A, Wolf E, Schnieke A, Flisikowska T (2014) Lable pigs with conditionally-activatable oncogenic KRAS mutation
262. Scheffzek K, Ahmadian MR, Kabsch W, Wiesmuller L, Lautwein A, et al. (1997) The Ras-RasGAP complex: structural basis for GTPase activation and its loss in oncogenic Ras mutants. *Science* 277: 333-338.
263. Bos JL (1989) ras oncogenes in human cancer: a review. *Cancer Res* 49: 4682-4689.
264. Drayton S, Rowe J, Jones R, Vatcheva R, Cuthbert-Heavens D, et al. (2003) Tumor suppressor p16INK4a determines sensitivity of human cells to transformation by cooperating cellular oncogenes. *Cancer Cell* 4: 301-310.
265. Boehm JS, Hession MT, Bulmer SE, Hahn WC (2005) Transformation of human and murine fibroblasts without viral oncoproteins. *Mol Cell Biol* 25: 6464-6474.
266. Denning C, Dickinson P, Burl S, Wylie D, Fletcher J, et al. (2001) Gene targeting in primary fetal fibroblasts from sheep and pig. *Cloning Stem Cells* 3: 221-231.
267. Newbold RF, Overell RW (1983) Fibroblast immortality is a prerequisite for transformation by EJ c-Ha-ras oncogene. *Nature* 304: 648-651.
268. Wei W, Hemmer RM, Sedivy JM (2001) Role of p14(ARF) in replicative and induced senescence of human fibroblasts. *Mol Cell Biol* 21: 6748-6757.
269. Zindy F, Eischen CM, Randle DH, Kamijo T, Cleveland JL, et al. (1998) Myc signaling via the ARF tumor suppressor regulates p53-dependent apoptosis and immortalization. *Genes Dev* 12: 2424-2433.
270. Shay JW, Pereira-Smith OM, Wright WE (1991) A role for both RB and p53 in the regulation of human cellular senescence. *Exp Cell Res* 196: 33-39.
271. Beausejour CM, Krtolica A, Galimi F, Narita M, Lowe SW, et al. (2003) Reversal of human cellular senescence: roles of the p53 and p16 pathways. *EMBO J* 22: 4212-4222.
272. Brenner AJ, Stampfer MR, Aldaz CM (1998) Increased p16 expression with first senescence arrest in human mammary epithelial cells and extended growth capacity with p16 inactivation. *Oncogene* 17: 199-205.
273. Payal Agarwal, Farruk Mohammad Lutful Kabir, Patricia DeInnocentes and Richard Curtis Bird (2012). *Tumor Suppressor Gene p16/INK4A/CDKN2A and Its Role in Cell Cycle Exit, Differentiation, and Determination of Cell Fate, Tumor Suppressor Genes*, Dr. Yue Cheng (Ed.), ISBN: 978-953-307-879-3, InTech, DOI: 10.5772/27882. Available from: <http://www.intechopen.com/books/tumor-suppressor->

- genes/tumor-suppressor-gene-p16-ink4a-cdkn2a-and-its-role-in-cell-cycle-exit-differentiation-and-determina
274. Hampar B, Boyd AL, Derge JG, Zweig M, Eader L, et al. (1980) Comparison of properties of mouse cells transformed spontaneously by ultraviolet light-irradiated herpes simplex virus or by simian virus 40. *Cancer Res* 40: 2213-2222.
 275. Sherr CJ, McCormick F (2002) The RB and p53 pathways in cancer. *Cancer Cell* 2: 103-112.
 276. Abercrombie M (1979) Contact inhibition and malignancy. *Nature* 281: 259-262.
 277. Seluanov A, Hine C, Azpurua J, Feigenson M, Bozzella M, et al. (2009) Hypersensitivity to contact inhibition provides a clue to cancer resistance of naked mole-rat. *Proc Natl Acad Sci U S A* 106: 19352-19357.
 278. Freedman VH, Shin SI (1974) Cellular tumorigenicity in nude mice: correlation with cell growth in semi-solid medium. *Cell* 3: 355-359.
 279. Shields JM, Pruitt K, McFall A, Shaub A, Der CJ (2000) Understanding Ras: 'it ain't over 'til it's over'. *Trends Cell Biol* 10: 147-154.
 280. Stavropoulos DJ, Bradshaw PS, Li X, Pasic I, Truong K, et al. (2002) The Bloom syndrome helicase BLM interacts with TRF2 in ALT cells and promotes telomeric DNA synthesis. *Hum Mol Genet* 11: 3135-3144.
 281. Jackson EL, Olive KP, Tuveson DA, Bronson R, Crowley D, et al. (2005) The differential effects of mutant p53 alleles on advanced murine lung cancer. *Cancer Res* 65: 10280-10288.
 282. Mangerich A, Scherthan H, Diefenbach J, Kloz U, van der Hoeven F, et al. (2009) A caveat in mouse genetic engineering: ectopic gene targeting in ES cells by bidirectional extension of the homology arms of a gene replacement vector carrying human PARP-1. *Transgenic Res* 18: 261-279.
 283. Flisikowska T, Kind A, Schnieke A (2013) The new pig on the block: modelling cancer in pigs. *Transgenic Res* 22: 673-680.
 284. Mansour SL, Thomas KR, Capecchi MR (1988) Disruption of the proto-oncogene int-2 in mouse embryo-derived stem cells: a general strategy for targeting mutations to non-selectable genes. *Nature* 336: 348-352.
 285. Hanson KD, Sedivy JM (1995) Analysis of biological selections for high-efficiency gene targeting. *Mol Cell Biol* 15: 45-51.
 286. Niwa H, Yamamura K, Miyazaki J (1991) Efficient selection for high-expression transfectants with a novel eukaryotic vector. *Gene* 108: 193-199.
 287. Hasty P, Rivera-Perez J, Bradley A (1991) The length of homology required for gene targeting in embryonic stem cells. *Mol Cell Biol* 11: 5586-5591.
 288. Deng C, Capecchi MR (1992) Reexamination of gene targeting frequency as a function of the extent of homology between the targeting vector and the target locus. *Mol Cell Biol* 12: 3365-3371.
 289. Choulika A, Perrin A, Dujon B, Nicolas JF (1995) Induction of homologous recombination in mammalian chromosomes by using the I-SceI system of *Saccharomyces cerevisiae*. *Mol Cell Biol* 15: 1968-1973.
 290. Porteus MH, Baltimore D (2003) Chimeric nucleases stimulate gene targeting in human cells. *Science* 300: 763.
 291. Li S, Flisikowska T, Kurome M, Zakhartchenko V, Kessler B, et al. (2014) Dual fluorescent reporter pig for Cre recombination: transgene placement at the ROSA26 locus. *PLoS One* 9: e102455.
 292. Helleday T, Lo J, van Gent DC, Engelward BP (2007) DNA double-strand break repair: from mechanistic understanding to cancer treatment. *DNA Repair (Amst)* 6: 923-935.
 293. Mekeel KL, Tang W, Kachnic LA, Luo CM, DeFrank JS, et al. (1997) Inactivation of p53 results in high rates of homologous recombination. *Oncogene* 14: 1847-1857.
 294. Willers H, McCarthy EE, Alberti W, Dahm-Daphi J, Powell SN (2000) Loss of wild-type p53 function is responsible for upregulated homologous recombination in immortal rodent fibroblasts. *Int J Radiat Biol* 76: 1055-1062.

295. Bertrand P, Rouillard D, Boulet A, Levalois C, Soussi T, et al. (1997) Increase of spontaneous intrachromosomal homologous recombination in mammalian cells expressing a mutant p53 protein. *Oncogene* 14: 1117-1122.
296. Akyuz N, Boehden GS, Susse S, Rimek A, Preuss U, et al. (2002) DNA substrate dependence of p53-mediated regulation of double-strand break repair. *Mol Cell Biol* 22: 6306-6317.
297. Dominguez-Bendala J, Priddle H, Clarke A, McWhir J (2003) Elevated expression of exogenous Rad51 leads to identical increases in gene-targeting frequency in murine embryonic stem (ES) cells with both functional and dysfunctional p53 genes. *Exp Cell Res* 286: 298-307.
298. Solozobova V, Rolletschek A, Blattner C (2009) Nuclear accumulation and activation of p53 in embryonic stem cells after DNA damage. *BMC Cell Biol* 10: 46.
299. Aladjem MI, Spike BT, Rodewald LW, Hope TJ, Klemm M, et al. (1998) ES cells do not activate p53-dependent stress responses and undergo p53-independent apoptosis in response to DNA damage. *Curr Biol* 8: 145-155.
300. Solozobova V, Blattner C (2010) Regulation of p53 in embryonic stem cells. *Exp Cell Res* 316: 2434-2446.
301. Templeton NS, Roberts DD, Safer B (1997) Efficient gene targeting in mouse embryonic stem cells. *Gene Ther* 4: 700-709.
302. Willers H, McCarthy EE, Hubbe P, Dahm-Daphi J, Powell SN (2001) Homologous recombination in extrachromosomal plasmid substrates is not suppressed by p53. *Carcinogenesis* 22: 1757-1763.
303. Bunz F, Fauth C, Speicher MR, Dutriaux A, Sedivy JM, et al. (2002) Targeted inactivation of p53 in human cells does not result in aneuploidy. *Cancer Res* 62: 1129-1133.
304. Wiktor-Brown DM, Sukup-Jackson MR, Fakhraldien SA, Hendricks CA, Engelward BP (2011) p53 null fluorescent yellow direct repeat (FYDR) mice have normal levels of homologous recombination. *DNA Repair (Amst)* 10: 1294-1299.
305. Yun S, Lie ACC, Porter AC (2004) Discriminatory suppression of homologous recombination by p53. *Nucleic Acids Res* 32: 6479-6489.
306. Khanna KK, Jackson SP (2001) DNA double-strand breaks: signaling, repair and the cancer connection. *Nat Genet* 27: 247-254.
307. Essers J, Hendriks RW, Swagemakers SM, Troelstra C, de Wit J, et al. (1997) Disruption of mouse RAD54 reduces ionizing radiation resistance and homologous recombination. *Cell* 89: 195-204.
308. Bezzubova O, Silbergleit A, Yamaguchi-Iwai Y, Takeda S, Buerstedde JM (1997) Reduced X-ray resistance and homologous recombination frequencies in a RAD54-/- mutant of the chicken DT40 cell line. *Cell* 89: 185-193.
309. Yamaguchi-Iwai Y, Sonoda E, Buerstedde JM, Bezzubova O, Morrison C, et al. (1998) Homologous recombination, but not DNA repair, is reduced in vertebrate cells deficient in RAD52. *Mol Cell Biol* 18: 6430-6435.
310. Rijkers T, Van Den Ouweland J, Morolli B, Rolink AG, Baarends WM, et al. (1998) Targeted inactivation of mouse RAD52 reduces homologous recombination but not resistance to ionizing radiation. *Mol Cell Biol* 18: 6423-6429.
311. Takata M, Sasaki MS, Sonoda E, Fukushima T, Morrison C, et al. (2000) The Rad51 paralog Rad51B promotes homologous recombinational repair. *Mol Cell Biol* 20: 6476-6482.
312. Vasquez KM, Marburger K, Intody Z, Wilson JH (2001) Manipulating the mammalian genome by homologous recombination. *Proc Natl Acad Sci U S A* 98: 8403-8410.
313. Wesoly J, Agarwal S, Sigurdsson S, Bussen W, Van Komen S, et al. (2006) Differential contributions of mammalian Rad54 paralogs to recombination, DNA damage repair, and meiosis. *Mol Cell Biol* 26: 976-989.
314. Sarai N, Kagawa W, Fujikawa N, Saito K, Hikiba J, et al. (2008) Biochemical analysis of the N-terminal domain of human RAD54B. *Nucleic Acids Res* 36: 5441-5450.
315. Peitz M, Pfannkuche K, Rajewsky K, Edenhofer F (2002) Ability of the hydrophobic FGF and basic TAT peptides to promote cellular uptake of recombinant Cre recombinase:

- a tool for efficient genetic engineering of mammalian genomes. *Proc Natl Acad Sci U S A* 99: 4489-4494.
316. Peitz M, Jager R, Patsch C, Jager A, Egert A, et al. (2007) Enhanced purification of cell-permeant Cre and germline transmission after transduction into mouse embryonic stem cells. *Genesis* 45: 508-517.
 317. Mortensen RM, Conner DA, Chao S, Geisterfer-Lowrance AA, Seidman JG (1992) Production of homozygous mutant ES cells with a single targeting construct. *Mol Cell Biol* 12: 2391-2395.
 318. Nelson FK, Frankel W, Rajan TV (1989) Mitotic recombination is responsible for the loss of heterozygosity in cultured murine cell lines. *Mol Cell Biol* 9: 1284-1288.
 319. Wasmuth JJ, Vock Hall L (1984) Genetic demonstration of mitotic recombination in cultured Chinese hamster cell hybrids. *Cell* 36: 697-707.
 320. Bond JA, Wyllie FS, Wynford-Thomas D (1994) Escape from senescence in human diploid fibroblasts induced directly by mutant p53. *Oncogene* 9: 1885-1889.
 321. Rogan EM, Bryan TM, Hukku B, Maclean K, Chang AC, et al. (1995) Alterations in p53 and p16INK4 expression and telomere length during spontaneous immortalization of Li-Fraumeni syndrome fibroblasts. *Mol Cell Biol* 15: 4745-4753.
 322. Bond JA, Haughton MF, Rowson JM, Smith PJ, Gire V, et al. (1999) Control of replicative life span in human cells: barriers to clonal expansion intermediate between M1 senescence and M2 crisis. *Mol Cell Biol* 19: 3103-3114.
 323. Terzian T, Suh YA, Iwakuma T, Post SM, Neumann M, et al. (2008) The inherent instability of mutant p53 is alleviated by Mdm2 or p16INK4a loss. *Genes Dev* 22: 1337-1344.
 324. Classon M, Harlow E (2002) The retinoblastoma tumour suppressor in development and cancer. *Nat Rev Cancer* 2: 910-917.
 325. Mitnacht S (2005) The retinoblastoma protein--from bench to bedside. *Eur J Cell Biol* 84: 97-107.
 326. Funes JM, Quintero M, Henderson S, Martinez D, Qureshi U, et al. (2007) Transformation of human mesenchymal stem cells increases their dependency on oxidative phosphorylation for energy production. *Proc Natl Acad Sci U S A* 104: 6223-6228.
 327. Serrano M, Lee H, Chin L, Cordon-Cardo C, Beach D, et al. (1996) Role of the INK4a locus in tumor suppression and cell mortality. *Cell* 85: 27-37.
 328. Goessel G, Quante M, Hahn WC, Harada H, Heeg S, et al. (2005) Creating oral squamous cancer cells: a cellular model of oral-esophageal carcinogenesis. *Proc Natl Acad Sci U S A* 102: 15599-15604.
 329. Resnitzky D, Gossen M, Bujard H, Reed SI (1994) Acceleration of the G1/S phase transition by expression of cyclins D1 and E with an inducible system. *Mol Cell Biol* 14: 1669-1679.
 330. Resnitzky D, Reed SI (1995) Different roles for cyclins D1 and E in regulation of the G1-to-S transition. *Mol Cell Biol* 15: 3463-3469.
 331. Rane SG, Cosenza SC, Mettus RV, Reddy EP (2002) Germ line transmission of the Cdk4(R24C) mutation facilitates tumorigenesis and escape from cellular senescence. *Mol Cell Biol* 22: 644-656.
 332. Chatterjee SJ, George B, Goebell PJ, Alavi-Tafreshi M, Shi SR, et al. (2004) Hyperphosphorylation of pRb: a mechanism for RB tumour suppressor pathway inactivation in bladder cancer. *J Pathol* 203: 762-770.
 333. Tsutsui T, Kumakura S, Yamamoto A, Kanai H, Tamura Y, et al. (2002) Association of p16(INK4a) and pRb inactivation with immortalization of human cells. *Carcinogenesis* 23: 2111-2117.
 334. Laird PW, Jaenisch R (1996) The role of DNA methylation in cancer genetic and epigenetics. *Annu Rev Genet* 30: 441-464.
 335. Brenet F, Moh M, Funk P, Feierstein E, Viale AJ, et al. (2011) DNA methylation of the first exon is tightly linked to transcriptional silencing. *PLoS One* 6: e14524.
 336. Ekholm SV, Reed SI (2000) Regulation of G(1) cyclin-dependent kinases in the mammalian cell cycle. *Curr Opin Cell Biol* 12: 676-684.

337. Keyomarsi K, Conte D, Jr., Toyofuku W, Fox MP (1995) Deregulation of cyclin E in breast cancer. *Oncogene* 11: 941-950.
338. Erlandsson F, Wahlby C, Ekholm-Reed S, Hellstrom AC, Bengtsson E, et al. (2003) Abnormal expression pattern of cyclin E in tumour cells. *Int J Cancer* 104: 369-375.
339. Cassia R, Moreno-Bueno G, Rodriguez-Perales S, Hardisson D, Cigudosa JC, et al. (2003) Cyclin E gene (CCNE) amplification and hCDC4 mutations in endometrial carcinoma. *J Pathol* 201: 589-595.
340. Ohtsubo M, Roberts JM (1993) Cyclin-dependent regulation of G1 in mammalian fibroblasts. *Science* 259: 1908-1912.
341. Spruck CH, Won KA, Reed SI (1999) Deregulated cyclin E induces chromosome instability. *Nature* 401: 297-300.
342. Keck JM, Summers MK, Tedesco D, Ekholm-Reed S, Chuang LC, et al. (2007) Cyclin E overexpression impairs progression through mitosis by inhibiting APC(Cdh1). *J Cell Biol* 178: 371-385.
343. Pagano M, Pepperkok R, Verde F, Ansorge W, Draetta G (1992) Cyclin A is required at two points in the human cell cycle. *EMBO J* 11: 961-971.
344. Rosenblatt J, Gu Y, Morgan DO (1992) Human cyclin-dependent kinase 2 is activated during the S and G2 phases of the cell cycle and associates with cyclin A. *Proc Natl Acad Sci U S A* 89: 2824-2828.
345. Krude T, Jackman M, Pines J, Laskey RA (1997) Cyclin/Cdk-dependent initiation of DNA replication in a human cell-free system. *Cell* 88: 109-119.
346. Rosenberg AR, Zindy F, Le Deist F, Mouly H, Metezeau P, et al. (1995) Overexpression of human cyclin A advances entry into S phase. *Oncogene* 10: 1501-1509.
347. Resnitzky D, Hengst L, Reed SI (1995) Cyclin A-associated kinase activity is rate limiting for entrance into S phase and is negatively regulated in G1 by p27Kip1. *Mol Cell Biol* 15: 4347-4352.
348. De Boer L, Oakes V, Beamish H, Giles N, Stevens F, et al. (2008) Cyclin A/cdk2 coordinates centrosomal and nuclear mitotic events. *Oncogene* 27: 4261-4268.
349. den Elzen N, Pines J (2001) Cyclin A is destroyed in prometaphase and can delay chromosome alignment and anaphase. *J Cell Biol* 153: 121-136.
350. Geley S, Kramer E, Gieffers C, Gannon J, Peters JM, et al. (2001) Anaphase-promoting complex/cyclosome-dependent proteolysis of human cyclin A starts at the beginning of mitosis and is not subject to the spindle assembly checkpoint. *J Cell Biol* 153: 137-148.
351. Yam CH, Fung TK, Poon RY (2002) Cyclin A in cell cycle control and cancer. *Cell Mol Life Sci* 59: 1317-1326.
352. Pines J, Hunter T (1989) Isolation of a human cyclin cDNA: evidence for cyclin mRNA and protein regulation in the cell cycle and for interaction with p34cdc2. *Cell* 58: 833-846.
353. Maity A, McKenna WG, Muschel RJ (1995) Evidence for post-transcriptional regulation of cyclin B1 mRNA in the cell cycle and following irradiation in HeLa cells. *EMBO J* 14: 603-609.
354. Hwang A, Maity A, McKenna WG, Muschel RJ (1995) Cell cycle-dependent regulation of the cyclin B1 promoter. *J Biol Chem* 270: 28419-28424.
355. Welch PJ, Wang JY (1992) Coordinated synthesis and degradation of cdc2 in the mammalian cell cycle. *Proc Natl Acad Sci U S A* 89: 3093-3097.
356. Heald R, McLoughlin M, McKeon F (1993) Human wee1 maintains mitotic timing by protecting the nucleus from cytoplasmically activated Cdc2 kinase. *Cell* 74: 463-474.
357. Jin P, Hardy S, Morgan DO (1998) Nuclear localization of cyclin B1 controls mitotic entry after DNA damage. *J Cell Biol* 141: 875-885.
358. Kawamoto H, Koizumi H, Uchikoshi T (1997) Expression of the G2-M checkpoint regulators cyclin B1 and cdc2 in nonmalignant and malignant human breast lesions: immunocytochemical and quantitative image analyses. *Am J Pathol* 150: 15-23.
359. Soria JC, Jang SJ, Khuri FR, Hassan K, Liu D, et al. (2000) Overexpression of cyclin B1 in early-stage non-small cell lung cancer and its clinical implication. *Cancer Res* 60: 4000-4004.

360. Mashal RD, Lester S, Corless C, Richie JP, Chandra R, et al. (1996) Expression of cell cycle-regulated proteins in prostate cancer. *Cancer Res* 56: 4159-4163.
361. Grabsch H, Lickvers K, Hansen O, Takeno S, Willers R, et al. (2004) Prognostic value of cyclin B1 protein expression in colorectal cancer. *Am J Clin Pathol* 122: 511-516.
362. Hansel DE, Dhara S, Huang RC, Ashfaq R, Deasel M, et al. (2005) CDC2/CDK1 expression in esophageal adenocarcinoma and precursor lesions serves as a diagnostic and cancer progression marker and potential novel drug target. *Am J Surg Pathol* 29: 390-399.
363. Kallakury BV, Sheehan CE, Ambros RA, Fisher HA, Kaufman RP, Jr., et al. (1997) The prognostic significance of p34cdc2 and cyclin D1 protein expression in prostate adenocarcinoma. *Cancer* 80: 753-763.
364. Dulic V, Kaufmann WK, Wilson SJ, Tlsty TD, Lees E, et al. (1994) p53-dependent inhibition of cyclin-dependent kinase activities in human fibroblasts during radiation-induced G1 arrest. *Cell* 76: 1013-1023.
365. el-Deiry WS, Harper JW, O'Connor PM, Velculescu VE, Canman CE, et al. (1994) WAF1/CIP1 is induced in p53-mediated G1 arrest and apoptosis. *Cancer Res* 54: 1169-1174.
366. Harper JW, Adami GR, Wei N, Keyomarsi K, Elledge SJ (1993) The p21 Cdk-interacting protein Cip1 is a potent inhibitor of G1 cyclin-dependent kinases. *Cell* 75: 805-816.
367. Dulic V, Stein GH, Far DF, Reed SI (1998) Nuclear accumulation of p21Cip1 at the onset of mitosis: a role at the G2/M-phase transition. *Mol Cell Biol* 18: 546-557.
368. Niculescu AB, 3rd, Chen X, Smeets M, Hengst L, Prives C, et al. (1998) Effects of p21(Cip1/Waf1) at both the G1/S and the G2/M cell cycle transitions: pRb is a critical determinant in blocking DNA replication and in preventing endoreduplication. *Mol Cell Biol* 18: 629-643.
369. Zhan Q, Antinore MJ, Wang XW, Carrier F, Smith ML, et al. (1999) Association with Cdc2 and inhibition of Cdc2/Cyclin B1 kinase activity by the p53-regulated protein Gadd45. *Oncogene* 18: 2892-2900.
370. Jin S, Antinore MJ, Lung FD, Dong X, Zhao H, et al. (2000) The GADD45 inhibition of Cdc2 kinase correlates with GADD45-mediated growth suppression. *J Biol Chem* 275: 16602-16608.
371. Bunz F, Dutriaux A, Lengauer C, Waldman T, Zhou S, et al. (1998) Requirement for p53 and p21 to sustain G2 arrest after DNA damage. *Science* 282: 1497-1501.
372. Kastan MB, Zhan Q, el-Deiry WS, Carrier F, Jacks T, et al. (1992) A mammalian cell cycle checkpoint pathway utilizing p53 and GADD45 is defective in ataxia-telangiectasia. *Cell* 71: 587-597.
373. Chudnovsky Y, Adams AE, Robbins PB, Lin Q, Khavari PA (2005) Use of human tissue to assess the oncogenic activity of melanoma-associated mutations. *Nat Genet* 37: 745-749.
374. Starling JA, Maule J, Hastie ND, Allshire RC (1990) Extensive telomere repeat arrays in mouse are hypervariable. *Nucleic Acids Res* 18: 6881-6888.
375. Prowse KR, Greider CW (1995) Developmental and tissue-specific regulation of mouse telomerase and telomere length. *Proc Natl Acad Sci U S A* 92: 4818-4822.
376. Wright WE, Shay JW (2000) Telomere dynamics in cancer progression and prevention: fundamental differences in human and mouse telomere biology. *Nat Med* 6: 849-851.
377. Jiang L, Carter DB, Xu J, Yang X, Prather RS, et al. (2004) Telomere lengths in cloned transgenic pigs. *Biol Reprod* 70: 1589-1593.
378. Vaziri H, Schachter F, Uchida I, Wei L, Zhu X, et al. (1993) Loss of telomeric DNA during aging of normal and trisomy 21 human lymphocytes. *Am J Hum Genet* 52: 661-667.
379. Fradiani PA, Ascenzioni F, Lavitrano M, Donini P (2004) Telomeres and telomerase activity in pig tissues. *Biochimie* 86: 7-12.
380. Wong SC, Ong LL, Er CP, Gao S, Yu H, et al. (2003) Cloning of rat telomerase catalytic subunit functional domains, reconstitution of telomerase activity and enzymatic profile of pig and chicken tissues. *Life Sci* 73: 2749-2760.

381. Ben-Porath I, Weinberg RA (2005) The signals and pathways activating cellular senescence. *Int J Biochem Cell Biol* 37: 961-976.
382. Huot TJ, Rowe J, Harland M, Drayton S, Brookes S, et al. (2002) Biallelic mutations in p16(INK4a) confer resistance to Ras- and Ets-induced senescence in human diploid fibroblasts. *Mol Cell Biol* 22: 8135-8143.
383. Harvey M, Sands AT, Weiss RS, Hegi ME, Wiseman RW, et al. (1993) In vitro growth characteristics of embryo fibroblasts isolated from p53-deficient mice. *Oncogene* 8: 2457-2467.
384. Dirac AM, Bernards R (2003) Reversal of senescence in mouse fibroblasts through lentiviral suppression of p53. *J Biol Chem* 278: 11731-11734.
385. Wei W, Herbig U, Wei S, Dutriaux A, Sedivy JM (2003) Loss of retinoblastoma but not p16 function allows bypass of replicative senescence in human fibroblasts. *EMBO Rep* 4: 1061-1066.
386. Montalto MC, Phillips JS, Ray FA (1999) Telomerase activation in human fibroblasts during escape from crisis. *J Cell Physiol* 180: 46-52.
387. Badie S, Escandell JM, Bouwman P, Carlos AR, Thanasoula M, et al. (2010) BRCA2 acts as a RAD51 loader to facilitate telomere replication and capping. *Nat Struct Mol Biol* 17: 1461-1469.
388. Saharia A, Stewart SA (2009) FEN1 contributes to telomere stability in ALT-positive tumor cells. *Oncogene* 28: 1162-1167.
389. Fan Q, Zhang F, Barrett B, Ren K, Andreassen PR (2009) A role for monoubiquitinated FANCD2 at telomeres in ALT cells. *Nucleic Acids Res* 37: 1740-1754.
390. Thompson LH, Hinz JM (2009) Cellular and molecular consequences of defective Fanconi anemia proteins in replication-coupled DNA repair: mechanistic insights. *Mutat Res* 668: 54-72.
391. Cesare AJ, Reddel RR (2010) Alternative lengthening of telomeres: models, mechanisms and implications. *Nat Rev Genet* 11: 319-330.
392. Ellis NA, Groden J, Ye TZ, Straughen J, Lennon DJ, et al. (1995) The Bloom's syndrome gene product is homologous to RecQ helicases. *Cell* 83: 655-666.
393. Lafferty-Whyte K, Cairney CJ, Will MB, Serakinci N, Daidone MG, et al. (2009) A gene expression signature classifying telomerase and ALT immortalization reveals an hTERT regulatory network and suggests a mesenchymal stem cell origin for ALT. *Oncogene* 28: 3765-3774.
394. Henson JD, Hannay JA, McCarthy SW, Royds JA, Yeager TR, et al. (2005) A robust assay for alternative lengthening of telomeres in tumors shows the significance of alternative lengthening of telomeres in sarcomas and astrocytomas. *Clin Cancer Res* 11: 217-225.
395. Pipas JM (2009) SV40: Cell transformation and tumorigenesis. *Virology* 384: 294-303.
396. Lin CY, Loven J, Rahl PB, Paranal RM, Burge CB, et al. (2012) Transcriptional amplification in tumor cells with elevated c-Myc. *Cell* 151: 56-67.
397. Nie Z, Hu G, Wei G, Cui K, Yamane A, et al. (2012) c-Myc is a universal amplifier of expressed genes in lymphocytes and embryonic stem cells. *Cell* 151: 68-79.
398. Shimizu T, Ishikawa T, Sugihara E, Kuninaka S, Miyamoto T, et al. (2010) c-MYC overexpression with loss of Ink4a/Arf transforms bone marrow stromal cells into osteosarcoma accompanied by loss of adipogenesis. *Oncogene* 29: 5687-5699.
399. Rubio R, Garcia-Castro J, Gutierrez-Aranda I, Paramio J, Santos M, et al. (2010) Deficiency in p53 but not retinoblastoma induces the transformation of mesenchymal stem cells in vitro and initiates leiomyosarcoma in vivo. *Cancer Res* 70: 4185-4194.
400. Rodriguez R, Rubio R, Menendez P (2012) Modeling sarcomagenesis using multipotent mesenchymal stem cells. *Cell Res* 22: 62-77.
401. Mizejewski GJ (1999) Role of integrins in cancer: survey of expression patterns. *Proc Soc Exp Biol Med* 222: 124-138.
402. Hood JD, Cheresch DA (2002) Role of integrins in cell invasion and migration. *Nat Rev Cancer* 2: 91-100.
403. Mita H, Toyota M, Aoki F, Akashi H, Maruyama R, et al. (2009) A novel method, digital genome scanning detects KRAS gene amplification in gastric cancers: involvement of

- overexpressed wild-type KRAS in downstream signaling and cancer cell growth. *BMC Cancer* 9: 198.
404. Wagner PL, Perner S, Rickman DS, LaFargue CJ, Kitabayashi N, et al. (2009) In situ evidence of KRAS amplification and association with increased p21 levels in non-small cell lung carcinoma. *Am J Clin Pathol* 132: 500-505.
 405. Birkeland E, Wik E, Mjos S, Hoivik EA, Trovik J, et al. (2012) KRAS gene amplification and overexpression but not mutation associates with aggressive and metastatic endometrial cancer. *Br J Cancer* 107: 1997-2004.
 406. McCubrey JA, Steelman LS, Abrams SL, Lee JT, Chang F, et al. (2006) Roles of the RAF/MEK/ERK and PI3K/PTEN/AKT pathways in malignant transformation and drug resistance. *Adv Enzyme Regul* 46: 249-279.
 407. Braun BS, Tuveson DA, Kong N, Le DT, Kogan SC, et al. (2004) Somatic activation of oncogenic Kras in hematopoietic cells initiates a rapidly fatal myeloproliferative disorder. *Proc Natl Acad Sci U S A* 101: 597-602.
 408. Orkin RW, Gehron P, McGoodwin EB, Martin GR, Valentine T, et al. (1977) A murine tumor producing a matrix of basement membrane. *J Exp Med* 145: 204-220.
 409. Futaki S, Hayashi Y, Yamashita M, Yagi K, Bono H, et al. (2003) Molecular basis of constitutive production of basement membrane components. Gene expression profiles of Engelbreth-Holm-Swarm tumor and F9 embryonal carcinoma cells. *J Biol Chem* 278: 50691-50701.
 410. Riddell SR, Elliott M, Lewinsohn DA, Gilbert MJ, Wilson L, et al. (1996) T-cell mediated rejection of gene-modified HIV-specific cytotoxic T lymphocytes in HIV-infected patients. *Nat Med* 2: 216-223.
 411. Morris JC, Conerly M, Thomasson B, Storek J, Riddell SR, et al. (2004) Induction of cytotoxic T-lymphocyte responses to enhanced green and yellow fluorescent proteins after myeloablative conditioning. *Blood* 103: 492-499.
 412. Rosenzweig M, Connole M, Glickman R, Yue SP, Noren B, et al. (2001) Induction of cytotoxic T lymphocyte and antibody responses to enhanced green fluorescent protein following transplantation of transduced CD34(+) hematopoietic cells. *Blood* 97: 1951-1959.
 413. Mercier-Letondal P, Deschamps M, Sauce D, Certoux JM, Milpied N, et al. (2008) Early immune response against retrovirally transduced herpes simplex virus thymidine kinase-expressing gene-modified T cells coin fused with a T cell-depleted marrow graft: an altered immune response? *Hum Gene Ther* 19: 937-950.
 414. Pellegata NS, Sessa F, Renault B, Bonato M, Leone BE, et al. (1994) K-ras and p53 gene mutations in pancreatic cancer: ductal and nonductal tumors progress through different genetic lesions. *Cancer Res* 54: 1556-1560.
 415. Gao HG, Chen JK, Stewart J, Song B, Rayappa C, et al. (1997) Distribution of p53 and K-ras mutations in human lung cancer tissues. *Carcinogenesis* 18: 473-478.
 416. Vahakangas KH, Bennett WP, Castren K, Welsh JA, Khan MA, et al. (2001) p53 and K-ras mutations in lung cancers from former and never-smoking women. *Cancer Res* 61: 4350-4356.
 417. Dellaire G, Lemieux N, Belmaaza A, Chartrand P (1997) Ectopic gene targeting exhibits a bimodal distribution of integration in murine cells, indicating that both intra- and interchromosomal sites are accessible to the targeting vector. *Mol Cell Biol* 17: 5571-5580.

10 Appendix

The tables show the fold-change values and the associated p-values for a series of cancer-related genes differentially expressed in stepwise genetically modified porcine MSC derivatives (neo14/K-, neo14/K67/-, neo14K67/1.1+cMyc) and porcine sarcoma derived tumour cells (pPTC, rePTC) compared to wild-type pMSCs. Tables were grouped as five categories: key genes of cellular transformation, ALT-associated genes, cell cycle regulatory genes, p53 target genes and tissue invasion and metastatic marker genes.

SYMBOL	DESCRIPTION	neo14/K-		neo14/K67/-		neo14/K67/1.1+cMyc		pPTC		rePTC	
		p-value	Fold-Change	p-value	Fold-Change	p-value	Fold-Change	p-value	Fold-Change	p-value	Fold-Change
TP53	tumour protein p53 (TP53)	2.82E-08	-6.33E+00	1.10E-03	2.27E+00	2.31E-03	1.95E+00	1.62E-05	2.64E+00	1.98E-02	1.51E+00
KRAS	v-Ki-ras2 Kirsten rat sarcoma viral oncogene homolog	1.52E-01	1.69E+00	4.95E-01	1.31E+00	1.01E-01	1.83E+00	1.08E-03	3.31E+00	7.83E-06	7.00E+00
APC	adenomatous polyposis coli (APC)	3.86E-03	1.45E+00	3.23E-01	1.13E+00	1.53E-02	1.35E+00	1.72E-01	1.15E+00	5.12E-03	-1.37E+00
ARF	p14ARF protein (P14ARF)	5.70E-02	1.74E+00	1.50E-03	3.16E+00	3.85E-02	1.84E+00	3.09E-04	2.91E+00	7.65E-04	2.63E+00
RB1	retinoblastoma 1	4.63E-01	1.24E+00	9.82E-02	-1.75E+00	8.88E-01	1.04E+00	8.55E-01	-1.05E+00	1.75E-04	-3.30E+00
TERT	telomerase reverse transcriptase	8.13E-01	1.03E+00	5.36E-01	-1.10E+00	2.13E-02	-1.40E+00	5.30E-02	-1.27E+00	3.40E-02	-1.30E+00
cMyc	v-myc myelocytomatosis viral oncogene homolog (avian)	2.18E-03	1.27E+00	2.12E-01	1.10E+00	1.45E-07	1.80E+00	1.78E-09	2.01E+00	8.91E-08	1.70E+00

Table 5: Fold-change values and associated p-values for a series of key genes of cellular transformation

SYMBOL	DESCRIPTION	neo14/K-		neo14/K67-		neo14/K67/1.1+cMyc		pPTC		rePTC	
		p-value	Fold-Change	p-value	Fold-Change	p-value	Fold-Change	p-value	Fold-Change	p-value	Fold-Change
TERT	telomerase reverse transcriptase	8.13E-01	1.03E+00	5.36E-01	-1.10E+00	2.13E-02	-1.40E+00	5.30E-02	-1.27E+00	3.40E-02	-1.30E+00
FEN1	flap structure-specific endonuclease 1	2.59E-10	1.43E+01	1.67E-09	1.38E+01	7.34E-11	1.81E+01	9.20E-11	1.18E+01	5.42E-11	1.29E+01
FANCD2	Fanconi anemia, complementation group D2	6.53E-10	1.20E+01	1.57E-08	9.30E+00	3.91E-09	9.02E+00	3.90E-10	9.31E+00	2.97E-09	6.97E+00
FANCA	Fanconi anemia, complementation group A (FANCA)	1.79E-03	1.94E+00	1.17E-04	2.73E+00	4.00E-05	2.71E+00	4.36E-06	2.84E+00	1.57E-04	2.13E+00
RAD51	RAD51 homolog (S. cerevisiae)	2.18E-12	5.87E+00	1.78E-10	4.39E+00	3.21E-12	5.61E+00	1.69E-12	4.75E+00	8.69E-12	4.05E+00
RAD51D	RAD51 homolog D (S. cerevisiae)	2.56E-03	1.27E+00	3.34E-04	1.41E+00	8.98E-07	1.68E+00	3.24E-06	1.50E+00	2.40E-04	1.32E+00
RAD52	RAD52 homolog (S. cerevisiae) (RAD52)	5.34E-01	-1.06E+00	2.19E-01	1.15E+00	7.34E-01	-1.03E+00	1.60E-03	1.38E+00	9.39E-01	1.01E+00
RAD54B	RAD54 homolog B (S. cerevisiae)	6.34E-08	7.59E+00	4.89E-06	5.05E+00	3.88E-08	8.18E+00	4.55E-08	6.04E+00	3.18E-07	4.75E+00
BRCA2	breast cancer type 2 susceptibility protein-like (LOC100153762), partial mRNA.	2.39E-07	3.66E+00	8.44E-05	2.43E+00	1.71E-07	3.78E+00	2.29E-08	3.80E+00	4.92E-01	1.10E+00
MRE11A	MRE11 meiotic recombination 11 homolog A (S. cerevisiae)	7.71E-06	2.16E+00	1.02E-03	1.70E+00	1.88E-05	2.04E+00	2.76E-06	2.06E+00	6.34E-01	-1.05E+00
BLM	Bloom syndrome, RecQ helicase-like (BLM)	6.55E-14	2.19E+01	7.81E-12	1.26E+01	3.27E-14	2.52E+01	1.36E-14	1.92E+01	1.81E-14	1.82E+01
WRN	Werner syndrome, RecQ helicase-like	3.02E-04	3.31E+00	5.53E-02	1.83E+00	3.27E-04	3.27E+00	1.40E-04	3.07E+00	6.15E-03	2.04E+00
POT1	protection of telomeres 1 homolog (S. pombe)	5.93E-03	2.19E+00	3.92E-01	1.28E+00	2.00E-02	1.89E+00	7.99E-03	1.91E+00	2.05E-01	-1.33E+00
TERF1	telomeric repeat binding factor (NIMA-interacting) 1	1.59E-03	2.43E+00	9.82E-01	1.01E+00	1.44E-01	1.43E+00	4.51E-02	1.55E+00	1.29E-01	1.38E+00
TERF2	telomeric repeat binding factor 2	3.34E-05	1.18E+00	2.57E-02	1.08E+00	6.12E-06	1.21E+00	5.09E-07	1.22E+00	2.03E-08	1.29E+00

Table 6: Fold-change values and associated p-values of ALT-associated genes

SYMBOL	DESCRIPTION	neo14/K-		neo14/K67/-		neo14/K67/1.1+cMyc		pPTC		rePTC	
		p-value	Fold-Change	p-value	Fold-Change	p-value	Fold-Change	p-value	Fold-Change	p-value	Fold-Change
RB1	retinoblastoma 1	4.63E-01	1.24E+00	9.82E-02	-1.75E+00	8.88E-01	1.04E+00	8.55E-01	-1.05E+00	1.75E-04	-3.30E+00
E2F3	transcription factor E2F3-like (LOC100154407)	1.03E-06	2.56E+00	3.41E-01	1.14E+00	1.67E-07	2.94E+00	7.69E-06	1.99E+00	2.88E-07	2.45E+00
CDK1	cyclin-dependent kinase 1	2.15E-08	1.73E+01	9.00E-07	1.12E+01	2.55E-08	1.67E+01	7.90E-09	1.42E+01	1.05E-08	1.34E+01
CDK2	cyclin-dependent kinase-2 alpha, transcript variant 2 (LOC100154715)	6.24E-12	5.88E+00	7.09E-10	4.24E+00	6.54E-12	5.85E+00	2.25E-11	4.09E+00	3.06E-12	4.99E+00
CDK4	cyclin-dependent kinase 4 (CDK4)	6.16E-08	1.54E+00	3.04E-06	1.43E+00	2.00E-07	1.48E+00	1.00E-07	1.43E+00	5.01E-08	1.46E+00
CDK6	cyclin-dependent kinase 6	1.49E-08	2.06E+00	8.09E-06	1.64E+00	2.83E-07	1.79E+00	2.04E-09	2.05E+00	6.99E-06	1.48E+00
CCNA1	cyclin-A1-like (LOC100627814), partial mRNA.	7.18E-01	-1.05E+00	3.11E-02	1.43E+00	6.41E-01	-1.07E+00	5.04E-01	1.08E+00	1.11E-01	1.22E+00
CCNA2	cyclin A2	2.52E-11	3.87E+01	6.82E-10	2.65E+01	4.15E-11	3.43E+01	1.81E-10	1.61E+01	1.03E-09	1.18E+01
CCNB1	cyclin B1 (CCNB1)	8.13E-10	5.27E+01	1.26E-08	3.90E+01	1.27E-09	4.68E+01	2.08E-10	4.32E+01	1.34E-10	4.83E+01
CCNB2	cyclin B2	7.30E-14	7.25E+01	1.87E-12	4.86E+01	2.64E-13	5.16E+01	8.03E-14	3.99E+01	4.06E-14	4.71E+01
CCNB3	cyclin B3	7.34E-16	4.13E+01	2.41E-14	2.80E+01	1.62E-15	3.44E+01	4.31E-16	2.80E+01	2.13E-16	3.26E+01
CCND1	cyclin D1	4.00E-06	1.98E+00	3.98E-05	1.87E+00	9.57E-05	1.67E+00	1.65E-04	1.52E+00	1.88E-06	1.87E+00
CCND2	cyclin D2 (CCND2)	1.41E-02	1.26E+00	1.58E-01	1.15E+00	8.58E-05	1.54E+00	9.63E-02	1.14E+00	4.39E-07	1.80E+00
CCND3	cyclin D3	3.83E-01	-1.22E+00	3.84E-01	-1.25E+00	6.63E-01	1.10E+00	4.20E-01	1.17E+00	1.62E-02	-1.67E+00
CCNE1	cyclin E1	8.63E-08	2.20E+00	3.23E-04	1.55E+00	9.36E-08	2.19E+00	3.08E-05	1.53E+00	2.49E-05	1.54E+00
CCNE2	cyclin E2	4.48E-11	8.18E+00	1.03E-07	3.95E+00	2.90E-11	8.70E+00	1.06E-10	5.58E+00	4.45E-07	2.59E+00

Table 7: Fold-change values and associated p-values of cell cycle regulatory genes

SYMBOL	DESCRIPTION	neo14/K-		neo14/K67/-		neo14/K67/1.1+cMyc		pPTC		rePTC	
		p-value	Fold-Change	p-value	Fold-Change	p-value	Fold-Change	p-value	Fold-Change	p-value	Fold-Change
TP53	tumour protein p53 (TP53)	2.82E-08	-6.33E+00	1.10E-03	2.27E+00	2.31E-03	1.95E+00	1.62E-05	2.64E+00	1.98E-02	1.51E+00
MDM2	Mdm2 p53 binding protein homolog (mouse)	4.92E-06	-3.10E+00	2.11E-07	-5.05E+00	3.08E-05	-2.62E+00	1.84E-06	-2.89E+00	1.50E-02	-1.49E+00
TP63	tumor protein p63, transcript variant 1 (TP63)	1.64E-01	1.52E+00	9.27E-02	1.77E+00	7.19E-01	1.11E+00	1.57E-02	1.95E+00	7.85E-03	2.12E+00
CDKN1A	cyclin-dependent kinase inhibitor 1A (p21, Cip1)	5.17E-13	-5.98E+00	4.03E-12	-5.75E+00	3.93E-13	-6.17E+00	5.14E-13	-4.71E+00	1.84E-06	-1.72E+00
CDKN1B	cyclin-dependent kinase inhibitor 1B (p27, Kip1) (CDKN1B)	4.59E-01	-1.12E+00	1.78E-01	-1.27E+00	1.82E-02	-1.49E+00	5.99E-02	-1.31E+00	6.38E-06	-2.38E+00
GADD45A	growth arrest and DNA-damage-inducible, alpha (GADD45A)	4.57E-06	-1.60E+00	3.49E-06	-1.72E+00	8.05E-07	-1.72E+00	1.33E-02	-1.18E+00	4.89E-01	-1.04E+00
CCNG1	cyclin G1	3.13E-07	-2.28E+00	1.37E-06	-2.27E+00	1.70E-08	-2.77E+00	6.25E-06	-1.75E+00	8.27E-05	-1.56E+00

Table 8: Fold-change values and associated p-values of some p53 target genes

SYMBOL	DESCRIPTION	neo14/K-		neo14/K67/-		neo14/K67/1.1+cMyc		pPTC		rePTC	
		p-value	Fold-Change	p-value	Fold-Change	p-value	Fold-Change	p-value	Fold-Change	p-value	Fold-Change
TIMP1	TIMP metalloproteinase inhibitor 1	2.26E-04	-1.29E+00	2.04E-04	-1.33E+00	1.97E-02	-1.15E+00	2.41E-10	-1.91E+00	2.83E-01	1.05E+00
TIMP2	TIMP metalloproteinase inhibitor 2	1.69E-06	-1.33E+00	7.53E-07	-1.40E+00	8.39E-08	-1.43E+00	7.51E-09	-1.44E+00	1.31E-09	-1.51E+00
TIMP3	TIMP metalloproteinase inhibitor 3	1.49E-03	-1.17E+00	6.72E-02	-1.10E+00	1.32E-05	-1.30E+00	1.97E-06	-1.30E+00	1.78E-14	-2.57E+00
TIMP4	TIMP metalloproteinase inhibitor 4	1.58E-01	-1.28E+00	1.51E-02	-1.66E+00	1.02E-01	-1.34E+00	3.34E-02	-1.40E+00	3.09E-02	-1.41E+00
MMP1	matrix metalloproteinase 1 (interstitial collagenase)	2.70E-01	-2.40E+00	1.09E-01	-4.29E+00	9.15E-01	1.09E+00	6.59E-01	1.35E+00	1.45E-03	1.28E+01
MMP3	matrix metalloproteinase 3 (stromelysin 1, progelatinase)	5.75E-01	1.07E+00	6.45E-01	1.07E+00	4.85E-10	5.09E+00	5.10E-11	5.15E+00	2.28E-16	3.75E+01
MMP10	matrix metalloproteinase 10 (stromelysin 2)	5.18E-01	1.11E+00	1.17E-01	1.34E+00	1.60E-08	5.22E+00	4.30E-09	4.80E+00	1.65E-14	3.57E+01
MMP12	matrix metalloproteinase 12 (macrophage elastase)	8.13E-03	1.47E+00	6.83E-01	1.06E+00	1.65E-03	1.62E+00	2.89E-01	1.13E+00	1.97E-11	6.17E+00
VEGFA	vascular endothelial growth factor A	4.00E-03	1.61E+00	1.71E-01	1.26E+00	2.02E-01	1.21E+00	5.12E-02	1.30E+00	9.25E-09	3.80E+00
THBS1	thrombospondin 1	1.74E-03	1.29E+00	7.08E-01	1.03E+00	7.69E-02	1.14E+00	1.56E-07	1.67E+00	2.14E-03	-1.24E+00
THBS2	thrombospondin-2-like (LOC100153940)	5.15E-10	-1.81E+01	2.45E-10	-3.01E+01	6.56E-10	-1.73E+01	3.18E-05	-2.97E+00	7.50E-13	-4.76E+01
THBS3	thrombospondin 3	9.21E-09	-3.83E+00	2.72E-08	-4.02E+00	3.88E-07	-2.78E+00	6.51E-04	1.58E+00	3.28E-03	1.45E+00

Table 9: Fold-change values and associated p-values of some tissue invasion and metastatic marker genes

11 Acknowledgement

Ich bedanke mich bei meiner Betreuerin, Frau Professor Angelika Schnieke, für die Bereitstellung des äußerst interessanten und spannenden Projektes. Die hilfreichen und anregenden Ideen und Diskussionen und ihre Unterstützung. Vielen Dank auch dafür, dass ich an so vielen Konferenzen teilnehmen durfte und unsere Forschungsarbeiten präsentieren konnte.

Mein weiterer Dank gilt meinem Zweitprüfer, Herrn Professor Dieter Saur, für die Begutachtung dieser Thesis. Des Weiteren möchte ich mich bei ihm und Stefan Eser für die Planung und Durchführung der Zellimplantationen und der Isolierung der porzinen Tumorzellen, sowie bei Vanessa Klein für die Anfertigung der Tumorschnitte bedanken.

Zudem bedanke ich mich bei Frau Professor Irene Esposito für die histologische Charakterisierung der porzinen Tumore. Morgane Ravon und Ulrich Certa danke ich für die Durchführung und Auswertung der Transkriptomanaylsen. Und vielen Dank für den sehr netten und eindrucksvollen Tag bei Roche in Basel.

Bei Viola und Steffen Löbnitz bedanke ich mich recht herzlichst für die Aufzucht und die liebevolle Betreuung von "Poldi". Besonders dafür, dass sie ihn immer wieder mit leckeren Äpfeln und extra Streicheleinheiten verwöhnt haben. Mein weiterer Dank gilt Frau Dr. Barbara Kessler für die Durchführung der Zellimplantationen in "Poldi".

Ein ganz besonderer Dank gilt meiner Mentorin, Frau Dr. Claudia Merkl. Ich danke dir so sehr dafür, dass du deine Erfahrungen und dein fachliches Wissen mit mir geteilt hast. All deine Ratschläge und Anregungen, deine Zeit und Geduld, die du in mich investiert hast, und dass du mich bei meiner wissenschaftlichen Ausbildung unterstützt und gefördert hast.

Tausend Dank dafür!

I would like to thank Dr. Alex Kind for all the help, great ideas and corrections of publications, manuscripts and abstracts. You are excellent in "pimping up" drafts! Bei Dr. Tatiana Flisikowska bedanke ich mich für all ihre Hilfe und Ratschläge während meiner Promotion und für all die netten und unterhaltsamen Gespräche außerhalb der Arbeit. PS: Tatiana, du solltest viel öfter deutsch sprechen, denn du hast einen so niedlichen Akzent! Dr. Krzysztof Flisikowski danke ich für die Einführung in die Welt der quantitativen real-time PCR und der Bisulfit-Sequenzierung. Vielen Dank auch für deine „stupid jokes“ während der Kaffeepausen!!! Bei Dr. Simone Kraner-Scheiber bedanke ich mich für die exzellente Vorauswahl der Studenten.

Meinen Studenten Susan Kläger, Lena Glashauser, Cornelia Brönner, Ferdinand Sedlmayer, Daniela Fellner und Monika Honz möchte ich sagen, ihr wart großartig! Es war mir eine Freude, euch zu betreuen und mein Wissen an euch weiterzugeben.

Ein dickes Dankeschön gebührt all meinen ehemaligen Mitstreitern: Tobias Richter, Marina Durkovic, Simon Leuchs, Tina Landmann und Alexander Tschukes für all die schöne und unterhaltsame Zeit während der Pausen, das Brainstorming und all eure Tipps und Tricks im Labor. Aber auch vielen Dank für all die schönen und lustigen Momente außerhalb der Arbeit. All meinen jetzigen Mitstreitern: Konrad Fischer, Erica Schulze, Beate Rieblinger, Rahul Dutta, Daniela Fellner und Carolin Wander wünsche ich weiterhin ganz viel Erfolg und gutes Gelingen mit ihren Projekten. Und ich hoffe, keiner muss je wieder sagen, "Oh mein Gott, ich bin verloren"!

Ein herzliches Dankeschön an Benedikt Baumer, den ich auch im Privatleben schätzen und lieben gelernt habe. Vergesse nicht: "Shit onto the wall, tomorrow comes the painter"! Und wie hast du immer so nett gesagt: "It's me so what from sausage"!

Liebe Bärbel, dir danke ich für deine liebevolle Fürsorge, die Planung und Organisation der Betriebsausflüge und Weihnachtsfeiern und einfach dafür, dass du all den bürokratischen Schreibkram für uns erledigst. Mit deinem herzlichen Lachen, deinen orangen Haaren und deinem bunten Kleidungsstil hast du stets soooo viel Farbe in meinen oft tristen Laboralltag gebracht.... Danke dafür!!!

Ein fettes Dankschön gebührt auch all den TA's, denn ihr seid die gute Seele des Lehrstuhls! Die Zeit mit euch war soooo wunderbar unterhaltsam, lehrreich und lustig.

Ich würde gerne Danke sagen an Angela Zaruba, denn durch sie habe ich erst gelernt, wie das Feilschen richtig geht. An Margret Bahnweg für die schönen Tanzeinlagen zu Freddie Mercury. An Sulith Christan für all die ruhigen, emotionalen und spirituellen Gespräche abseits des stressigen Laboralltags. An Kristina Mosandl, für ihre offene und herzliche Art. Und vielen Dank für deine Offenheit während deiner Schwangerschaft, denn somit wissen wir nun alle, was uns noch bevorstehen wird... Vielen Dank auch an unsere Reiseleitung, Marlene Edlinger, für die Planung und Organisation der Rafting- und Paddelwochenenden, sowie für all die nette Zeit außerhalb der Arbeit. Toni Kuhnt, du bist einfach großartig und eine Bereicherung für unseren Lehrstuhl. Dein Humor ist echt der Hammer! Vielen Dank, für all den „Kuatsch“, den wir gemacht haben und für all die Tränen, die ich geweint habe vom vielen Lachen. Und unserem jüngsten im Team möchte ich auch danken, Alexander Carrapeiro, dem „Cloning King“.

Liebste Peggy, mein allergrößter Dank gebührt dir. Du hast mich nicht nur immer hilfsbereit und tatkräftig im Labor unterstützt und mir auch des Öfteren das Denken abgenommen, sondern du warst auch als Freundin immer für mich da. Wir konnten uns alles anvertrauen und haben Freud' und Leid geteilt, -nur deine Marmelade hast du nicht so gerne mit mir teilen wollen... Ich danke dir für all deine maßlosen Übertreibungen, deiner Schwäche für Sprichwörter und den Gebrauch mir vorher völlig unbekannter Wörter, die mir sogar jetzt noch -wenn ich so daran denke- ein Lächeln ins Gesicht zaubern. Peggy, mein Sonnenschein, ich danke dir für all die Jahre voller Freude, Spaß und Harmonie!

Meiner Familie möchte ich von ganzem Herzen dafür danken, dass sie es mir ermöglicht hat, diesen Weg zu gehen. Lieber Papa, lieber Thomas, ich danke euch, dass ihr mir in der schwersten Zeit unseres Lebens so wahnsinnig viel Trost und Zuversicht zugesprochen habt! Ich finde, wir können wahnsinnig stolz auf uns sein und dankbar, dass wir uns haben!

Mein lieber Flo, dir danke ich für deine Geduld, dein Verständnis und deine Unterstützung während der letzten Monate. Aber am meisten danke ich dir für deine unendliche Liebe! Irgendwie danke ich auch dem Schicksal dafür, dass sich unsere Wege gekreuzt haben und ich einen so wunderbaren, humorvollen und „nicht nur hochintelligenten, sondern auch wunderschönen“ Partner an meiner Seite habe. Babe, ich liebe dich!

Der langen Rede kurzer Sinn:

Etz mal was auerich...

.... Fertsch der Lack ▽▽▽▽
○○○○

12 Curriculum Vitae**Persönliche Daten**

Name Anja B. E. Saalfrank
 Geburtsdatum 23.01.1985
 Geburtsort Marktredwitz, Deutschland

Ausbildung

- | | |
|--------------------|--|
| 01/2010 – 12/ 2014 | Promotionsstudium, Molekulare Biotechnologie,
Technische Universität München
<u>Thesis:</u> „Modelling the multi-step process of tumorigenesis in pigs“ |
| 10/2007 – 12/2009 | Master of Science, Molekulare Biotechnologie,
Technische Universität München
Abschlussnote: 1,2
<u>Thesis:</u> „Generation of rat induced pluripotent stem cells“ |
| 10/2004 – 09/2007 | Bachelor of Science, Molekulare Biotechnologie,
Technische Universität München
Abschlussnote: 1,6
<u>Thesis:</u> „Milchdrüsenspezifische Expressionskonstrukte“ |
| 09/1996 – 06/2004 | Luisenburg Gymnasium, Wunsiedel
Allgemeine Hochschulreife
Abschlussnote: 2,0 |

Veröffentlichungen und Präsentationen**Peer-reviewed Originalmanuskripte**

- Li S, Edlinger M, **Saalfrank A**, Flisikowski K, Tschukes A, Kurome M, Zakhartchenko V, Kessler B, Saur D, Kind A, Wolf E, Schnieke A, Flisikowska T.
 Viable pigs with a conditionally-activated oncogenic KRAS mutation.
 Transgenic Res. 2015 Jun;24(3):509-17
- Merkl C, **Saalfrank A**, Riesen N, Kühn R, Pertek A, Eser S, Hardt MS, Kind A, Saur D, Wurst W, Iglesias A, Schnieke A.
 Efficient generation of rat induced pluripotent stem cells using a non-viral inducible vector.
 PLoS One. 2013;8(1):e55170
- Flisikowski K, Venhoranta H, Bauersachs S, Hänninen R, Fürst RW, **Saalfrank A**, Ulbrich SE, Taponen J, Lohi H, Wolf E, Kind A, Andersson M, Schnieke A.
 Truncation of MIMT1 gene in the PEG3 domain leads to major changes in placental gene expression and stillbirth in cattle.
 Biol Reprod. 2012 Dec 21;87(6):140

Leuchs S*, **Saalfrank A***, Merkl C, Flisikowska T, Edlinger M, Durkovic M, Rezaei N, Kurome M, Zakhartchenko V, Kessler B, Flisikowski K, Kind A, Wolf E, Schnieke A.
Inactivation and inducible oncogenic mutation of p53 in gene targeted pigs.
PLoS One. 2012;7(10):e43323

* Diese Autoren haben gleichermaßen zur Veröffentlichung beigetragen

Merkl C, Leuchs S, **Saalfrank A**, Kind A, Schnieke A.
RNA interference in pigs: comparison of RNAi test systems and expression vectors.
Mol Biotechnol. 2011 May;48(1):38-48

Clavel T, **Saalfrank A**, Charrier C, Haller D.
Isolation of bacteria from mouse caecal samples and description of *Bacteroides sartorii* sp. nov.
Arch Microbiol. 2010 Jun;192(6):427-35

Veröffentlichte Kurzfassung

Flisikowska T, Leuchs S, **Saalfrank A**, Eser S, Kind A, Wolf E, Saur D, Schnieke A.
Porcine models for human cancer
Reproduction Fertility and Development 12/2012; 25(1):321-2

Vortrag

Saalfrank A, Flisikowska T, Tschukes A, Schnieke A
Animal model for early detection of pancreatic cancer
Vortragstagung der Deutschen Gesellschaft für Züchtungskunde e.V. und der Gesellschaft für Tierzuchtwissenschaften e.V. am 6/7. September 2011 in Weihenstephan

Posterpräsentationen

Saalfrank A, Flisikowska T, Flisikowski K, Eser S, Wolf E, Saur D, Schnieke A
The pig as a model for human cancer
23rd Biennial Congress of the European Association for Cancer Research, July 5th-8th, 2014, Munich

Flisikowska T, **Saalfrank A**, Flisikowski K, Eser S, Wolf E, Saur D, Schnieke A
Genetic engineering in Livestock: Porcine Cancer Models
3rd Munich Biomarker Conference, November 26th-27th 2013, Munich

Flisikowska T, Leuchs S, **Saalfrank A**, Eser S, Kind A, Wolf E, Saur D, Schnieke A.
Porcine models for human cancer
6th Mildred Schell Cancer Conference, June 5th-7th 2013, Bonn

Saalfrank A, Flisikowska T, Leuchs S, Eser S, Edlinger M, Müller-Fliedner P, Wolf E, Saur D, Schnieke A
The pig as a model for human cancer
7th International Meeting Stem Cell Network North Rhine Westphalia, April 23rd-24th 2013, Cologne

Saalfrank A, Flisikowska T, Flisikowski K, Eser S, Wolf E, Saur D, Schnieke A
The pig as a model for human cancer
17th International AEK Cancer Congress, March 20th-22nd 2013, Heidelberg

Saalfrank A, Flisikowska T, Leuchs S, Eser S, Wolf E, Saur D, Schnieke A
The pig as a model for human cancer
2nd Munich Biomarker Conference, November 22nd-23rd 2012, Munich